MERIWA

FINAL REPORT

ON

Evaluation of Monorail Haulage in Metalliferous Underground Mining

BY

A/Prof. Emmanuel Chanda
&
Dr. Mahinda Kuruppu

22 MAY 2009

Executive summary

The decline is a major excavation in metalliferous mining since it provides the main means of access to the underground and serves as a haulage route for underground trucks. However, conventional mining of the decline to access the ore body poses economic and technical challenges that require innovative responses. The average cross-sectional area of mine declines in Australia is 5m wide x 5m high. The large excavations associated with current underground mining practices are economically and geotechnically inappropriate, especially for narrow vein mining conditions. The decline gradient of 1:7 (8^{o}) designed to accommodate truck haulage results in a significantly longer decline compared to a decline mined at a steeper gradient. Further, the current drill-blast-load-haul cycle does not allow rapid development of the decline to access the ore body since the cycle is made up of discontinuous segments. The use of diesel equipment poses health risks and increases ventilation requirements. The heat load and air borne exhaust contaminants emitted by large diesel engines create an unacceptable demand on mine ventilation, resulting in substandard working conditions. As mines get deeper, there is a tendency to increase the truck and loader fleet – which results in traffic congestion in the decline. Metal prices in the current boom may have helped to offset some of the shortcomings of current practices, and although the good times may continue, a down-turn could find many operations exposed.

This study was prompted by the need to investigate the potential of the monorail haulage system in metalliferous mining, particularly in decline development and main haulage in view of shortcomings of the current practices. Monorails are being used in mines around the world for material transport and man-riding but their utility in rock transport has not been fully investigated. Hence, it is proposed to replace non-shaft component of the mine haulage system with roof/back mounted monorail technology using continuous conductor technology to provide competitive haulage rates in substantially smaller excavations at steeper gradient than is currently achievable. It is proposed that a suite of

equipment can be adapted or modified to enable development of the decline supported by the monorail system.

To this end, a drill system mounted on the monorail accompanied by a pneumatic system for loading rock into monorail containers is proposed. The decline gradient for the monorail decline is 1:3 (or 20^0) with a cross-sectional area of 4m wide x 4m high. Systems analysis, engineering economics and computer simulation are used to evaluate the feasibility of the monorail mining system for decline development. Technical data relating to the operation of monorails in underground mining was obtained form Scharf Mining Solutions of Germany, a company that manufactures monorails. Monorail haulage has definite advantages over conventional haulage; these include use of electrical power instead of diesel, steeper gradients (up to 36^o), smaller excavations (3mx3m), tighter horizontal and vertical turning radii and potential for automation. The concepts are applied to a narrow vein ore deposit with results indicating that the monorail system delivers significant savings in terms of time and cost of decline development in this specific application.

In this report we present: the design of the monorail system for decline development and an evaluation of cost and productivity associated with the monorail system in comparison with the conventional decline development.

The main conclusion from this study is that the monorail haulage system is a feasible proposition for decline development in metalliferous underground mining. It is not being suggested that the monorail will replace current truck haulage systems, but it is evident that monorail technology will deliver significant benefits to the narrow vein mining industry.

Acknowledgements

The Authors would like to thank Minerals and Energy Research Institute of Western Australia (MERIWA) and Newmont for financial support of the monorail research project at Western Australian School of Mines (WASM) and Scharf Mining Solution for providing technical data and cost information on the Electric Monorail Transport System.

The author would also like to express sincere thanks to the following people for their invaluable contribution and useful suggestions to this research;

- Mr. B. Besa a PhD student who has been working and will continue working on this project for his PhD thesis;
- Mr. William Darcy who worked on the project before Mr. Besa took over;
- Mr. Mick Roberts, who provided advice on practical aspects of the system; and
- Mr. Stefan Meyer of SMT Scharf - Solutions for Mining Transport.

Table of Contents

Page

List of Figures

Page

List of Tables

Page

Nomenclature

Symbol	Description	Units
f	Friction factor	[-]
ρ	Density	[Kg/m^3]
μ	Viscosity of fluid	[kg/ms]
λ	Friction factor	[-]
μ_d	Dynamic internal friction factor	[-]
l_p	Plug length	[m]
ξ_p	Ratio of cross sectional area of conveying plug to that of pipe	[-]
ℓ_b	Bulky density of the material in the plug	[Kg/m^3]
ξ_i	Factor of internal friction	[-]
u_a	Air velocity	[m/s]
u_k	Permeating air velocity	[m/s]
u_p	Plug velocity	[m/s]
l_a	Length of air cushion	[m]
η	Efficiency	[%]
h_f	Friction head loss	[m]
μ_k	Coefficient of kinetic friction	[-]
μ_s	Coefficient of static friction	[-]
ΔP_{acc}	Pressure loss in acceleration zone	[kPa]
ΔP_{sts}	Pressure loss in steady state zone	[kPa]
A	Cross sectional area of pipe	[m^2]
A	Particle projected area	[m^2]
A_h	Contact area between plug and retarded bed	[m^2]
A_w	Contact area between plug and the wall	[m^2]
C	Curve length	[m]
C_d	Development cost	[A$]

$C_{1,2}$	Constants with index 1 and 2	[-]
C_D	Drag coefficient	[-]
C_m	Decline development cost per meter	[A$/m]
D	Diameter of pipe	[m]
d_p	Particle diameter	[m]
D	Drag diameter	[m]
e	Pipe roughness	[m]
E_c	Power of conveying system	[kW]
F_{BK}	Braking force	[kN]
F_d	Drag force	[kN]
$F_{FR\text{-}HH}$	Horizontal frictional forces at base of horizontal stabilisers	[kN]
$F_{FR\text{-}HL}$	Lateral frictional forces at base of vertical stabilisers	[kN]
$F_{FR\text{-}HV}$	Vertical frictional forces at base of horizontal stabilisers	[kN]
$F_{FR\text{-}VH}$	Horizontal frictional forces at base of vertical stabilisers	[kN]
F_{HS}	Forces in horizontal stabilisers	[kN]
F_M	Feed force from the monorail drilling system	[kN]
F_{MS}	Force suspending monorail train	[kN]
F_{MS}	Force suspending monorail train	[kN]
F_{MW}	Force due to weight of monorail train (plus weight of two drilling booms)	[kN]
Fr	Froude Number	[-]
F_{VS}	Force in vertical stabilisers	[kN]
F_w	Gravitational force of rock particle	[kN]
H	Thickness of stagnant bed	[m]
H_T	Pump head	[m]
L	Euclidean length	[m]
L	Length of pipe	[m]
m	gradient	[-]
m*	Mass flow ratio	[-]
M_a	Mass flow rate of air	[kg/s]
M_p	Mass of plug	[kg]
M_s	Mass flow rate of solids	[kg/s]
P	Pressure drop	[kPa]

P_1,P_2	Pressure at front and back side of plug	[kPa]
P_c	Total conveying pressure	[kPa]
Pr	Normal pressure in the plug	[kPa]
Q	Conveying rate	[m3/h]
r	radius	[m]
r	Monorail turning radius	[m]
Re	Reynolds Number	[-]
R_h	Friction resistance at the surface of stagnant bed	[N]
R_W	Friction resistance at the inner surface of a pipe	[N]
U	Difference of permeating air velocity and plug velocity	[m/s]
v_s	Superficial velocity of solids	[m/s]
v	Velocity	[m/s]
V	Volumetric flow rate	[m^3/s]
z	Vertical displacement	[m]
α	Decline gradient	[Deg]
β	Angle of inclination of pipe	[Deg]
ε	Porosity of conveying material	[-]
φ	Shape factor	[-]

Abbreviations

Symbol	Description
AusIMM	Australasian Institute of Mining and Metallurgy
BCM	Bank Cubic Metre
BHP	Brake horsepower
DF	Design Factor
EMTS	Electric Monorail Transport System
FEL	Front End Loader
FoS	Factor of Safety
GPSS	General Purpose Simulation System
LHD	Load Haul Dump
MERIWA	Mineral and Energy Research Institute of Western Australia
PID	Proportional-Integral-Derivative
PLC	Programmable Logic Control
ROM	Run-of-mine
SG	Specific Gravity

Chapter 1

1.0 Introduction

1.1 Underground mine access and haulage

Most underground mines in Western Australia (WA) are accessed by means of declines or shafts. However, the majority of mines in WA adopt declines as a means of accessing underground resources. In conventional truck haulage mining, declines are usually excavated at a gradient of 1:7 with an average width of 5mW x 5mH. From the decline, cross-cuts are mined at regular vertical intervals to access the orebody. Transportation of ore and waste from underground to surface as well as men and material to and from underground is done via the decline. The average cost of mining a decline in Australia is in the order of A$2500/metre.

The decline method of accessing the orebody and its subsequent use as a transport excavation has been a huge success for the Australian underground industry. However, the system does not meet the specific needs of narrow vein mining and the challenge posed by mining at greater depths (greater than 600m) in the Australian context. Large excavations typical of many Australian mines are not suitable for narrow vein type deposit and are unlikely to be suitable at greater depths from both geotechnical and economic perspectives. Specific problems associated with conventional decline development and haulage include airborne exhaust contaminants emitted by large diesel engines, slow advance rates, increased ventilation requirements, increased rock reinforcement costs, traffic congestion and carbon footprint. Metal prices in the current boom have

helped to offset some of the challenges associated with large declines; a down-turn in commodity prices could find many operations exposed. The need to develop innovative responses to these challenges is clearly evident.

1.2 The monorail system

One system that has the potential to overcome the above challenges, in part, is the monorail haulage system. This research work was conducted in order to determine the technical and economic feasibility of monorail application in mine decline development. It is postulated that the monorail system would result in rapid decline development by reducing the mining cycle, hence accessing the orebodies faster and at a lower cost in comparison to conventional method of using jumbos, loaders and trucks. The monorail decline can be mined at steeper gradient of up to 36^0, hence reducing the total length of the decline. Further, due to the reduction of excavation dimension, the monorail system would result in lower support costs, less seismic risk and lower excavated rock volumes. In relation to underground transport, the Electric Monorail Transmission System (EMTS) will reduce reliance on diesel powered equipment by replacing it with quasi-mobile main powered electrical transport and development methods. Other benefits include reduction in ventilation air volumes, elimination of diesel exhaust fumes and reduction in heat load in underground workings, reduction in quantity of rock required to be mined and improved grade control by reducing the amount of external waste mined.

Monorail technology has been used in the mining industry for material and personnel transport and in a limited way for rock haulage. The proposal of this project is to replace the non-shaft components of the mine transport system with roof/back mounted monorail which provides mobile motive energy whilst simultaneously functioning as the second level electrical reticulation system. The system is designed to integrate drilling, blasting, loading and hauling during the development of a decline, serving as the rock transport system from the underground to the surface.

It must be stated here that monorail haulage is not necessarily being proposed as a total replacement or direct competitor to the large tonnage autonomous machines currently in use, although the capability does exist and can be implemented as appropriate. The system has a lot of potential for narrow vein type of deposits and deep mines where large excavations pose seismic risks.

1.3 Research objectives

The primary objective of this project is to evaluate the techno-economic feasibility of the application of the EMTS in metalliferous underground mines in Australia.

Specific objects of this study are to;

- Design a pneumatic loading system that uses a monorail train to clean the development face;
- Design a drilling system that uses a monorail train to drill the development face;
- Design decline haulage with application of the monorail system in ore bodies which cannot be economically accessed by existing practices;
- Estimate capital and operating expenditures for the designed decline haulage (that uses the monorail system) and compare these with conventional decline haulage development;
- Design system control and automation with the objective of reducing personnel requirements, thereby lowering operating costs; and
- Review Mining and Safety Regulations so as to include operations and applications of the designed monorail system.

1.4 Research approach

To achieve the objectives stated in Section 1.3 above, the following approach was used: collection of technical, productivity and cost data from the manufacturer of the

system and mines around the world where the system is currently being used; conceptual design of the system for a hypothetical decline development project; evaluation of cost and productivity of the system and comparison with conventional bulk application to a case study mine. While monorail technology is proven, its application in metalliferous mining as the main transport system has not been studied in detail to provide mine planners with an alternative. In this study, an integrated drill-blast-load-haul system based on monorail platform is presented. The idea is to reduce the main cycle allowance for rapid development of the decline to access the orebody. The concept involves mounting a twin-boom jumbo on the roof-mounted monorail and using a pneumatic (supersucker) system to load the broken rock into the monorail containers via a hopper. The containers are lifted by the monorail and transported to the surface via the decline. The performance and cost of the system are estimated from first principles using the data supplied. A computer simulation model was developed to check the validity of the results. The results for the case study (Jundee) are compared to those based on conventional decline development.

1.5 Report structure

The outline of the report is as follows:

Chapter 2 presents the current state of monorail technology and its application in the mining industry. The advantage of the system and its operations are discussed in comparison with the conventional method.

Chapter 3 provides a detailed description of the available mathematical models and experimental explanations of pneumatic conveying systems. Since loading of broken rock from the development face will be done using a pneumatic suction unit, this chapter reviews literature on pneumatic suction principles. The chapter is intended to bring about pneumatic suction theory that is used during the design of the monorail pneumatic loading system.

Chapter 4 outlines the design of the drilling system for the monorail. The drill jumbo is not an independent unit but mounted on the monorail. To drill the

round, monorail is advanced to the face and hydraulic props are used to stabilise the drilling system. Drilling may occur simultaneously with loading.

Chapter 5 discusses the design of a pneumatic loading system. The system is based on the principle of a vacuum cleaner. The rock fragments are sucked from the face into the hopper which loads the containers that are transported to the surface. The use of pneumatic loading provides a much more continuous system compared to the use of boggers.

Chapter 6 discusses the application of the monorail mining and haulage system to the Jundee orebody. This case study clearly shows that the proposed system would improve the economics of mining the Nexus orebody, one of the South Deeps structures.

Chapter 7 describes the simulation model and the results obtained – these are compared with analytical estimates of productivity.

Chapter 8 presents conclusions drawn from this study and recommendations for future work.

Chapter 2

2.0 Monorail technology

2.1 Introduction

This chapter reviews the literature on current state of monorail technology and its application in the mining industry. The chapter provides background information about the design of decline access using conventional as well as monorail technology. The advantage of the monorail system and its operations are discussed in comparison with the conventional method

2.2 Background to monorail technology

Aerial ropeways (Figure 2.1), which can be considered as early forerunners of monorails, have long been recognised as less expensive transportation devices (Oguz and Stefanko, 1971). According to Oguz and Stefanko (1971), the first aerial rope way was installed for surface transportation in Germany in 1860. However, the most important disadvantage of an aerial ropeway installation for underground application is slack in the carrying rope and the difficulty arrangement of pulling at horizontal curves. An important underground aerial rope installation was in the San Francisco Mine of Mexico Limited at San Francisco Del Oro, Chihuahua, in Mexico (Metzger, 1940). According to Metzger (1940) the underground portion of this installation was 930.86m (3054 ft).

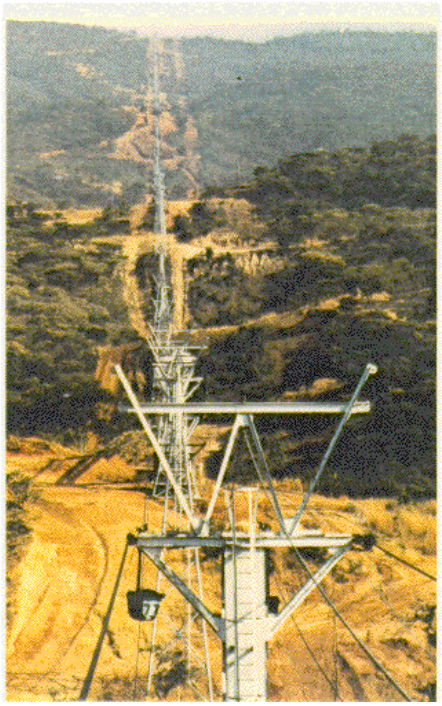

Figure 2.1: Aerial rope way at Maamba Collieries Limited, Zambia (Courtesy – Boyd, 1993)

One of the first monorail systems was developed in Germany early during Second World War using old, flat-bottomed rails to transport relatively heavy material (Oguz and Stefanko, 1971). This was the beginning of the old Bacorite monorail system (Parfitt and Griffin, 1963). The more recent developments of monorail systems at the end of the 1950's and early 1960's in Germany and in England are remarkable (Oguz and Stefanko, 1971).

2.2.1 Electric Monorail Transport System (EMTS) Technology

2.2.1.1 What is EMTS technology?

Monorail haulage systems are not new in the world of materials handling (Oguz and Stefanko, 1971). Their early application can be traced to Germany during the Second World War (Toler, 1965). The EMTS system consists of a track of jointed section rails, which can easily be extended to the desired length and suspended by means of chains or rigid brackets to roof bolts or support beams (Figure 2.2).

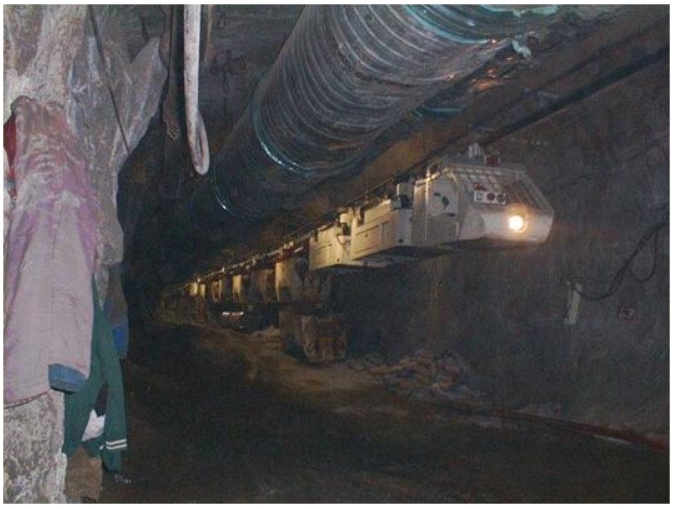

Figure 2.2: EMTS in an underground haulage (Courtesy – Scharf, 2007).

The containers or carriages hang by its wheels on the bottom flange of the track and are powered by electric motors. Monorail systems use a roof suspended I-profile rail, which completely prevents any derailment of the train. Depending on the transportation task, the monorail system can be equipped with man-riding cabins, material container and bottom discharge hoppers (Guse and Weibezhn, 1997). With a load carrying capacity of up to 30 tonnes and the ability to negotiate gradients of up to 36^0, the EMTS can make transport in decline development considerably more efficient than conventional truck haulage system. Variable drive units and load - carrying beams with payload capacities of up to 30 tonnes allow the monorail system to negotiate horizontal and vertical curves with a minimum radius of 4m and 10m respectively.

2.2.1.2 Components of a monorail system

The monorail system consists of the following main components (see also Figure 2.3) which are flexibly joined to each other via coupling rods.

a) Driver's cabin
b) Drive units
c) Power pack
d) Bulk material containers

e) Hoist units

f) Power supply and control unit

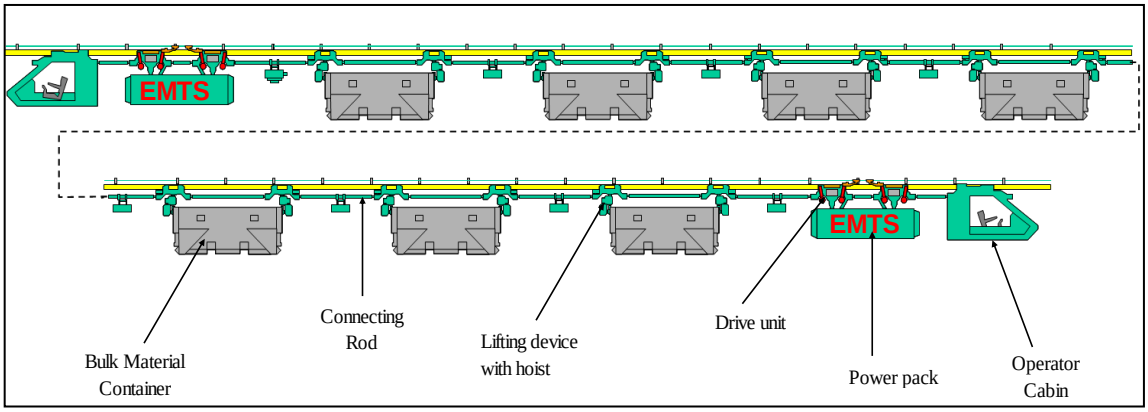

Figure 2.3: Components of monorail system (Courtesy – Scharf, 2007)

(a) Operator's cabin

On at least one end of the monorail system there is an operator's cabin (Figure 2.4) which serves to control and operate the system. The cabin contains an ergonomic operator seat, a joystick and a panel with the signalling and control devices (Figure 2.4). Additionally, each cabin is equipped with a head light and a tail light which can be switched according to the travelling direction.

(a)

(b)

Figure 2.4: Monorail train (a) drivers cabin with ergonomic operator seat; (b) Joystick with panel (Courtesy – Scharf, 2007)

(b) Drive units

Figure 2.5 shows the drive unit for the monorail system. Each drive unit consists of 2 x 29 kW electric motors controlled by frequency converters and programmable controllers that are coupled to the drive wheel through gears. The special design drive units using frequency converter powered motors allows to feed back electrical power into the power supply. This results in approximately 30% average power saving of the electrical power needed for the operation of the trains. The drive unit is controlled from either end of the train from the operator's cabins. Up to four drive units can be used within one train. Monorail trains operated by friction drives are generally equipped with 2 or 3 hydraulic drive units each with a nominal traction force of 40kN. Each drive unit also comprise two spring tensioned hydraulically released emergency brakes. The drive unit weighs approximately 2 tonnes and has maximum length of 2m.

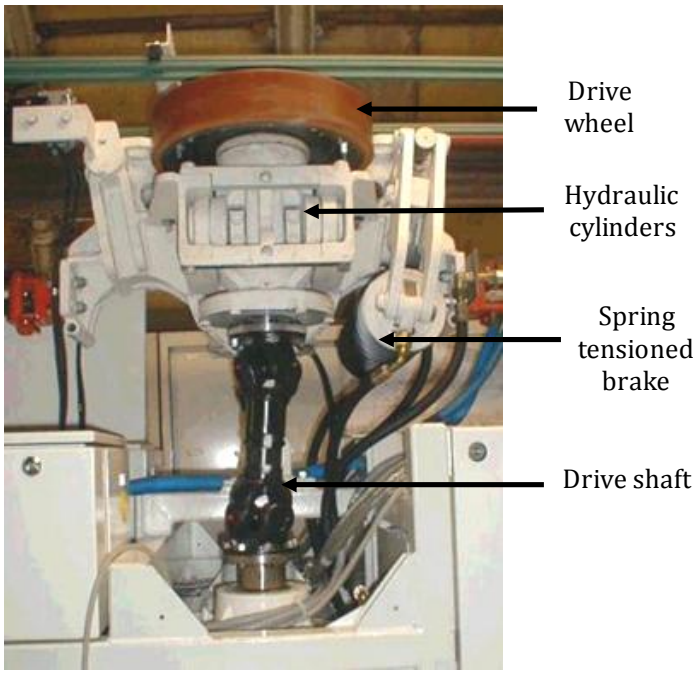

Figure 2.5: Monorail train drive unit (Courtesy – Scharf, 2007)

(c) Monorail system power pack

The monorail system drive unit consists of two electric motors. Therefore, the power pack (Figure 2.6) provides power to these two electric motors which then propel the drive units.

Figure 2.6: Power pack for monorail train (Courtesy – Scharf, 2007)

Because the monorail train can have up to four drive units, each electric motor propels one drive unit which subsequently runs one pair of friction drive wheels. There is also a small hydraulic power pack mounted on the rear of the driver's cabin that provides power to the hydraulic release cylinders of the spring loaded brake system.

(d) Bulk material containers

Figure 2.7 shows the standard monorail container. The standard containers are 1.2m high, 1.1m wide and 3.5m in length. Each container holds 2.5m^3 of material, weighs 1 tonne when empty and has lifting devices that are designed to handle a payload of 5 tonnes. The monorail train can carry a maximum of 6 containers.

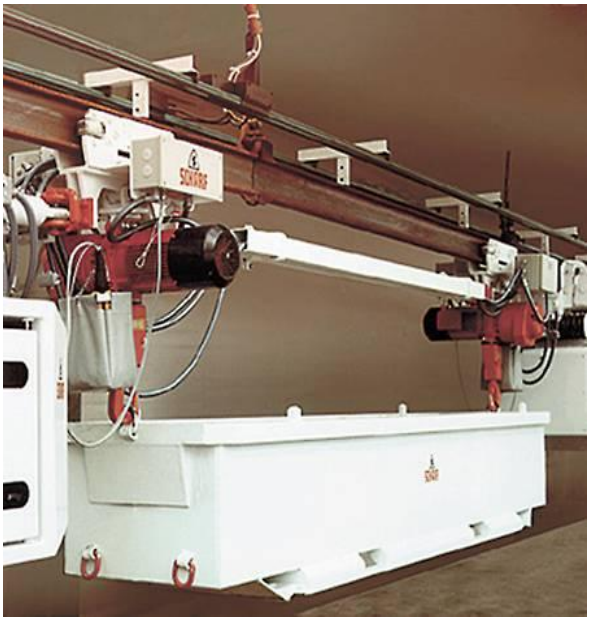

Figure 2.7: Monorail standard container (Courtesy – Scharf, 2007).

The payload may be increased by upgrading the lifting beams that requires the use of stronger chains and use of twin trolley on each lifting beam. Customised containers and carrying frames for heavy loads as well as rock containers can

easily be coupled to the lifting beams and this permits a great deal of flexibility and high utilisation of the machine.

A system of load distribution limits the roof bolt/suspension bracket load to 50 kN. This allows single load of maximum 30 tonnes to be transported. The lifting beams are available with load measuring devices to prevent an overloaded train from being operated. The load measuring system allows the internal Programmable Logic Control (PLC) to adapt the system's setting according to the actual total train weight.

(e) Hoist units

The monorail system is equipped with hoist carriages (Figure 2.8). Each carriage incorporates a hoist able to take load up to maximum of 30 tonnes. The hoists are controlled either from the operator's cabin or directly from the hoist unit.

(a)

(b)

Figure 2.8: Monorail system hoist unit

(f) Switches and power supply

All components of the power supply and the control unit are installed in switch boxes. These are suspended on a load beam with two carriages. The carriages include the current collectors supplying the train with power from the conductor rail (Figure 2.9). Several types of swiches are also avalaible which can be remote controlled by EMTS driver or by dispatcher. They can also be activated hydraulically, pneumatically or electrically and consists of fail-safe locking system.

(a)

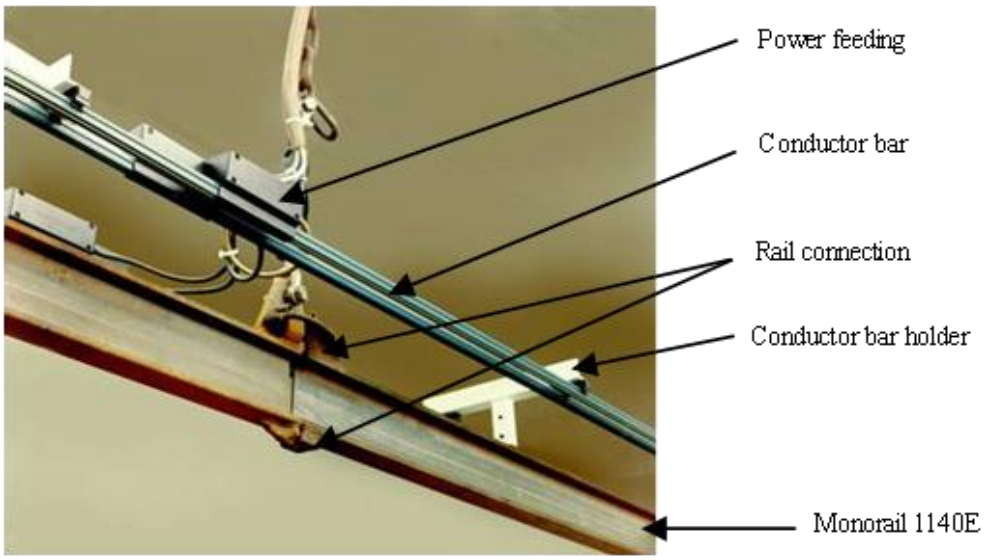

(a)

Figure 2.9: Monorail train power unit (a) switch (b) power supply unit (Courtesy – Scharf, 2007).

2.2.1.3 EMTS automation and control system

The heart of the EMTS control is a PLC that controls the entire monorail system through a programme (software). The PLC manages different drive modes in which the EMTS operates including the ascending and descending functions. The software also incorporates a fault-finding facility and records all operational details. The EMTS can also apply soft and emergency braking modes through the PLC system. PLC systems have proven to be extremely reliable in mining environments, and their application in longwall controllers and belt starters has become commonplace (Novak and Kohler, 1998).

Safety features incorporated in the PLC include the ability to control and limit speed of train which can be slowed down automatically when approaching rail switches or stations. Different types of switches allow adaptation to any mine layout. Furthermore, the operations of the system can be remote controlled combined with video cameras. This could result in the reduction of mine operating personnel when compared to truck operations.

2.2.1.4 Monorail system application in mining

The following are some of the potential applications of the monorail system in mining:

- The monorail system could find wide applications in horizontal development, ore stoping operations and in ore / waste haulage from underground to the surface.
- In some instances, the monorail system may replace truck and / or train haulage.
- The monorail system could also be installed in combination with conveyor haulage system.
- It is also conceivable that the system could be used in lateral haulage to the ore pass system for further materials handling.
- The system can also find wide application in transport of machinery and equipment up to 30 tonnes per single load (Figure 2.10) as well as transport of men by mounting man-riding carrier of up to 20 men per carrier (Figure 2.11).

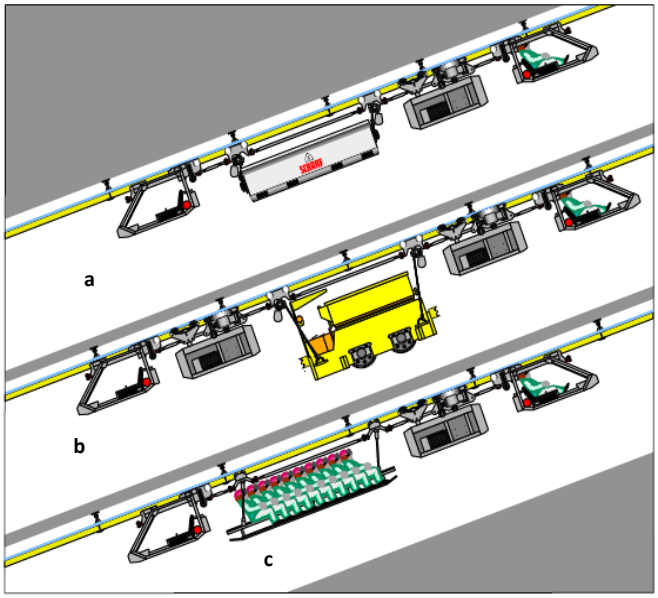

Figure 2.10: Conceptual applications of monorail system (a) Bulk Transport, (b) Machinery and Equipment and (c) Transport of men (Courtesy - Scharf, 2007).

Figure 2.11: Transport of men (Courtesy - Scharf, 2007).

2.2.1.5 An overview of monorail Installation

Monorail installation is a combination of three major activities i.e. drilling, roof bolting and placing new rail section. It is reported (Oguz and Stefanko, 1971) that preparatory activities such as lining, marking the hole and collaring of drill holes are important phases in drilling of holes for monorail installation. Drill holes for monorail installation are normally drilled to a depth of 2m and require a 41mm diameter hole. Collaring and eventually drilling a hole precisely are very important because incorrect drilling results in the monorail being off-line and this creates unnecessary friction on the monorail by the rollers.

Once holes are drilled, roof bolts are inserted into the holes. Selecting the support structure for the monorail deserves attention (Oguz and Stefanko, 1971). This is to avoid roof bolts coming out of the sockets due to the weight of the rail and the monorail. The Hilti OneStep anchor bolt is used as the suspension bolt for the monorail. This type of anchor bolt has increased working safety and has reduced anchor settling time. After installing the roof anchor, a special eyebolt is attached on the threaded end of the bolt. A shackle provides easy connection of the chain to the roof bolt. From the shackle the distance is

carefully measured to obtain the length of the chain for horizontal track installation. This restricts the lateral movement of the rail during monorail system movements. Details of monorail installation are described in Chapter 8.

2.2.2 Benefits of EMTS

Monorail haulage system has tremendous benefits as compared to truck haulage. The following are some of the potential benefits of the monorail system:

- Ability to negotiate declines at steeper gradients (up to 36^0) with less power demand. This tremendously reduces the decline length;
- Ability to negotiate horizontal curves to the radius of 4m and vertical radius of 10m;
- Reduction in size of excavations - minimum operating drive dimension is 1.7m wide and 2.9m high – this improves stability of underground excavations;
- Small excavations means less heat generated from rock, hence reduced ventilation and need for air conditioning;
- Reduced haulage costs per tonne per kilometre because of less power consumption (Generally, rail transport systems have low friction energy loss);
- High availability of more than 95%;
- Multi purpose haulage system for men, material and rock;
- Small and medium sized ore bodies can be mined with less initial investment;
- Require no floor preparation and are not affected by wet or weak floor conditions;
- No diesel fumes since it uses electricity for operations;
- Can be controlled by PLC System which opens the possibility of significant personnel savings and hence cost saving; and
- Low system operating costs – a must for small / medium-sized high grade ore bodies, hence improved profitability of narrow vein ore deposits.

2.3 Monorail system versus conventional decline development

2.3.1 What is decline access?

In underground mining, accessing ore body can be achieved via a decline or ramp system, vertical shaft or adit (Hartman, 2002). The decisions related to the primary development openings of a mine must be made early in the mine planning stage. The decisions normally concern the type, shape and size of main openings. In Australia, most mines are accessed by means of declines. Declines are spiral, which are in rectangular form and which circle either the flank of the deposit or the deposit itself (Figure 2.12).

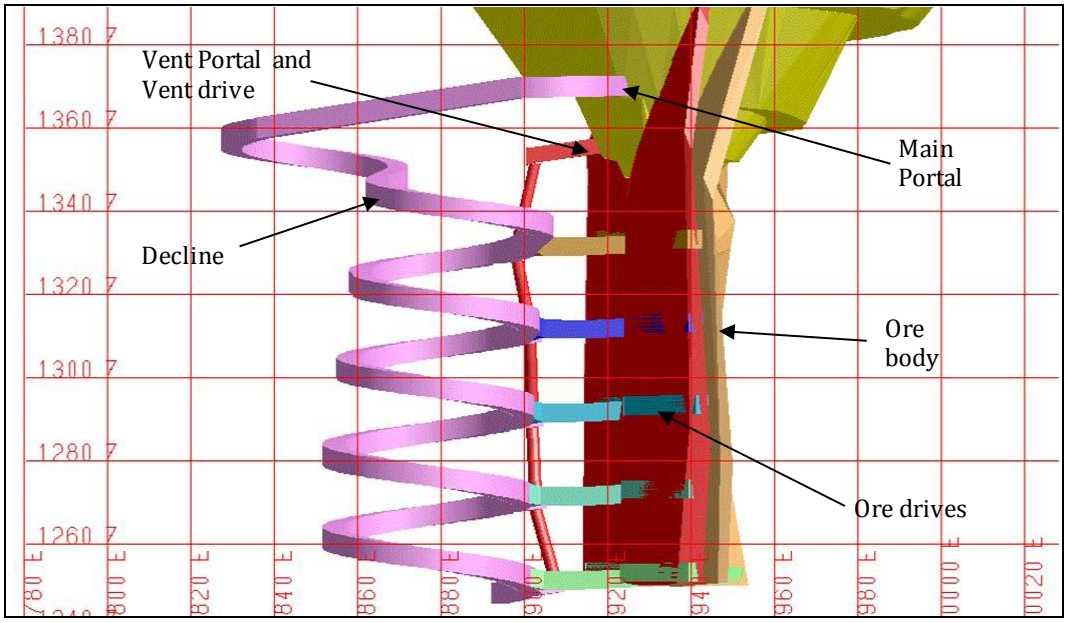

Figure 2.12: Conventional decline access (Chanda and Roberts, 2005)

The decline begins with a box cut, which is the portal to the surface, or from an open pit. A box cut is a small open cut created to provide a secure and safe portal as access to a decline in an underground mine. Levels are then excavated horizontally off the decline to access the ore body.

Australia is a world leader in the design and operation of mine accessed by declines and the number of metaliferous underground mines using the decline

system are increasing steadily (Chanda and Roberts, 2005; Chanda and Corbett, 2003). This increase has generated a great deal of interest in underground haulage systems in future.

2.3.2 Conventional decline development

Australian underground mines utilise hybrid system of underground haulage appropriate to the ore body being mined and layout (Isokangas and White, 1993). Most mines in Australia adapt decline access and the use of truck haulage (Robertson, 1998). Therefore, mine planning and design parameters for decline access are greatly influenced by available haulage system that the mining engineer can choose from. The following are the design parameters used in conventional decline development in Western Australia.

2.3.2.1 Design parameters for conventional decline access

(a) Size of decline access

In most Australian mines, the size of decline access is designed for truck haulage with the minimum standard opening cross-sectional area of 5.5mW x 5.5mH. The size of declines is ordinarily driven to allow free access to any level of the mine with diesel-powered equipment. The size of decline provides a means of utilising mobile equipment throughout the mine without limitations. Generally, declines are sized to accommodate the largest equipment to be used with added room for ventilation, drainage and personnel (Pond, 2000). This means that the bigger the equipment, the bigger the decline dimensions. Therefore, the size of these openings and the design of curves must be carefully matched to the equipment used in the mine and must allow room for tubing that is used for ventilation. Thus, for narrow deposits the minimum dimension requirement of decline development and material handling are costly and as a result, they fail to clear economic hurdles.

(b) Decline gradient

Decline gradient generally refers to the slope of the decline access. It is used to express the steepness of slope of the decline where zero indicates level (horizontal) and increasing (or decreasing) numbers correlate to more vertical inclinations upwards or downwards. Decline gradient has fundamental importance in decline access development because it affects the length of the decline. In Australian mines, the standard decline gradient used in conventional decline development is 1:7 (8^0). According to Chanda and Corbett (2000) steeper gradients require trucks to operate under higher loads for longer periods per kilometre travelled, thereby increasing maintenance and operating costs.

(c) Turning radius

The turning radius of an underground decline access is the radius of the smallest circular turn that the truck is capable of making. This is illustrated using Figure 2.13.

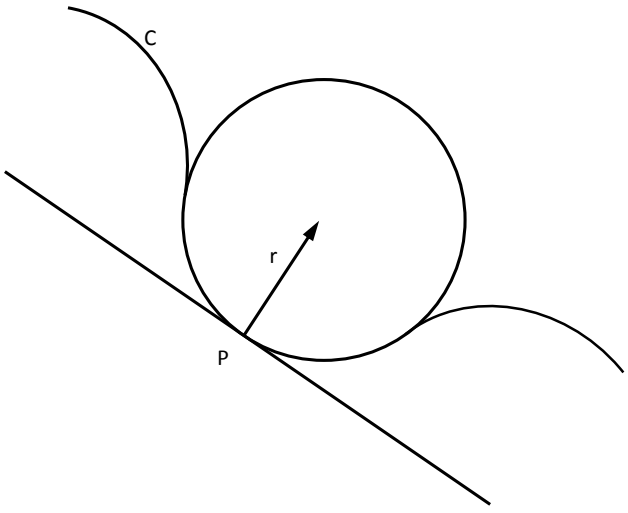

Figure 2.13: Relationship between curvature and curve length (Wikipedia, 2007).

For a plane curve ***C***, the curvature at a given point ***P*** has a magnitude equal to the reciprocal of the radius (**1/*r***) of an oscillating circle (Wikipedia, 2007). The smaller the radius ***r*** of the oscillating circle the larger the magnitude of the

curvature. Therefore, where a curve is "nearly straight", the curvature will be close to zero i.e. length of the curve will be longer, and where the curve undergoes a tight turn, the curvature will be large in magnitude giving smaller curve radius.

2.3.2.2 Effects of designed parameters on decline development

Decline access design parameters have tremendous effects on decline length, waste material excavated, and duration of decline development. The parameters also have some influence on decline development costs. The following are the effects of design parameters on decline development.

(a) Effects of size of decline

The size of decline access has fundamental impacts on decline development. Reduction in decline dimension has the effects of reducing both the development costs and duration of decline development and vice versa. It can also be argued that large dimensions speed up the rate of development through the use of large and more productive machines. However, large and more productive machines have an effect of increasing both the initial capital costs and the development cost per meter. Similarly, with large machines, mining of thin and vein type deposits become very expensive making mining operations uneconomic. According to Chanda and Burke (2007) the large access excavations typical of many Western Australian mines are likely to be unsustainable at increased mining depths, from both geotechnical and economic perspectives. This means, for decline dimensions smaller than the conventional 5.5mW x 5.5mH, developments will reduce and as such narrow deposits can be extracted since smaller drives in the ore body are necessary to reduce mining dilution (Chanda and Roberts, 2005). Smaller excavation reduces the need for costly ground support, increases the safety of mine workers and reduces ventilation requirements. However, smaller decline dimension entails finding suitable

haulage equipment since truck haulage can no longer be applicable. Other effects of size of decline are summarised below:

- The amount of development outside the ore body is huge resulting in more waste material being excavated. The increase in waste development has an effect of increasing development costs as well as transport costs;
- With large decline dimensions, infrastructure requirements to support openings for decline truck haulage may be too expensive to economically extract narrow ore bodies; and
- The duration of decline development is also longer for declines with large dimensions than those with smaller ones due to the fact that more time is spent excavating huge quantity of material in declines with larger dimensions.

(b) Effects of decline gradient

(i) Effects on development meters

Decline gradient has significant effects on decline development meters. According to Chanda and Burke (2007) with increasing depths of mining and further tightening on safety requirements, the price of a typical decline excavation in Australia is likely to increase further. It is reported (Chanda and Roberts, 2005) that at decline gradient of 1:7, to reach a theoretical 700m vertical depth ore body, the decline distance would be 4950m while at steeper gradient the decline length would be less. This is illustrated using Figure 2.14:

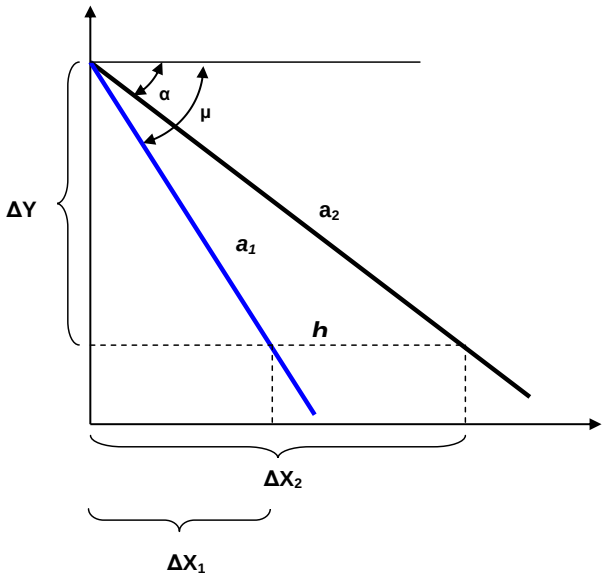

Figure 2.14: Relationship between gradient and length of a line.

Theoretically, for linear functions, the gradient of a line (**m**) is calculated as indicated in Equation 2.1:

$$m = \frac{\Delta y}{\Delta x} \qquad 2.1$$

and according to Figure 2.14, a_1 has steeper gradient than a_2. The length of a_1 and a_2 is calculated using Equation 2.2 and 2.3 respectively.

$$a_1 = \frac{\Delta Y}{\sin\mu} \qquad 2.2$$

$$a_2 = \frac{\Delta Y}{\sin\alpha} \qquad 2.3$$

According to Equation 2.2 and 2.3, it can be seen that to reach horizontal level ***h***, the length a_1 will be less than a_2 because a_1 has steeper gradient than a_2. This is also confirmed by numerical calculations of *Euclidean Length*, **L**, using Equation 2.4 (Brazil et al., 2003). From Equation 2.4, it is evident that as decline gradient increases, the decline length reduces and vice versa. This is also supported by Mohammed (2005). Therefore, the deeper the depth of the ore body, the more will be the decline length.

$$L = z\sqrt{1+\frac{1}{m^2}} \qquad [m] \qquad 2.4$$

Where:

L is the Euclidean Length

m is the decline gradient

z is the vertical displacement [m]

Although the gradient in Equation 2.4 varies from 1 in 9 and 1 in 7 for conventional mining the equation also applies for steeper gradients. Thus, if decline gradient is reduced below the conventional 1:7, the decline length will be shorter. Figure 2.15 shows results of recent studies on the effects of decline gradient on decline lengths (Chanda and Roberts, 2005).

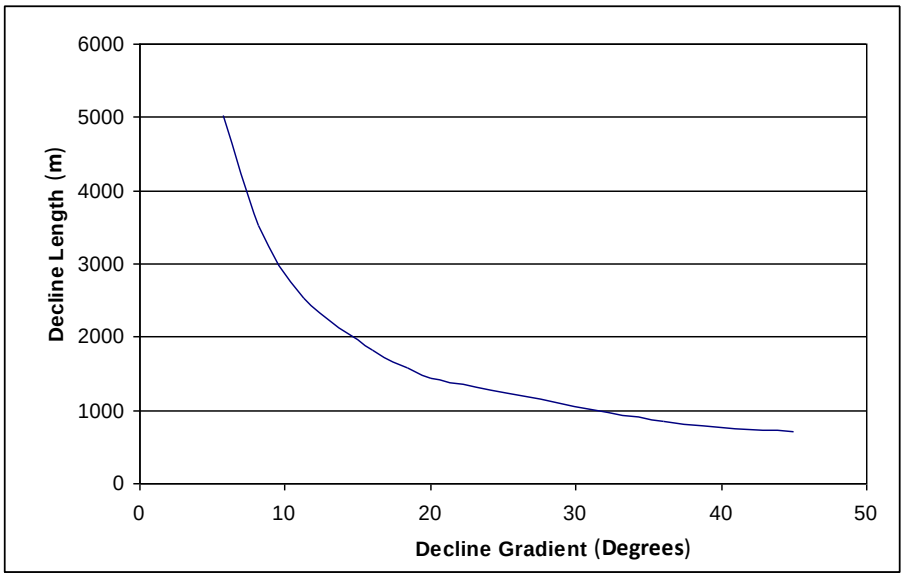

Figure 2.15: Effects of decline gradient on decline length (Chanda and Roberts, 2005)

Figure 2.15 shows that the decline gradient is inversely proportional to the decline length, i.e. an increase in decline gradient results in a reduction in decline length and vice versa. According to a study by Chanda and Roberts (2005) an increase in decline gradient from 1:7 (8^0) to 1:2.7 (20^0) resulted in 50% reduction in decline development meters.

(ii) Effects on duration of decline development

Duration of decline development is also inversely proportional with decline gradient. This means that, as the decline gradient is increased, the duration of decline development reduces and vice versa. Thus, if we let **X** be the average daily advance, the duration of development can be determined using Equation 2.5:

$$\text{Duration of development} = \left[\frac{Z\sqrt{1+\frac{1}{m^2}}}{\text{X}} \right] \qquad 2.5$$

A study conducted by Mohammed (2005) indicates that it would take 825 days to develop a decline to a depth of 700m with conventional 1:7 decline gradient at 6m advance per day. However, with a gradient of 1:2.7, it would take 451 days with the same advance rate. The study therefore shows that there is a reduction of almost 50% in decline development period with the reduction of decline gradient from 1:7 to 1:2.7.

(iii) Effects on development cost

The cost of decline development is also directly related to the decline gradient. As indicated earlier, the steeper the decline gradient, the less the development meters required to reach the ore body and vice versa. It is reported (Brazil et al, 2003) that with steeper gradient, the development costs reduce because the decline length is reduced, thereby reducing the total development cost. Equation 2.6 (Brazil et al, 2003) confirms the reduction in development costs as the decline gradient is increased.

$$C_d = C_m\left[\text{z}\sqrt{1+\frac{1}{m^2}} \right] \qquad 2.6$$

Where:

C_d is the development cost

C_m is the decline development costs per meter

According to literature (Chanda and Roberts, 2005) development cost per meter for conventional decline development (5.5mW x 5.5mW) is approximately A$2200. At such cost, the results of their study showed that the longer the decline length (low decline gradient), the more development costs will be incurred as compared to steep decline gradient (Figure 2.16). The results also indicated that an increase in decline gradient from 1:7 to 1:2.7 resulted in more than 50% reduction in development costs.

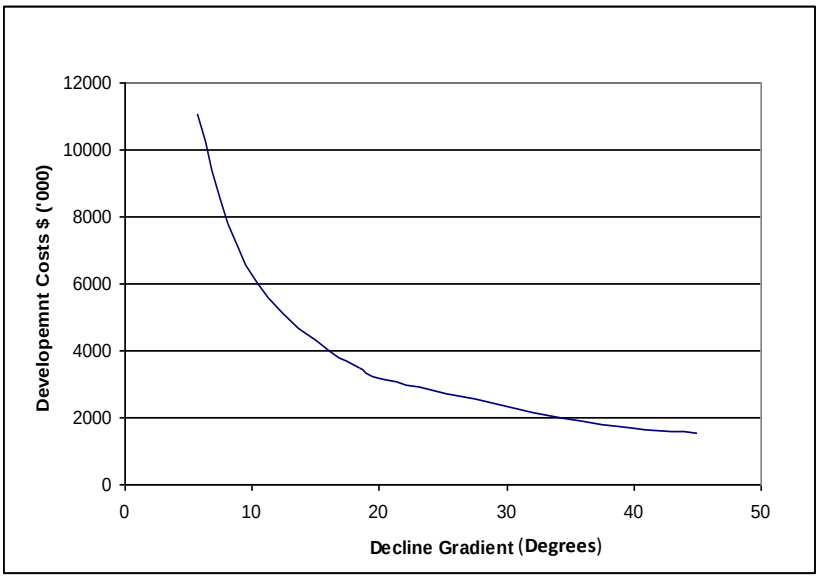

Figure 2.16: Relationship between decline gradient and development costs (Chanda and Roberts, 2005)

(c) Effects of turning radius

The effects of the turning radius can be illustrated by calculating the arc length ***AB*** using Figure 2.17.

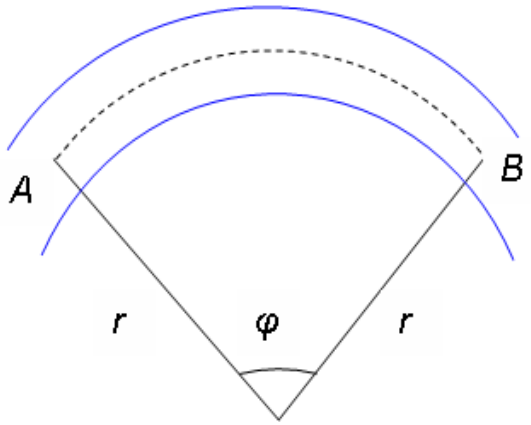

Figure 2.17: Relationship between turning radius and curve length

In Figure 2.17, considering ***AB*** as the curve length with turning radius ***r***, the distance between ***A*** and ***B*** is found using Equation 2.7.

$$C = \frac{\varphi}{180}\pi r \qquad \text{[m]} \qquad 2.7$$

Where:

C is the curve length	[m]
r is the curve radius	[m]
φ angle formed by arc **AB**	[degrees]

From Equation 2.7, it can be seen that the larger the turning radius ***r***, the longer will be the curve length. In Australian underground mines, a turning radius of 15 – 20m is adopted for decline access. This means curve lengths in conventional decline development are excessively longer compared with a monorail system which can negotiate curve radius of up to 4m.

2.3.2.3 Productivity in conventional decline development

Productivity in conventional decline development involves the following unit operations:

- Drilling and blasting;
- Waste removal from the face to stockpile area; and
- Loading and transport of waste from stockpile area to the surface.

(a) Drilling and blasting

Table 2.1 shows the drilling and blasting cycle time according to the studies conducted in Western Australia (Leppkes, 2005):

Table 2.1: Drilling and blasting cycle times

No	Unit operation	Cycle time (Minutes)
1	Drill face - using twin boom jumbo (48 face holes and 32 support holes @ 4 min per hole)	320
2	Charging the face	39
3	Other activities (e.g. mark face, tie blast, evacuate blast area, evacuate blast fumes etc)	114
	Total Cycle time	**473**

According to Leppkes (2005), in competent ground surface, ground support with a wire mesh is only required by statutory regulations in Western Australia where the height of the face exceed 3.5m. Therefore, since the development face studied by Leppkes was 3m x 3m in competent ground surface, no time to install wire mesh was allowed as indicated in Table 2.1. However, where the height of the decline exceeds 3.5 metres, as later indicated, the time to install support would be included in the mining cycle.

(b) Waste removal from the face to stockpile area

In conventional decline development LHD units are used for waste removal at face in combination with Front End Loaders (FELs). Cycle time at the face involves loading muck from the development face into LHD units and transporting the waste material to a stockpile area at another level. When all the muck pile is removed, face drilling commences. According to studies by Leppkes (2005) the cycle time to load one truck ranged from 3.6 minutes to 6 minutes.

However, to load and transport muck from a 3.7m cut to the stockpile area was estimated to take 78 minutes (1.3 hours).

(c) Waste removal from stockpile area to the surface.

When all muck is removed from the face, stockpiled muck is then loaded into 32.4 tonne payload trucks and transported to the surface. Table 2.2 shows an example of cycle times to transport muck from the stockpile area to the surface according to Leppkes (2005):

Table 2.2: Truck cycle time to move waste from stockpile area to surface

No	Unit operation	Cycle time (Minutes)
1	Loading time	6
2	Travel time (loaded) – 2000 m @ 6.8 km/h	17.64
3	Dump time	1
4	Travel time (Unloaded) - 2000 m @ 23 km/h	5.22
	Total Cycle time	**29.86**

According to Leppkes (2005) a 3m wide by 3m high by 3.7m long cut produces a muck pile of 33.3 Bank Cubic Metre (BCM) of material or 93.2 tonnes at Specific Gravity (SG) of 2.8. Therefore, with a 32.4 tonne payload truck and 29.9 min/cycle, the total cycle time to load and transport 93.2 tonnes from the stockpile to the surface in conventional truck haulage system takes approximately 90 minutes (1.5 hours) for a 2000m spiral decline length. Therefore, the total cycle time to load muck from face to surface with stockpiling in a 3.7m cut is 168 minutes (2.8 hours) as shown in Table 2.3:

Table 2.3: Total load-haul cycle time with stockpiling

No	Unit operation	Cycle time (Minutes)
1	Total cycle time to load and transport muck to stockpile area.	78
2	Total cycle time to load and transport muck from stockpile to surface	90
	Total Cycle Time	**168**

(d) Truck productivity versus decline length

Decline access is normally attractive for shallow ore bodies. However, as the depth of mining operations increases, productivity of trucks decreases. McCarthy and Livingstone (1993) simulated the productivity of 50 tonne and 40 tonne trucks and the results of their modelling showed that productivity of trucks reduces as the depth of mining increases (Figure 2.18). The decrease in truck production is attributed to long cycle times trucks have to make due to increase in decline length.

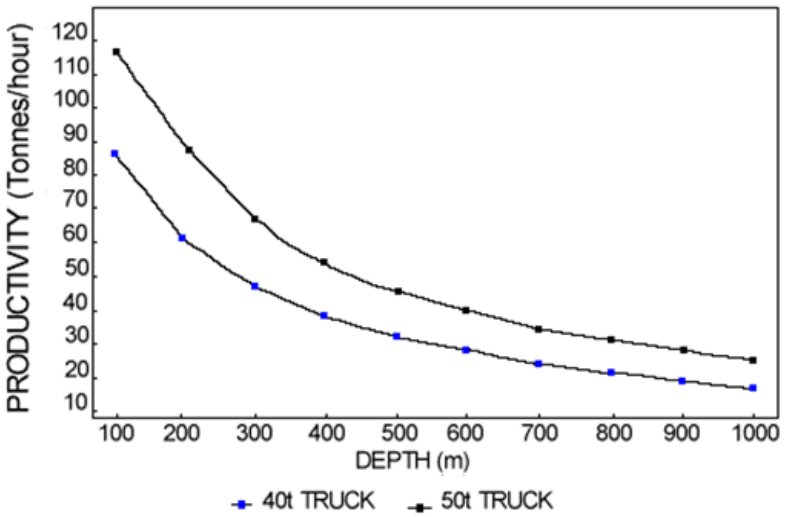

Figure 2.18: Relationship between productivity of trucks and depth of mining (McCarthy and Livingstone, 1993)

According to studies (Leppkes, 2005) on truck cycle times conducted in Western Australia where a 32.4 payload Hitachi 400D trucks was loaded with Elphinstone R1700G, two trucks were required to develop a decline up to a vertical depth of 377m and three trucks thereafter. This confirms results by McCarthy and Livingstone (2005) that productivity of trucks reduces with increase in mining depths. It is a well known fact that the LHDs in decline development have limitations which include the need for dump bays, not effective over distances exceeding 100m, soft floors, confined to certain gradients and the need for constant road maintenance.

2.3.2.4 Costs in conventional decline development

Generally, mining costs are governed by the ratio of excavated tonnes of ore to tonnes of excavated waste including waste resulting from capital development. With respect to the recent liberal use of decline as mine access, the ratio of capital waste development tonnes to mined ore tonnes has been excessive especially in narrow vein, high grade small deposits (Brazil et al, 2003). In conventional decline access development costs are categorised in two types i.e. capital costs and operating costs for LHD trucks.

(a) Capital Costs

Capital costs for conventional decline development involves purchase of LHD trucks as well as boggers / loaders. According to literature (Leppkes, 2005) the cost of an underground Hitachi AH400D truck is A$720,000.

(b) Operating costs

Operating costs associated with operations of a 32.4 tonne payload Hitachi AH400-D truck commonly used in conventional decline development are summarised in Tables 2.4

Table 2.4: Operating costs for Hitachi AH400-D truck (Leppkes, 2005).

No.	Description	Operating costs (A$/h)
1	Maintenance parts	13.36
2	Fuel	21.00
3	Tyres	7.74
4	Maintenance labour	6.14
5	Oil and Lubricants	0.94
	Total	49.18

2.3.3 Application of monorail technology in decline development

Application of monorail technology in decline development requires changes to design parameters of the decline access. This section, therefore, reviews literature as it relates to design parameters of the decline access with monorail system application.

2.3.3.1 Decline design parameters

(a) Size of decline

The monorail system is designed to operate on declines of cross-sectional area less than the 5.5mW x 5.5mH used in conventional decline development. According to manufacturers of monorail train (Scharf, 2007), the monorail system has dimensions 1.1mW x 1.3mH but considering safety and ventilation requirements of the decline access, decline dimension of 3mW x 3mH is suggested by Scharf as being suitable for monorail system application (Figure 2.19). For two monorail trains, decline dimension of 3.8mW x 3.0mH is recommended.

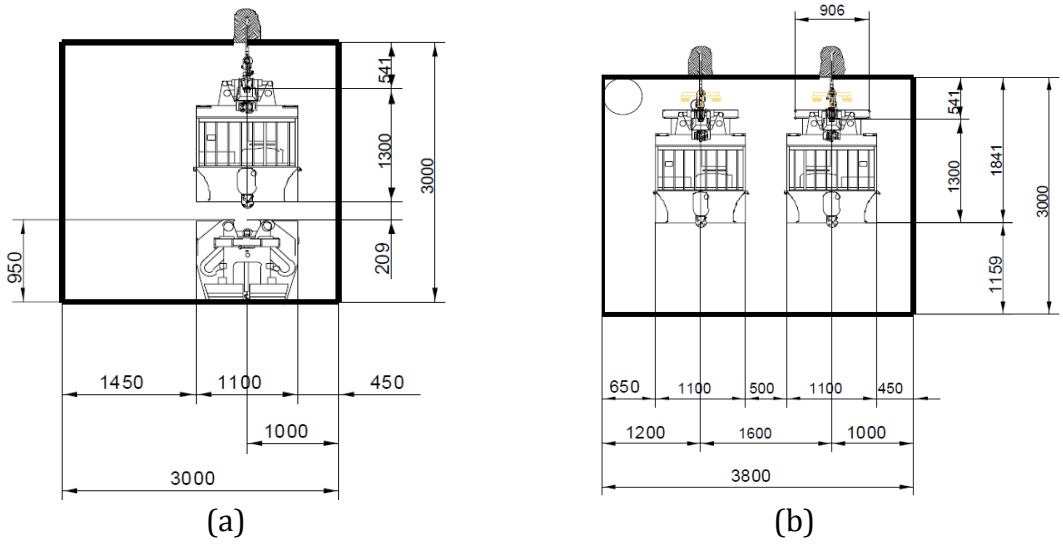

Figure 2.19: Decline opening requirements (a) one monorail train (b) two monorail trains (Scharf, 2007)

Therefore, the smaller decline dimensions with monorail system application reduces the need for costly ground support – an important measure for health and safety of mine workers and for energy savings – reduces ventilation requirements. Generally, the implication of smaller cross-sectional area of decline access is that considerable savings can be made in underground development.

(b) Decline gradient

Decline access for monorail system application is developed at a steeper gradient than 1:7 (8^0) used in conventional decline development since the system has the ability to negotiate steeper gradients. It is reported (Chanda and Roberts, 2005) that monorail train can negotiate gradients up to 36^0 when specially installed rack and pinion drives are used. At such gradient, it is reported (Meyer, 2007) that the monorail speed can go up to 12.5km/h with a load of up to 30 tonnes.

(c) Turning radius consideration

Design of vertical and horizontal radius for monorail application is also of paramount importance in decline development. Horizontal curves with a minimum radius of 4m as well as vertical curves of 10m can easily be negotiated by the monorail train of width 1.1m and length 3.7m. Networks can also be built up using manually or pneumatically operated rail switches. However, calculations for turning radius (***r***) for monorail cars with varying dimensions can be done as outlined below using Figure 2.20 (Oguz and Stefanko, 1971).

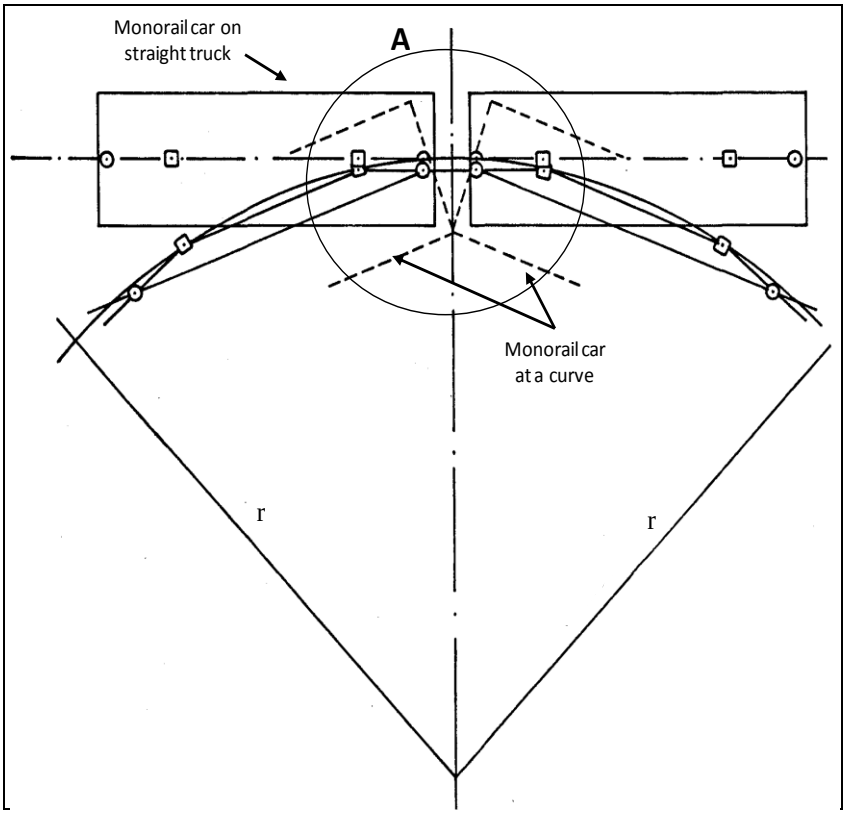

(a)

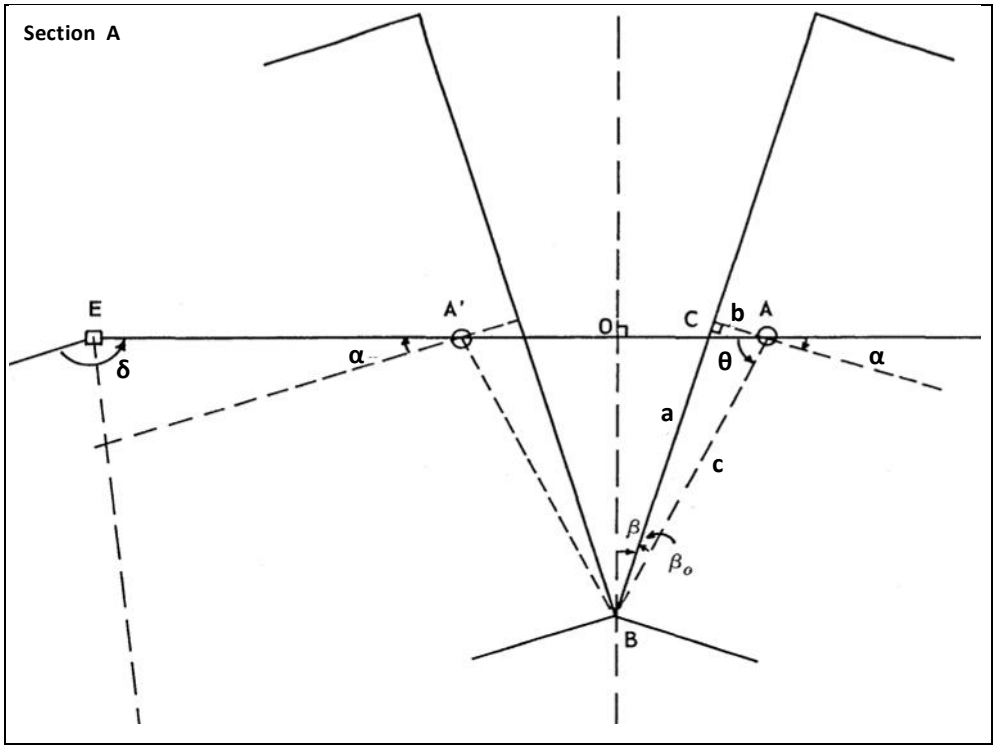

(b)

Figure 2.20: Solution to the minimum required curve radius (Oguz and Stefanko, 1971)

According to Figure 2.20, the minimum turning radius between two monorail cars can be determined using Equation 2.8 given the parameters below:

- Length of the car
- Width of the car
- Distance between cars (length of drawbars); and
- Distance from hanging point to the edge of the car (shown as ***b*** in Figure 2.20).

$$r = \frac{EO}{Cos\left(\frac{\delta}{2}\right)} \qquad 2.8$$

This means at turning radius ***r***, the monorail cars will just touch on a curve. Therefore, to be on the safe side, any curve for the monorail system should be more than ***r***. As reported by Oguz and Stefanko (1971) a turning radius less than 4m develops unnecessary stresses on the truck beam and on the rollers, causing excessive wear on the track and damage to the roller bearings.

2.3.3.2 Effects of designed parameters on decline development

Decline design parameters for monorail system application have effects on decline development. Table 2.5 summarises the effects of the parameters and the benefits resulting from their use.

Table 2.5: Effects of monorail design parameters

No	Design Parameter	Effects	Benefits
1	Decline dimension (small cross-sectional area)	• Less waste to be drilled and blasted; • Less waste to be transported; • Less ground support needed	• Less development costs • Less ventilation costs
2	Decline gradient (steep gradients)	• Have an effect of reducing decline length.	• Faster developments; • Less development costs • Less waste to be transported;
3	Turning radius (Small radius)	• Have an effect of reducing decline length.	• Faster developments; • Less development costs • Less waste to be transported.

2.3.3.3 Monorail system productivity

The rock loading subsystem is a critical component of monorail haulage. Loading is part of the mining cycle that involves the following activities:

- Drill and blast; and
- Removal of rock from face.

However, the cycle times of the drill and blast operation are dependent on the efficiency of the mucking and transport system. A fully installed underground monorail system in decline development consists of the following unit operations:

- Loading of monorail containers with Front End Loader (FEL); and
- Transport of material to the surface by monorail train.

(a) Monorail system productivity with FEL

Productivity of the monorail system with FEL at a workface consists of a loader (Side Dump Loader) that loads material from the face directly into monorail containers. Therefore, the cycle time for the loader is the total time to load all 6 containers of the monorail train. According to the study done by Leppkes (2005) it was estimated that it takes 33 minutes to load all 6 monorail containers of 6 tonne capacity using a FEL. This was based on monorail containers located 20m from the face.

(b) Transport of material to the surface by monorail train

Once all the monorail containers are loaded, they are lifted up by the lifting beam of the monorail train and transported to surface. The cycle time for the monorail system therefore, involves lifting of containers and transporting muck from the development face to the surface. Table 2.6 shows the cycle times for loading and hauling muck using a monorail system for a 3.7m cut development face.

Table 2.6: Cycle time for loading and hauling using a monorail

No	Unit operation	Cycle time (Minutes)
1	Loading time	33
2	Travel time (loaded) – 2000 m @ 6.5 km/h	18.46
3	Dump time (1 minute / container)	6
4	Travel time (Unloaded) - 2000 m @ 12.6 km/h	9.52
	Total Cycle time	**66.98**

Therefore, with 93.2 tonne material from the 3.7m box cut, it would take 208 minutes (3.5 hours) to clean the face with monorail system of payload 30 tonnes.

2.3.3.4 Monorail system costs

The costs associated with operations of the monorail system are classified into two:

- Capital costs; and
- Operating costs.

(a) Capital Costs

Capital costs for monorail system operations consist of purchase and installation of a monorail train in the decline. Table 2.7 shows capital costs, for the purchase of a monorail train with two drive cabins, four drive units and six lifting beams and containers with a payload of 30 tonnes (Meyer, 2007). Table 2.8 shows the capital costs for monorail installation per meter.

Table 2.7: Capital costs for purchase of monorail train (Meyer, 2008)

No.	Unit	A$	Comments
1	Monorail Train	1,200,000	Price by Scharf
2	Containers	16,000	Price by Scharf
3	Monorail Tools	25,000	Price by Scharf
4	Shunting Trolley	49,000	Price by Scharf
5	Dispenser (For roof bolt installation)	26,000	Price by Hilti
	Total	**1,316,000**	

Table 2.8: Capital costs for monorail train installation (Meyer, 2008)

No.	Unit	A$/m	Comments
1	Rail component	125.00	Price by Scharf
2	Electrical Components	250.00	Price by Scharf
3	Bolts (2 bolts / 3m section)	72.00	Price by Hilti
4	Rail Suspension components	75	Price by Scharf
5	Labour	51.04	Estimated
6	Jumbo Drill (for roof bolt installation)	4.45	Estimated
	Total	**577.49**	

(b) Operating costs

Table 2.9 shows operating costs for the monorail train. The installed power on the train is 232kW.

Table 2.9: Operating costs for Monorail train

No.	Description	Operating costs (A$/h)
1	Maintenance parts	12.00
2	Power	34.40
3	Maintenance labour	2.59
	Total	48.99

2.3.3.5 Power requirements for monorail system operations

Monorail trains are controlled from the driver's cabin at either end of the train. Each monorail train has a power pack equipped with 2 x 29 kW electric motors providing a total of 58 kW power to each drive unit. The monorail trains are controlled by frequency converters and PLC, coupled to the drive wheels through gears to control the speed of the train. When the train is braking (e.g. while travelling downhill) the EMTS is working in a generating mode. That means the braking forces are not wasted by creating heat but they generate electrical power which is fed back into the power supply system. The average saving by generating electrical power is approximately 30% of the electrical power needed

for the operation of the trains. The special design feature of the frequency converters allows such a cost saving mode of operation. There are also emergency and parking brakes and a twin 3-phase AC power pick-up. Up to four drive units are implemented into one monorail train for more traction forces. Therefore, the total power installed on one monorail train is 232kW.

(a) Monorail power consumption

A single monorail train with 232kW of installed power requires a transformer with a minimum capacity of 167kVA every 800m although a 200kV transformer is selected for a single monorail (World Mining Equipment, 1996). According to Leppkes (2005) power alone contributes to 70% of total operating costs (Table 2.9) based on power costs of A$0.29 per kWh using site based diesel power generators. Table 2.10 shows power consumption for the monorail train.

Table 2.10: Power consumption for Monorail train (Leppkes, 2005)

Description	Units	Value	Comments
Installed Power	kW	232	4 drives @ 58kW per drive.
Power Required	kWhrs	170.1	40 minutes per hour full load and 20 minutes per hour 20% of load
Power saved (in generating mode)	kWhrs	51.6	30% of full load power recovered
Power Required	kWhrs	118.6	Power Required minus power saved

Leppkes assumed that for 40 minutes in an hour, power would be consumed at the full installed power and for 20 minutes in the hour, 20% of installed power would be consumed. He also assumed that one third of the full load power consumed would be saved when the train is operating in generating mode. Therefore, the total power consumption for four drive units is 118.6kWh (or 29.65kWh for each drive unit). The results by Leppkes (2005) coincided with results obtained by Oguz and Stefanko (1971) who obtained a power consumption of 30kWh per drive unit during their study of monorail train.

(b) Effects of power on monorail operating costs

Cost of power has the effect of increasing or decreasing operating costs of monorail train depending on its cost per kWh. Figure 2.21 shows that the operating costs are directly proportional to the cost of power (Leppkes, 2005).

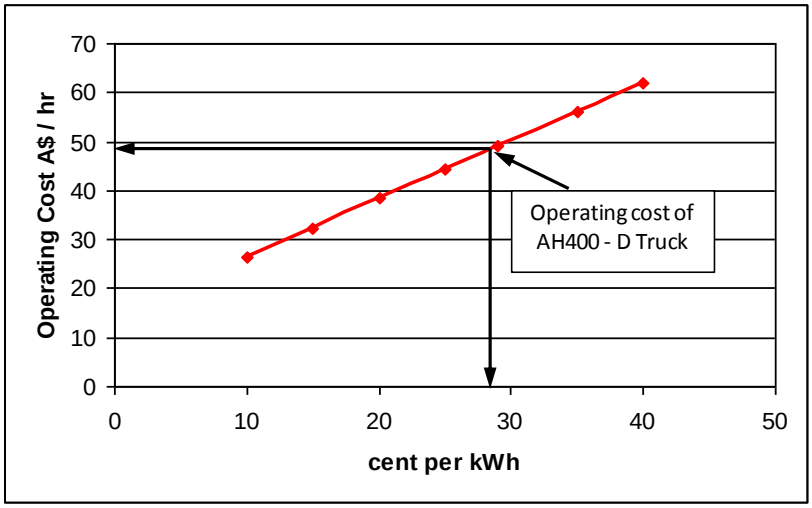

Figure 2.21: Effects of power on operating costs (Leppkes, 2005).

(c) Effects of monorail speed on power consumption

According to the study (Oguz and Stefanko, 1971) acceleration and speed of the monorail train affects power consumption (Figure 2.22 and 2.23). According to their results, power demand for empty run was higher than for the loaded run because of the higher travel speed of the former.

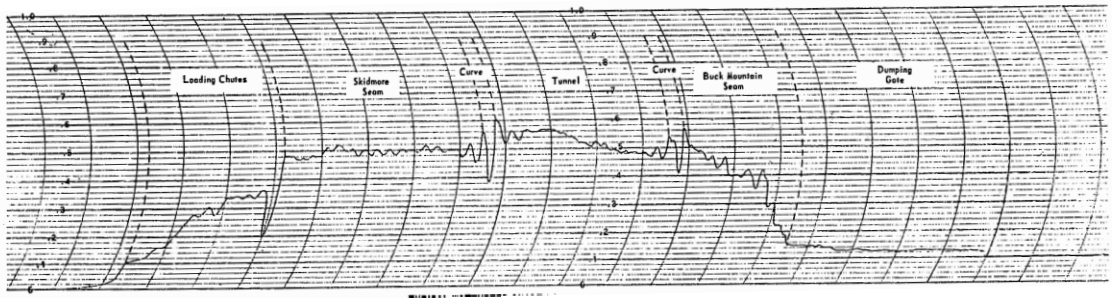

Figure 2.22: Wattmeter chart for empty trip at faster monorail speed (Oguz and Stefanko, 1971)

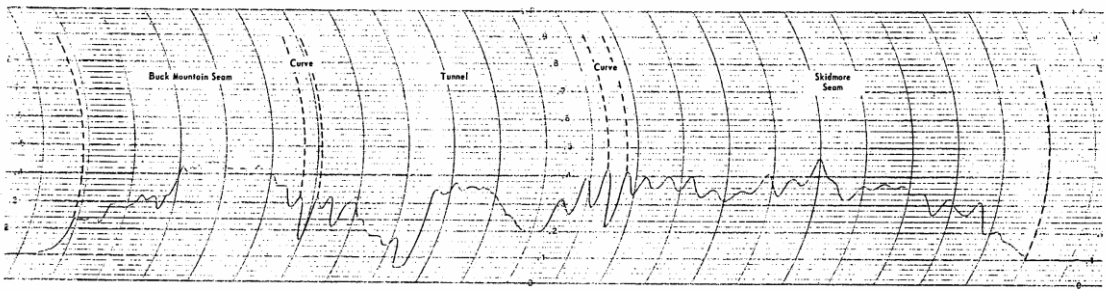

Figure 2.23: Wattmeter chart for loaded trip at slow monorail speed (Oguz and Stefanko, 1971)

2.3.4 Conventional versus monorail system decline development

A comparison between conventional (truck) haulage method and monorail haulage system was done. This section presents the results of the comparisons.

Literature has revealed that to reach the ore body in conventional decline development, significant amount of waste material is excavated. However, with monorail application less amount of waste material would be extracted due to smaller size of the decline opening and steeper gradient, reducing both the development costs and the duration of development. It is also evident that decline gradient and turning radius play an important role in reducing the decline length. Therefore, with monorail application there is significant reduction in development meters and ore bodies will be accessed more quickly and cheaply.

Monorail system productivity is greatly affected by the loading mechanism. According to literature, it takes longer time to load monorail containers when compared to trucks and this increases monorail cycle times (Figure 2.24).

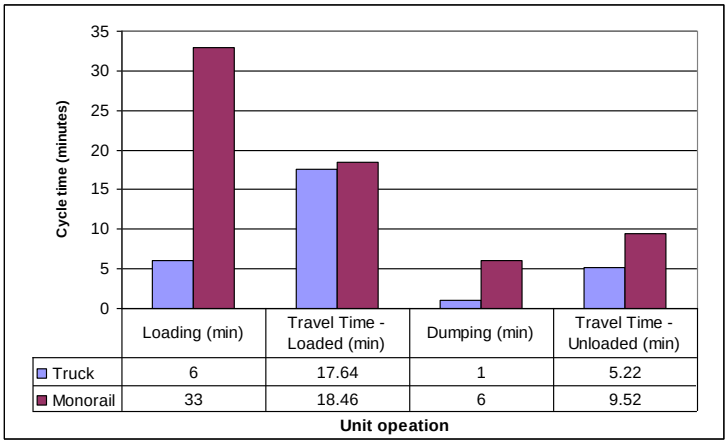

Figure 2.24: Graph showing cycle times for monorail and truck haulage systems.

However, significant reduction in cycle times will be achieved if the monorail system is loaded with some continuous loading system. The system will make monorail system cycle times comparable with conventional LHD truck techniques whilst eliminating the need for stockpiling. Capital cost for monorail is significantly higher than for a similar payload truck (Figure 2.25). However, the higher capital costs of monorail system will be overshadowed by the huge saving resulting from decline development.

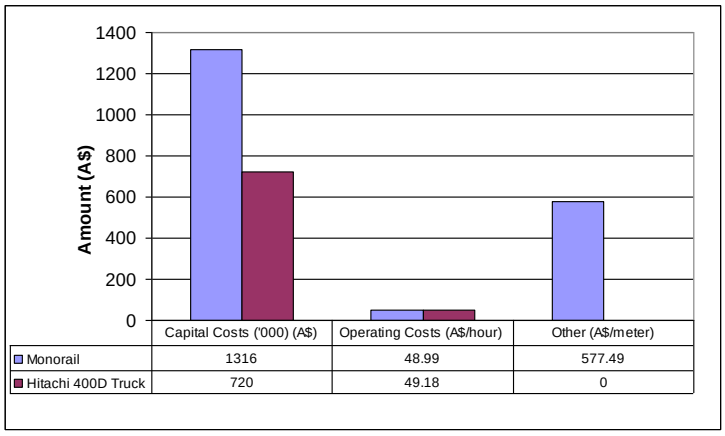

Figure 2.25: Capital and operating costs for monorail and truck haulage systems.

Although power consumption is critical in monorail system operations, operating cost of the monorail system was estimated to be the same as a similar payload underground truck i.e. A$49 per hour. Operating cost for monorail

system would be less than a similar payload truck if the cost of power was significantly reduced. Mining operations using monorail system have proved to be very cost-effective in most major mining countries of the world (Leppkes, 2004).

2.3.5 Monorail system productivity with continuous system

From the reviewed literature, it has been determined that loading time is the main drawback to high advance rates in monorail application. Therefore, to improve advance rates the monorail system should be loaded by some continuous system that will quickly remove the rock from the face onto the monorail containers. According to literature, the cycle time for the development of a decline using monorail system without stockpiling was greater than using conventional LHD and truck in combination with stockpiles. The increase in cycle time for monorail system resulted from the inefficiency of the loader and the number of cycles the loader had to make to fill the monorail containers. The proposed new concept requires an independent drilling unit with its own power supply attached to the monorail train. A pneumatic suction unit that uses monorail technology could load the blasted material into monorail containers via the hopper. The concept is illustrated in Figure 2.26.

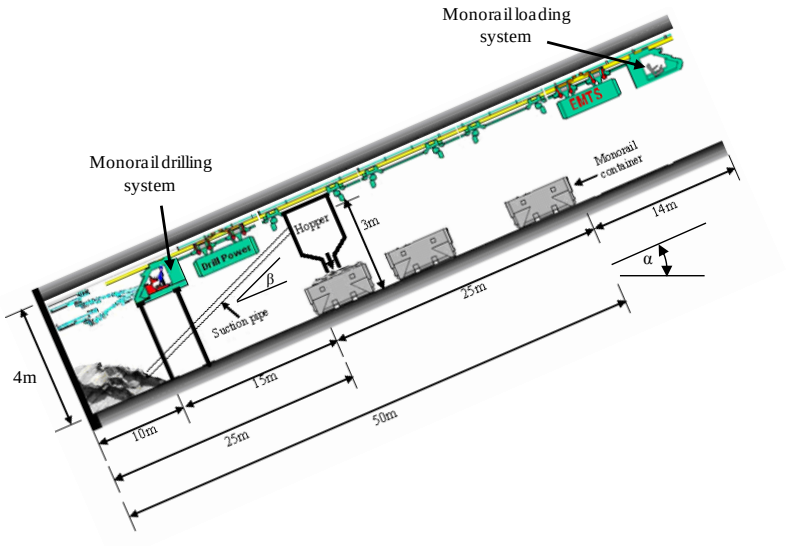

Figure 2.26: Proposed configuration of the monorail drill-blast-load-haul system

The concept would allow part of the face to be drilled while blasted material is being loaded into the monorail containers using pneumatic loading system. When the containers are full they will be transported on surface by the monorail train. However, the drilling unit would continue drilling the top part of the face whilst waiting for the monorail train which is powered by another motor to return from surface.

2.4 Summary

The reviewed literature shows that the current method of accessing ore bodies by conventional decline method has proved to be expensive. It suggests that more waste material is being extracted because of the size of decline openings adopted. The conventional 1:7 decline gradient and turning radius of 20m makes the decline excessively longer whereas at steeper gradients and small turning radius, decline lengths will be reduced and ore bodies will be accessed more cheaply and quickly.

It is also evident that the monorail system offers an alternative to truck haulage system at reduced costs. However, the rock loading system is a critical component of monorail system haulage. The cycle time of the drill and blast operation is dependent on the efficiency of the mucking and transport system. In monorail system operations, the loading time is the main drawback to high advance rates.

It is therefore suggested that the monorail system be loaded by some continuous system that will quickly remove the rock from the face onto the monorail containers. The proposed system offers fundamental reduction in capital expenditure and significant savings in mine operating costs. Therefore, in the next chapter extensive literature regarding pneumatic conveying system is presented. The literature will be used during the design of a pneumatic loading system that uses monorail technology.

Chapter 3

3.0 Pneumatic conveying system

3.1 Introduction

A continuous monorail loading system is fundamental in improving advance rates in decline development. In the previous chapter, it was revealed that to improve advance rates in decline development, the monorail system should be loaded by some continuous system that quickly removes blasted rock fragments from the development face onto the monorail containers. The proposed monorail loading system uses pneumatic (vacuum) conveying system to suck blasted rock fragments (via inclined suction pipe) into the hopper. Thus, the design of the system involves an analysis of application of fluid flow. Although the classic hydraulic principles apply, the monorail pneumatic loading system is complicated since suction involves solids which make significant changes in the rheological or flow characteristics of the liquid. Therefore, in order to gain an understanding of the flow phenomenon in different sections of pneumatic conveying system and how different research addressed these issues a detailed literature survey is done on the gas-solids flow in a pipeline. This Chapter therefore reviews literature regarding pneumatic conveying system.

3.2 Pneumatics and its applications

Pneumatics comes from the Greek word "*Pneumatikos"* which means coming from the wind. It is a branch of physics dealing with systems that use pressurized gas, especially air, as a power source. It was first successfully used in 1860s for transporting lightweight material such as wood shavings, sawdust and waste papers. The technology of pneumatic transport has steadily improved

and found increasing use in the last 150 years. Currently, the applications of pneumatic conveying systems can be seen in many industrial sectors such as transportation of pulverised and crushed Run-Of-Mine (ROM) coal through pipelines (Wypych et al 1990; Kerttu 1985). Pneumatic conveying is also used at harbours, barge terminals and rail terminals for loading and unloading bulky material such as grain, cement, fertilisers etc. Other applications include chemical process industry, pharmaceutical industry, mining industry, agricultural industry etc. Pneumatic transport system also finds wide application in dredging of sand and other sea-bottom materials (Herbich, 2000). According to Ratnayake (2005) a list of more than 380 different products have been successfully conveyed pneumatically including very fine powders, as well as big crystals such as quartz rock of size 80 mm.

3.3 Pneumatic conveying system

Pneumatic conveying system is the use of air or another gas to transport powdered or granular solids through pipes (Kraus 1980). This is a counterpart of slurry pipeline, using a gas instead of a liquid as the medium to transport solids. Thus using either positive or negative pressure of air or other gases, the material to be transported is forced through pipes and finally separated from the carrier gas and deposited at the desired destination. Because of high intensity of pneumatic transport and the abrasion (wear) of material transported, such pipelines are for transport over short distances only, usually less than 1km although most often only a few hundred meters or shorter.

The following are some of the advantages of pneumatic conveying:

- Economical over short-distance transport of bulk material;
- Automatic and labour-saving;
- Avoid or minimise human contact with the material being transported, thus enhancing safety and security;
- Flexibility in routing; and
- Dust free conveying system.

3.3.1 Types of pneumatic conveying systems

Generally there are three types of pneumatic pipeline conveying systems i.e. negative-pressure (or suction) system, positive pressure system and combined (negative-positive pressure) system. In this study, only details of negative pressure system are discussed in detail since it is the system that is used in the design of monorail loading system.

Negative pressure systems are sometimes called the suction systems and they behave like a vacuum cleaner. With this method, the absolute gas pressure inside the system is lower than atmospheric pressure. The vacuum inside the hopper and the suction pipe is created by the prime mover (e.g. air pump) such that the solid-air mixture is sucked through the pipe and solids discharged into the hopper. Because the maximum pressure differential across a pipe and hopper that can be developed by suction system is always less than one atmospheric pressure, the suction can only be used for relatively short distances, normally not more than 30m (Liu 2003). According to Liu (2003) the smallest suction system is the vacuum cleaner while the largest suction systems are those used at Disney World in Orlando, Florida. The latter system consists of an underground network of pipes for collecting the trash from various buildings to a central station. Figure 3.1 shows the schematic configuration of the negative pressure system.

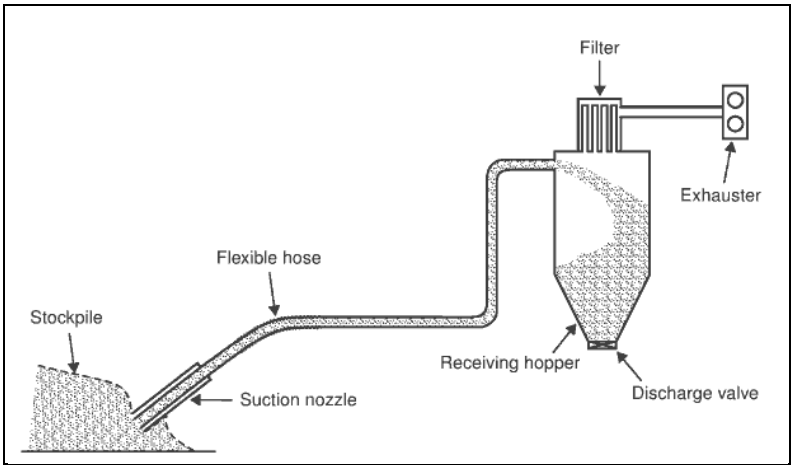

Figure 3.1: Vacuum conveying from open storage (Mills, 2004)

3.3.2 Components of pneumatic conveying system

A number of different components exist in a pneumatic conveying plant. A typical conveying system comprises different zones where distinct operations are carried out. In each of these zones, some specialised pieces of equipment are required for the successful operation of the plant. According to Klinzing et al (1997) typical modern pneumatic conveying system consists of the following major components:

(a) The prime mover

The prime mover is an essential element in pneumatic conveying system. A wide range of compressors, blowers, fans and vacuum pumps are used to provide the necessary energy to the conveying gas.

(b) Feeding, mixing and acceleration zone

This zone is considered critical in pneumatic conveying system. In this zone, the solids are introduced into the flowing gas stream. Because the solids are essentially at rest, large change in momentum occurs when solids are mixed with the flowing gases.

(c) The conveying zone

The conveying zone consists of a pipe to convey the solids from point A to point B over a certain distance. The selection of piping is based on a number of factors including the abrasiveness of the product, pressure required etc.

(d) Gas-solid separation zone

At the end of any negative or positive pneumatic conveying system, a separator is needed that separates the solids from the carrier gas or air in order to recover the solids transported. The selection of an adequate gas-solid separation system

is dependent upon a number of factors, the primary factor being the size of solids requiring to be separated from the gas stream.

3.3.3 Modes of pneumatic conveying

The pneumatic conveying of particulate solids is broadly classified into three flow regimes according to the concentration of solids in the pipeline i.e. according to the air mass flow ratio i.e. dilute, medium or dense phase. The classifications are indicated in Table 3.1. In this study, only two regimes i.e. dilute-phase and dense-phase will be discussed in detail.

Table 3.1: Classification of pneumatic conveying regimes

Description	**Solid loading ratio – m***
Dilute (lean) phase	m*<10
Medium phase	10<m*<50
Dense phase.	m*>50

(m*is the solid loading ratio - See Equation 5.3)

Several researchers have adopted m* as the basis of definition for dense and dilute phase conveyance e.g. Mason et al (1980) have suggested that dense phase conveyances normally operate with m* greater than 40 whilst Jones (1989) indicates that m* for dense phase is greater than 50. Wypych (1994) also revealed that m* of 20 is typical of dilute phase contrary to classification of pneumatic conveying regimes in Table 3.1.

Wypych and Arnold (1984) also suggests that the above forms of definitions are inadequate since m* is dependent upon the pipeline length for a given air mass flow rate (as highlighted by Mills et al., 1982). Thus, based on the above, it was assumed, in this study, that m* for dense phase conveyance is above 50 whilst for dilute / medium phase m* is less than 50. According to Jones (1989) dilute phase systems are the most common applicable method of broken rock conveyance in the mines. These methods are comparatively cheap to install and operate but

have relatively low productivity. Therefore, since dilute / medium phase has been proved and works well in suction of broken rock from the mines, it is adopted in this design.

3.3.3.1 Dilute phase transport

Rhodes (2001) described dilute phase transport system as a system which is characterised by high gas velocities (greater than 20m/s), low solid concentration (less than 1% by volume) and low pressure drop per unit length of transport line. With this method, the bulk material is carried by an air stream of sufficient velocity to entrain and re-entrain it for a distance depending on the available pressure. Under these dilute conditions, the solid particles behave independently fully suspended in the gas and fluid-particle forces dominate. Until quite recently, most pneumatic transport was done in dilute suspension using large volume of air at high velocity. Figure 3.2 shows an example of dilute phase transport of fines (Rhodes 2001)

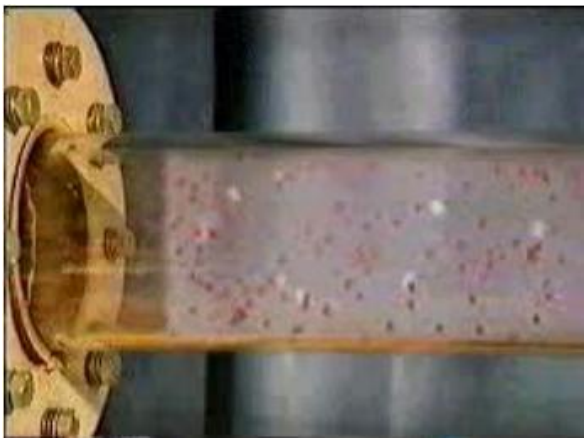

Figure 3.2: Dilute phase transport (Rhodes, 2001)

Dilute phase transport systems are comparatively cheap to install and operate, use low pressure compressed air and can be used over long distances. On the other hand their relatively high conveying velocities cause degradation (wear) of material and they are low tonnage systems.

3.3.3.2 Dense phase transport

Dense phase involves reduction of gas velocity such that bulk materials are transported in stratification mode with non-uniform concentration of solids over the pipe cross-section (Wypych and Arnold 1984). Thus with this method, the material is pushed through a pipeline as a plug which occupies the whole cross-section or as a moving bed for a pressure dependant distance. Thus in this method, particles in a pipeline are not fully suspended and there is much interaction between particles. Dense phase pneumatic transportation of bulk solids is continually gaining interest and popularity for a variety of industrial applications. Examples include coal-fired power stations, blast furnace injection, dry disposal of fly ash and the transportation of materials in the plug phase mode. The attraction of dense phase transport lies in its low air requirements meaning low energy requirement. Also according to Liu (2003) in dense phase conveyance, most of the pipe interior is filled with the solids to be transported or solid-to-air weight ratio is very high i.e. greater than 100.

3.3.4 Operations of pneumatic conveying system

Various flow regimes exist inside the pipeline in a pneumatic conveying system, spanning the entire range of conveying conditions from extrusion flow to fully dilute suspension flow. Through numerous experimental studies together with visual observations using glass tubes, etc., scientists have deduced these varieties of flow regimes. It has been seen that these different flow regimes could be explained easily in terms of variations of gas velocity, solids mass flow rate and system pressure drop. This clarification also explains the general operation of a pneumatic conveying system. Most research workers and industrial system designers have used a special graphical technique to explain the basic operation of a pneumatic conveying system.

This technique utilises the interaction of gas-solid experienced inside the conveying pipeline in terms of gas velocity, solids mass flow rate and pressure

gradient in pipe sections in a way of graphical presentation, which was initially introduced by Zenz and Othmer (1960) and Zenz (1964). Some researchers named this diagram 'pneumatic conveying characteristics curves', while others call them phase diagrams. The superficial air velocity and pressure gradient of the concerned pipe section are usually selected as the *x* and *y* axes of the diagram and a number of different curves are produced on this set of axes in terms of different mass flow rates of solids. There is a distinguishable difference between the relevant flow regimes for horizontal and vertical pipe sections. On the other hand, the particle size and particle size distribution also have influence on the flow patterns inside the pipelines.

3.3.4.1 Horizontal conveying

Figure 3.3 shows the typical horizontal phase diagram with various cross-sectional diagrams showing the state of possible flow patterns at different flow situations.

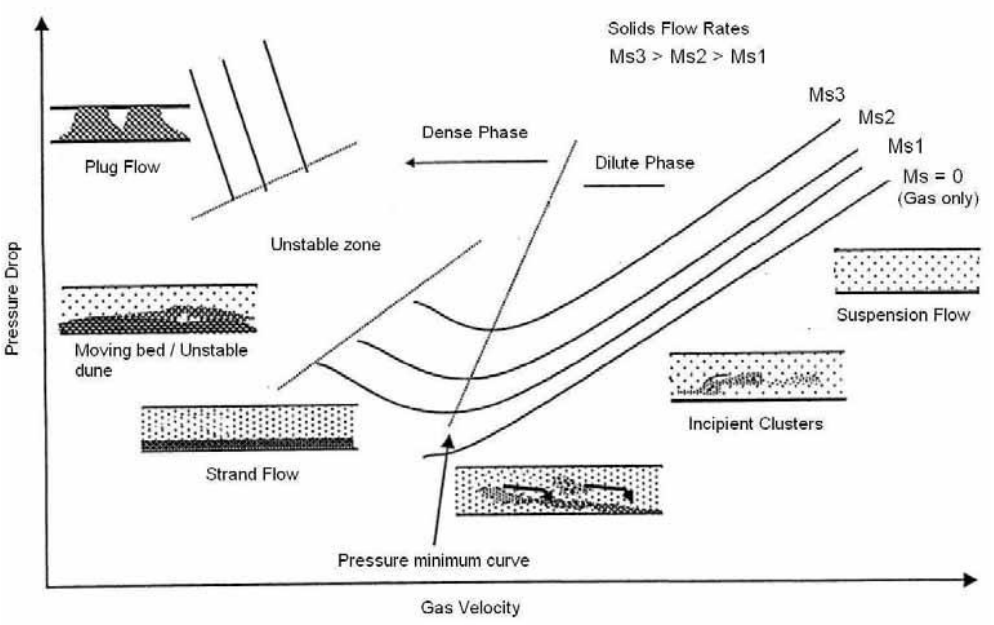

Figure 3.3: A typical conveying characteristic curves: horizontal flow (Ratnayake 2005)

The curves in Figure 3.3 show the variations of constant solids mass flow rate contours, when the conveying gas velocity and system pressure drop varies independently. The gas only line shows the pressure drop vs. gas velocity curve, which is characteristically a single phase flow. When the solids particles are introduced to the system with a particular solids mass flow value, the pressure drop increases to a higher value than in case of gas only transport even though the gas velocity is maintained constant. By keeping the solids flow rate constant and reducing the gas velocity further, pressure drop decreases down to a certain point where the minimum pressure drop is experienced. The pressure minimum curve connects such points for different solid flow rate values. Generally, the flow regimes up to this point from the right side could be categorized as the dilute phase flow with low values of mass loading ratios. Further reduction of gas velocity leads to particle deposition in pipe bottom and then the flow mode is called dense phase conveying. Pressure drop can be seen increasing, when gas velocity is decreasing. After an unstable flow region, the conveying pattern shows a plug flow characteristic, which will cause the pipeline to be totally blocked in attempts at further reduction of gas velocity.

The figure shows the different boundaries of the conveying characteristic curves. One boundary is the extreme right hand side limitation, which depends on the air volume flow capacity of the prime mover. The upper limit of the solid flow rate is influenced by the allowable pressure value of compressed air supply. The left-hand side boundary is fixed by the minimum conveying velocity, which will be discussed in detail later in this chapter.

3.3.4.2 Vertical Conveying

Figure 3.4 shows the typical vertical phase diagram with various cross-sectional diagrams showing the state of possible flow patterns at different flow situations. The orientation of the pipe has a considerable effect on the flow patterns and conveying regimes, because of the influence of gravity force. Consequently, the cross-sectional diagrams are totally different for the vertical pipe sections from those of horizontal sections, although the general appearances of the mass flow

rate contours are similar to each other. Figure 3.4 shows a typical phase diagram of a vertical pipe section, together with various cross-sectional diagrams showing the representative state of possible flow patterns at different flow situations.

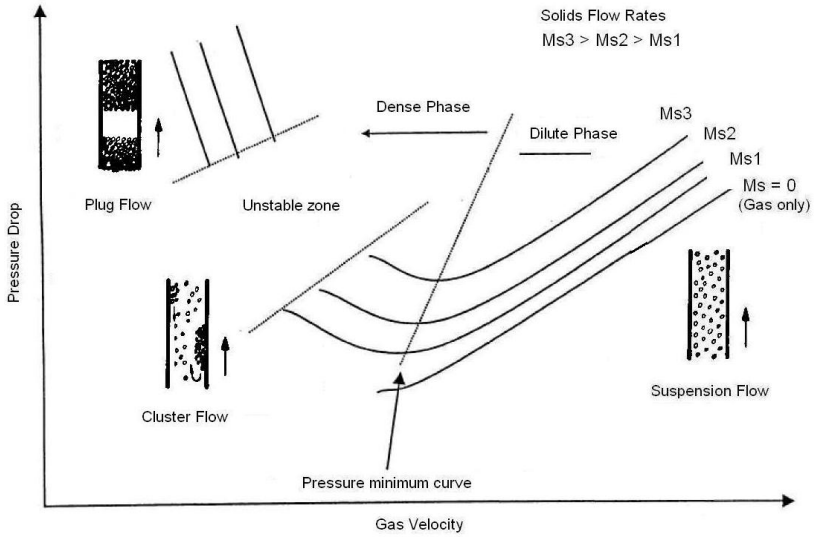

Figure 3.4: A typical conveying characteristic curves: vertical flow (Ratnayake, 2005).

3.4 Fundamentals of pneumatic (suction) principles

All pneumatic conveying systems, whether they are of the positive or negative pressure type, conveying continuously or in a batch-wise mode can be considered to consist of the basic elements i.e. feeding system, air and material pipeline (horizontal, vertical or inclined) and separation system (Figure 3.5)

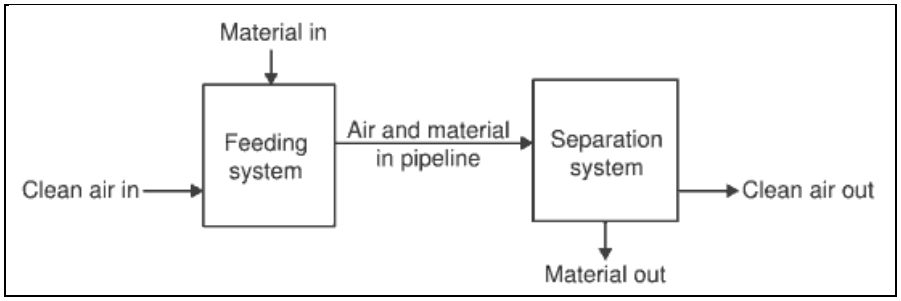

Figure 3.5: Elements of a pneumatic conveying system (Mills, 2004)

Therefore, in order to gain an understanding of the flow phenomenon in different sections of pneumatic conveying system, literature survey was done on the gas-solids flow in pipes. The review starts from the beginning of the conveying line and proceeds along the pipeline up to the end of transport line by considering different sections.

3.4.1 Feeding and entry section

Material feeding device is particularly critical to the successful operation of the pneumatic loading system. According to Klinzing and Dhodapkar (1993) the nature of the pressure fluctuation and smoothness of the flow are strongly dependent on the design of the feed section. According to their research, the feed section plays an important role in the development of flow pattern. Thus, the basic requirement of any feeding device is that the pressure loss across the device should be as low as possible in low pressure systems and as small a proportion of the total as possible in high pressure systems (Mills, 2004). Thus, if the feeder takes an unnecessary proportion of the total pressure drop from the air source, less pressure will be available for conveying the material from the pipeline.

In vacuum systems, the material feeding is invariably at atmospheric pressure and so the pipeline can either be fed directly from a supply hopper or by means of suction nozzles from a storage vessel or stockpile. In this case, there will be no adverse pressure gradient against which the material has to be fed. This means that there will be no leakage of air across the device when feeding material in the pipeline.

Usually, the feeding systems are classified on the basis of pressure limitations. In terms of commercially available feeding devices, it is convenient to classify feeders in three pressure ranges:

- Low pressure - maximum 100 kPa
- Medium pressure – maximum 300 kPa
- High pressure – maximum 1000 kPa

Below are commonly used feeding devices with their relevant pressure ranges:

- Rotary valves – low pressure
- Screw feeders – medium pressure
- Venturi feeder – low pressure (operate up to 20 kPa)
- Vacuum nozzle – negative pressure
- Blow tanks – high pressure

3.4.2 Pressure drop determination in pipes

Since the suction pipe for monorail loading system is inclined, this section presents literature on pressure loss determination through straight sections of an inclined pipe.

The accurate prediction of pressure drop is becoming an increasingly important requirement for many pneumatic conveying applications. According to Pan and Wypych (1992) to predict accurately the total pipeline air pressure drop in pneumatic conveying, an essential step involves the determination of pressure drop due to the solids-air flow in each straight section of pipe. In the literature, there is no lack of theoretical and empirical studies on the determination of the pressure drop across the pipe. However, most of these studies have their limitations. For example, a number of theoretical models are restricted to the dilute-phase conveying of coarse particles of relatively narrow size distribution (Yang, 1977; Tsuji, 1982). The usual assumption of pressure drop determination in gas-solid two-phase flow is correlated best when expressed as the sum of two functions (Morikawa et al, 1978; Bradley, 1989; Mills, 1990; Pan and Wypych, 1992; Pan and Wypych, 1997) as indicated in Equation 3.1.

$$\Delta p_t = \Delta p_a + \Delta p_s \qquad 3.1$$

Where:

Δp_t = is the total pressure drop in the suspension

Δp_a = is pressure drop due to gas (air-alone)

Δp_s = is pressure drop attributed to the solid particles

Determination of each of these components of pressure drop is considered separately and is presented in this section.

3.4.2.1 Air-alone pressure drop

Determination of the air-only pressure drop is straight forward in single phase flow. As a gas flows along a pipeline, the pressure resulting from the frictional resistance to the flow causes the gas to expand, i.e. the density of the gas decreases and consequently the average velocity of the gas across a section of the pipe must increase in the direction of the flow. Thus, using Darcy formula, the pressure drop in a gas of density ρ_a flowing along a pipeline of diameter D and length L is given as follows:

$$\Delta P_a = 4 f \frac{L}{D} \frac{\rho_a v_a^2}{2} \qquad 3.2$$

Where:

v_a = the average velocity of the flowing gas [m/s]

f = is the friction coefficient for the gas

D = Diameter of pipe [m]

L = Length of pipe [m]

ρ_a = density of air [kg/m^3]

The friction coefficient for the gas f can be determined as follows according to Blausius equation (for Re < 10^5):

$$f = \frac{0.316}{\mathrm{Re}^{0.25}} \qquad 3.3$$

Where Re is the Reynolds number determined as follows:

$$\mathrm{Re} = \frac{\rho v D}{\mu} \qquad 3.4$$

Where:

$\boldsymbol{\mu}$ is the viscosity of the fluid [kg·m^{-1}·s^{-1}]

Alternatively, the value of f can be calculated using Colebrook formula (Equation 3.5) or Moody Chart (Figure 3.6).

$$\frac{1}{\sqrt{f}} = -2 \cdot \log\left[\frac{e/D}{3.7} + \frac{2.51}{\mathrm{Re}\sqrt{f}}\right] \qquad 3.5$$

Where:

$\boldsymbol{e}$ is relative roughness of pipe [mm]

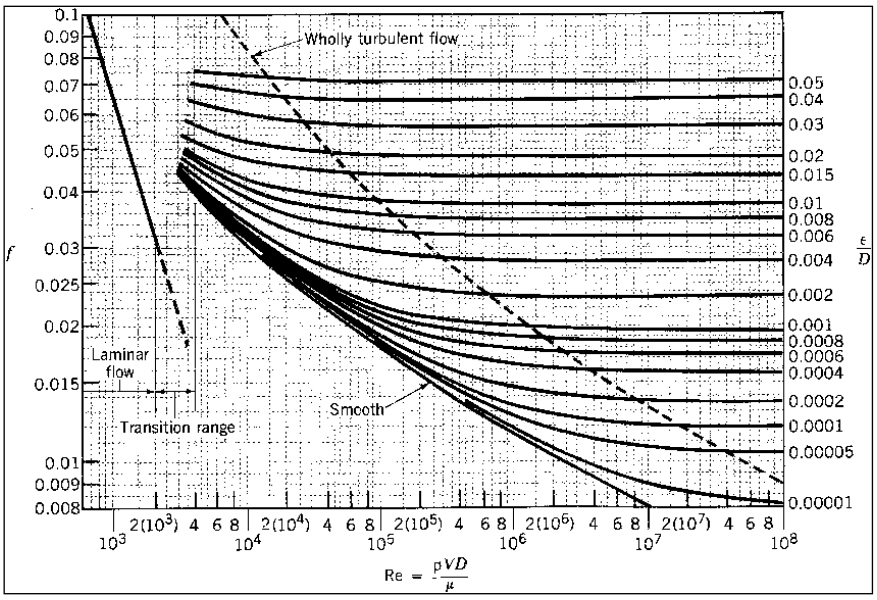

Figure 3.6: Moody Chart (Klinzing and Dhodapkar 1993)

The Koo equation can also be used to determine the friction coefficient f for the gas for turbulent flow as indicated below:

$$f = 0.0014 + \frac{0.125}{\mathrm{Re}^{0.32}} \qquad 3.6$$

For incompressible flow, the commonly used formulas are:

a) Laminar flow (i.e., 0 < Re < 2300)

$$\Delta \mathrm{P_a} = \lambda_a \rho_a v_a^2 \frac{\Delta \mathrm{L}}{2\mathrm{D}} \qquad 3.7$$

(Note the $\lambda_a = 4f$)

b) Turbulent flow i.e., *Re* > 2300 f is calculated as follows:

$$\lambda_a = \frac{1.325}{\left[\mathrm{In}\left(\frac{\varepsilon}{3.7\mathrm{D}} + \frac{5.74}{\mathrm{Re}^{0.9}}\right)\right]^2} \qquad 3.8$$

(For $10^{-6} \leq \frac{\varepsilon}{D} \leq 10^{-2}$ and $5 \times 10^3 \leq \mathrm{Re} \leq 10^8$ - as sited by Ratnayake, 2005)

Wypych and Pan (1991) modified Equations 3.3 and Equation 3.8 and proposed to replace the values of constants of Equation 3.8 by number of coefficient (i.e. $x_1 \ldots x_5$), which could be determined by minimising the sum of squared errors of pressures at different points on conveying line.

$$\lambda_a = \frac{x_1}{\left[\mathrm{In}\left(\frac{\varepsilon}{3.7\mathrm{D}} + \frac{x_2}{\mathrm{Re}^{x3}}\right)\right]^2} \qquad 3.9$$

$$f = \frac{x_4}{\mathrm{Re}^{x_5}} \qquad 3.10$$

Based on an empirical relationship, Klinzing et al (1997) proposed the following equation to calculate the pressure drop in straight pipe for compressed air pipe works.

$$\Delta P_a = 1.6\times10^{3} V^{1.85} \frac{L}{D^{5} P_1} \qquad 3.11$$

Where:

V = volumetric flow rate [m^3/s]

L = pipe length [m]

P_1 = Initial pressure [kPa]

To calculate the air only pressure drop in the pipeline, Wypych and Arnold (1984) proposed the following empirical formula.

$$\Delta P_a = 0.5 \left[\left(01^{2} + 0.004567 m_a^{1.85} L D^{-5} \right) \right] 101 \qquad 3.12$$

Where;

m_a = mass flow rate of air [m^3/s]

3.4.2.2 Pressure drop due to solids in straight inclined pipes

According to Pan and Wypych (1992) the pressure drop due to solids through a straight section of pipe can be considered as a function of many variables, such as superficial air velocity v_a, air density ρ_a, pipe diameter D, length ΔL, air viscosity μ_a, pipe roughness ε, product mass flow rate m_s, particle density ρ_S, mean particle diameter d_p, particle shape factor φ, friction coefficient between pipe wall and particle velocity v_s. Inclination of conveying pipe also affects the pressure during gas-solid fluid flow (Mills, 2004). For a given product and pipe material, it can be assumed that d_p, z, ρ_s and v_s are constant.

Although the possibility of the existence of a unique mathematical model to determine the pressure drop component due to the presence of dispersed solid

particles is very low, because of the complex nature of two-phase gas-solid flow in pipes, many correlating equations have been proposed by various authors in different publications. When the friction factor of gas-solid mixture is considered, the total pressure drop for horizontal pipes as presented by Pan and Wypych (1992) can be presented as below:

$$\Delta P_s = \mathrm{m}^* \lambda_s \frac{\rho_s \Delta \mathrm{L} v_s^2}{2D} \qquad 3.13$$

λ_s is the frictional factor of solid and can be calculated in horizontal pipes as follows as suggested by Pan and Wypych (1992).

$$\lambda_s = 2\mathrm{k}\left(\frac{\pi}{4}\right)\mathrm{Re}\left(\frac{\varepsilon}{D}\right)\left(\frac{\Delta \mathrm{L}}{D}\right) \qquad 3.14$$

Since Equation 3.14 is applicable for horizontal pipes, Aziz and Klinzing (1990) proposed the frictional approach for the inclined sections and used the following equation to determine the friction factor:

$$\lambda_s = \frac{D}{2v_s^2}\left[\frac{3C_D \varepsilon_s^{-4.7} \rho_a \left(v_s\right)^2}{4\left(\rho_s - \rho_a\right) d_p} - g\sin\theta\right] \qquad 3.15$$

Where:

θ is the inclination of the pipe.

Hirota et al. (2002) carried out an experimental investigation on inclined conveying of solids in high-dense and low-velocity. They found a linear relationship between Froude Number, Fr and friction factor of the gas-solid mixture, which can be presented in the following form.

$$\lambda_s = 2\left(\sin\theta + C_1 \mu_d \cos\theta\right)\frac{1}{\mathrm{Fr}} \qquad 3.16$$

Where:

μ_d = the dynamic internal friction factor

C_1 = a constant between 1 and 2 (1.5 is recommended).

In addition, they found that the pressure drop is maximum between 30°- 45° inclination angles as cited by Ratnayake (2005).

Pneumatic pressure loss in incline pipes for dense phase was also investigated by Kano (1985). Figure 3.7 (a) and (b) shows the basis for which the study was based. In the force pattern, a plug of length l_p slides successively on a stagnant bed of thickness h piled up at the bottom of an inclined pipe of thickness D .

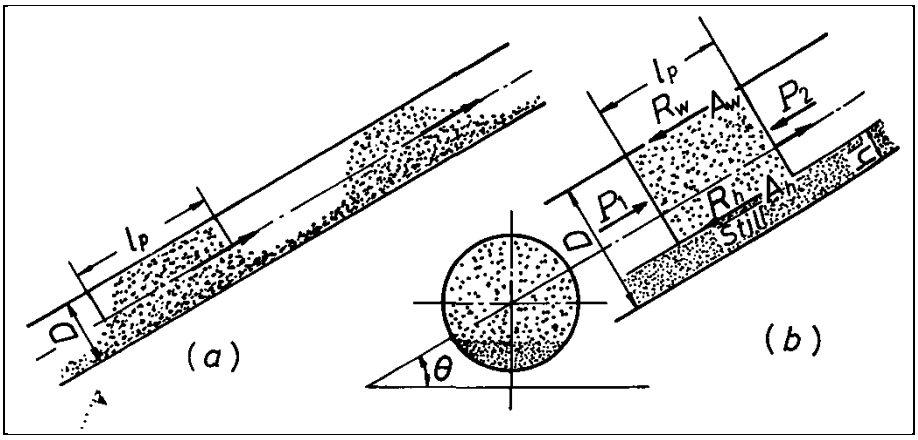

Figure 3.7: Schematic diagram of conveying incline pipe (a) dense pneumatic condition (b) acting forces (Kano, 1985)

The pressure at the front and back side of the plug are p_1 and p_2 respectively and their difference $\Delta p_p = p_1 - p_2$. Kano (1985) assumed balance of the forces acting at the plug in the flow direction, the pressure difference and related to the component of gravity $M_p.g.\sin\theta$, the wall friction resistance R_w and the frictional resistance R_h at the surface of the retarded bed as follows:

$$\Delta p_p \zeta_p A = M_p g \sin\theta + R_w + R_h \qquad 3.17$$

Where:

ζ_p is ratio of the cross sectional area of conveying plug to that of a pipe

M_p is mass of plug. [kg]

A is cross sectional area of pipe. [m^2]

The above parameters are calculated as indicated below:

$$M_p = \zeta_p A l_p \ell_b \qquad 3.18$$

Where:

ℓ_b is bulk density of the material in the plug.

$$R_w = \xi_w p_r A_w \qquad 3.19$$

Where:

ξ_w is a factor of wall friction; and

p_r is a normal pressure to the pipe wall.

$$R_h = \xi_i \left(M_p g \cos\theta + p_r A_h \right) \qquad 3.20$$

Where ξ_i is a factor of internal friction. A_h is the contact area between plug and retarder bed calculated as follows:

$$A_h = 2 l_p \sqrt{D - h\, h} \qquad 3.21$$

Kano (1985) also determined the contact area A_w between the plug and the wall as indicated below:

$$A_w = \left(1 - \frac{\cos^{-1}\left(1 - \frac{2h}{D}\right)}{\pi}\right)\pi D l_p \qquad 3.22$$

Thus, the pressure loss over the whole plug as determined by Kano (1985) is as indicated below:

$$\Delta p_p = \left[\ell_b g \sin\theta + \xi_w \frac{4p_r}{\zeta_p D}\left(1 - \frac{\cos^{-1}\left(1 - \frac{2h}{D}\right)}{\pi}\right) + \xi_i\left(\ell_b g \cos\theta + \frac{8p_r\sqrt{2Dh - h^2}}{\zeta_p \pi D^2}\right)\right] l_p \qquad 3.23$$

As cited by Kano (1985), Ergun (1952) expressed Δp_p as indicated below:

$$\Delta p_p = \Delta p_k + \frac{\rho_a}{2}\left(u_a^2 - u_k^2\right) \qquad 3.24$$

Where Δp_p denotes the permeating pressure drop in the plug and can be calculated as shown below:

$$\Delta p_p = \left(1.75 + \frac{1.50(1-\varepsilon)}{\mathrm{Re}}\right)\frac{\rho_a U}{d_s}\left(\frac{1-\varepsilon}{\varepsilon^3}\right) l_p \qquad 3.25$$

Where ρ_a is the air density, and U and u_p is determined according to the equation below:

$$U = u_k - u_p = \frac{u_a}{\varepsilon} - u_p \qquad 3.26$$

Where:

U = Difference of permeating air velocity and plug velocity

And

$$\mathrm{Re} = \frac{U\rho_a d_s}{\mu} \qquad 3.27$$

Where:

u_a is calculated mean air velocity i.e. the quotient of the total air volume divided by the cross-sectional area of the pipe.

u_k is permeating air velocity

u_p is plug velocity

ε is porosity of the conveying material in the pipe

If it is assumed that the length l_p and l_a of the plugs and the air cushions between the plugs, respectively stay constant over the whole pipe length L, the total conveying pressure p_c in the pipe is determined as follows:

$$p_c = \Delta p_p \frac{L}{l_p + l_a} \qquad 3.28$$

Where:

Δp_p is the conveying pressure related to a single plug.

3.5 Force balance in incline suction pipe in a decline

This section provides an overview of force balance of solids in incline pipe during solid transport in pneumatic conveying system. The equations of fluid dynamics that are required have been well known for centuries and have been presented by many researchers (Dorricott and Jones, 1984; Biegaj, 2002; Jones 1989). Figure 3.3 shows the principle on which these equations are based.

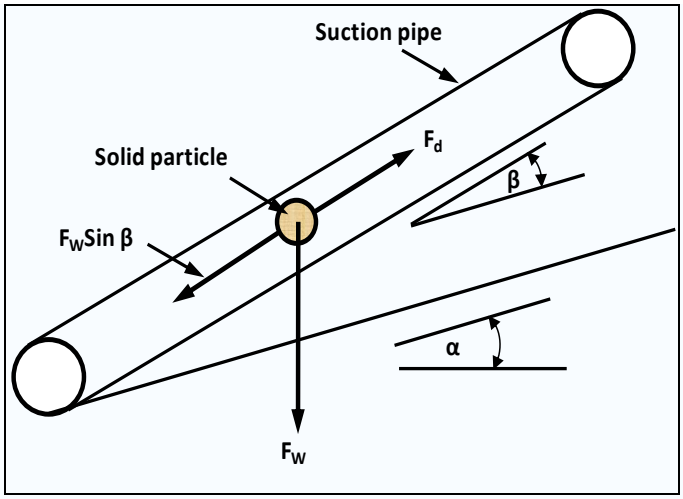

F_w = Gravitational force of rock particles
F_d = Drag force of rock particles
β = Inclination of suction pipe (degrees)
α = decline gradient (degrees)

Figure 3.8: Forces on a rock particle

According to Figure 3.8, the movement of a particle in a fluid is subjected to two forces i.e. gravitational force and drag force (Biegaj, 2002; Jones, 1989). Gravitational force is as a result of the particle weight while drag force is the force that resists the movement of solid particles through a fluid. Drag force is made up of frictional forces and pressure forces. Therefore, for transport of solid particle into and along the pipe to take place, the suction pressure across the particle must exceed its weight (F_wSinβ).

$$F_w \sin \beta < F_d \qquad 3.29$$

The gravitational force on a spherical particle as given by Terence (1997) is given by equation 3.30:

$$F_w = \frac{4}{3}\pi r^3 g \rho_s \quad \text{[kg]} \qquad 3.30$$

Where:

ρ_s is the density of solid [kg/m^3]

g is the acceleration due to gravity [m/s^2]

However, in laminar flow i.e. fluid flow in which the fluid travels smoothly or in regular paths, the particle is subjected to air resistance as indicated in Equation 3.31.

$$F_w = \frac{4}{3}\pi r^3 g(\rho_s - \rho_a) \quad \text{[kg]} \qquad 3.31$$

Where:

ρ_a is the density of air [kg/m^3]

With inclined suction pipe, gravitational force is given as indicated in Equation 3.32.

$$F_w = \frac{4}{3}\pi r^3 g(\rho_s - \rho_a)\sin\beta \qquad 3.32$$

However, the gravitational force on a spherical particle in a vertical duct as given by Terence (1997) is given by Equation 3.33.

$$F_w = \frac{\pi d^3}{6}(\rho_s - \rho_a)g \quad \text{[kg]} \qquad 3.33$$

Where:

d is the drag diameter of spherical particle (i.e. diameter of the cross-sectional area of the particle perpendicular to the direction of motion).

Therefore, with inclined suction pipe the gravitational force on a spherical particle is given by Equation 3.34:

$$F_w = \frac{\pi d^3}{6}(\rho_s - \rho_a)g\sin\beta \quad \text{[kg]} \qquad 3.34$$

However, the movement of solid particles in a stream gives rise to drag force F_d which acts in the opposite direction. It comprises frictional forces and pressure forces and is given by the Equation 3.35 (Terence, 1997):

$$F_d = \frac{1}{2} C_D \rho_a v_s^2 A \text{ [kg]} \qquad 3.35$$

Where:

C_D is the drag coefficient (for rough unstreamlined objects C_D is 1 and for smooth objects it is much less (Terence, 1997))

v_s is the velocity of the rock particle in a suction pipe [m/s]

A is particle projected area [m^2]

Many experiments have been carried out (Terence, 1997) to determine the relationship between settling velocity of particle and unique relationship between drag coefficient and Reynolds Number which reduces to Stokes equation at low Reynolds Numbers.

Stokes Law states that,

> *"if particles are falling in the viscous fluid by their own weight, then a terminal velocity is reached when drag force exactly balance the gravitational force."*

At high velocities, the drag increases above that predicted by Stokes equations due to great turbulent and particles settle more slowly than the Law predicts (Terence, 1997).

Thus, the terminal velocity of particles is found in Stokes Law by equating drag and gravitational forces on the particle as given by Equation 3.8.

$$F_w = F_d \qquad 3.36$$

3.6 Minimum entry velocity consideration

Mills (2004) described entry velocity as the superficial velocity at the point where the material is fed into the pipeline. Because of the continuous expansion

of the conveying gas over the conveying distance, the gas velocity at the start of the pipeline is the lowest gas velocity in the conveying system having a constant bore size. Thus, the entry velocity must be greater than the required minimum conveying velocity to ensure successful conveying of material. In vacuum conveying system, it is approximately equal to the free air velocity i.e. the superficial velocity of the air when evaluated at free air condition. Thus, to avoid pipeline blockages and to facilitate an efficient conveying without high particle degradation, an optimum value of the start gas velocity should be chosen at the entry section of the conveying line.

In vacuum conveying systems, pickup velocity has been defined as the gas velocity required to cause solids, initially at rest, to be totally suspended by the air flow. From theory of pneumatic transport of solids, it is known that particles become suspended when the vertical component of turbulence (i.e. turbulent velocity fluctuation) is greater than the settling velocity of the particle in the fluid. Considerable literature has been published by various authors (Dorricott and Jones, 1984; Biegaj, 2002; Jones 1989) on the determination of minimum air velocity required to convey material in a pipe in gas-solid pneumatic transport system. According to Jones (1989) the minimum air velocity in the conveying pipeline must exceed the terminal velocity of the largest particle if choking is to be avoided. The terminal velocity for spherical particles in vertical pipes can therefore be obtained as follows:

$$v_t = \sqrt{\frac{4d(\rho_s - \rho_a)g}{3C_D\rho_a}} \qquad 3.37$$

Therefore, with inclined pipe equation 3.38 can be written as follows:

$$v_t = \sqrt{\frac{4d(\rho_s - \rho_a)g\sin\beta}{3C_D\rho_a}} \qquad 3.38$$

However, according to (Dorricott and Jones, 1984; Biegaj, 2002; Jones, 1989), the upward velocity of the air stream must exceed this value by a factor (DF) for the largest particle to be transported satisfactorily.

$$v_t = \mathrm{DF}\left[\sqrt{\frac{4d(\rho_s - \rho_a)g\sin\beta}{3C_D\rho_a}}\right] \qquad 3.39$$

For design purposes, it is unwise to have superficial velocities too near the critical velocity because of the danger of choking the system. Therefore, to avoid choking, Jones (1989) recommended a factor of 1.5 – 2.0 although at high velocities, high frictional losses prevail. As an example when conveying rock fragments in shaft sinking, high air velocity in suction pipes i.e. 150m/s – 200m/s gives rise to high frictional losses (Jones, 1989).

Since the rock particles are non-spherical and will be in turbulent flow, the difficulty arises in which particles will fall in random orientation in the laminar flow region. However, particles will orientate themselves to give maximum resistance to drag in the turbulent region (Terence, 1997). Therefore, the terminal velocity as given by Holland (1973) is calculated from Equation 3.40.

$$v_t = \mathrm{DF}\left[\sqrt{\frac{4\varphi d(\rho_s - \rho_a)g\sin(\beta+\alpha)}{3C_D\rho_a}}\right] \quad [\mathrm{m/s}] \qquad 3.40$$

Where:

φ is factor of smoothness and varies from 0.5 - 1 (where 0.5 is very rough material and 1 is perfectly smooth material (Alwyn, 1991)).

3.7 Effects of Material Physical Characteristics

The characterization of the material to be conveyed plays a very large part in the selection of the velocity regime. The conveying velocity and hence air flow rate is greatly influenced by material characteristics. Particle size distribution, particle

shape distribution, hardness and particle density, all have an effect on minimum conveying velocity, pressure drop, air flow, etc. Properties such as moisture content, cohesiveness and adhesiveness may cause flow problems during conveyance. This section highlights the effects of material physical characteristics on the conveying system.

a) Particle size distribution

Particle size distribution can be readily measured by various means for a product and is considered to be one of the most important material properties in relation to dense phase conveying. In conventional systems, materials with a wide size distribution are generally more problematic than fine powders such as cement or pulverized fuel ash. Also the natural force of attraction increases with the decreasing particle size. Mean diameter, volume diameter, surface diameter and Stokes diameter are a few of the commonly used terms to define the particle size.

b) Particle shape

This is a more difficult parameter to measure, but a qualitative assessment of the particle shapes of a material can often be made. It is evident however that particle shape distribution has to be considered in conjunction with particle size distribution. Usually, the shape of the constituent particles in a bulk solid is an important characteristic as it has a significant influence on their packing and flowing behaviour. Highly irregular shaped and fibrous particle can interlock thereby increasing the resistance of a bulk solid to flow.

c) Hardness

Particle hardness like shape and size has a superficially obvious effect on wear rate of pipeline. Thus it is important to take it into account when a pneumatic conveying installation is being designed to avoid undue erosive wear of the system components.

d) Density of particles

The density of particles in gas-solid pneumatic conveying systems is also an important parameter to be considered. Like hardness, the density of the particle will have effects on wear rate of pipeline.

In pneumatic conveying, many different kinds of materials can be transported. The properties of these materials are different from one to another but the materials can be classified in a few groups. Geldart's work (Geldart, 1973), which has been used as a base for many other experiments, is worthwhile to take into account. Based on experimental evidence, Getdart found that most products, when fluidised by a gas, are likely to behave in a manner similar to one of four recognisable groups and these groups of materials can be represented graphically as shown in Figure 3.9.

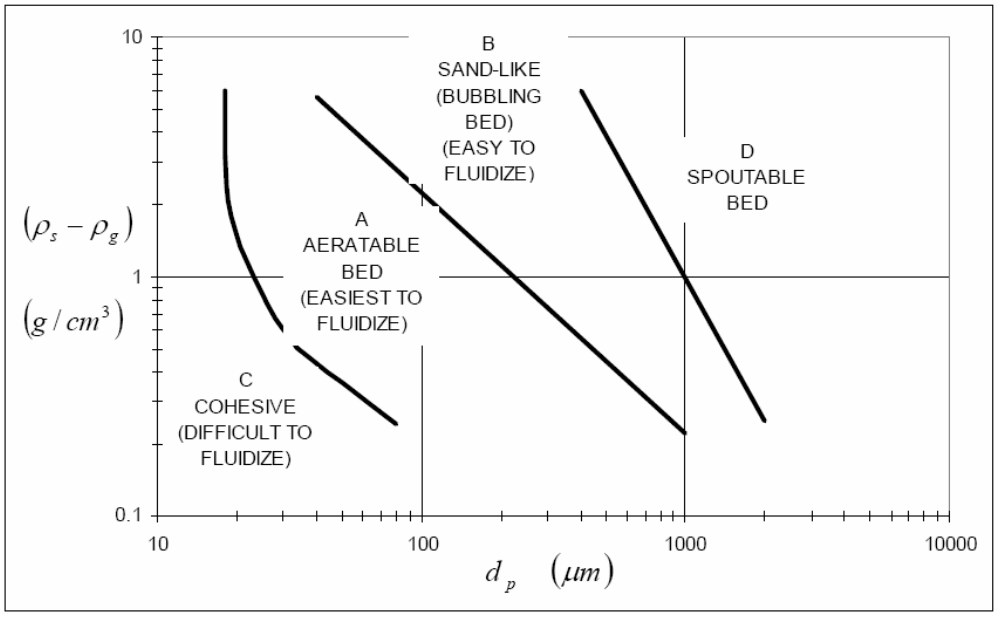

Figure 3.9: Geldart's classification of materials (Geldart, 1973)

Geldart found that materials can be classified by four characterized groups (called Groups A, B, C, and D) by the size and density difference between particle and gas. Each material group has its own characteristic property as follows:

a) **Group A**: Powders, ideal for fluidization, the non-bubbling fluidization occurs at the minimum fluidization gas velocity and bubbling occurs as fluidization gas velocity increases.
b) **Group B**: Start bubbling at minimum fluidization velocity.
c) **Group C:** Very fine and cohesive material, very hard to be fluidized.
d) **Group D**: Coarse solids

3.8 Gas-solid separation

Transportation of solids is terminated in the gas-solid separation zone. In gas-solid separation zone, the solids are separated from the gas stream in which they have been conveyed. Particles in this zone are decelerated and are separated from the gas stream by means of a cyclone. Therefore, the separation unit is critical in gas-solid phase and should receive attention in pneumatic conveying system. According to Klinzing et al. (1997) the gas solid segregation unit can have profound influence on the performance of a pneumatic system. The selection of adequate gas-solid separation system depends on a number of factors, the most important being the size of solids requiring to be separated.

3.9 Pneumatic conveying power requirement

Pneumatic conveying power requirement is also critical in ensuring smooth flow of material in the suction pipe. The power consumption of the prime mover is the rate at which work is done to convey rock fragments through the suction pipe over a vertical distance. Therefore, the amount of work done by the prime mover is the product of the weight of material moved and the vertical distance through which it is moved (Sharp, 1988). The power requirement for pneumatic conveying system E_c is calculated as indicated in Equation 3.41 (Kano, 1985):

$$E_c = \frac{Q\Delta p}{60\times 1000\eta} \qquad 3.41$$

Where:

Q is the air conveying rate [m^3/s]

p is pressure loss in all pneumatic lines of the system [kPa]

η is total efficiency of blower (usually in the range 0.6 – 0.75)

3.10 Summary

The reviewed literature indicates that pneumatic (vacuum) conveying of solids is possible in mines. However, many factors such as pressure loss and minimum transport velocity in the suction pipe and material characteristics should be considered during the design of the pneumatic conveying system. It is also important that the mode of pneumatic conveyance i.e. whether dense-phase or dilute phase is decided during the design process. Selection of the pump to give the required negative pressure is also critical in smooth conveyance of the solids in the pipeline. The type of pump selected will determine the efficiency of the pneumatic conveyance system. Since pneumatic conveying is generally suited to the conveyance of fine and lighter particles, it has a limitation in terms of productivity when larger and denser particles are being conveyed i.e. it gives low productivity for larger particles. Therefore, it is necessary to set up a pilot plant where the performance in terms of productivity of the pneumatic system is determined.

Chapter 4

4.0 Design of monorail drilling system

4.1 Introduction

This Chapter outlines the design of the drilling system for monorail application. The concept involves mounting twin-boom drilling jumbo on to the monorail system and stabilising the system during drilling operations. Hydraulic props are used to stabilise the system during operations. This chapter also determines the required forces in these hydraulic props i.e. in both horizontal and vertical stabilisers to make the system stable.

4.2 Configuration of monorail drilling system

The monorail drilling system is designed such that it is coupled with two independent drilling units as indicated in Figure 4.1.

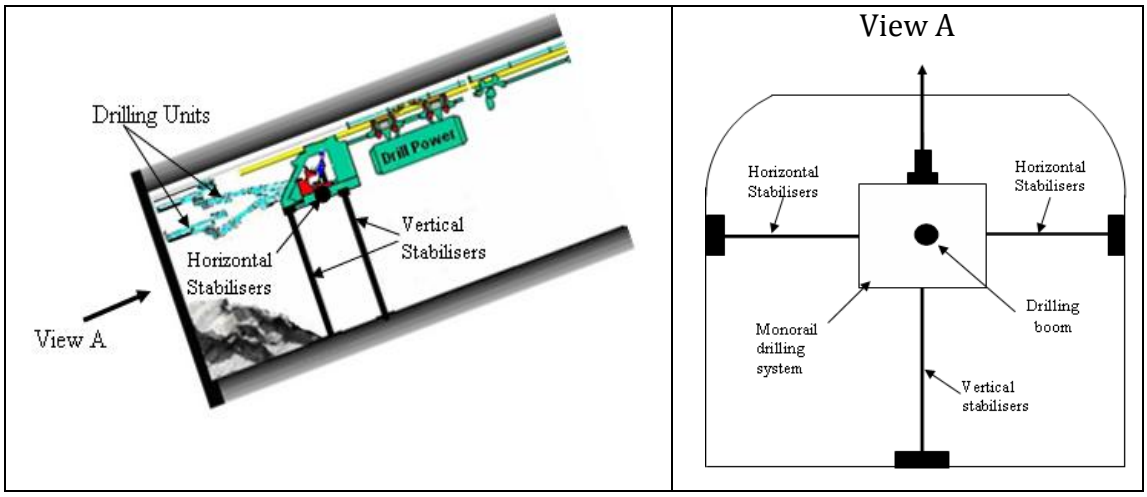

Figure 4.1: Configuration of monorail drilling system

The system has its own power supply attached to it with two horizontal and two vertical hydraulic stabilisers to act as supports during drilling operations. The operation of the drilling system allows for drilling of the top part of the development face to commence as the monorail pneumatic loading system continues to clean the blasted material at the development face. The advantage of this system is that drilling of the face continues whilst monorail loading system cleans the face. This would increase the daily advance of decline development.

4.3 Components of a monorail drilling unit

A wide and varied range of drilling units is available for underground tunnelling and many factors influence their choice in development projects. The drilling units, loading and rock removal equipment must be selected so that its combined efficiency is optimised (Atlas Copco Manual, 1982). The choice of drilling unit to be coupled to the monorail drilling system is therefore, worth attention. Figure 4.2 shows drilling boom with components to be coupled to the monorail drilling system.

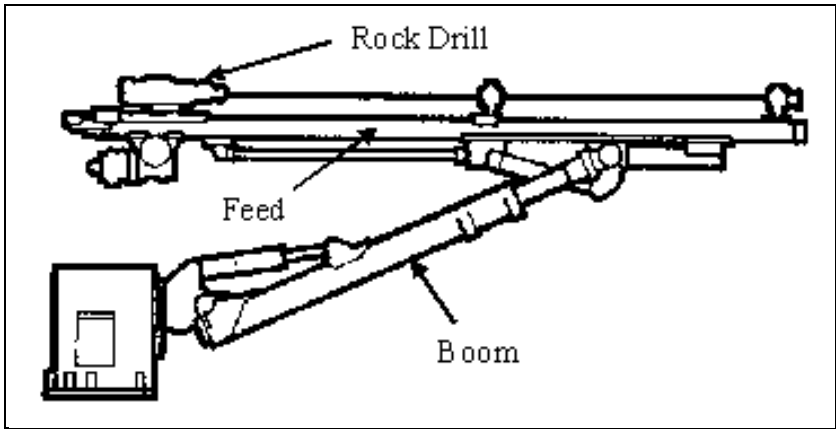

Figure 4.2: Drilling boom with components (Atlas Copco Manual, 1982)

4.3.1 Rock Drill

A rock drill is a machine or device use for penetrating the rock (i.e. drilling holes in a rock) so that the hole may be blasted (Figure 4.3).

Figure 4.3: COP 1638 Rock drill (Atlas Copco Manual, 1982)

It is usually driven by compressed air although it may also be driven by electricity. In most underground tunnelling machines, the rock drill is mounted onto the feed. Therefore, feed should be equipped with extremely fast rock drill with advanced drilling controls. This is in order to drill out the face quickly, accurately and efficiently. Thus, the reliability and productivity of the drilling equipment depend on the rock drill used. Also the efficiency of the rock drill gives lower cost per meter drilled. Therefore, the monorail drilling system will be equipped with high performance pneumatic rock drills with ergonomic controls and automated drilling control system. Table 4.1 shows the types of rock drills available with their technical specifications.

Table 4.1: Rock drill parameters (Sandvik Mining and Construction, 2007; Atlas Copco Manual, 1982)

Supplier	Rock Drill Type	Power (kW)	Weight (kg)	Max Pressure (bars)		Hole Size (mm)
				Percussion	Rotation	
Sandvik	HLX5	20	210	225	175	43 – 64
	HLX5T	22	218	245	175	43 – 64
	HL 510 S	16	130	175	175	43 – 51
	Hydrastar 200	6 - 10	115	200	210	30 - 45
Atlas Copco	COP 1638	16	170	200	310	33 - 76
	COP 1838 ME-07	20	171	230	240rpm	45 - 64
	COP 1838ME-05	20	171	230	300rpm	45 - 64
	COP 3038	30	165	200	380	43 - 64

4.3.2 Feed

Feed is a metal channel on which a rock drill is fed forward as drilling progresses. In percussive drilling, as much as possible of the impact energy from the rock drill has to be transmitted to the rock in order to do the drilling work. In top-hammer drilling, the drill is mounted on a cradle, which runs on a feed. Feeding can take place mechanically, utilising a chain or screw or hydraulically (Figure 4.4).

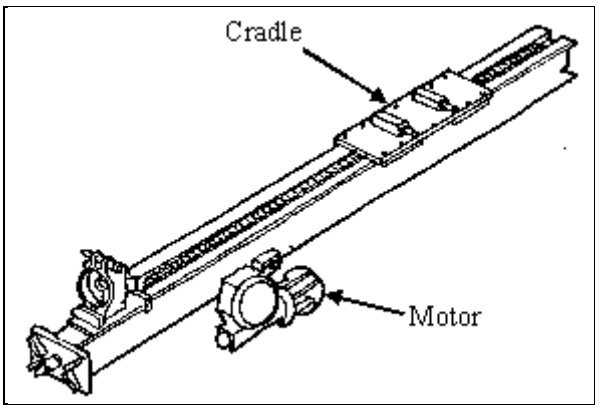

Figure 4.4: Feed with feed motor and cradle (Atlas Copco Manual, 1982).

The feed force varies according to the nature of the rock to be drilled and the mass of the drill rig and the drill steel. When drilling is done by the rotary crushing method the feed force is utilised to drive the buttons of the roller bit into rock and a very high feed force will be required. Thus the life of the bit depends on the feed force and on the properties of the rock being drilled. Table 4.2 shows feed parameters for different types of feeds.

Table 4.2: Feed parameters (Sandvik Mining and Construction, 2007; Atlas Copco Manual, 1982)

Supplier	Type	Maximum Feed Force (kN)	Net Weight (kg)	Feed Length (m)
Sandvik	TF 500 – 10’	25	470	4.66
	TF 500 – 12’	25	500	5.27
	TF 500 – 14’	25	530	5.88
	TF 500 – 16’	25	560	6.49
Atlas Copco	BMH 2831	15	474	4.68
	BMH 2833	15	494	5.29
	BMH 2840	15	514	5.59
	BMH 2843	15	524	5.90
	BMH 2849	15	541	6.51
	BMH 6812	20	601	5.287
	BMH 6814	20	631	5.882
	BMH 6816	20	665	6.502
	BMH 6818	20	696	7.102

It is therefore essential for the rig to be firmly erected, so that the feed is secure and the feed force sufficient to ensure that the bit is constantly in contact with the rock. Insufficient thrust produces several undesirable effects including reduced speed, damage to the drill caused by the piston shrinking the front head and heating of the drill rod and bits due to conversion of unabsorbed energy to heat. With increase in thrust, penetration speed improves progressively until an optimum level is attained (Atlas Copco Manual, 1982). Further increase gives rise to interference in the operation of the percussive mechanism because the bit is no longer able to rotate freely and the length of the piston stroke and thereby the power of the impact is reduced (Figure 4.5). The percussive drill can only produce its full stroke if the rods are allowed to rotate because the two movements are coupled. Therefore, optimum thrust can be considered as the maximum level conducive with satisfactory results and that at which any increase of thrust brings undesirable consequences.

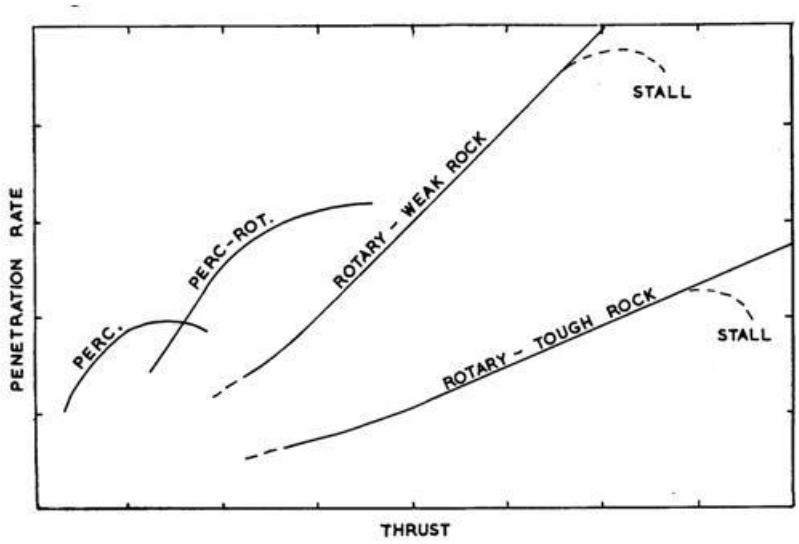

Figure 4.5: Effects of thrust on penetration rate (McGregor, 1967)

4.3.3 Drill Boom

A drill boom (Figure 4.6) is a telescoping, hydraulically adjustable powered steel arm projecting from the drill carriage to carry a drill and hold it in selected positions (AusIMM, 2007).

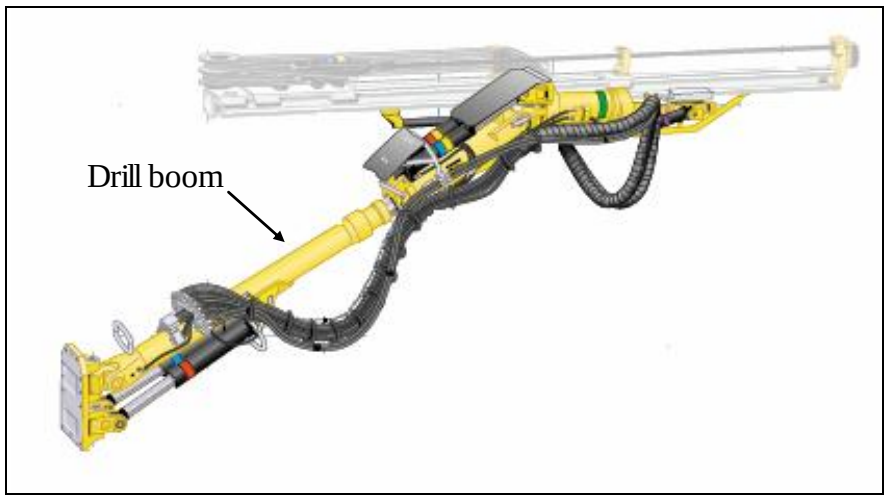

Figure 4.6: BUT 28 Drill Boom (Atlas Copco Manual, 1982)

Most of the booms have automatic parallel holding of the feed which results in easy positioning of the boom and maximises the advance per round. The boom consists of two hydraulic cylinders coupled between the support plate and the

boom and located on each side of the boom so that both cylinders are loaded by the weight of the boom, which makes the boom very stable in all positions. In monorail drilling system, the drill boom carries the feed beam for rock drill and is universally pivoted to the monorail train. Table 4.3 shows boom parameters for Sandvik and Atlas Copco.

Table 4.3: Boom parameters (Sandvik Mining and Construction, 2007; Atlas Copco Manual, 1982)

Supplier	Type	Boom Wt (kg)	Boom Length	Telescopic Boom Ext. (m)	Feed roll-over	Coverage area	Max. Lifting angle		Max. Swing angle
Sandvik	TB 60	2250		1.2	358^0	54	55	-25	$\pm45^0$
	TB 40	1850		1.05	358^0	44.5	55	-30	$\pm40^0$
	B 26XL F	1960		1.7	360^0	41.4	54	-16	$\pm50^0$
	B 26 F	1850		1.2	360^0	38.9	45	-16	$\pm45^0$
Atlas Copco	BUT 4B	1100	1.50	0.90	360^0	23	$+55^0$	-45^0	±30
	BUT 28	1750	1.25	1.25	360^0	48	$+65^0$	-30^0	$\pm45^0$
	BUT 32	2075	1.80	1.25	360^0	41	$+65^0$	-30^0	$\pm45^0$
	BUT 35G	**2860**	1.80	**1.60**	**360^0**	**92**	**$+65^0$**	**-30^0**	**$\pm45^0$**

4.4 Forces acting on the monorail drilling system

In hard rock drilling, the economical blast hole drilling requires drilling equipment that is capable of both rotation and percussion. The tools used in drilling i.e. whether percussive or rotary, handheld or mounted are subjected to great strains during drilling operations. Thrust describes the force which must be applied by the drilling system to hold a bit to the rock, make it penetrate and feed it forward as chippings are removed during drilling. Therefore, the drilling efficiency of the monorail drilling system depends on its thrust as well as its resistance to forces from the drilling unit. The stability of the monorail drilling system during drilling operations is of paramount importance in achieving high drilling performance. Therefore, both the analysis and the design of a monorail drilling system involve determining reaction forces that stabilise the monorail drilling system during drilling operations. Figure 4.7 and 4.8 summarise the forces acting on the monorail drilling system during drilling operations.

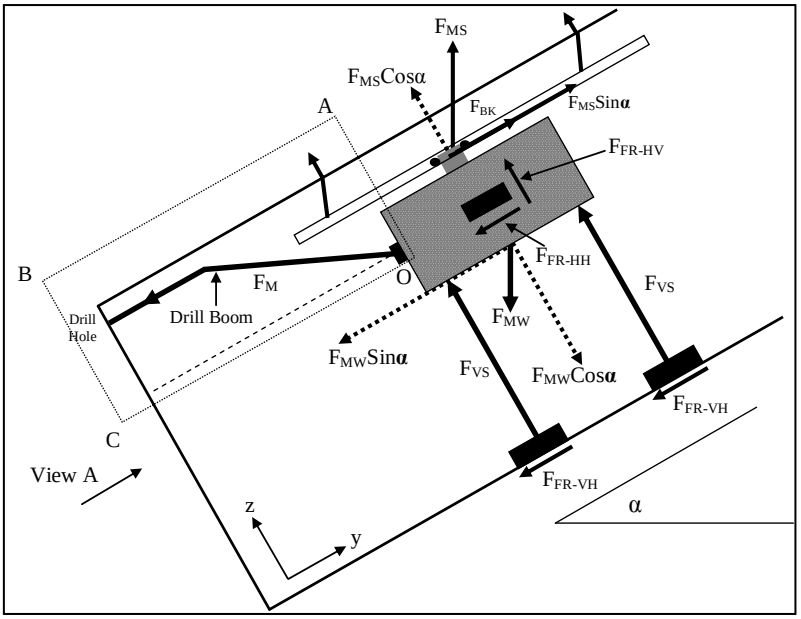

F_M	=	Feed force from the monorail drilling system
F_{MS}	=	Force suspending monorail train
F_{MW}	=	Force due to weight of monorail train (plus weight of two drilling booms)
F_{VS}	=	Force in vertical stabilisers
F_{FR-VH}	=	Horizontal frictional forces at base of vertical stabilisers
F_{FR-HH}	=	Horizontal frictional forces at base of horizontal stabilisers
F_{FR-HV}	=	Vertical frictional forces at base of horizontal stabilisers
F_{BK}	=	Braking force
α	=	Decline gradient (Degrees)

Figure 4.7: Longitudinal section showing forces on the monorail drilling system

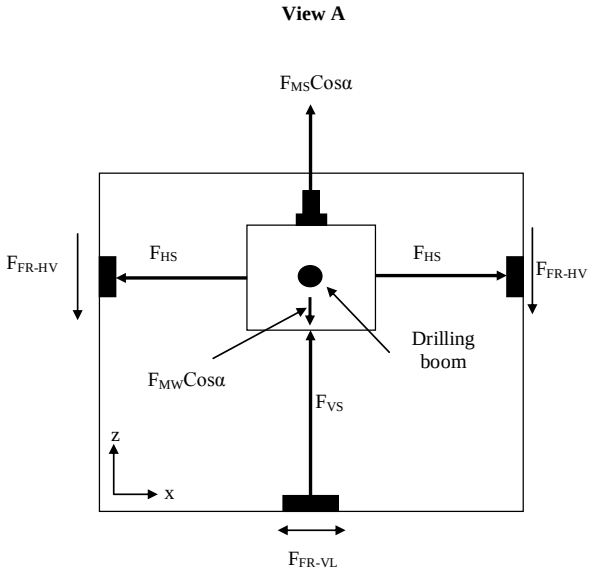

F_{MS}	=	Force suspending monorail train
F_{MW}	=	Force due to weight of monorail train (plus weight of two drilling booms)
F_{VS}	=	Force in vertical stabilisers
F_{FR-HV}	=	Vertical frictional forces at base of horizontal stabilisers
F_{HS}	=	Forces in horizontal stabilisers
F_{FR-HL}	=	Lateral frictional forces at base of vertical stabilisers
α	=	Decline gradient (Degrees)

Figure 4.8: Cross- section showing forces on the monorail drilling system

The monorail drilling system is acted upon by forces in horizontal, vertical and lateral directions depending on the drilling direction of the two drilling booms. Therefore, whether the monorail drilling system remains stable during drilling operations depends on the forces in horizontal and vertical stabilisers, the frictional forces at the base of the two horizontal stabilisers and the brake forces of the monorail system. Reaction forces in horizontal stabilisers act on lateral forces from the two drilling units; vertical stabilisers oppose vertical forces from the drilling units while frictional forces at the base of the two horizontal stabilisers and brake forces resist horizontal force (i.e. resists horizontal movement of the system during drilling).

4.5 Forces from the monorail drilling system

As indicated in the previous sections, three force components result from the drilling unit in X (lateral forces), Y (horizontal forces) and Z (vertical forces) directions with respect to the cross section plane. The magnitude of these forces varies depending on the magnitude and direction of the two drilling booms. Thus, the reaction forces from the monorail drilling system also vary according to the magnitude and direction of the three force components. This section therefore summarises the three reaction force components from the monorail drilling system.

4.5.1 Horizontal Forces

4.5.1.1 Forces due to weight of monorail drilling system

Since the monorail drilling system is inclined at decline gradient $\boldsymbol{\alpha}$, the weight of the monorail drilling system exerts horizontal force on the drilling unit equal to $\mathbf{F_{MW}Sin\alpha}$ (see Figure 4.7). This force is fixed and opposes forces from the drilling unit.

4.5.1.2 Brake force

Brake force is a fixed force that results from applied brakes during monorail drilling. These forces prevent horizontal movements of the monorail drilling system during drilling operation. According to manufacturers of monorail train, Scharf, the braking force is calculated as follows:

$$\text{Braking Force} = 1.5 \times \text{Pulling force} \qquad 4.1$$

The braking force differs depending on the type of monorail, the number of drive units and the number of brakes it has. For EMTS with four drive units, 6 brakes with pulling force of 64kN, the braking force is 96kN.

4.5.1.3 Horizontal frictional forces

Friction results from the two surfaces being pressed together closely causing intermolecular attractive forces between molecules of different surfaces (Ferdinand et al, 2002). As such, friction depends upon the nature of the two surfaces and the degree to which they are pressed together. Friction force often opposes the motion of an object and it balances the net force tending to cause motion. When the force tending to cause motion is zero, equilibrium requires that there be no friction. As can be seen from Figure 4.9, as the opposing force (F) is increased, the friction must be equal and opposite to force tending to cause motion (P) as long as equilibrium exits.

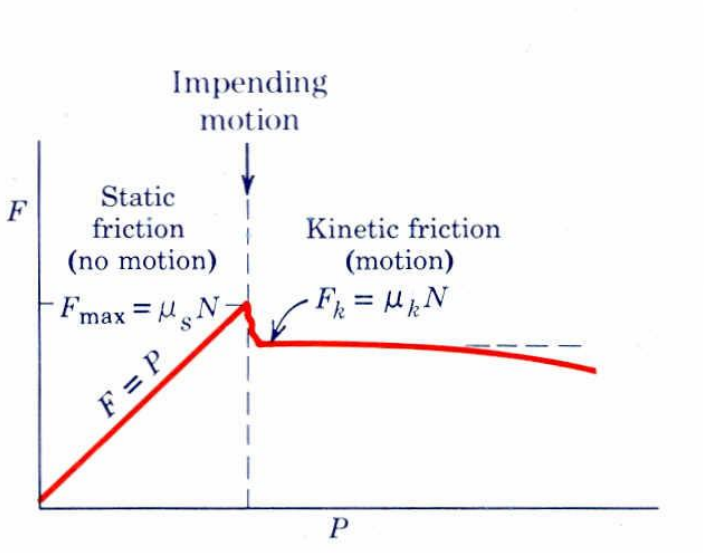

μ_s and μ_k are coefficient of static and kinetic friction

Figure 4.9: Static and kinetic frictional forces (Meriam and Kraige, 1993)

However, friction force reaches maximum value which causes the block to slip and to move in the direction of applied force. At the same time, frictional force drops slightly and rather abruptly to a lower value. Here it remains constant for an interval but then drops. After slippage occurs, a condition of kinetic friction accompanies the ensuing motion.

With monorail drilling, horizontal friction forces ($F_{FR\text{-}HH}$) exist at the contact point between the base of the two horizontal stabilisers and the decline surface (Figure 4.7). This means, $F_{FR\text{-}HH}$ depends on normal forces in horizontal stabilisers. The maximum amount of friction force which a surface can exert upon an object just before sliding can be calculated using Coulomb friction formula as indicated in Equation 4.2 (Ferdinand et al, 2002). Therefore, maximum horizontal frictional force on the monorail drilling system is determined using Equation 4.2:

$$F_{FR\text{-}HH\ (max)} = \mu_s F_{HS} \qquad 4.2$$

Where:

μ_s is coefficient of static friction

F_{HS} is normal force in horizontal stabilisers.

Therefore, for a condition of static equilibrium, when motion is not impending, the static friction force is:

$$F_{FR\text{-}HH} < \mu_s F_{HS\,(max)} \qquad 4.3$$

4.5.2 Vertical forces

4.5.2.1 Force due to weight of monorail

According to Figure 4.7 and 4.8, the monorail drilling system exerts downward forces due to its weight equal to $\mathbf{F_{MW}Cos\alpha}$. This force is fixed and does not change during drilling operations.

4.5.2.2 Monorail suspension forces

Monorail suspension forces are forces suspending the monorail drilling system when the system is at rest i.e. when the system is not drilling. Suspension forces depend on the anchorage forces in the rock bolts used during monorail installation. Therefore, these forces must be high enough to suspend the monorail drilling system at rest. According to Figure 4.8, monorail suspension force is found using $\mathbf{F_{MS}Cos\alpha}$.

4.5.2.3 Vertical frictional forces

Vertical frictional forces ($F_{FR\text{-}HV}$) in the two horizontal stabilisers tend to oppose the vertical movement of the monorail drilling system. These forces depend on the normal forces in vertical stabilisers and the coefficient of static friction between the base of the two horizontal stabilisers and the decline surface.

4.5.2.4 Forces in vertical stabilisers

To stabilise the monorail drilling system in vertical direction, two vertical stabilisers are used. The forces in stabilisers oppose resultant vertical forces from the two drilling units. Thus, whether or not the monorail drilling system fails under any given loading depends on the ability of the two vertical stabilisers to withstand drilling forces.

4.5.3 Lateral forces

4.5.3.1 Lateral forces from the drilling unit

Lateral stabilisation of the monorail drilling system is achieved using forces in horizontal stabilisers (F_{HS}) as shown in Figure 4.8. The forces in horizontal stabilisers oppose the drilling forces tending to cause motion of the system in lateral direction. Thus, to counteract lateral forces resulting from the two drilling units, there should be equal and opposite forces from the monorail drilling system in a lateral direction.

4.5.3.2 Lateral frictional forces

Lateral frictional forces ($F_{FR\text{-}VL}$) also exist between the base of the two vertical stabilisers and the decline floor during drilling operations as indicated in Figure 4.8. The direction of action of these forces always opposes the motion or impending motion and depends on the position of the drilling booms with respect to the Z-Axis. These forces also depend on the normal forces in vertical stabilisers and the coefficient of static friction.

4.6 Forces from the monorail drilling unit

Since the drilling boom can be defined as a directed line segment in space, it can be represented as a vector **OV** in 3D space as indicated in Figure 4.10. Thus, during drilling with maximum drill force F_M, three force components (i.e. F_X, F_Y and F_Z) results from the drilling unit in X, Y and Z direction respectively. In mechanics involving 3D forces, it is often necessary to resolve a force into its three mutually perpendicular components during the analysis (Meriam and Kraige, 1993; Hall et al 1999).

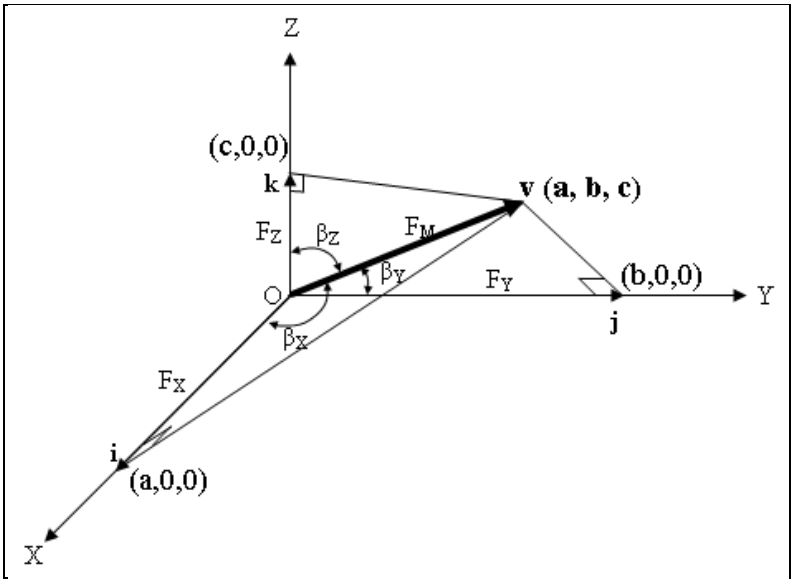

Figure 4.10: Drilling boom represented as line segment in 3D space

4.6.1 Resolution of drill force F_M into its components

From Figure 4.10, ***v*** (representing a drill boom) can be represented as a vector in 3D positioned so that its initial point is at the origin, **O** (representing pivoting point of drill boom with monorail train) of the rectangular coordinate system. The coordinates (***a, b, c***) of the terminal point of ***v*** can be written as ***v*** = (***a, b, c***) with vector, ***v*** = ***a*****i** + ***b*****j** + ***c*****k** and direction angles[1] β_X, β_Y and β_Z (Meriam and Kraige, 1993; Hall et al 1999). Thus, according to Howard (1984) and Thomas

[1] Direction angles β_X, β_Y and β_Z are angles the vector ***v*** makes with the positive x, y and z-axis.

and Finney (2003) the length of the vector ***v***, denoted by $\|v\|$ is the distance from the origin, **O**, to the point (***a, b, c***) and can be found as:

$$\|v\| = \sqrt{a^2 + b^2 + c^2} \qquad 4.4$$

With the monorail drilling system, the components of drilling force F_M depend on the direction angles of the drilling boom (i.e. position in space of the drilling boom) and the coordinates in 3D of the terminal point of force F_M (i.e. the length of drilling boom). Therefore, to determine the direction angles of the drilling boom, direction cosines of the vector ***v*** = ***a*****i** + ***b*****j** + ***c*****k** are used as follows:

$$Cos\beta_X = \frac{a}{\|v\|} \qquad 4.5$$

$$Cos\beta_Y = \frac{b}{\|v\|} \qquad 4.6$$

$$Cos\beta_Z = \frac{c}{\|v\|} \qquad 4.7$$

Given F_M as the pushing force of the drilling system through origin O, the line of action of the drilling boom is inclined to three mutually perpendicular axes O_X, O_Y, and O_Z with direction angles β_X, β_Y, and β_Z respectively. Therefore, to determine the component forces from the drilling unit acting on the monorail drilling system, the resultant force F_M is regarded as the diagonal of a rectangular parallelepiped whose sides are ***a, b*** and ***c*** in the direction ***v*** = ***a*****i** + ***b*****j** + ***c*****k**. Thus, considering the triangle XOV (Figure 4.10), which is right angled with X-Axis, gives $\mathbf{F_X = F_M Cos\beta_X}$. Similarly, for triangle YOP and ZOP we see that $\mathbf{F_Y = F_M Cos\beta_Y}$ and $\mathbf{F_Z = F_M Cos\beta_Z}$ respectively. Therefore, three force components result from the drilling unit and their magnitude depends on the pushing force (F_M), the coordinates ***a, b,*** and ***c*** and the boom length $\|v\|$. The three force components of F_M in X, Y and Z- direction, are summarised in Figure 4.11.

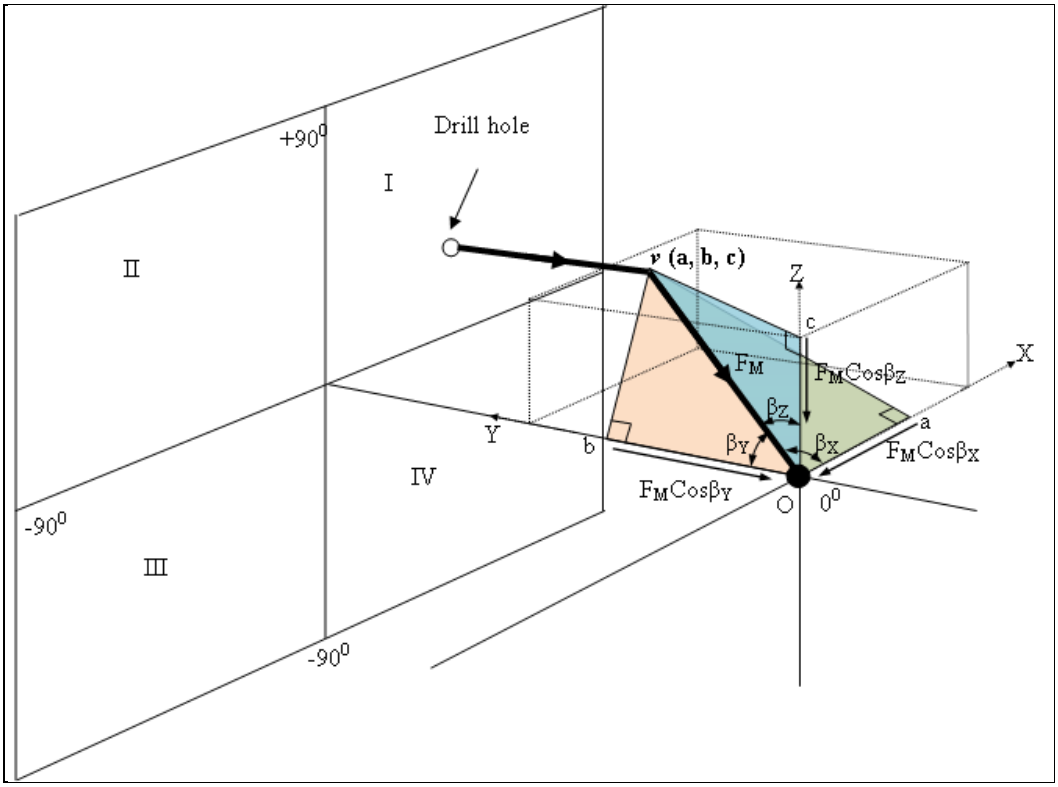

Figure 4.11: Forces acting on the monorail drilling system from the drilling unit

However, two drilling units will be coupled to the monorail drilling system, therefore the force components from the second drilling unit are given as follows:

(i) $F_X = F_M{}^1 \text{Cos}\beta^1{}_X$

(ii) $F_Y = F_M{}^1 \text{Cos}\beta^1{}_Y$

(iii) $F_Z = F_M{}^1 \text{Cos}\beta^1{}_Z$

Where:

$F_M{}^1$ is the pushing force from the second drilling boom;

$\beta^1{}_X$, $\beta^1{}_Y$, $\beta^1{}_Z$ are direction angles of the second drilling boom to three mutually perpendicular axes i.e. O_X, O_Y, and O_Z respectively.

Therefore, when two drilling booms are coupled to the drilling system, at least two forces from the two drilling units act on the monorail drilling system in each

of the X, Y and Z directions. The forces acting in each direction are indicated below:

(i) $F_X = F_M Cos\beta_X + F^1_M Cos\beta^1_X$ (Lateral)

(ii) $F_Y = F_M Cos\beta_Y + F^1_M Cos\beta^1_Y$ (Horizontal)

(iii) $F_Z = F_M Cos\beta_Z + F^1_M Cos\beta^1_Z$ (Vertical)

4.6.2 Drilling boom vector definition

As indicated in the previous section, the forces on the monorail drilling system are determined by the position in space of the two drilling booms with respect to the X, Y and Z-Axes. Therefore, to determine the components of drilling force, the boom length and direction of the two drilling booms are critical. Hence, depending on the direction and magnitude of the two drilling booms, the action forces on the monorail drilling unit will differ.

Considering the origin, O (i.e. the pivoting point) as the starting point, the vectors $\boldsymbol{v}$ and $\boldsymbol{v^1}$ (i.e. positions of two drilling booms) can be described by specifying their end points in Cartesian coordinates $\boldsymbol{(a, b, c)}$ and $\boldsymbol{(a^1, b^1, c^1)}$ respectively. This means that the two monorail drilling booms can be described in vector form with coordinates $\boldsymbol{(a, b, c)}$ and $\boldsymbol{(a^1, b^1, c^1)}$ in 3D where $\boldsymbol{a, b}$ and $\boldsymbol{c}$ and $\boldsymbol{a^1, b^1}$ and $\boldsymbol{c^1}$ are real numbers. Therefore, the position vectors $\boldsymbol{v}$ and $\boldsymbol{v^1}$ of the two drilling booms at any point are the vectors represented by two line segments from the origin O, to end points $\boldsymbol{v}$ and $\boldsymbol{v^1}$.

In development face drilling, the coordinates $\boldsymbol{(a, c)}$ and $\boldsymbol{(a^1, c^1)}$ depend on the size of the development face being drilled i.e. the coordinate $\boldsymbol{a}$ represents the distance from the origin O to the side walls of the decline while **c** represents distance from origin, O to the roof or floor of the decline. In defining the two drilling booms as vectors, the monorail installation dimensions (Figure 4.12) are used. These dimensions give the exact position of the origin O, (i.e. pivoted position of drilling booms) relative to the development face being drilled.

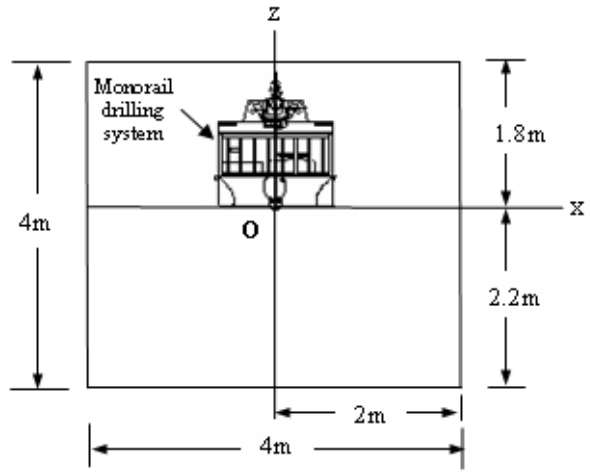

Figure 4.12: Position of monorail dimensions for vector determination

According to Figure 4.10 and Figure 4.11, the two drilling booms can be represented as vectors with end point having coordinates **(a, b, c)** and **(a^1, b^1, c^1)** respectively as follows;

$$\boldsymbol{v} = a\mathbf{i} + b\mathbf{j} + c\mathbf{k}$$
$$\boldsymbol{v^1} = a^1\mathbf{i} + b^1\mathbf{j} + c^1\mathbf{k}$$

The vector components **bj** and **b^1j** represents the horizontal (y-axis) i.e. from the origin O, to the development face. According to Figure 2.20 (Chapter 2), the monorail drilling system drills from a distance of 10m from the development face. Therefore, the total distance of the drilling boom from the joint O to the drill face is 10m. This means the total boom length (i.e. feed length plus boom length) of the system is 10m.

In this study, it is assumed that the monorail drilling system has a fixed boom segment of 2.5m. Therefore, the values of vector **b** and **b^1** have a minimum value of 2.5m and maximum value of 10m. The range of values for ***a, b*** and **c** are summarised below:

$$-2\text{m} \le a \le 2\text{m} \qquad -2\text{m} \le a^1 \le 2\text{m}$$
$$2.5\text{m} \le b \le 10\text{m} \qquad 2.5\text{m} \le b^1 \le 10\text{m}$$
$$-2.2\text{m} \le c \le 1.8\text{m} \qquad -2.2\text{m} \le c^1 \le 1.8\text{m}$$

4.7 Stabilisation of the monorail drilling system

4.7.1 Horizontal Stabilisation

According to Figures 4.7 and 4.8, the monorail drilling system remains horizontally stable during drilling operations when the sum of all action and reaction horizontal forces on the system are equal to zero i.e.:

$$\sum F_Y = 0 \qquad 4.8$$

Where:

$\sum F_Y$ are sum of horizontal forces acting on monorail drilling system

However, horizontal forces acting on the monorail drilling system are:

(i) Forces from two drilling units i.e. $F_M Cos\beta_Y + F^1{}_M Cos\beta^1{}_Y$

(ii) Braking forces i.e. F_{BK}

Horizontal reaction forces from monorail drilling system are:

(i) Forces from monorail weight i.e. $F_{MW} Sin\alpha$

(ii) Horizontal frictional forces in the two vertical stabilisers i.e. $2F_{FR\text{-}VH}$

(iii) Horizontal frictional forces in the two horizontal stabilisers i.e. $2F_{FR\text{-}HH}$

In equilibrium, action and reaction forces on the system will be equal. Therefore:

$$F_{MW} Sin\alpha + 2F_{FR\text{-}VH} + 2F_{FR\text{-}HH} = F_M Cos\beta_Y + F^1{}_M Cos\beta^1{}_Y + F_{BK} \qquad 4.9$$

Since the line of action of maximum horizontal forces from the two drilling units is symmetrical to the horizontal stabilisers, most of the reaction forces from the drilling system are through horizontal frictional forces ($F_{FR\text{-}HH}$). This means that there are very low horizontal frictional forces at the base of the two vertical stabilisers.

Assumption

In this study it is assumed that all the action forces from the two drilling units are opposed by horizontal friction forces in the two horizontal stabilisers and brake forces. This means that frictional forces at the base of the two vertical stabilisers will be zero ($F_{FR\text{-}VH} = 0$). It was further assumed that the forces from the drilling units will not affect monorail suspension forces ($F_{MS}Sin\alpha$) indicating that there will be no change in $F_{MS}Sin\alpha$ (i.e. $\Delta F_{MS}Sin\alpha = 0$) during drilling operation. Therefore, with the above assumptions, $F_{FR\text{-}HH}$ can be determined as indicated in equation 4.10.

$$F_{FR-HH} = \frac{1}{2}\left[F_M Cos\beta_Y + F_M^1 Cos\beta_Y^1 + F_{BK} - F_{MW} Sin\alpha\right] - F_{FR-VH} \qquad 4.10$$

However, from Equation 4.6 $Cos\beta_Y = \frac{b}{\|v\|}$ and $Cos\beta_Y = \frac{b^1}{\|v^1\|}$, and hence equation 4.10 can be written as follows:

$$F_{FR-HH} = \left[F_M \times \frac{b}{\|v\|} + F_M^1 \times \frac{b^1}{\|v^1\|} + F_{BK} - F_{MW} Sin\alpha - F_{FR-VH}\right] \qquad 4.11$$

4.7.1.1 Minimum horizontal force

Minimum frictional forces in horizontal stabilisers of the monorail drilling system result when drilling at extreme points on the face along the X-axis i.e. at maximum values of ***a*** and ***a¹***. However, as vectors ***a*** and ***a¹*** approach maximum i.e. 2m, the vectors ***c*** and ***c¹*** approach maximum value i.e. ***c*** and ***c¹***→ 1.8m. From Section 4.6.2, it was assumed that the minimum boom length in 2.5m, thus the minimum value of vectors ***b*** and ***b¹*** is 2.5m. This means also that the minimum horizontal force is determined when ***b*** = ***b¹*** → 2.5m, ***a*** = ***a¹***→2m and as ***c*** = ***c¹***→ 1.8m. Therefore, to determine the minimum horizontal force, the two drilling booms will have vectors ***v*** = **2i** + **2.5j** + **1.8k** and ***v¹*** = **2i** + **2.5j** + **1.8k** with

minimum boom length $\|v\|$ of 3.67m. Thus, with this minimum boom length, as ***a***, ***a¹,*** c and ***c¹*** approach maximum, the maximum swing angle (in lateral direction) of the drilling booms will be 33^0 (calculated from trigonometry).

4.7.1.2 Maximum horizontal force

Maximum horizontal frictional force on the drilling system results when the two drilling booms are drilling horizontally, i.e. the values of ***a*** = ***a¹***→0 and ***c*** = ***c¹***→0. Therefore, as ***a*** = ***a¹***→0 and ***c*** = ***c¹***→0, the values of ***b*** = ***b¹*** approach maximum or minimum value i.e. 2.5m or 10m making the two drilling booms horizontal. This also indicates that, regardless of the length of the drilling booms, horizontal forces will be the same.

4.7.2 Vertical Stabilisation of the monorail drilling system

According to Figure 4.7 and Figure 4.8, the monorail drilling system will remain in vertical equilibrium when the sum of action and reaction vertical forces on the system is equal to zero:

$$\sum F_Z = 0 \qquad 4.12$$

Where:

$\mathbf{\sum F_Z}$ is sum of vertical forces on monorail drilling system

Thus,

$$\sum \text{Upward Forces} = \sum \text{Downward Forces} \qquad 4.13$$

For two drilling units and two vertical stabilisers Figures 4.7 and 4.8 gives the following upward and downward forces:

$$\sum \text{Upward forces} = 2F_{VS} + F_{MS}\text{Cos}\alpha + 2F_{FR\text{-}HV} \qquad 4.14$$

$$\sum \text{Downward Forces} = F_{MW}\,\text{Cos}\,\alpha + F_M\text{Cos}\beta_Z \text{ and } F^1{}_M\text{Cos}\beta^1{}_Z \qquad 4.15$$

However, for the monorail drilling system to be in vertical equilibrium, the upward forces must be equal to the downward forces. Therefore, equating Equation 4.14 and 4.16 gives:

$$2F_{VS} + F_{MS}Cos\alpha + 2F_{FR\text{-}HV} = F_{MW}\,Cos\,\alpha + F_{M}Cos\beta_{Z} \text{ and } F^{1}{}_{M}Cos\beta^{1}{}_{Z} \quad 4.16$$

Assumption

Since there should be no relative movement (i.e. no friction) between the base of horizontal stabilisers and the surface (decline wall), it is assumed that vertical reactions from the drilling system is through vertical stabilisers only. This means that there is no change in vertical frictional force ($F_{FR\text{-}HV}$) in horizontal stabilisers i.e. ($\Delta F_{FR\text{-}HV} = 0$). Therefore, from equation 4.16, the minimum force in each vertical stabiliser can be determined as follows:

$$F_{VS} = \frac{1}{2}\left(F_{M}Cos\beta_{Z} + F_{M}^{1}Cos\beta_{Z}^{1}\right) + \frac{1}{2}Cos\alpha\left(F_{MW} - F_{MS}\right) - F_{FR-HV} \quad 4.17$$

Thus with $\Delta F_{FR\text{-}HV} = 0$ and $\Delta F_{MS}Sin\alpha = 0$ equation 4.17 can be written as:

$$F_{VS} = \frac{1}{2}\left(F_{M}Cos\beta_{Z} + F_{M}^{1}Cos\beta_{Z}^{1}\right) + \frac{1}{2}F_{MW}Cos\alpha \quad 4.18$$

Thus, whether or not the monorail drilling system will resist vertical drilling forces depends on force F_{VS}. From equation 4.7 $Cos\beta_{Z} = \frac{c}{\|v\|}$ and $Cos\beta_{Z}{}^{1} = \frac{c^{1}}{\|v^{1}\|}$, therefore, Equation 4.18 can be written as follows:

$$F_{VS} = \left[\frac{1}{2}\left(F_{M}\frac{c}{\|v\|} + F_{M}^{1}\frac{c^{1}}{\|v^{1}\|} + F_{MW}Cos\alpha\right)\right] \quad 4.19$$

4.7.2.1 Minimum vertical force

The minimum force in vertical stabilisers results when the system is drilling centre holes on the development face, i.e. as $\boldsymbol{a} = \boldsymbol{a^1}$ and $\boldsymbol{c} = \boldsymbol{c^1}$ approaches zero ($\boldsymbol{a} = \boldsymbol{a^1} \rightarrow 0$; $\boldsymbol{c} = \boldsymbol{c^1} \rightarrow 0$). This indicates that as the value of $\boldsymbol{a}$ and $\boldsymbol{a^1} \rightarrow 0$ and $\boldsymbol{c}$ and $\boldsymbol{c^1} \rightarrow 0$, the values of $\boldsymbol{b}$ and $\boldsymbol{b^1}$ approach minimum or maximum value i.e. 2.5m or 10m respectively (minimum and maximum boom length). Therefore, the two drilling booms form vectors $\boldsymbol{v} = \mathbf{0i + 2.5j + 0k}$ (or $\boldsymbol{v} = 0\mathbf{i} + \mathbf{10j} + \mathbf{0k}$) and $\boldsymbol{v^1} = \mathbf{0i} + \mathbf{2.5j} + \mathbf{0k}$ (or $\boldsymbol{v^1} = \mathbf{0i} + 10\mathbf{j} + \mathbf{0k}$), with boom lengths of 2.5m and 10m. Thus, all the forces are along the y-axis, i.e. in horizontal direction.

Since the monorail drilling system is suspended on the monorail (i.e. in the decline roof), drilling of downholes will exert upward vertical forces on the monorail system. This means that the maximum downward lifting angle of the system should be enough to enable the drilling system to drill the holes at the lowest point (bottom) of the drill face. Thus, as $\boldsymbol{c}$ and $\boldsymbol{c^1}$ approach maximum, i.e. -2.2m, and as $\boldsymbol{a}$ and $\boldsymbol{a^1}$ approach 0, $\boldsymbol{b}$ approaches minimum value i.e. 2.5m. Also the vectors $\boldsymbol{v} = \mathbf{0i} + \mathbf{2.5j} - \mathbf{2.2k}$ and $\boldsymbol{v^1} = \mathbf{0i} + \mathbf{2.5j} - \mathbf{2.2k}$, will have minimum boom length of 3.33m. The resultant force is negative meaning that the force acts upwards i.e. it pushes the monorail drilling system upwards. Therefore, computing the swing angle of the two vectors using trigonometry, gives the maximum downward swing angle of 41^0. However, for the monorail system to be stable, the weight of the system ($F_{MW}Cos\alpha$) must be more than the upward force from the drilling unit (i.e. $F_MCos\beta_Z + F^1{}_MCos\beta^1{}_Z < F_{MW}Cos\alpha$).

4.7.2.2 Maximum vertical force

According to equation 4.19, maximum vertical force in vertical stabilisers results when the drilling system is drilling extreme up holes along the Z-axis on the development face, i.e. as $\mathbf{c} = \boldsymbol{c^1}$ approaches maximum (i.e. $\boldsymbol{c = c^1} \rightarrow 1.8m$), $\boldsymbol{a}$ and $\boldsymbol{a^1} \rightarrow \boldsymbol{0}$ and $\boldsymbol{b = b^1}$ approaches minimum i.e. 2.5m. Therefore, the vectors $\boldsymbol{v} = \mathbf{0i} + \mathbf{2.5j} + \mathbf{1.8k}$ and $\mathbf{v^1} = \mathbf{0i} + \mathbf{2.5j} + \mathbf{1.8k}$ have maximum length (i.e. boom length) of

3.1m. Computing the maximum upward lifting angle using trigonometry gives 35^0.

4.7.3 Lateral stabilisation of the monorail drilling system

For the monorail drilling system to be in lateral equilibrium during drilling operations, the sum of all lateral forces (along X-axis) i.e. the sum of action forces from the drilling unit and reaction forces from the drilling system must be equal to zero:

$$\sum F_X = 0 \qquad 4.20$$

Where

$\mathbf{\sum F_X}$ is sum of lateral forces on monorail drilling system

Thus,

$$\sum \text{Lateral forces from drilling units} = \sum \text{Lateral Forces from monorail drilling system} \qquad 4.21$$

The maximum lateral force on the monorail drilling system is exerted when the two drilling units are drilling on the same side of the Z-axis with drilling boom horizontal (i.e. along the X-axis). Therefore, all the lateral forces from the drilling unit are opposed by one horizontal stabiliser opposite to the direction of force. From Figures 4.7 and 4.8, for two drilling units and two horizontal stabilisers, the following lateral forces exist:

$$\sum \text{Lateral forces from the drilling unit} = F_M Cos\beta_X + F^1{}_M Cos\beta^1{}_X \qquad 4.22$$

$$\sum \text{Lateral Forces from monorail drilling system} = F_{HS} + 2F_{FR-VL} \qquad 4.23$$

Therefore, equating Equation 4.22 and 4.23 gives:

$$F_{HS} + 2F_{FR-VL} = F_M Cos\beta_x + F_{M^1} Cos\beta^1{}_x \qquad 4.24$$

Assumption

All the lateral forces from the two drilling units are opposed by the force in horizontal stabilisers. Therefore, there will be no lateral frictional force ($F_{FR\text{-}VL}$ = 0) at the base of the vertical stabilisers. This is because there should be no lateral movement at the base of the vertical stabilisers during drilling operations.

Determining the minimum force in each horizontal stabiliser (F_{HS}) from equation 4.24 gives the following:

$$F_{HS} = F_M Cos\beta_X + F_M^1 Cos\beta_X^1 - 2F_{FR-VL} \qquad 4.25$$

With $F_{FR\text{-}VL}$ = 0, equation 4.25 can be written as:

$$F_{HS} = F_M Cos\beta_X + F_M^1 Cos\beta_X^1 \qquad 4.26$$

From Equation 4.5 $Cos\beta_Z = \frac{a}{\|v\|}$ and $Cos\beta_Z = \frac{a^1}{\|v\|}$, therefore, Equation 4.26 can be written as indicated below:

$$F_{HS} = F_M \frac{a}{\|v\|} + F_M^1 \frac{a^1}{\|v\|} \qquad 4.27$$

4.7.3.1 Minimum lateral force

The minimum lateral force results when the system is drilling horizontal holes along the Y-axis i.e. when ***a*** and ***a¹*** approach zero (***a*** = ***a¹*** → 0) and ***c*** and ***c¹*** approach 0 (***c*** and ***c¹*** → 0). Therefore, as ***a***, ***a¹***, ***c*** and ***c¹*** tend to zero, ***b*** and ***b¹*** approach minimum or maximum value i.e. 2.5m or 10m. This also means that the drilling boom will have vector ***v*** = **0i** + **2.5j** + **0k** (or ***v*** = **0i** + **10j** + **0k**) and ***v¹*** = **0i** + **2.5j** + **0k** (or ***v¹*** = **0i** + **10j** + **0k**) with drilling boom length varying from minimum 2.5m to maximum 10m along Y-axis.

4.7.3.2 Maximum lateral force

The maximum lateral force is exerted on the system when drilling extreme holes along the X-axis i.e. when $\boldsymbol{a}$ and $\boldsymbol{a^1}$ approach maximum (i.e. as $\boldsymbol{a}$ and $\boldsymbol{a^1} \rightarrow$ 2m) and $\boldsymbol{c}$ and $\boldsymbol{c^1}$ approach zero (i.e. as $\boldsymbol{c}$ and $\boldsymbol{c^1} \rightarrow$ 0). From Section 4.7.1.1, it was determined that the maximum swing angle was 33^0. Therefore, as $\boldsymbol{a}$ and $\boldsymbol{a^1} \rightarrow$ 2m and $\boldsymbol{c}$ and $\boldsymbol{c^1} \rightarrow$ 0 the boom length approaches 3.67m. Also $\boldsymbol{b}$ and $\boldsymbol{b^1}$ approach 2.5m. This means that the two drilling booms have vectors $\boldsymbol{v}$ = **2i** + **2.5j** + **0k** and $\boldsymbol{v^1}$ = **2i** + **2.5j** + **0k**, with maximum boom length of 3.67m.

4.8 Design of monorail drilling system

The previous sections have revealed that the monorail drilling system is acted upon by forces from the drilling unit in vertical, horizontal and lateral directions. These forces make the monorail system unstable during drilling operations. Therefore, to stabilise the drilling system it is necessary to determine the magnitude of reaction forces in horizontal vertical and lateral directions of the monorail drilling system. These reaction forces will oppose forces resulting from the drilling unit and by so doing making the system stable.

4.8.1 Method

In determining reaction forces for the monorail drilling system, equilibrium equations presented earlier were used to determine minimum and maximum reaction forces of the drilling system. Using maximum feed force of 25kN (Table 4.2), maximum and minimum possible reaction forces from the monorail drilling system have been determined.

4.8.2 System Assumptions

The following assumptions were made during the analysis:

(i) Braking force (F_{BK}) of the monorail drilling system is 96kN.

(ii) According to manufacturers of the monorail train, Scharf, the weight of the monorail system with four drive units is 92kN. However, the two drilling booms that are coupled to the drilling system increase the weight of the system. Therefore, in this study, total weight of two drilling booms is assumed to be is half the weight of the monorail train. Thus, the total weight of the two drilling booms is 46kN giving the total weight of the train as 138kN.

(iii) Horizontal action forces from the two drilling units are opposed by forces in the two horizontal stabilisers. This means frictional forces at the base of the two vertical stabilisers is zero ($F_{FR\text{-}VH} = 0$).

(iv) All vertical reactions forces from the drilling system is through vertical stabilisers only. This means the vertical frictional force ($F_{FR\text{-}HV}$) in horizontal stabilisers is zero ($F_{FR\text{-}HV} = 0$).

(v) The drilling boom has a lifting angle of -41^0 and $+35^0$, and swing angle of 33^0

(vi) No lateral frictional force ($F_{FR\text{-}VL} = 0$) at the base of the vertical stabilisers. This is because there should be no lateral movement at the base of the vertical stabilisers during drilling operations.

(vii) Decline gradient $\alpha = 20^0$

4.8.3 Monorail horizontal stabilisation forces

4.8.3.1 Minimum frictional forces

The minimum frictional force in horizontal stabilisers is determined using Equation 4.11 under the following condition i.e.

$$F_{FR\text{-}HH} \left| \begin{array}{l} \boldsymbol{a} \rightarrow 2\text{m}; \boldsymbol{b} \rightarrow 2.5\text{m}; \\ \boldsymbol{c} \rightarrow 1.8\text{m}; \|v\| \rightarrow 3.67m \end{array} \right. \qquad F_{FR\text{-}HH} \left| \begin{array}{l} \boldsymbol{a^1} \rightarrow 2\text{m}; \boldsymbol{b^1} \rightarrow 2.5\text{m}; \\ \boldsymbol{c^1} \rightarrow 1.8\text{m}; \|v^1\| \rightarrow 3.67m \end{array} \right.$$

Therefore, using the maximum feed force of 25kN and decline gradient $\boldsymbol{\alpha} = 20^0$, minimum frictional forces in horizontal stabilisers were determined as indicated in Table 4.4. The Table shows that the minimum frictional force ($F_{FR\text{-}HH} = F_Y$) required in horizontal stabilisers is 82kN.

Table 4.4: Minimum horizontal frictional forces ($F_{FR\text{-}HH}$)

Max. drill force (F_M)	Vector coordinates			$b = b^1$ (m)	$\|v\|$ (m)	$\|v^1\|$ (m)	F_Y (kN)	$F_{FR\text{-}HH\ (min)}$ (kN)
	$a = a^1$	$b = b^1$	$c = c^1$					
25	2	2.5	1.8	2.5	3.67	3.67	82	82

4.8.3.2 Maximum frictional forces

Maximum frictional force in horizontal stabilisers was also determined using Equation 4.11 under the following condition i.e.

$$F_{FR\text{-}HH} \begin{vmatrix} 2.5\text{m} \le \boldsymbol{b} \le 10\text{m}; \\ \boldsymbol{a} = \boldsymbol{c} = 0;\ 2.5\text{m} \le \|v\| \le 10\text{m} \end{vmatrix} \qquad F_{FR\text{-}HH} \begin{vmatrix} 2.5\text{m} \le \boldsymbol{b^1} \le 10\text{m}; \\ \boldsymbol{a^1} = \boldsymbol{c^1} = 0;\ 2.5\text{m} \le \|v^1\| \le 10\text{m} \end{vmatrix}$$

Using the maximum drill force of 25kN, maximum horizontal force was determined as indicated in Table 4.5.

Table 4.5: Maximum frictional force in horizontal stabilisers ($F_{FR\text{-}HH}$)

Max. drill force (F_M)	Vector coordinates			$b = b^1$ (m)	$\|v\|$ (m)	$\|v^1\|$ (m)	F_Y	$F_{FR\text{-}HH\ (max)}$ (kN)
	$a = a^1$	$b = b^1$	$c = c^1$					
25	0	2.5	0	2.5	2.5	2.5	25	99
25	0	10	0	10	10	10	25	99

According to Table 4.5, at maximum feed force, the maximum horizontal friction force of 99kN results from drilling operations. The table also shows that regardless of the length of the boom during drilling, horizontal drilling will always give the same maximum frictional force. This means also that any normal

force in horizontal stabilisers less than 99kN will cause the system to slide since $\mu > 1$. Therefore, to stabilise the system, i.e. to avoid slippage, normal force greater than 99kN is required in horizontal stabilisers.

4.8.4 Monorail vertical stabilisation forces

4.8.4.1 Minimum forces in vertical stabilisers

Minimum force in vertical stabilisers is determined using Equation 4.19 under the following conditions:

$$F_{VS} \left| \begin{array}{l} \boldsymbol{c = c^1} \rightarrow 0;\ \boldsymbol{a = a^1} \rightarrow 0 \\ 2.5\text{m} \le\ \text{b} \le 10\text{m};\ 2.5\text{m} \le \|v\| \le 10m \end{array} \right. \qquad F_{VS} \left| \begin{array}{l} \boldsymbol{c = c^1} \rightarrow 0;\ \boldsymbol{a = a^1} \rightarrow 0 \\ 2.5\text{m} \le\ \text{b}^1 \le 10\text{m};\ 2.5\text{m} \le \|v^1\| \le 10m \end{array} \right.$$

With maximum feed force of 25kN, minimum forces in vertical stabilisers are determined and are indicated in Table 4.6.

Table 4.6: Minimum force in vertical stabilisers (F_{VS})

Max. drill force (F_M)	**Vector coordinates**			***c = c¹*** **(m)**	$\|v\|$ **(m)**	$\|v^1\|$ **(m)**	**F_Z (kN)**	**F_{VS} (kN)**
	a = a¹	***b = b¹***	***c = c¹***					
25	0	2.5	0	0	2.5	2.5	64	64
25	0	10	0	0	10	10	64	64
25	0	2.5	-2.2	-2.2	3.33	3.33	48	48.3

Table 4.6 shows that minimum forces in vertical stabilisers ($F_{VS} = F_Z$) occur when the monorail drilling system is drilling horizontal holes (i.e. $\boldsymbol{a = a^1} \rightarrow 0$) along Z-axis. This is because as $\boldsymbol{a = a^1} \rightarrow 0$ and $\boldsymbol{c = c^1} \rightarrow 0$, all the forces concentrate along the horizontal plane. However, when the system is drilling down holes (i.e. with maximum boom lifting angle of -41^0 with $\boldsymbol{c = c^1} \rightarrow -2.2$) the vertical force

from the drilling units will be 48.3kN acting upwards and against the weight of the monorail drilling system.

4.8.4.2 Maximum forces in vertical stabilisers

According to section 4.7.2.2, maximum forces in vertical stabilisers ($F_{VS} = F_Z$) occur under the following conditions:

F_{VS} | $\boldsymbol{c = c^1} \rightarrow 1.8$; $\boldsymbol{a = a^1} \rightarrow 0$; $\boldsymbol{b = b^1} \rightarrow 2.5\text{m}$; $\|v\| \rightarrow 3.1\text{m}$

F_{VS} | $\boldsymbol{c = c^1} \rightarrow 1.8$; $\boldsymbol{a} = \boldsymbol{a^1} \rightarrow 0$; $\boldsymbol{b = b^1} \rightarrow 2.5\text{m}$; $\|v^1\| \rightarrow 3.1\text{m}$

Therefore, using Equation 4.19, maximum forces in vertical stabilisers were determined as indicated in Table 4.7. The table shows that the maximum drilling force in each vertical stabiliser should be 87.3kN.

Table 4.7: Maximum force in vertical stabilisers

Max. drill force (F_M)	Vector coordinates			$c = c^1$ (m)	$\|v\|$ (m)	$\|v^1\|$ (m)	F_Z (kN)	F_{VS} (kN)
	$a = a^1$	$b = b^1$	$c = c^1$					
25	0	2.5	1.8	1.8	3.1	3.1	87.3	87.3

4.8.5 Monorail lateral stabilisation forces

4.8.5.1 Minimum lateral forces

Minimum lateral force ($F_{HS} = F_X$) of the monorail system was determined using Equation 4.27 under the following conditions.

F_{HS} | $\boldsymbol{a = a^1} \rightarrow 0$; $2.5\text{m} \leq \boldsymbol{b} \leq 10\text{m}$; $\boldsymbol{c = c^1} = 0$; $2.5\text{m} \leq \|v\| \leq 10\text{m}$

F_{HS} | $\boldsymbol{a = a^1} \rightarrow 0$; $2.5\text{m} \leq \boldsymbol{b^1} \leq 10\text{m}$; $\boldsymbol{c = c^1} = 0$; $2.5\text{m} \leq \|v^1\| \leq 10\text{m}$

Table 4.8 shows the minimum lateral forces in horizontal stabilisers.

Table 4.8: Minimum lateral force (F_{HS}) in horizontal stabilisers

Max. drill force (F_M)	Vector coordinates			$a = a^1$ (m)	$\|v\|$ (m)	$\|v^1\|$ (m)	F_X (kN)	F_Y (kN)	F_Z (kN)	F_{HS} (kN)
	$a = a^1$	$b = b^1$	$c = c^1$							
25	0	2.5	0	0	2.5	2.5	0	50	0	0
25	0	10	0	0	10	10	0	50	0	0

According to Table 4.8, minimum force in horizontal stabilisers is 0kN and is obtained when the monorail drilling system is drilling horizontal holes. The minimum lateral force is 0kN indicating that vectors $\boldsymbol{v} = \mathbf{0i} + \mathbf{2.5j} + \mathbf{0k}$ (or $\boldsymbol{v} = \mathbf{0i} + \mathbf{10j} + \mathbf{0k}$) and $\boldsymbol{v^1} = \mathbf{0i} + \mathbf{2.5j} + \mathbf{0k}$ (or $\boldsymbol{v^1} = \mathbf{0i} + \mathbf{10j} + \mathbf{0k}$) will have all the forces directed along the horizontal axis (Y-axis).

4.8.5.2 Maximum lateral forces

According to Section 4.7.3.2, maximum lateral force ($F_{HS} = F_X$) on the system was determined using Equation 4.27 under the following conditions:

$$F_{HS} \Big| \boldsymbol{a = a^1} \rightarrow 2;\ \boldsymbol{b = b^1} \rightarrow 2.5\text{m};\ \boldsymbol{c = c^1} \rightarrow 0;\ \|v\| = 3.67\text{m} \qquad F_{HS} \Big| \boldsymbol{a = a^1} \rightarrow 2;\ \boldsymbol{b} = \boldsymbol{b^1} \rightarrow 2.5\text{m};\ \boldsymbol{c = c^1} = 0;\ \|v^1\| = 3.67\text{m}$$

Table 4.9 shows the maximum lateral forces on the drilling system.

Table 4.9: Maximum lateral force (F_{HS}) in horizontal stabilisers

Max. drill force (F_M)	Vector coordinates			$a = a^1$ (m)	$\|v\|$ (m)	$\|v^1\|$ (m)	F_X (kN)	F_{HS} (kN)
	$a = a^1$	$b = b^1$	$c = c^1$					
25	2	2.5	0	2	3.67	3.67	27.2	27.2

Table 4.9 shows that the maximum lateral force in hydraulic stabilisers should be 27.2kN. Thus with the two drilling units drilling in the same quadrant i.e. either I, II, III or IV (see Figure 4.11) all the lateral forces from the drilling units are opposed by one horizontal stabiliser opposite to the direction of force. Therefore, the minimum force in each stabiliser is equal to the total lateral force from the two drilling units.

4.8.6 Coefficient of static friction at base of horizontal stabilisers

The coefficient of static friction (μ_s) depends on the normal forces in the two hydraulic stabilisers (F_{HS}) and the maximum frictional forces in horizontal stabilisers ($F_{FR\text{-}HH(max}$). The results obtained show that the maximum frictional force at the base of horizontal stabilisers is larger than the normal forces in hydraulic stabilisers i.e. $F_{FR\text{-}HH(max)}$ = 99kN > F_{HS} = 27.2kN. Also according to Equation 4.2, the maximum possible friction force between the two surfaces before sliding begins is the product of the coefficient of static friction and the normal force. Thus, from the results obtained, at the point of equilibrium the coefficient of friction is larger than 1 indicating that the system will slide during drilling operations. Therefore, the normal forces in hydraulic stabilisers should be large enough to avoid sliding.

Just before sliding takes place, $F_{FR\text{-}HH(max)} = \mu F_{HS}$ i.e. μF_{HS} should have a value of 99kN. However, according to Equation 4.3 for the system to remain static, μF_{HS} should be larger than 99kN.

Assumptions

In this study, it is assumed that the normal force in horizontal stabilisers (F_{HS}) is twice the maximum frictional force at the base of horizontal stabilisers ($F_{FR\text{-}HH(max)}$). Therefore, F_{HS} will have a value of 198kN. This means also that at this normal force, the system will not slide during operation since $\mu<1$.

4.9 Factor of safety

The Factor of Safety (FoS) also known as safety factor is used to provide a design margin over the theoretical design capacity. This is in order to allow for uncertainty in the design process (Ferdinand et al, 2002). The FoS is a multiplier applied to the maximum expected load to which a component or assembly is subjected. The uncertainty could be any one of a number of the components of the design process including calculations, material strengths, manufacture quality etc. The selection of the appropriate factor of safety to be used in design of components is essentially a compromise between the associated additional cost and weight and the benefit of increased safety and/or reliability. An appropriate factor of safety is chosen based on several considerations. Prime considerations are the accuracy of load and wear estimates, the consequences of failure and the cost of over-engineering the component to achieve that FoS. For example, components whose failure could result in substantial financial loss, serious injury or death usually use a FoS of four or higher (often ten). Non-critical components generally have a safety factor of two.

4.9.1 Factor of safety in monorail drilling system

Factor of safety in monorail drilling system is applied to horizontal and vertical stabilisers. The maximum load that these stabilisers are allowed to carry under normal conditions of utilisation is considerably smaller than the ultimate load. The smaller load is referred to as the allowable load. Thus, only a fraction of the ultimate load capacity in the hydraulic stabilisers is utilised when the allowable load is applied. The remaining portion of the load carrying capacity of the member is kept in reserve to ensure its safe performance. Thus, the FoS of the hydraulic stabilisers is the ratio of the ultimate load to the allowable load and is calculated as indicated in Equation 4.28:

$$\text{Factor of Safety} = \frac{\text{Ultimate load}}{\text{Allowable load}} \qquad 4.28$$

Assumption

Since hydraulic stabilizers will be made with known materials with certification and will be operated in reasonably constant environmental conditions with subjected loads and stresses that can be determined using qualified design procedures, a **Factor of Safety of 2.0** will be used in the design.

However, regular inspection and maintenance of the system is required to achieve maximum and safe performance. Table 4.10 shows maximum and minimum reaction forces from the monorail drilling system after applying a safety factor of 2.0.

Table 4.10: Summary reaction forces of the monorail drilling system with FoS

Parameter	Design parameters without FoS		Factor of Safety	Design parameters with FoS	
	Minimum Force (kN)	Maximum Force (kN)		Minimum Force (kN)	Maximum Force (kN)
Force in vertical stabiliser (F_{VS})	48	87.3	2	96	174.4
Forces in horizontal stabilisers (F_{HS})	0	198	2	0	396

Therefore, the coefficient of static friction between the decline wall and the base of horizontal stabilisers of the monorail system can be found as follows:

$$\mu_s = \frac{F_{FR-HH\,(\max)}}{F_{HS\,(\max)}} \qquad 4.29$$

$$\mu_s = \frac{99}{396} = 0.25$$

Since the coefficient of static friction is less than unit (μ_s <1), the monorail drilling system will be stable and will not slide during drilling operations.

4.10 Monorail suspension forces

The strength of roof bolts and suspension chains for monorail suspension is also critical in ensuring the monorail drilling system remains suspended during operations. The monorail consists of a suitable steel section hung by chains from rock bolts. Therefore, stronger chains and rock bolts with high tensile strength are required to suspend the monorail train. If rock bolts and chains with less strength are used, they may lead to collapse of the monorail together with the train. As an example a serious accident occurred at Impala Platinum 1 Shaft where there was failure of the rock bolts supporting the overhead rail (SRK-Turgis Report, 2002) resulting in trains falling onto the footwall. Therefore, it is necessary to determine the minimum force in rock bolts and chains that is required to suspend the monorail train.

4.10.1 Total weight of the monorail system

The minimum strength of the rock bolts and chains to suspend the monorail drilling system depends on the total weight of the monorail system (i.e. together with two drilling booms, feed and rock drills). Thus, for monorail system to remain suspended, the anchorage forces in rock bolts as well as in supporting chains should be more than or equal to the total weight of the monorail drilling system i.e. $F_{MW} \text{ Cos } \alpha < F_{MS}$. Figure 4.13 shows forces acting on the rock bolt and supporting chains by the weight of the drilling system.

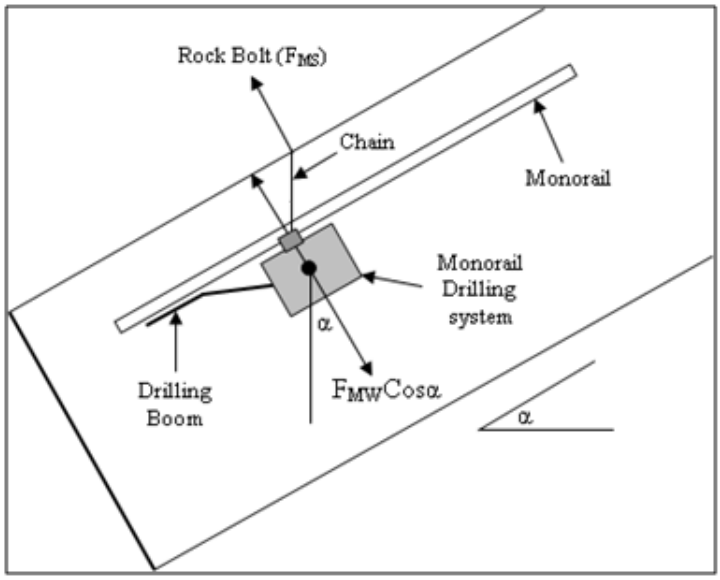

Figure 4.13: Forces in rock bolts (F_{MS}) and monorail drilling weight ($F_{MW}Cos\alpha$)

Thus, at equilibrium i.e. just before rock bolt and suspension chain failure, the total weight of the monorail drilling system is equal to the suspension forces in roof bolts as indicated in Equation 4.30.

$$F_{MS} = F_{MW} \, Cos \, \alpha \qquad 4.30$$

However, to be able to suspend the monorail train requires that the forces in rock bolts and suspension chains be more than the total weight of the system i.e. $F_{MS} > F_{MW} \, Cos \, \alpha$.

4.10.2 Strength of rock bolts and suspension chains

From the previous section, it has been determined that suspending the monorail drilling system requires that the forces in rock bolts and suspension chains be greater than the total weight of the system. Since the allowable load on the rock bolt before failure is $F_{MS} = F_{MW} \, Cos \, \alpha$, the rock bolt and suspension chain ultimate load should be more than the allowable load. However, the classical approach used in designing engineering structures is to consider the relationship between the capacity (ultimate load) of the rock bolts and suspension chains and the

allowable weight of monorail (allowable load). According to Equation 4.28 failure is assumed to occur when the factor of safety is less than 1. Therefore, failure occurs when the weight of the monorail drilling system is more than the ultimate strength of the rock bolt and suspension chains.

Therefore, the net weight of the monorail drilling system (F_{MW}) is determined as follows:

F_{MW} = Weight of train + weight of two drilling booms
= 92 + 46
= 138kN

Since the allowable load of the rock bolts and suspension chains is 138kN, applying a factor of safety of 2 gives the minimum strength of rock bolts and suspension chains i.e. ultimate load of 276kN. Therefore, the forces in the rock bolts and monorail suspension chains to support the monorail drilling system should have a minimum strength of approximately 276kN.

4.11 Summary

It has been determined that the stability of the monorail drilling system is critical in ensuring high performance of the drilling system. Stabilisation of the system requires determination of the horizontal, vertical and lateral forces of the system. According to the findings, these forces depend on the vector position of the two drilling booms with respect to the origin (pivoting point). Due to configuration and positioning of the monorail drilling system, the swing angles and lifting angles need to be determined accurately for the system to be able to cover the whole drill face.

In order for horizontal and vertical stabilisers not to slide against the decline wall, the coefficient of static friction is also critical. This implies that the material

which the stabilisers are to be made of should be carefully selected. Table 4.11 summarises the design parameters for the monorail drilling system.

Table 4.11: Summary of design parameters for monorail drilling system

Parameter	Value	
	Minimum	**Maximum**
Force in vertical stabiliser (F_{VS})	96	174.4
Forces in horizontal stabilisers (F_{HS})	0	396
Factor of safety	2	-

Chapter 5

5.0 Design of pneumatic monorail loading system

5.1 Introduction

Transportation of broken rock in mines is often discontinuous involving the use expensive equipment which takes up considerable space and injects pollutants into the air stream. In Chapter 2, literature revealed that a continuous monorail loading system is fundamental in improving advance rates in decline development. According to literature, to improve advance rates in decline development, the monorail should be loaded by some continuous loading system that quickly removes blasted rock fragments from the development face onto the monorail containers. In Chapter 3, extensive literature has been reviewed on pneumatic conveying theory which will be used in the design of monorail pneumatic loading system. This Chapter therefore, focuses on the design of monorail loading system that uses pneumatic (vacuum) conveying principles to suck broken rocks from the decline face. Pneumatic transport systems are being increasingly used in a wide variety of industries and their wider use in the mining industry could lead to more efficient and cost effective rock loading system and better ventilated mines.

5.2 Structure of the monorail loading system

Figure 5.1 shows the structure and configuration of the monorail loading system. The system consists of an incline suction pipe that is connected to the storage hopper. The high pressure fan connected to the storage hopper creates negative pressure inside the hopper that enables transport of blasted material from the

development face into the hopper to take place. Thus, rock fragments from the development face are sucked into the hopper through an incline suction pipe.

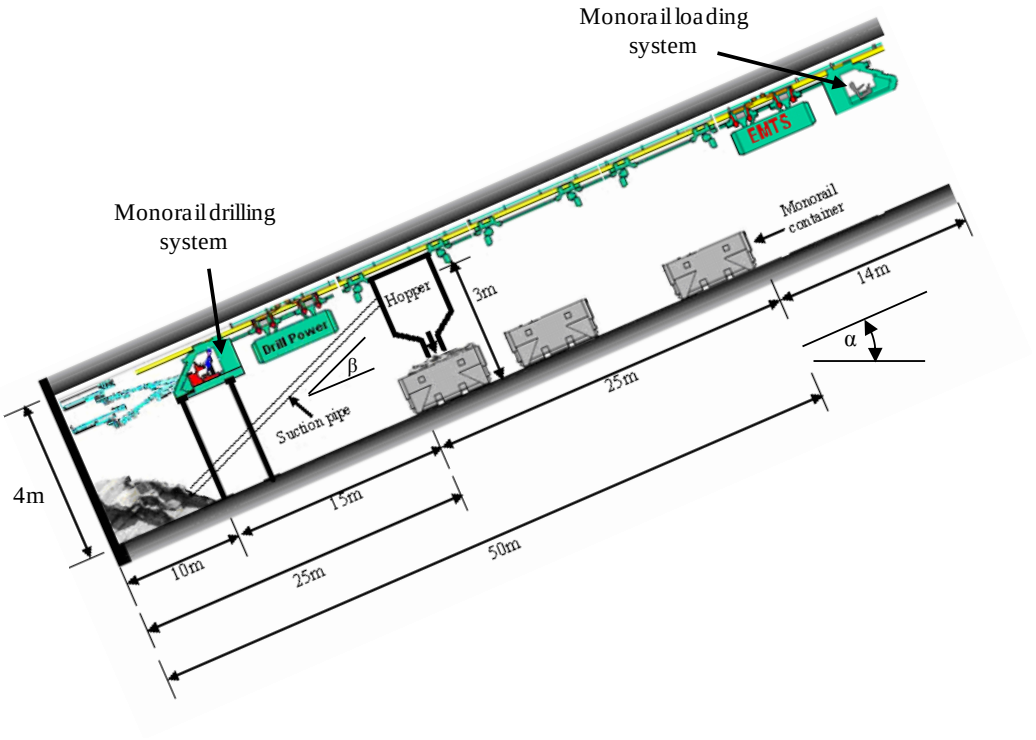

β is inclination of suction pipe from the decline floor to hopper; **α** is the decline gradient

Figure 5.1: Continuous loading principle of monorail system.

Once the hopper is full, the suction pipe is disconnected from the hopper and the hopper is pulled by the monorail train to the position of an empty container where automatic discharge of material takes place. According to the manufacturers of monorail train (Scharf), the dead weight of each monorail container is 1 tonne and the maximum payload per container is 4 tonnes. Therefore, in this study, the storage hopper has been designed with a capacity of 4 tonnes. This is in order to allow material from the hopper to be loaded in each monorail container in one pass. The movement of the storage hopper during loading of material into containers is done by coupling and uncoupling the hopper to the monorail train (Figure 5.2).

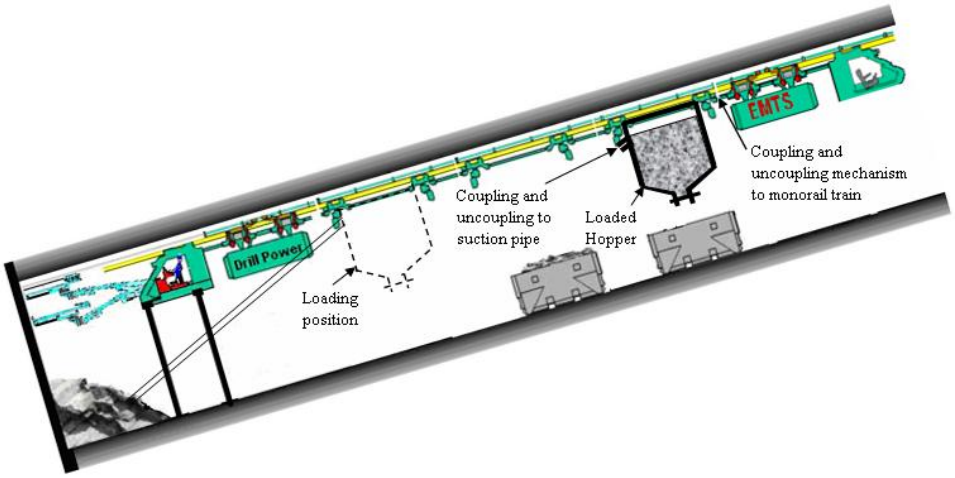

Figure 5.2: Movement of hopper during loading mechanism

Thus, the monorail train will have a mechanism that allows coupling and uncoupling of the hopper. This implies that when the hopper is fully loaded, it will be coupled to the monorail train that will pull it to the position of an empty monorail container where automatic discharge of material takes place. Once the monorail container is filled up, the empty hopper is pushed by the monorail train back to the loading position where the next loading takes place.

5.3 Design of monorail loading system

As highlighted by Mills (2004) design of any pneumatic conveying system for a new application is always difficult due to lack of sufficient knowledge and published data. Determination of parameters such as type of solids to be transported, pipe diameter, length and fittings needs a pilot plant test or a full-length test to determine accurately the design parameters such as what conveying speed should be used, and at what loading rate. Also data must be available so that pressure drop along the pipe can be accurately predicted. With the pressure drop known, one can then size the air pump and determine its horsepower. However, without the above information, it is difficult to accurately design the new system. Therefore, due to absence of the pilot test, only theory is used in the design of the monorail pneumatic conveying system. This means that

where information is lacking assumptions have been made and this may affect the results obtained.

5.3.1 Design purpose and method

The purpose of the pneumatic monorail loading system is to load blasted rock fragments from the development face in a decline to the hopper of the monorail system. According to Figure 5.1, material is conveyed from the development face a vertical distance of 3m using incline suction pipe connected to the hopper. The system will load 25m horizontal distance from the development face giving a pipe inclination from the decline floor of 6.84^0 i.e. calculated using trigonometry. In designing the monorail loading system, a model was created in spread sheet in which the relationship between theoretical suction principle equations presented in Chapter 3 and the loading parameters were studied. The sensitivity of each loading parameter on the performance of the loading system was examined using the model.

5.3.2 Material conveying characteristics

According to research on suction units used in sucking of broken rocks in shaft sinking (Jones, 1989), the ideal average diameter of suction pipes used varies from 203mm - 258mm. Therefore, in this study, a suction pipe diameter of 220mm is used. During the analysis, material density is varied from 2400 - 3000kg/m^3 while rock fragments (i.e. particle diameter) are varied from 50 – 200mm. The decline gradient (α) of 20^0 and pipe inclination from the decline floor (β) of 6.84^0 are also used. Therefore, the total pipe inclination from the horizontal is 26.84^0. A decline gradient of 20^0 is adopted since it is the gradient at which decline access is developed during mine design case study. It is also assumed that a total of 4 tonnes is loaded in each monorail container which is the maximum payload for each monorail container. Therefore, the loading time of the system refers to loading 4 tonnes of blasted material in a hopper.

5.3.3 Mode of solid conveying

According to the research (Jones, 1989), dilute phase systems are the most common applicable method of broken rock conveyance in the mines. These methods are comparatively cheap to install and operate although they have relatively low productivity. Therefore, dilute phase method is used to design the monorail pneumatic loading system.

5.3.4 Solid loading ratio (m*)

Since dilute phase mode of conveyance is used in the design of the pneumatic loading system, the solid loading ratio (**m***) of the conveyance should be less than 50 (i.e. **m***<50). Therefore, during this study a maximum solid loading ratio of 50 is used.

5.3.5 Transport velocity

Though a considerable number of research works has been carried out in the field of pneumatic conveying, currently there is no general procedure to predict the minimum conveying velocity. Since this study is theoretical, results of some experimental work which give good correlations with the theory are used. According to Jones (1989) the conveying air velocity in suction pipes used in shaft sinking maybe as high as 150 - 200m/s (i.e. for vertical distance of >100m) although this velocity results in high frictional losses.

Determining the terminal velocity of the largest particle (i.e. 200mm) using Equation 3.40, with solid loading ratio of 50 and voidage of 0.7, the largest particle (i.e. with maximum density of 3000kg/m^3) will only be suspended in the suction pipe at velocity of 66.4m/s. Therefore, the upward velocity of the conveying air should be higher than the terminal velocity of the largest particle in the suction pipe. Thus, using 1.5 as a factor of safety, the minimum upward

conveying air velocity should be 100m/s. This air velocity is used as minimum conveying air velocity in the model with maximum being 300m/s. However, since the maximum negative pressure cannot exceed 0.6 bars (60kPa), the range of conveying air velocities at maximum negative pressure is determined during the study.

5.3.6 Air flow rate

To determine the mass flow rate of air through the conveying line, air velocity as explained in Section 5.2.5 and a pipe diameter of 220mm are used. Thus, using the relationships in Equation 5.1 and 5.2, mass flow rate of air is determined as indicated in Figure 5.3.

$$Q_a = A.v_a \qquad 5.1$$

Where:

Q_a is the air flow rate

A is the cross-section area of pipe

v_a is the velocity of air

$$\mathrm{M}_a = Q_a.\rho_a \qquad 5.2$$

Where:

M_a is the mass flow rate of air

ρ_a is the density of air (1.2kg/m^3) and was assumed constant.

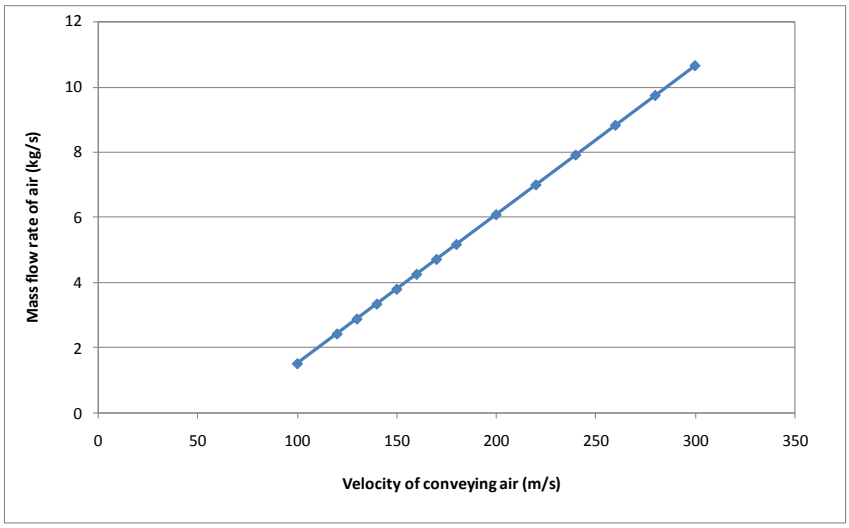

Figure 5.3: Mass flow rate of air at varying air velocities

Figure 5.3 shows that as the velocity of the conveying air increases, the mass flow rate of air in the suction pipe also increases linearly.

5.3.7 Mass flow rate of solids

Since the mass flow rate of air and solid loading ratio are known, therefore, the mass flow rate of solids in the suction pipe is determined using the relationship in Equation 5.3.

$$m^* = \frac{M_s}{M_a} \qquad 5.3$$

Where:

M_s is the mass flow rate of solids in the pipe [t/h]

M_a is the mass flow rate of air in the pipe [t/h]

m*is the solid loading ratio

Figure 5.4 shows the mass flow rates (i.e. at different solid loading ratios) at different air velocities.

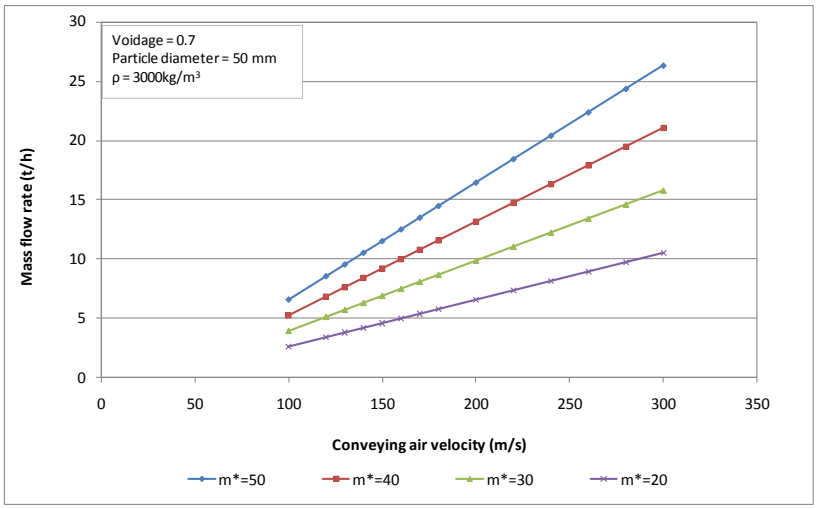

Figure 5.4: Mass flow rate of solids in the suction pipe at different solid loading ratios

According to Figure 5.4, the mass flow rate of solids in the suction pipe increases with increase in conveying air velocity. The figure also reveals that as the solid loading ratio increases, the mass flow rate of solids in the suction pipe also increases. This means that as the solid loading ratio increases, the more solids will be transported in the suction pipe resulting in high tonnage.

5.3.8 Superficial velocity of solids in the pipe

To estimate the transport velocity of solids in the suction pipe, Equation 5.4 is used as proposed by Dorricott and Jones (1984). Figure 5.5 shows the superficial velocity profile of solid phase in the suction pipe according to the density of the material being conveyed.

$$v_s = \frac{4M_s}{\pi D^2 \rho_s} \qquad 5.4$$

Where:

v_s is the superficial velocity of solids in the pipe.

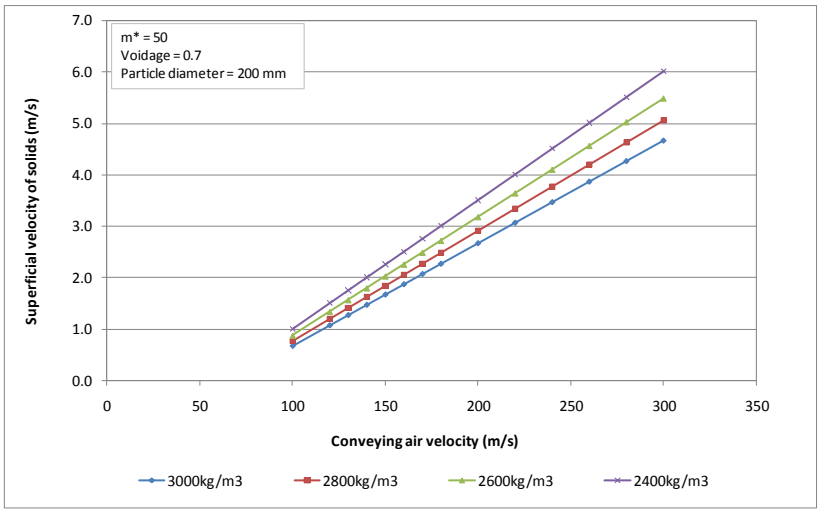

Figure 5.5: Superficial velocity of solids of different densities in the suction pipe

Figure 5.5 indicates that superficial velocity of solids in the suction pipe is proportional to the velocity of conveying air and also to the density of the material being transported. Figure 5.5 reveals that heavier particles have less superficial velocity as compared to lighter particles. The figure also shows that at higher conveying velocity more solids are transported as compared to low air velocity.

5.3.9 Pressure drop in incline suction pipe

The pressure drop prediction in incline suction pipe of the monorail pneumatic conveying system is divided into three zones i.e. acceleration zone, conveying zones and separation zone. However, since this study is theoretical and due to the difficult nature of predicting pressure loss in the separation zone, only the pressure losses in acceleration and conveying zones are determined as indicated in Equation 5.5.

$$\Delta p_t = \Delta p_{acc} + \Delta p_{sts} \qquad 5.5$$

Where:

Δp_t is total pressure loss in the suction pipe

Δp_{acc} is pressure loss in acceleration zone

Δp_{sts} is pressure loss in steady state zone (conveying zone)

5.3.9.1 Pressure loss in acceleration zone

In monorail conveying system, the solids to be transported i.e. rock fragments are at atmospheric pressure and are also at rest. As the rock fragments are accelerated from rest to some average conveying velocity, a rapid change in momentum takes place with associated high pressure loss. To determine the pressure loss in this zone, Equation 5.6 as recommended by Ottjes et al. (1976) was used. Results of the calculations of pressure loss in an acceleration zone for materials of different density are shown in Figure 5.6 and Figure 5.7.

$$\Delta p_{acc} = \frac{4 M_s v_s}{\pi D^2} \qquad 5.4$$

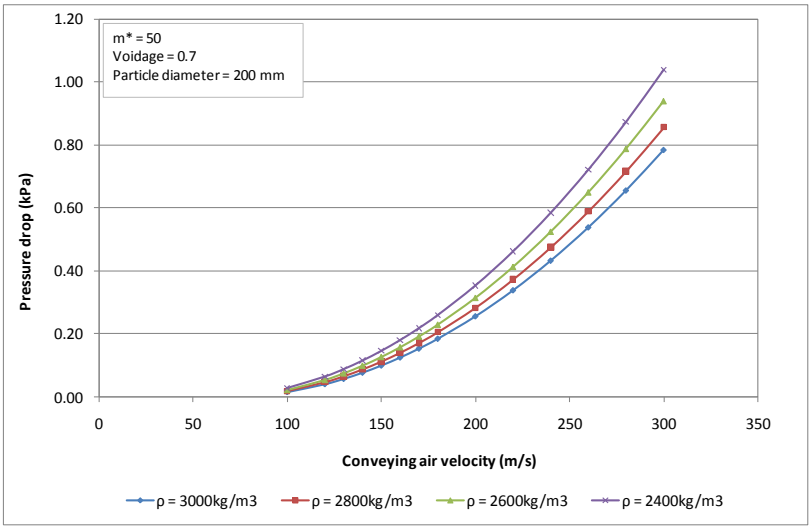

Figure 5.6: Pressure loss in acceleration zone for 200mm size rock particle with different densities

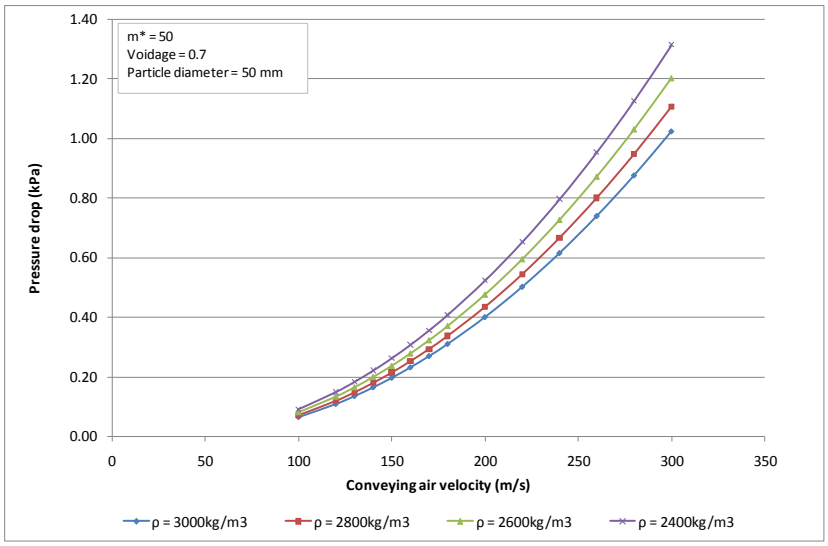

Figure 5.7: Pressure loss in acceleration zone for 50mm size rock particle with different densities

Figure 5.6 and Figure 5.7 show that the pressure drop in the acceleration zone increases with decrease in particle density. Results from the two figures show that as the density of rock fragments increases i.e. from 2400kg/m^3 to 3000kg/m^3 the pressure drop of the system decreases for both smaller and larger rock particles. However, as the air velocity increases, the pressure loss in the acceleration zone also increases. The two figures also reveal that rock fragments with smaller particle diameter results in larger pressure drop than larger particles.

5.3.9.2 Pressure drop in steady state zone

Pressure drop in steady state zone is determined using Darcy equation as indicated in Equation 3.13. To avoid choking in the suction pipe, a voidage of 0.7 with drag coefficient of 1 are used. Since the suction pipe for the system is inclined, Equation 3.15, as suggested by Aziz and Klinzing (1990) is used to determine the friction factor. In Figure 5.8 and Figure 5.9 the pressure drop per unit length of conveying pipe is shown as a function of the conveying air velocity in steady state zone. The maximum achievable negative pressure i.e. 0.6 bars (60kPa) is also indicated in the two figures.

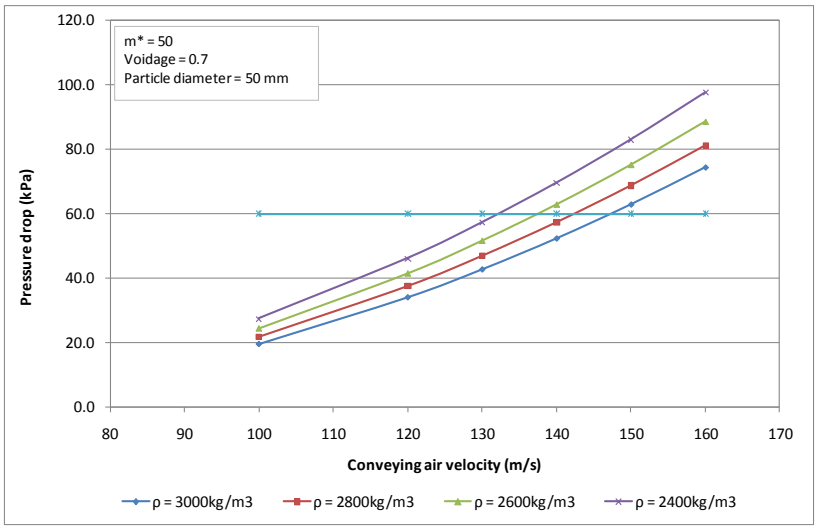

Figure 5.8: Pressure loss in steady state zone for material with 50mm particle diameter.

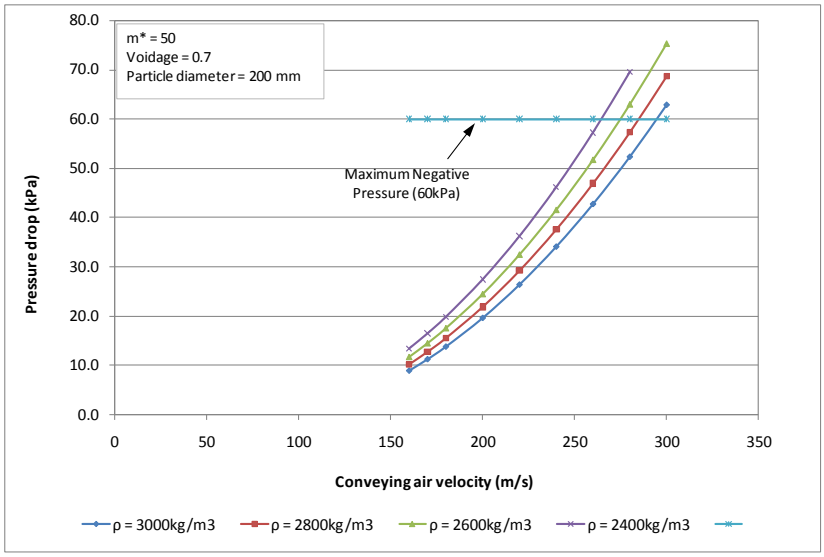

Figure 5.9: Pressure loss in steady state zone for material with 200mm particle diameter

5.4 Effects of design parameters

5.4.1 Effects of particle size on conveying velocity

Fragmentation (particle size) is the rock breakage carried out to fragment masses of rock. It attempts to break rocks into manageable sizes by chemical energy in blasting (Hartman, 2002). It is recognized that particle size being

sucked has strong effects on the productivity of the pneumatic system. Therefore, particle size affects the monorail pneumatic loading system depending on the size of rock fragments being loaded. The influence of particle diameter on pressure drop of the system at different conveying air velocities was assessed. The result of the assessment is shown in Figure 5.10 and Figure 5.11.

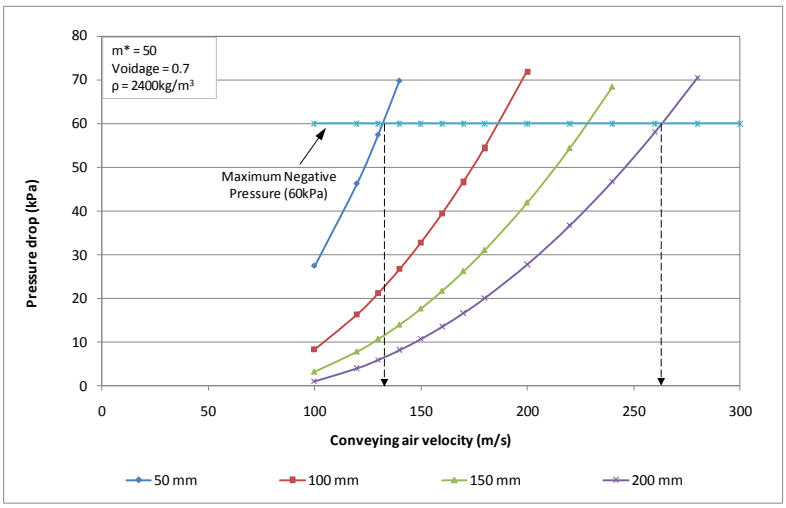

Figure 5.10: Effects of particle size on pressure loss of the system for material with density 2400kg/m^3

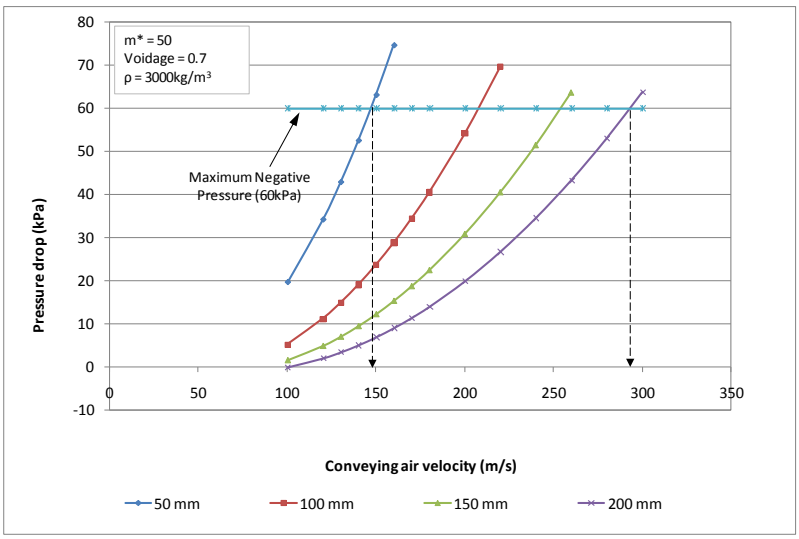

Figure 5.11: Effects of particle size on pressure loss of the system for material with density 3000kg/m^3

Figure 5.10 and Figure 5.11 reveal that as the particle size of rock fragments reduces the pressure drop of the system increases. The same scenario has been

observed for rock fragments with density 2400kg/m^3 and 3000kg/m^3. Results also show that particles with smaller diameter results in higher pressure drop than those with larger diameters. The increase in pressure drop for smaller particle size is attributed to the fact that as the particle size reduces, its mass also reduces thereby increasing the transport velocity of the particle in the pipe. From Darcy equation, an increase in particle velocity results in an increase in pressure loss in the suction pipe. According to Figure 5.9 (for material with density 2400kg/m^3) at maximum negative pressure, the conveying air velocity of the system varies from 132m/s (for particles with diameter 50mm) to 263m/s (for particle with diameter 200mm). For material with density 3000kg/m^3, the conveying velocity varies from 147m/s to 293m/s for 50mm and 200mm size particles respectively.

5.4.2 Effects of particle size on mass flow rate of solids

The effects of particle size on mass flow rate of solids of the pneumatic loading system at maximum negative pressure were also studied. Figure 5.12 and Figure 5.13 shows the results obtained for material with density 2400kg/m^3 and 3000kg/m^3.

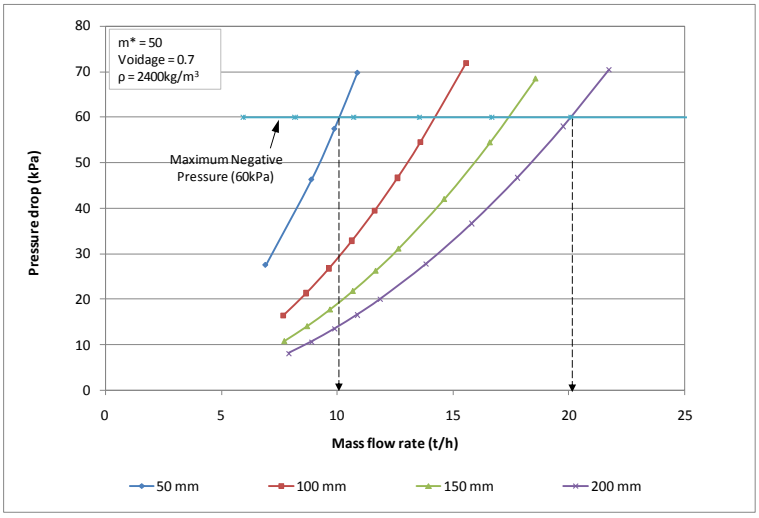

Figure 5.12: Effects of particle size on mass flow rate of solids of the system for material with density 2400kg/m^3

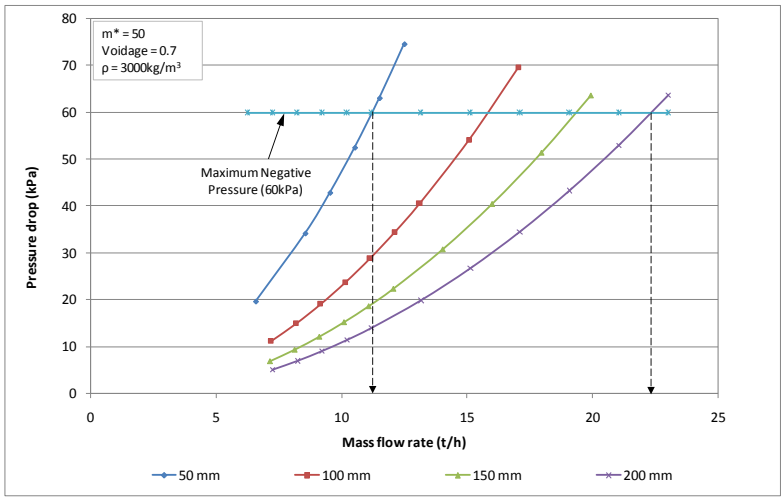

Figure 5.13: Effects of particle size on mass flow rate of solids of the system for material with density 3000kg/m^3

According to the results obtained (Figure 5.12 and 5.13), at maximum negative pressure, rock fragments with 50mm particle diameter results in lower mass flow rate than particles with size 200mm. From Figure 5.12 (rock density 2400kg/m^3), it is clear that particles with 50mm size result in mass flow rate of 10t/h while rock fragments with size 200mm gives 20t/h. Similarly, particles with density 3000kg/m^3 result in mass flow rate of 11t/h (for 50mm size particles) and 23t/h (for 200mm size particles). The larger mass flow rate resulting from larger particle size is attributed to the fact that at maximum negative pressure, larger particles require larger conveying (pushing) velocity than smaller particles.

5.4.3 Effects on power consumption

The power input to a pneumatic conveying system is through the air supply. Therefore, the power of the system is a function of air flow rate and pressure drop of the system. Equation 3.41 is used to determine the power consumption of the pneumatic system for rock fragments with density 2400kg/m^3 and 3000kg/m^3. Figures 5.14 and 5.15 show the results obtained at maximum negative pressure.

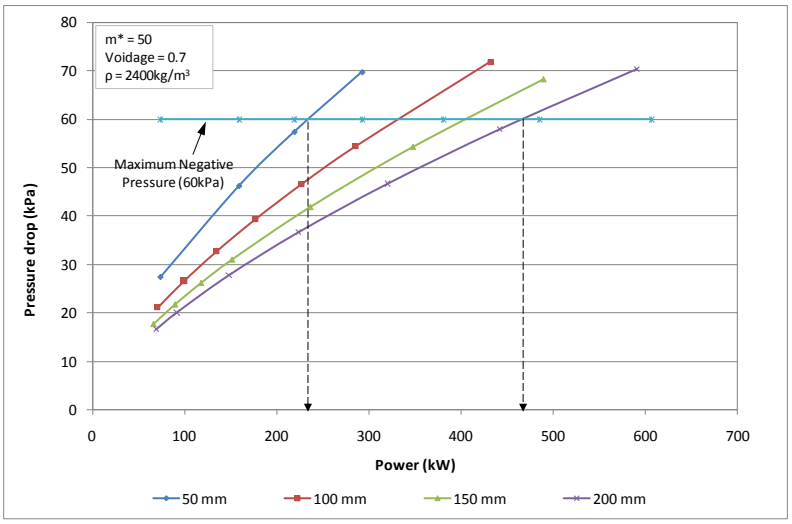

Figure 5.14: Effects of the system on power consumption for material with density 2400kg/m^3

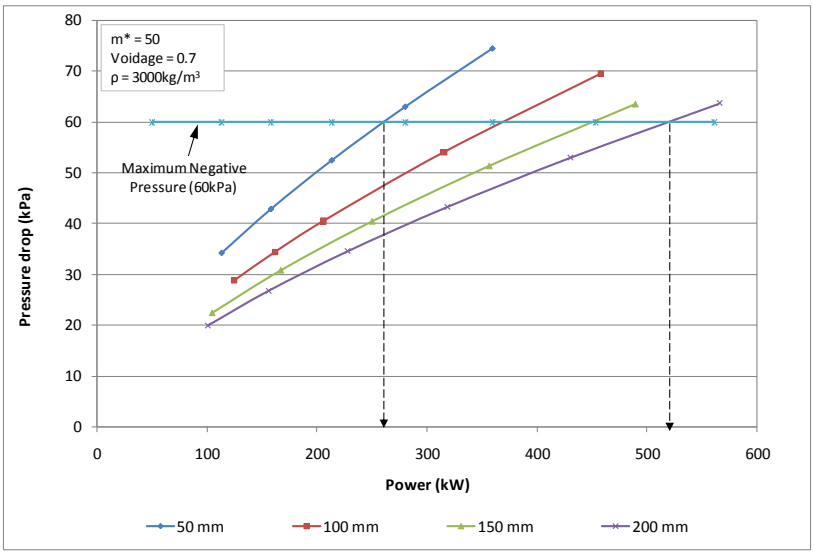

Figure 5.15: Effects of the system on power consumption for material with density 3000kg/m^3

According to Figure 5.14 and Figure 5.15, the power increases in proportion to the density and size of rock fragment being conveyed. At maximum negative pressure, rock particles (with density 2400kg/m^3 and 3000kg/m^3) with smaller diameter (i.e. 50mm) result in smaller power than larger particles (i.e. 200mm). As can be seen from Figure 5.14 (ρ= 2400kg/m^3), at maximum negative pressure, the power varies from approximately 220kW to 460kW for 50mm and 200mm particle size respectively. Similarly, for rock fragments with density 3000kg/m^3,

power varies from approximately 270kW to 540kW for 50mm and 200mm rock particles respectively. The increase in power is attributed to the high air velocity required to convey larger and denser particles as compared to lighter and smaller particles.

5.5 Optimum operating parameters

5.5.1 Optimum mass flow rate of the pneumatic system

According to Figure 5.12 and Figure 5.13, the mass flow rate of solids in the suction pipe of the system depends on the conveying air velocity at maximum negative pressure the density of rock fragments and also on rock fragmentation. Results show that the optimum mass flow rate of solids in the suction pipe at maximum negative pressure would vary from 10t/h to 23t/h depending on the density and rock fragmentation. Table 5.1 summarises the optimum capacity at maximum negative pressure.

Table 5.1: Mass flow rate of solids at maximum negative pressure.

Air Vel (m/s)	Density of rock fragments (kg/m^3)	Particle size (mm)	Max. Negative Pressure (kPa)	Mass flow rate (t/h)
132.0	2400	50	60	10.0
147.0	3000	50	60	11.2
263.0	2400	200	60	20.0
293.0	3000	200	60	22.3

5.5.2 Optimum power consumption

In section 5.4.3, the effects of rock density as well as rock fragmentation on system power consumption was discussed. According to the results, at maximum negative pressure, the optimum power would vary from 220kW to 540kW depending on the density and particle size of the rock fragments being conveyed.

5.5.3 Optimum loading time

Figure 5.16 and Figure 5.17 show the optimum loading time of the pneumatic loading system at maximum negative pressure for different rock fragments and rock density.

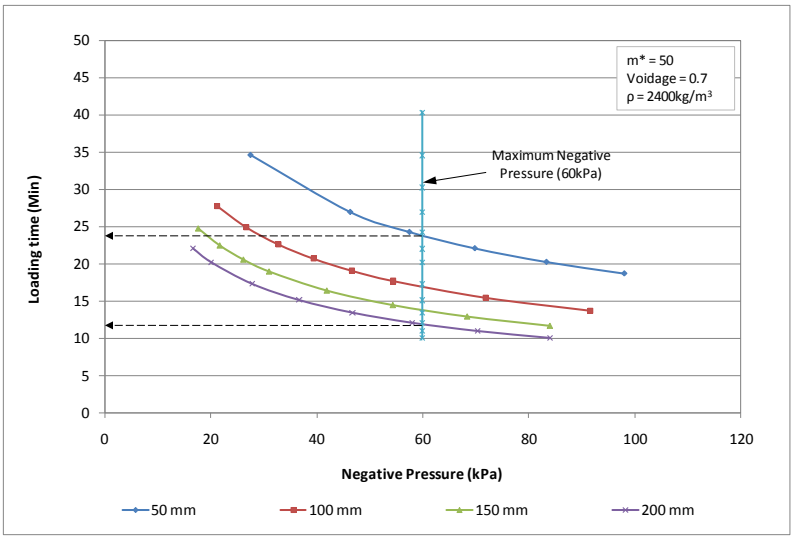

Figure 5.16: Optimum loading time for material with density 2400kg/m^3

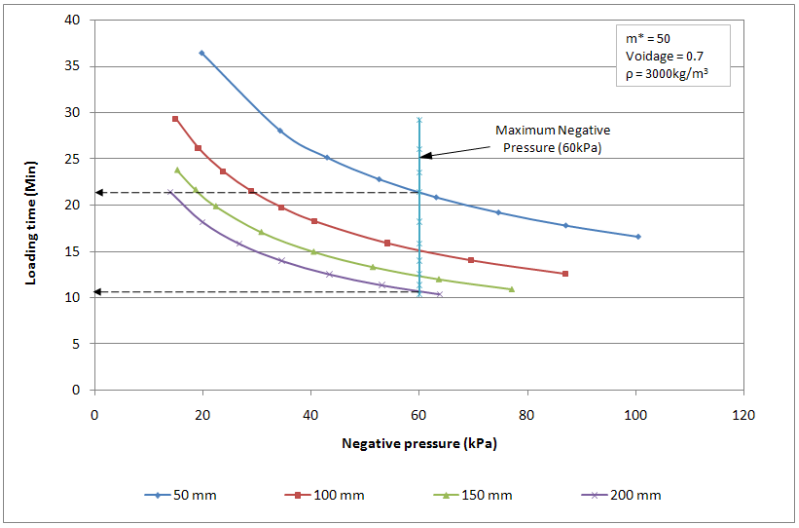

Figure 5.17: Optimum loading time for material with density 3000kg/m^3

Results show that the loading time of the pneumatic loading system depends on the conveying air velocity (or maximum negative pressure), the density of rock fragments as well as the fragmentation of the rocks being conveyed. At

maximum negative pressure, Figure 5.16 and Figure 5.17 reveal that the loading time for lighter and more fragmented rock is higher than for heavier and less fragmented rocks. As indicated in Figure 5.16 (ρ =2400kg/m^3), the loading time of the system varies from 12 minutes (for 200mm rock fragments) to 24 minutes (for 50 mm rock fragments). However, for rock fragments of density 3000kg/m^3 (Figure 5.17), the loading time varies from 11 minutes (for 200mm rock fragments) to 22 minutes (for 50 mm rock fragments). Therefore, the optimum loading time for the pneumatic system would vary from 11 minutes to 24 minutes depending on the density and size of rock fragments being conveyed.

5.5.4 Rock fragmentation

According to Franklin and Katsabanis (1996) rock fragmentation can mean anything from "the limit of breaking" to "the percentage passing, above or below a certain size." During pneumatic suction of broken rock, it should be recognised that rock fragmentation have strong effects on system productivity. Therefore, with monorail application, control of rock fragmentation is important in ensuring smooth suction of rock fragments by the pneumatic system. This means also that rock fragments after blasting should be carefully controlled to avoid choking of the suction pipe during the suction process. The blast design of the decline face for monorail application should, thus, optimise rock fragmentation so as to optimise productivity of the suction system.

5.5.4.1 Post-blast material size distribution

Fragment size measurement of blasted rock has become active research field as computers, digitizing and image analysis techniques progress (Franklin and Katsabanis, 1996). Fragment size distribution, the creation of new surface in blast-fragmented rock, energy consumption and rock strength properties are the most important interrelated variables. According to Franklin and Katsabanis (1996) the significant fractions after rock blasting can usually be classified as

oversize, fines and mid-range. In underground mines, the oversize can be boulder size above which secondary breakage is necessary before further handling normally above 300mm. Kuznestov characteristic-size and Roslin-Rammler distribution equations are valid starting points for modelling fragment distribution in rock blasting and their combination has resulted in the development of the Kuz-Ram model. Figure 5.18 shows an example of size distribution curve after rock blasting.

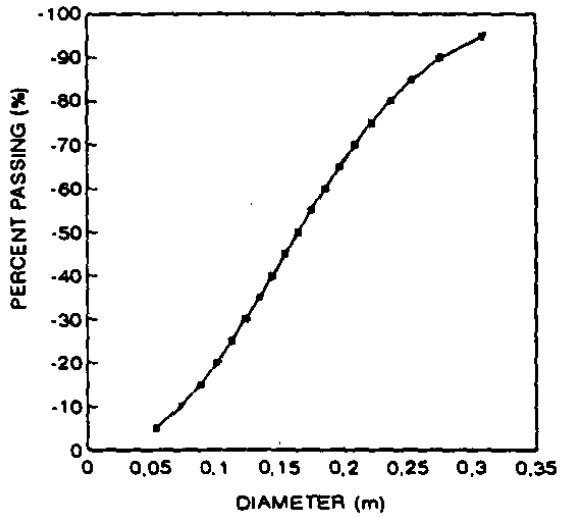

Figure 5.18: Size distribution curve (Franklin and Katsabanis, 1996)

5.5.4.2 Optimum rock fragmentation

The size of rock fragments in pneumatic conveying system plays an important role during solid conveyance. This means that the efficiency and performance of the pneumatic conveying system depends on the particle size being transported, conveying air velocity, density of rock fragments and the pipe diameter of the suction system. Therefore, it is essential that the optimum rock fragmentation that is handled economically by the monorail pneumatic loading system at different conveying velocities is determined. In this section, the optimum rock fragmentation of the monorail loading system is determined at maximum negative pressure (i.e. 60kPa). The optimal rock fragmentation for monorail pneumatic loading system is that which gives the maximum productivity at given conveying air velocity. Therefore, in determining the optimal rock fragmentation

for the loading system, the size of rock fragments that resulted in maximum mass flow rate was considered optimal. Thus, for each conveying air velocity, the size of rock fragments that gave the maximum mass flow rate in the suction pipe was determined. The optimum rock fragmentation for varying conveying air velocity was determined at m*=50. Figure 5.19 and Figure 5.20 shows the optimum particle size of the system.

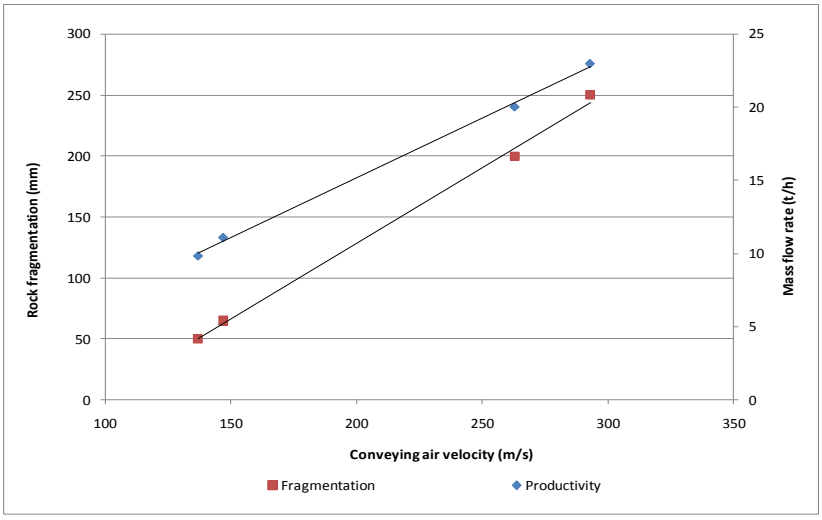

Figure 5.19: Rock fragmentation and mass flow rate at different conveying air velocities ρ=2400kg/m3 (Voidage = 0.7; Pipe diameter = 220mm)

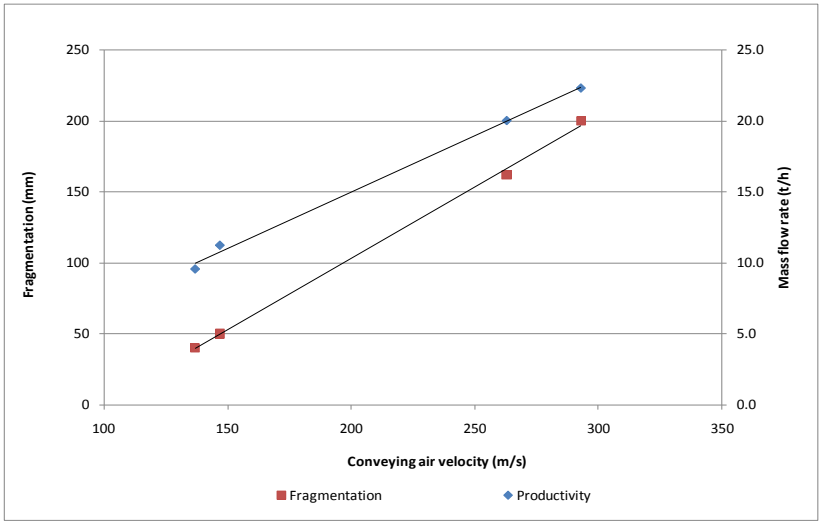

Figure 5.20: Rock fragmentation and mass flow rate at different conveying air velocities ρ=3000kg/m3 (Voidage = 0.7; Pipe diameter = 220 mm)

Figures 5.19 and 5.20 show that the optimal rock fragmentation is directly proportional to the conveying air velocity of the loading system. This means that as the conveying air velocity increases, the optimum rock fragments being sucked by the system also steadily increases. Results also indicate that rock fragmentation has direct effects on the mass flow rate (i.e. productivity) of the suction system. According to the results obtained, the more fragmented rock particles result in low productivity while larger particles have higher productivity. Therefore, optimal rock fragmentation from the development face would vary from 50mm to 200mm as indicated in Figure 5.21.

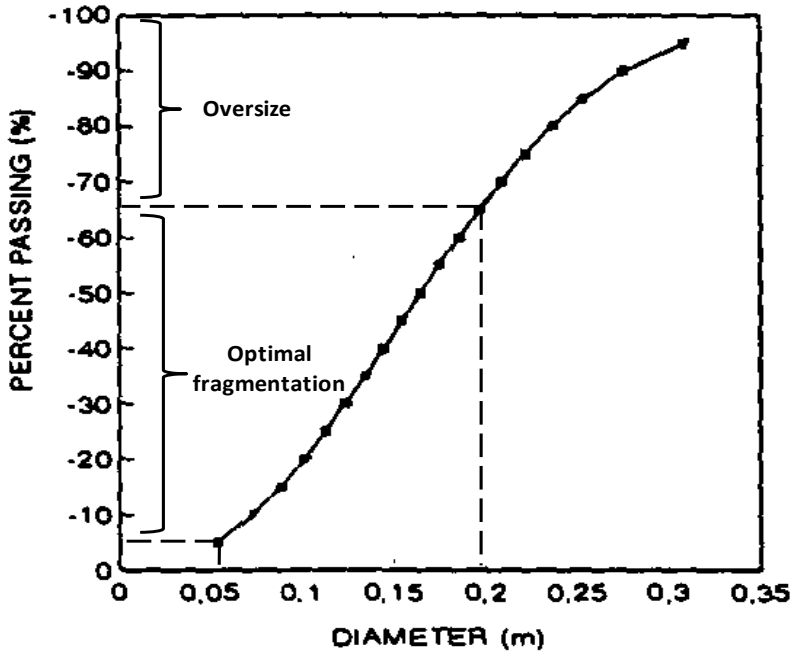

Figure 5.21: Size distribution curve showing optimal fragmentation range

Figure 5.21 also shows that only 65% of the rock fragments in a muck pile will be sucked at maximum conveying pressure leaving 35% as oversize rock fragments.

5.5.4.3 Dealing with oversize

According to Figure 5.21, the muck pile at the development face will contain 35% oversized fragments that will not be sucked by the pneumatic suction system. The oversized materials will create problems during pneumatic loading

operations and as such they will need to be reduced to manageable sizes by secondary breaking at the face. The following are the suggested method of reducing the oversize rock fragments to size fractions that can be sucked by the system.

- Segregating the oversize material at the face and using secondary blasting to reduce them to manageable size.
- Use impact hammer to fragment the oversize material at the face.

It is also suggested that to control rock fragmentation at the development face, more research be conducted so as to come up with blast design pattern that will reduce or minimize the percentage of oversize rock fragments after blasting.

5.5.4.4 Issues of dust generation

With monorail pneumatic conveying systems, dust is generated during gas-solid separation as well as during discharge of material in monorail containers. Much dust with this system results from suction of fine dust resulting from blasting operations and degradation of rock fragments in the conveying process. Thus, the amount of dust generated during suction and discharge processes is a function of conveying conditions in terms of conveying air velocity (or operating negative pressure) and the fineness of the material being conveyed. Therefore, with the monorail pneumatic loading system, the gas-solid separation device (i.e. the hopper) has two functions:

- To store conveyed rock fragments, and
- To minimise pollution of the working environment by the conveyed material especially during discharge process.

This means that extreme measures must be taken into account to prevent the escape of dust particles into the working environment during conveying and discharge process, particularly if potentially hazardous rock fragments are being

conveyed. Therefore, the storage hopper should be designed with dust control mechanism. The following dust control mechanism has been suggested for the monorail system.

(a) Use of gravity settling chambers

This is a type of equipment for separating solid material from gas stream. With this equipment, the velocity of the gas-solid stream is reduced and the residence time is increased. This will allow the particles to fall under gravity as the gas containing dust is collected as indicated in Figure 5.22.

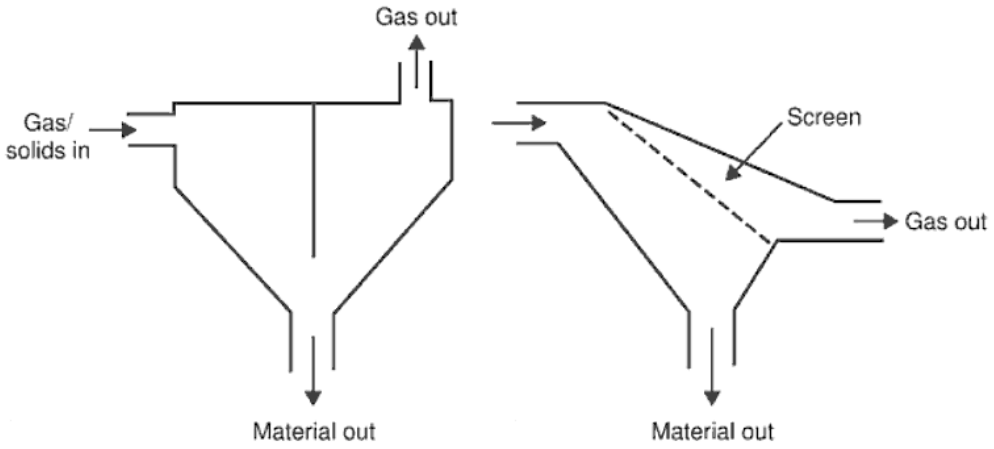

(a) (b)

Figure 5.22: Gravity settling chamber; (a) basic system (b) design incorporating screen (Mills, 2004)

(a) Use of dust suppression chemicals

The dust generated during discharge of material from the hopper into monorail containers is normally airborne and therefore, a misting based solution is the most practical approach to control it. Mist is normally mixed with dust suppression chemicals to increase the performance of suppressing airborne dust. Dust suppression using water sprayers is not recommended in this application as it has negative effects on the suction system i.e. combination of water and fine

material forms clayish material that blocks the suction pipe during suction process.

5.6 Pump selection for pneumatic loading system

Pump selection can be both arbitrary and specific i.e. for a given duty requirement, several alternative types of pump may be suitable when the choice of type may be based on "accept practice" or individual preference e.g. based on costs and performance. The choice can also be made purely on technical grounds. Based on technical grounds, pump selection for monorail pneumatic loading system can be done by analysis of the hydraulic system and the pump location and function. Therefore, the initial decision that must be made in applying a pump is the decision regarding the type of pump to use. According to literature (Bankston and Baker, 1994), centrifugal pumps are used in pneumatic sucker during shaft sinking. Therefore, a centrifugal pump is used for the design of monorail pneumatic loading system. According to Bankston and Baker (1994) before selecting a pump that fits one's needs, the following must be known:

1) The desired flow rate (pump capacity);
2) The total head or pressure against which it must operate;
3) The suction lift; and
4) Characteristics of the fluid.

5.6.1 Pump capacity

In order to select a pump that meets the requirements of the system in an efficient manner, the pump must be matched to the piping system and required flow rate. Therefore, the required capacity of the pump is dictated by the requirements of the system in which the pump is located. Normally, a process system is designed for a particular throughput. Therefore, in determining the pump capacity of the monorail pneumatic loading system, the maximum mass flow rate is used as pump capacity of the system. According to Table 5.1, at

maximum negative pressure, the pneumatic loading system has minimum capacity of 10t/h with maximum being 23t/h depending on the rock fragments being conveyed. Therefore, the maximum value is used to determine the pump capacity for the system.

5.6.2 Total Head

To determine the required size of a centrifugal pump for a particular application, all components of the system head in which the pump is to operate must be added up to determine the pump total head (TH). The monorail pneumatic loading system consists of three separate components of total head i.e.:

1. Static head
2. Friction head
3. Pressure head

Each of these three components must be considered for the system in which the pump is to operate, and the sum of these is the total head of the pump. Determination of total head in monorail system is achieved by the application of Bernoulli's equation (Equation 5.5) to the system as indicated in Figure 5.23:

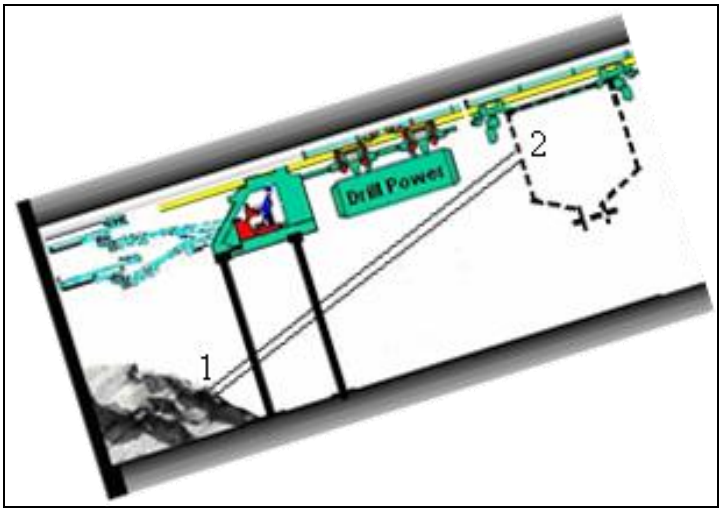

Figure 5.23: Monorail loading system total head determination.

$$\frac{P_1}{\rho g} + \frac{v_1^2}{2g} + z_1 = \frac{P_2}{\rho g} + \frac{v_2^2}{2g} + z_2 + h_f - H_T \qquad 5.5$$

Where:

H_T is total pump head [m]

h_f is friction head loss [m]

z is elevation at position 1 and 2

v is velocity of fluid at position 1 and 2

P_1 and P_2 is pressure at position 1 and 2 respectively

Since velocity is constant throughout the fluid flow in the suction pipe, the total head is therefore, given by Equation 5.6:

$$H_T = \frac{\Delta P}{\rho g} + \Delta Z + h_f \text{ [m]} \qquad 5.6$$

Where:

ΔZ is vertical height difference between point 1 and 2 (i.e. Static Head).

ΔP is the change in pressure (maximum negative pressure)

5.6.2.1 Static head

Static head (ΔZ) is the total elevation change that the solids must undergo during conveyance. In effect, static head represents the net change in height that the pump must overcome. For the monorail system the static head is the total elevation change from decline floor to the hopper i.e. the vertical distance from the muck pile to the hopper (Figure 5.24).

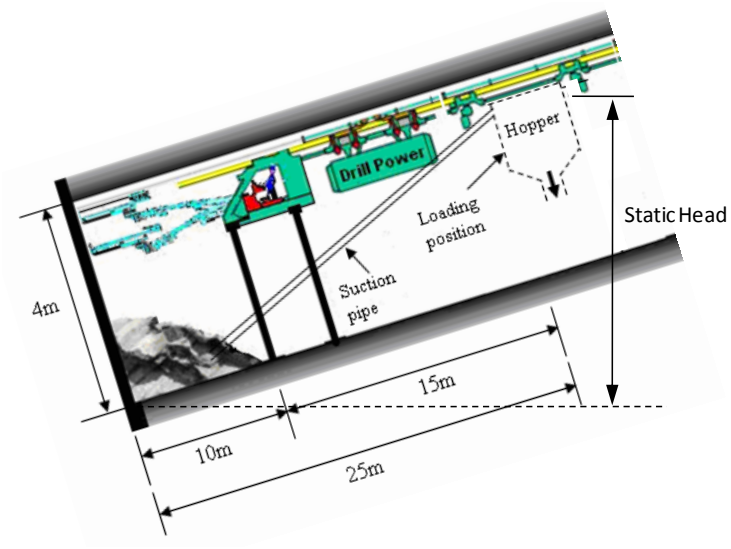

Figure 5.24: Static Head of the monorail pneumatic loading system

5.6.2.2 Friction head

Friction head (h_f) is the head necessary to overcome the friction losses in the piping, valves, and fittings for the system in which the pump operates. This is the amount of pressure (or head) required to 'force' fluid through pipe and fittings. When an incompressible fluid flows in a pipe and the flow is turbulent, the friction head loss is a function of the pipe length, diameter of pipe, surface roughness of the pipe wall, the velocity of the fluid in the pipe, the density of the fluid, and the viscosity of the transporting gas (i.e. air) in the pipe. Darcy-Weisbach equation (expressed in terms of friction head losses) as indicated in Equation 5.7 is generally used to calculate the frictional head losses in pipes. It is assumed that this is approximately valid for air which is a compressible fluid.

$$h_f = f \frac{L}{D} \frac{v^2}{2g} \qquad \text{[m]} \qquad 5.7$$

Where:

f is friction factor [m]

g is acceleration due to gravity [ms^{-2}]

Friction factor is determined for the turbulent flow regime, using the relationship between the relative roughness of pipe and the Reynolds Number i.e. using Colebrook or the Moody Chart. Therefore, friction head loss for monorail pneumatic loading system was determined using Equation 5.7. The friction factor is determined as outlined in Equation 3.15.

5.6.2.3 Pressure head

Pressure head is the head required to overcome a pressure or vacuum in the system upstream or downstream of the pump. For the monorail system, pressure head is determined using Equation 5.8.

$$H_p = \frac{\Delta P}{\rho g} \quad [\text{m}] \qquad 5.8$$

Table 5.2 shows the Pressure Head, Static Head, Friction Head as well as the total head of the monorail pneumatic loading system at maximum negative pressure (ΔP).

Table 5.2: Pressure head, Static head, Friction head and Total head of the monorail loading system at maximum negative pressure.

Conveying Air Vel (m/s)	Particle diameter (m)	Particle velocity (m/s)	Pressure Head Hp – (m)	Static Head ΔZ – (m)	Friction Head h_f - (m)	Total Head H_T – (m)
132.0	0.05	2.56	2.5	11.4	10.7	24.6
147.0	0.05	2.27	2.0	11.4	10.7	24.1
263.0	0.20	5.09	2.5	11.4	10.6	24.5
293.0	0.20	4.53	2.0	11.4	10.6	24.1

5.6.3 Pump performance curve

A pump's performance is shown in its characteristic performance curve where its capacity i.e. mass flow rate is plotted against its total head. The pump performance curve also show its Best Efficiency Point (BEP), required input

Brake-Horsepower (BHP), Net Positive Suction Head (NPSH), speed in Revolutions Per Minute (RPM), and other information such as pump size and type, impeller size, etc. This curve is plotted for a constant speed and a given impeller diameter. Typical performance curve is shown in Figure 5.25.

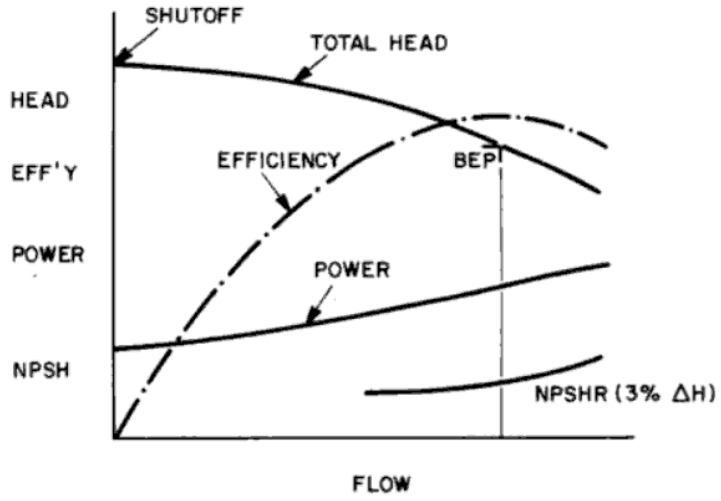

Figure 5.25: Typical pump performance curve

5.6.4 Brake-horsepower and Pump efficiency

The brake horsepower refers to the amount of energy (or actual amount of power) that must be supplied to operate a pump so as to obtain a particular flow and head. It is the input power to the pump or the required output power from the driver. Brake horsepower is determined using Equation 5.9.

$$\mathrm{BHP} = \frac{\mathrm{Q} \times \mathrm{H} \times \mathrm{s.g}}{3960 \times \eta} \qquad 5.9$$

Where:

Q is Flow rate [m^3/s]

H is the Total Head [m]

s.g is specific gravity

η is the pump efficiency.

The BHP required to operate a pump at a given point can also be obtained from the pump performance curve. On the pump performance curve, the brake horsepower curve runs below the total head (Figure 5.25). There is a brake horsepower curve for each different impeller trim usually provided by the manufacturer of the pump.

The efficiency of the pump can also be obtained from the pump performance curve. The pump efficiency normally measures the degree of its hydraulic and mechanical perfection. On the pump performance curve, the efficiency curve intersects with the head-capacity curve. Thus each pump will have its own maximum efficiency point. Therefore, the pump efficiency and brake-horsepower for monorail pneumatic loading system was determined using a 3600 rpm pump characteristic curve based on the maximum pump capacity i.e. 22.3t/h (7.4m^3/h) as well as maximum total head i.e. 24.6m (Figure 5.26).

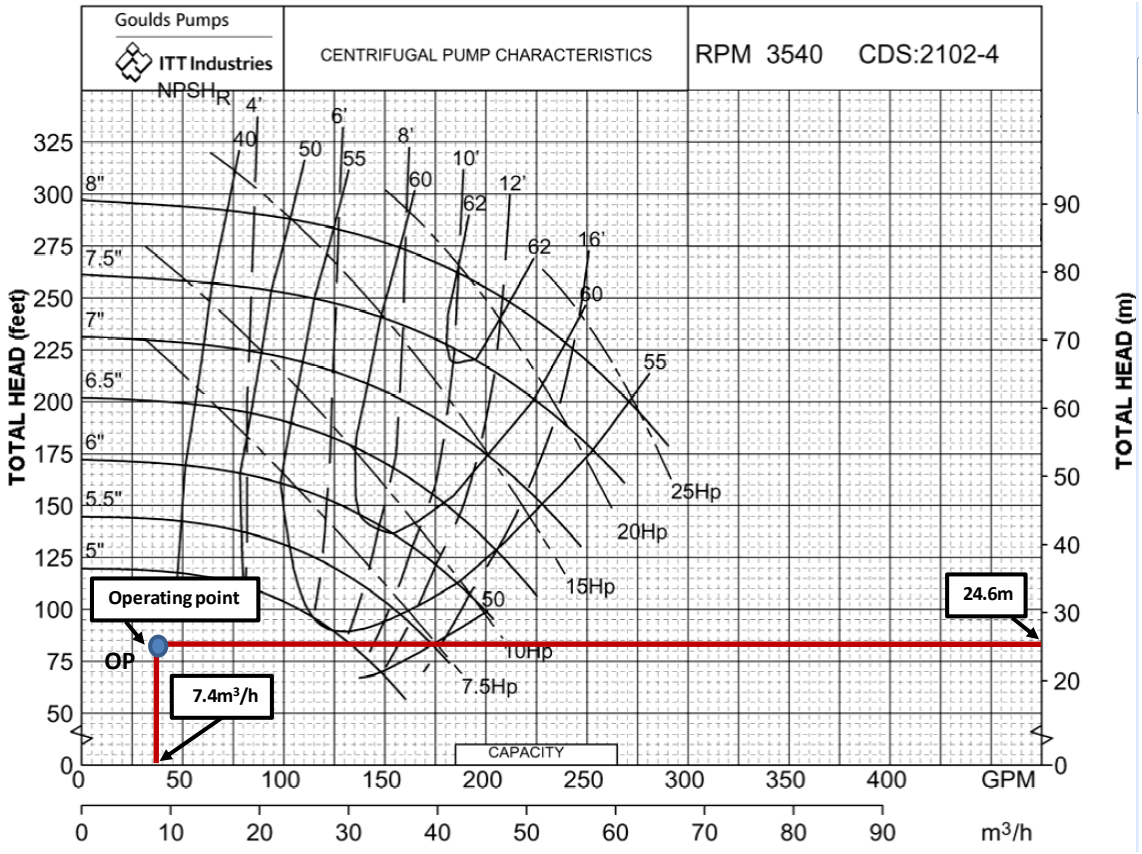

Figure 5.26: Performance curve showing operating point (OP) of the monorail pneumatic loading pump

The maximum capacity and total head of the pneumatic loading system were plotted on the 3600 rpm pump characteristic curve, to give the pump operating point shown as **OP** in Figure 5.26. According to Figure 5.26, the pump characteristics for the pneumatic loading system are indicated in Table 5.3.

Table 5.3: Pump characteristics for monorail pneumatic loading system

No.	Parameter	Value
1	Pump Horsepower	7.5HP
2	Pump Efficiency	40%
3	Impeller diameters or trims	5”

5.7 Summary

From the theoretical study, it has been determined that the transportation of rock fragments from development face into monorail containers is possible with the use of pneumatic loading system. Results have shown that the solid loading ratio determines the amount of solids in the suction pipe. Thus, the higher the solid loading ratio, the higher the mass flow rate of solids in the pipe. Results also indicate that the mass flow rate of solids depends on the maximum negative pressure, density of the rock fragments as well as rock fragmentation. At maximum negative pressure, larger rock fragments results in higher mass flow rate than more fragmented rock particles.

In terms of pressure loss, the study has revealed that the pressure loss of the system depends mostly on the rock fragmentation. It was observed that more fragmented rocks would result in more pressure loss due to their higher superficial velocity in the suction pipe than larger particles. Therefore, more fragmented rock particles would result in less mass flow rate than larger particles. Also due to higher velocity that is required to convey larger rock fragments, results show that more power is required to convey larger particles. Therefore, as a result of this high velocity, the loading time of larger rock fragments is lower than more fragmented particles.

Chapter 6

6.0 Simulation of monorail system

6.1 Introduction

In Chapters 4 and 5, the monorail drill-load-haul system was developed based on theory. It is therefore, necessary to determine the performance of the system using time and motion studies. The aim of this Chapter is therefore, to model the monorail drill-load-haul system and use computer simulation to determine the performance of the system in terms of advance rates per shift against which operational performance will be measured. GPSS/H simulation software and PROOF animation technology is used to simulate and animate the system respectively. During the simulation process, the sensitivity of the monorail system to variation in design parameters is explored.

6.2 Discrete-Event Simulation

Simulation is defined as "the process of designing a computerised model of the system (or process) and conducting experiments with this model for the purpose of either understanding the behaviour of the system or of evaluating various strategies for operations of the system" (Udo and James, 1993). The act of simulating generally entails representing certain key characteristics or behaviour of a selected physical or abstract system in order to identify and understand the factors which control the system and / or to predict the future behaviour of the system. The purpose of simulation is therefore, to shed light on the underlying mechanisms that control the behaviour of a system. More practically, simulation can be used to predict (forecast) the future behaviour of a system and determine what you can do to influence that future behaviour. This

means that simulation can be used to predict the way in which the system will evolve and respond to its surroundings. Therefore, during simulation process one can identify any necessary changes that will help make the system perform the way that is desired. It is a powerful and important tool because it provides a way in which alternative designs, plans and / or policies can be evaluated without having to experiment on a real system, which may be prohibitively costly, time-consuming, or simply impractical to do.

Because simulation is such a powerful tool to assist in understanding complex systems and to support decision-making, a wide variety of approaches and simulation tools exist (Fisherman, 2001). Modelling complex systems especially in engineering, health, management, mathematics, military, telecommunications and in transportation science uses discrete-event as a simulation tool. This is because it provides a relatively low-cost way of gathering information for decision making. Fisherman (2001) described discrete event system as a system in which one or more phenomenon of interest changes value or state at discrete points in time, rather than continuously with time. Thus, in discrete event system, the number of things taking place can be counted at any one instant in time (Sturgul, 2000).

Discrete event simulation has long been an integral part of the design process of complex engineering systems and modelling of natural phenomena (Carl, 2002). Many of the systems which we seek to understand or control can be modelled as digital systems. In digital model, we view the system at discrete instants of time in effect taking snapshots of the system at these instants. In designing, analysing and operating such complex systems, one is normally interested not only in performance evaluation but also in sensitivity analysis and optimization. Therefore, during simulation of the monorail system discrete-event simulation system is used.

6.3 Model Development

Fisherman (2001) defined a simulation model as an abstract logical and mathematical representation of a system that describes the relationship among objects in a system. Therefore, to model a system such as the monorail drill-load-haul system, one must first understand its working principles. Acquiring sufficient understanding of the system to develop an appropriate conceptual, logical and then simulation model, is one of the most difficult tasks in simulation analysis. Therefore, clear understanding of all working principles and processes of the monorail system is fundamental in coming up with a valid model. Figure 6.1 shows the model development cycle whilst Figure 6.2 offers an elaboration of the phases within each of these periods. The figures also depict the processes by which a modelling study transitions from one phase to another.

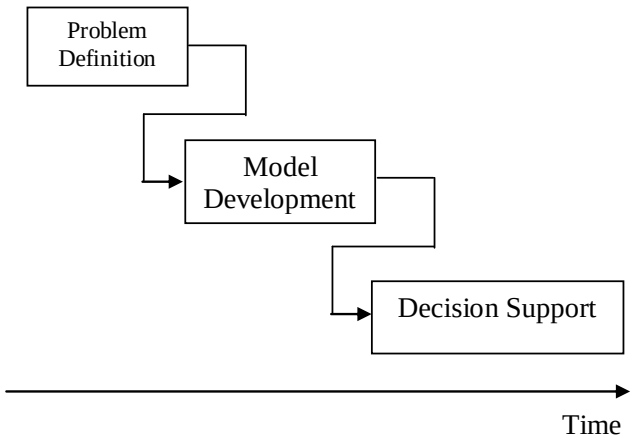

Figure 6.1: Chronological periods of the model life cycle (Nance, 1984)

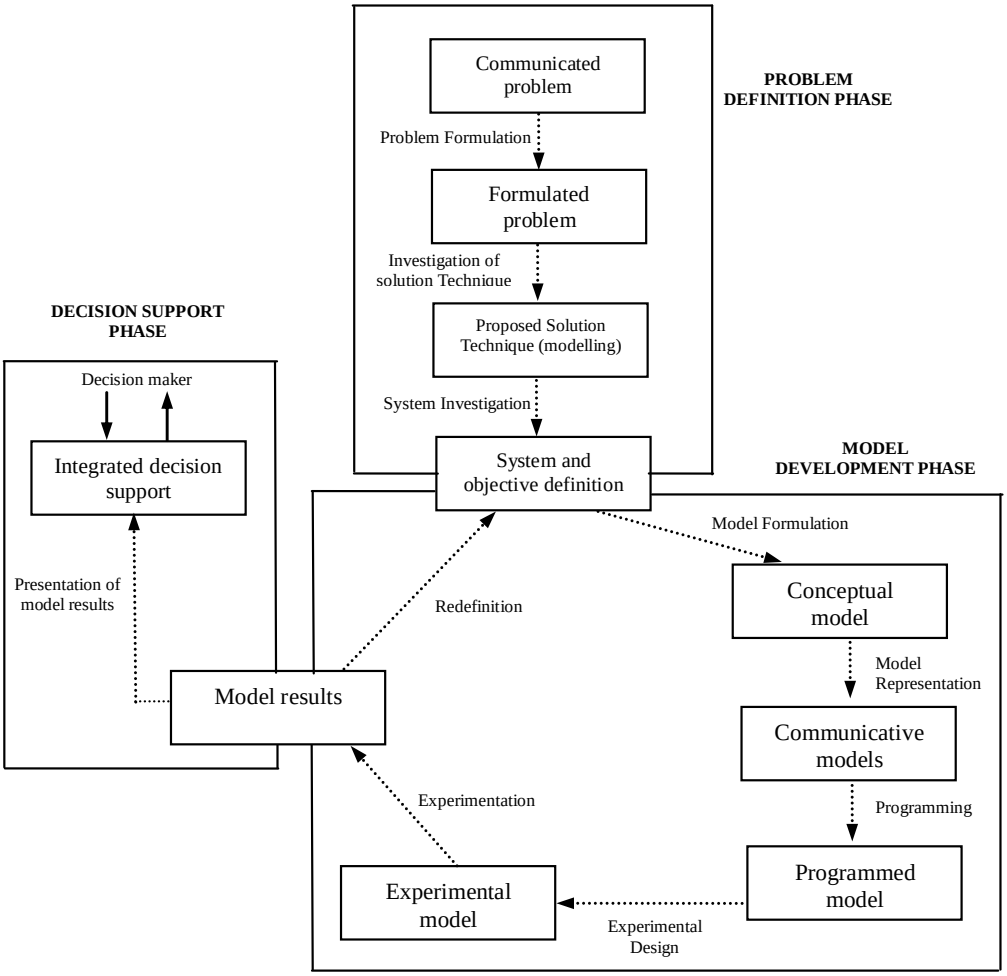

Figure 6.2: Phases in chronological periods of the model life cycle (Nance, 1984)

In general, having a definitive approach for conducting a simulation study is critical to the study's success and to developing a valid model in particular. Therefore, this section describes the approach that is followed during simulation of the monorail system.

6.3.1 Problem formulation

The first step in conducting a significant simulation project is to ensure that adequate attention is directed towards understanding what is to be accomplished by performing the study. During problem formulation, the problem of interest should be stated. According to Law (2005) the problem may

not be stated precisely or in quantitative terms. However, during this stage, an iterative process is often necessary. Chung (2003) also reviews that during problem formulation stage, the simulation practitioner can firmly establish the practicality of using simulation to analyse the system. Thus, at this stage the overall objectives as well as the specific questions to be answered by the study are highlighted.

6.3.2 Validity of conceptual model

To obtain best results from the simulation model, it is necessary to ensure that the conceptual model is valid. It is often necessary to perform a structured walk-through of the conceptual model to check its validity. If errors or omissions are discovered the conceptual model must then be corrected before programming commences.

6.3.3 Program the model

This stage involves programming of the model using simulation software. Selection of simulation software to be used during programming is critical at this stage. Software selection for simulation modelling is invariably a more complex process. It requires a careful and thoughtful approach to fully address the issues and impacts related to decisions.

After the model has been programmed into simulation software, verification and debugging of the programme follows. In general, verification focuses on the internal consistency of a model, while validation is concerned with the correspondence between the model and the reality. The term validation is applied to those processes which seek to determine whether or not a simulation is correct with respect to the "real" system. More prosaically, validation is concerned with the question "Are we building the right system?" Verification, on the other hand, seeks to answer the question "Are we building the system right?"

Verification checks that the implementation of the simulation model (program) corresponds to the model.

There are currently no algorithms or procedures available to identify specific validation techniques, statistical tests, etc., to use in the validation process (Sargent, 1991). Various authors e.g., Shannon (1975) suggest that, as a minimum, the three steps i.e. (1) Face validity, (2) Testing of the model assumptions, and (3) Testing of input-output transformations be made. Therefore, during monorail model development, it was prudent to validate and verify the model so as to get accurate (but not 100%) results from the model. Verification was done by performing tests on the model and by so doing errors were identified, and corrections made to the underlying model.

6.3.4 Model performance measure

The simulation models are often subject to errors caused by the estimated parameter(s) of underlying input distribution function. "What-if" analysis is needed to establish confidence with respect to small changes in the parameters of the input distributions. Performance measure is used to developing measurable performance indicators of the system. However, estimating system performance for several scenarios via simulation generally requires a separate simulation run for each scenario. Thus, a system performance measure is normally estimated by a value or series of values quantifying system behaviour as captured by the model and simulation (Standridge and Tsai, 1992). In simulating the monorail system, tasks / processes were reviewed, analysed and interpreted and by so doing performance requirements were revised. The following performance measures that relate to the monorail system itself as well as the system processes were of interest.

6.3.4.1 System performance measure

The overall performance value of the monorail system depends on its operational speed i.e. the efficiency with which the system completes the scheduled job. Thus, the performance of the monorail system is measured by the speed with which it completes drilling and cleaning the development face i.e. the number of development ends drilled and cleaned respectively during the shift. These parameters are determined as indicated in Equations 6.1 and 6.2:

$$\text{No. of ends drilled / shift} = \frac{\text{Total hours in a shift}}{\text{Time to drill face}} \qquad 6.1$$

$$\text{No. of ends cleaned / shift} = \frac{\text{Total hours in a shift}}{\text{Time to clean face}} \qquad 6.2$$

The system also needs targets against which the above performance can be judged. These targets determine the true capabilities of the system. The need for targets emphasises the point that operational performance can only be meaningful if measured against the system capabilities. Therefore, for the monorail system, the advance rate was determined at minimum loading time and is used as target to evaluate the system capability.

6.3.4.2 Process performance measure

Process performance measure relates to time interval that a process is delayed in the system. This means that the more time the process takes to be completed, the more inefficient will be the system and vice versa. During simulation of the monorail system, the following process performance measures were of interest:

- Time spent to drill the development face;
- Time spent to load rock fragments from the development into the hopper;
- Time spent to clean the development face; and

- Time to drill, blast, load and haul rock fragments from development face to surface.

Therefore, the performance of the monorail system is judged by its effectiveness and efficiency with which the above processes are fulfilled. This means also that the faster the system achieves the above processes, the more efficient is the system and vice versa.

6.4 Simulation of monorail system

6.4.1 Description of monorail simulation system

In this section all processes of the monorail drill-load-haul system are described. The section is intended to show the major processes of the monorail system that are modelled during simulation process. Figure 6.3 shows the process flow chart for the monorail drill-load-haul system.

According to Figure 6.3, the monorail drill-load-haul system consists of three processes i.e. drilling, loading and material haulage (including dumping) to surface. In the monorail system, these processes are interdependent and affect the drill-blast-load and haul cycle time and eventually performance of the system. Because the monorail drilling system depends on the pneumatic loading system, therefore, to determine the optimal drill-blast-load and haul cycle time of the system, sensitivity analysis of the pneumatic loading time on the total cycle time was performed during simulation studies.

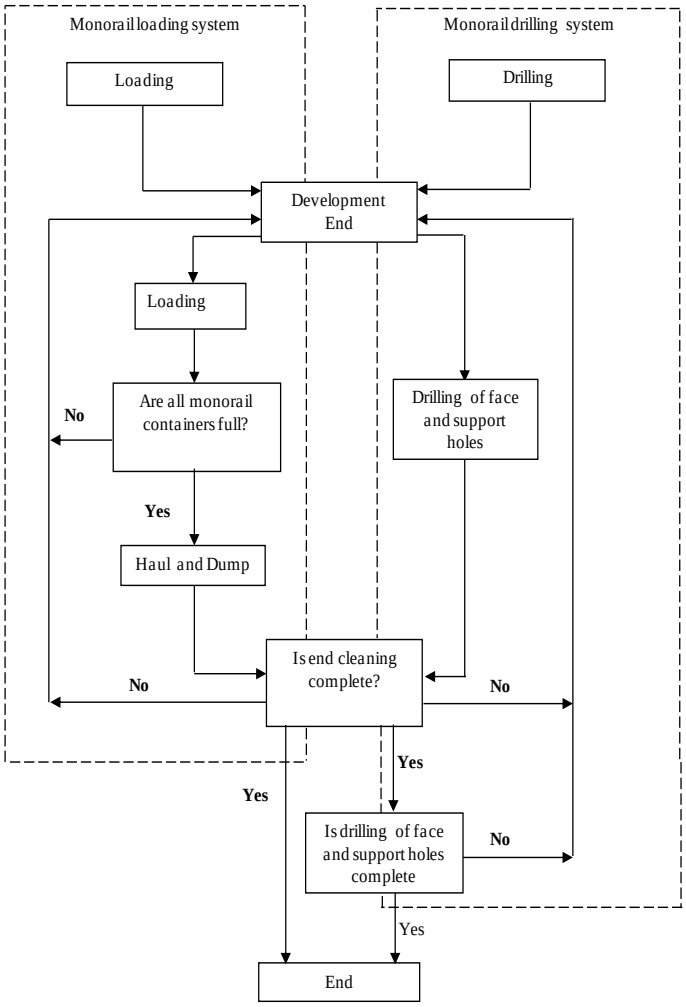

Figure 6.3: Process flow chart for monorail drill-load-haul system

(a) Drilling

Figure 6.3 shows that drilling of the development face commences immediately i.e. at the same time as cleaning of the face. The operation of the drilling system is such that drilling the top part of the face commences as the loading system continues cleaning the development face. According to Figure 6.3, drilling will not be completed as long as the development face is being cleaned. Drilling will also continue for some time after cleaning the face has been completed to allow drilling of down holes. Therefore, the monorail drilling system depends on the efficiency and operations of the loading system. Completion of the development drilling also depends on the number of holes being drilled as well as the time to drill one hole.

(b) Loading process

According to Figure 6.3, the operations of the monorail pneumatic loading system are such that when the development face is blasted and ready to be cleaned, the pneumatic loading system begins loading rock fragments into the hopper via the suction pipe. When the hopper is fully loaded, the suction pipe is disconnected from the hopper. The monorail train then pulls the hopper to the position of an empty container where automatic discharge of rock fragments into monorail container takes place. After material discharge, the monorail pushes the hopper back to the loading position where the suction pipe is reconnected to the hopper and the loading process resumes again. Figure 6.4 summarizes the loading process of the monorail loading system.

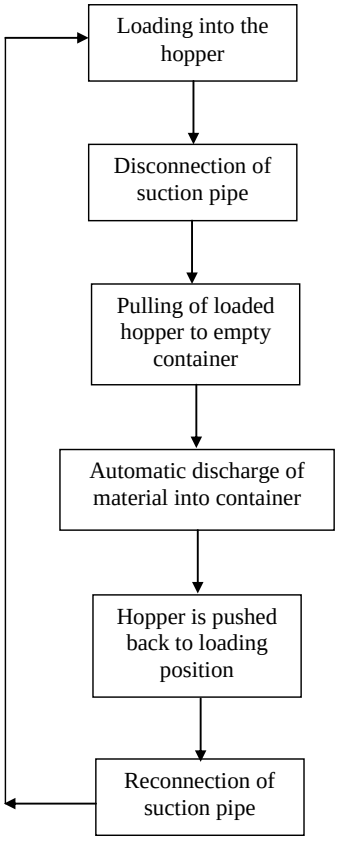

Figure 6.4: Process flow chart for monorail loading operation

The above processes are modelled during programming of the model for monorail loading system. Since the objective of the loading system is to clean the

development face within the shortest possible time, the sensitivity of the loading process (loading time) on drill-blast-load-haul cycle time is investigated. Therefore, during model simulation, the performance of the loading system at minimum loading time is determined.

(c) Hauling and dumping

When all the monorail containers are fully loaded, the hopper is disconnected from the monorail train and the train is moved to the container's lifting position where lifting of loaded containers takes place. Loaded containers are then transported to surface by the monorail train for material dumping. After material is dumped, the system returns underground where development face cleaning resumes until the face is completely cleaned. Before face cleaning resumes, monorail containers are lowered to the loading position by the monorail train. Figure 6.5 shows the hauling and dumping process of the monorail system.

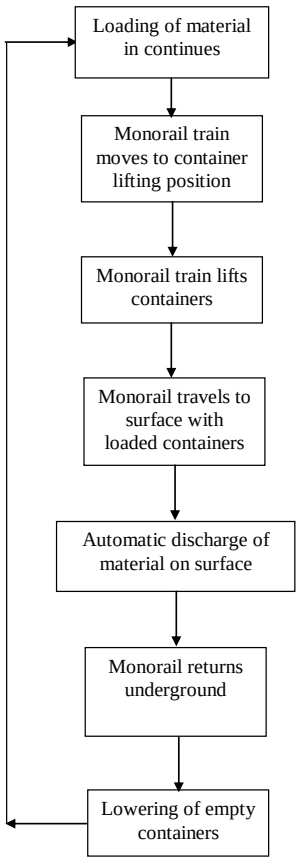

Figure 6.5: Process flow chart for material haulage to surface

The decline length also affects the drill-blast-load-cycle time of the system. This means that the longer the decline length, the longer the monorail system takes to haul and dump the material to the surface and return underground. Therefore, the decline length has an effect of increasing the drill-blast-load-haul cycle time of the system. However, because the monorail drilling system will continue drilling the development face when the material is being hauled to surface, drilling operation is not affected.

6.4.2 Model assumptions

Tables 6.1 and 6.2 show the assumptions used during simulation of the monorail system. Since the monorail is a new system, time estimates used in the model are based on the author's engineering judgement as well as the information from the manufacturers of the monorail train.

Table 6.1: Time estimates used during model simulation

No.	Process	Time (Sec)
1	Time to lower monorail container	30±10
2	Time to connect / disconnect pipe	30±10
3	Time to discharge material into containers	10±2
4	Waiting time before Monorail lifts containers	10±2
5	Time to lift containers	30±10
6	Dumping time on surface	90±10
7	Time to drill one hole	240
8	Time to drill and support one hole	240

Table 6.2: Assumptions made on monorail system during simulation

No	Description	Unit	Value
1	Number of holes (48 Face holes, 32 support holes and 6 monorail support holes)	-	86
2	Decline end size	m	4 x 4
3	Density factor	t/m^3	2.8
4	Total tonnage from the development face	t	136
5	Charging/Blasting/Fume dissipation and monorail extension	minutes	90

6.4.3 Model programming

GPSS/H programming language is selected for simulating the monorail system. The software is designed for studying systems represented by discrete events. According to literature, GPSS/H can solve variety of problems rapidly and accurately (Sturgul, 2000). GPSS/H has been proved to be extremely versatile for modelling mining and mining related operations and can also easily be coupled with PROOF for making animations (Sturgul, 2000). Appendix A shows the screen-shots and GPSS/H programme of the monorail system model used during simulation study.

6.5 Results of simulation model

The model was simulated for different loading times during the 12 hour shift. This section therefore presents results of the simulation process.

6.5.1 Effects of loading time on lashing speed

In this study, the "loading time" means the time the pneumatic suction system would take to suck rock fragments from the development face to fill the hopper. On the other hand, the "lashing speed" is the time the suction system would take to completely clean the development face (i.e. suck all rock fragments from the face). To determine the effects of the loading time on the lashing speed of the pneumatic loading system, the model was simulated with varying loading times. According to Section 4.5.3, the minimum and maximum loading times of the pneumatic system are 11 minutes and 24 minutes respectively. Therefore, the model was simulated from 10 minutes (600 seconds) to 24 minutes (1440 seconds) with 60 seconds being the interval time. For each loading time, the lashing speed of the pneumatic system was determined from the model. Figure 6.6 shows the simulation results obtained.

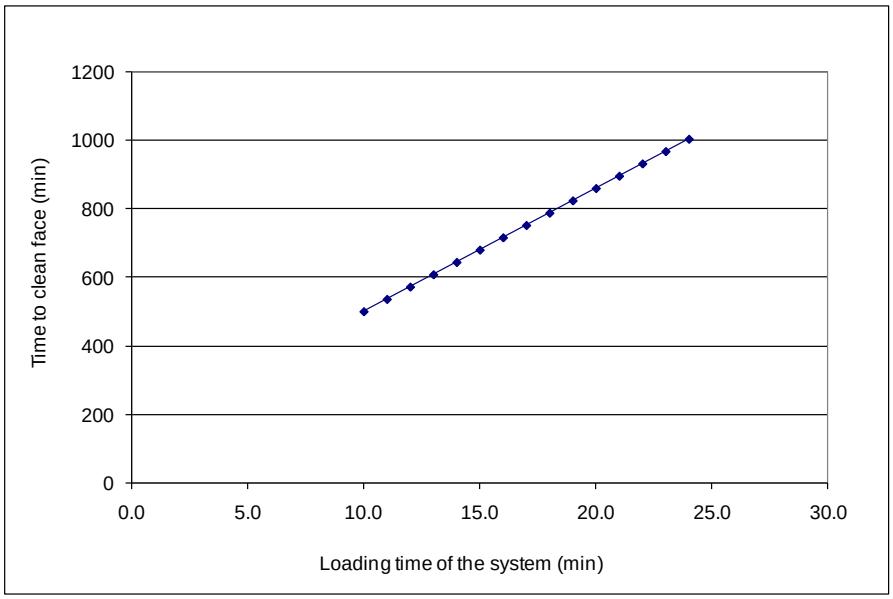

Figure 6.6: Effects of loading time on the lashing speed of the pneumatic system

According to Figure 6.6, the loading time of the pneumatic loading system is directly proportional to the lashing speed. Results indicate that an increase in the loading time of the pneumatic loading system (i.e. decrease in loading speed) results in an increase in time to clean the development face and vice versa. As an example, Figure 6.6 reveals that at minimum loading time i.e. 11 minutes the system would take approximately 537 minutes (8.9 hours) to clean the development face (i.e. load, haul and dump 93.2 tonnes) whilst at maximum loading time (24 minutes) it would take approximately 1005 minutes (16.7 hours) for the system to clean the face. It is therefore, evident from the results that an increase in loading time of the pneumatic loading system results in a steady increase in the time to clean the development face.

6.5.2 Effects of loading time on drilling speed

Figure 6.7 shows the effects of loading time of the pneumatic loading system on the drilling speed of the drilling unit.

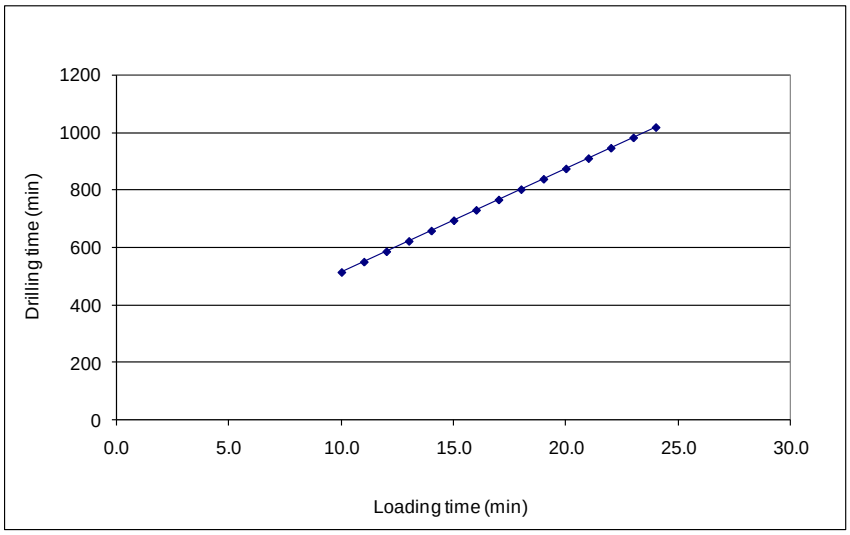

Figure 6.7: Effects of loading time of the pneumatic loading system on the drilling speed

The results indicate that the loading time of the system is directly proportional to the speed with which the development face is drilled. According to Figure 6.7, an increase in the loading time of the pneumatic loading system (i.e. system takes longer time) results in an increase in the drilling time of the drilling unit and vice versa. Results also indicate that the efficiency of the monorail drilling system depends on the efficiency and operations of the pneumatic loading system. Also, as can be seen from Figure 6.8, drilling of the development face always takes a relatively longer time to complete than face cleaning due to the fact that cleaning of the development face should be completed before face drilling is completed. Thus, drilling of the development face will not be completed as long as the development face is being cleaned. This is because the drilling time includes time to clean the face. This also means that the total cycle time to drill, blast, load and haul rock fragments from the development face depends on the efficiency of the pneumatic loading system. Figure 6.8 also indicates that when the loading time is reduced, the total drill-blast-load-haul cycle time will decrease and vice versa.

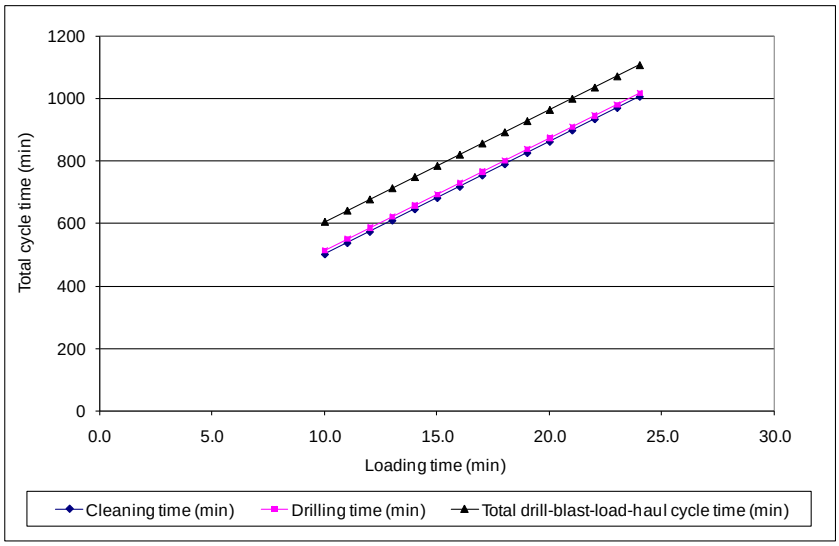

Figure 6.8: Relationship between loading, cleaning, drilling and total drill-blast-load-haul cycle time

6.5.3 Effects of loading time on total drill-blast-load-haul cycle time

The effects of the pneumatic loading system on the total drill-blast-load-haul cycle time were studied during model simulation. The total drill-blast-load-haul cycle time is the total time to drill, blast, clean and haul the material from the development face to the surface. Results of the simulation model are shown in Figure 6.9. The figure reveals that as the pneumatic loading time increases, the total drill-blast-load-haul cycle time also increases and vice versa. The increase in total cycle time is a result of the longer time it takes to clean the face that delays drilling, charging and blasting cycle time. As can be seen from Figure 6.9, at minimum loading time, i.e. 11 minutes, the total drill-blast-load-haul cycle time is 641 minutes (10.7 hours) whilst at maximum loading time (i.e. 24 minutes) the total cycle time would be 1106 minutes (18.5 hours).

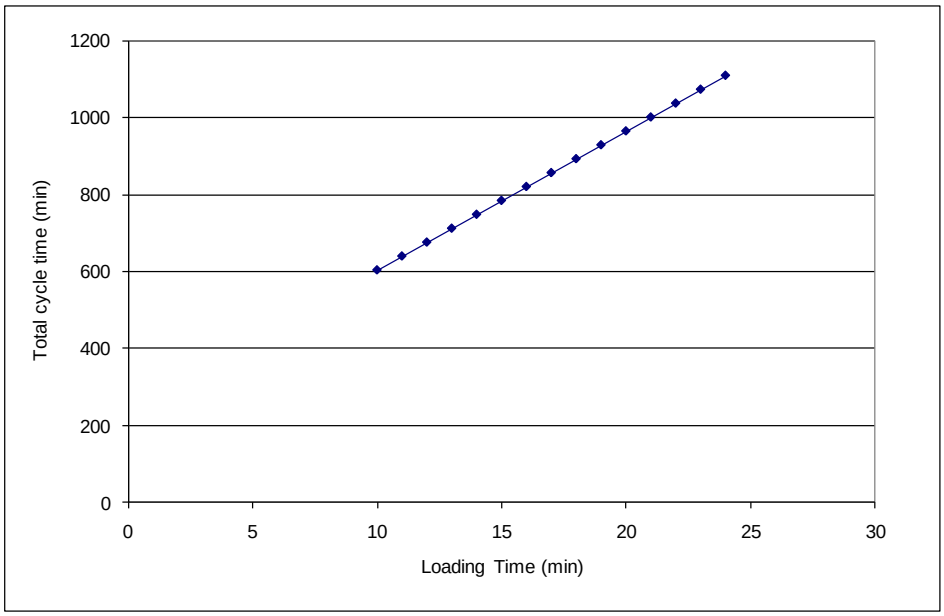

Figure 6.9: Effects of loading time on total drill-blast-load-haul cycle time

6.5.4 Effects of loading time on the number of blasts per shift

The productivity of the monorail system in terms of number of blasts it can achieve per shift was evaluated during simulation of the monorail system. During the analysis a restriction that prohibits blasting between shifts was considered. Figure 6.10 shows the simulation results in terms of the number of blasts per shift to be achieved by the monorail system.

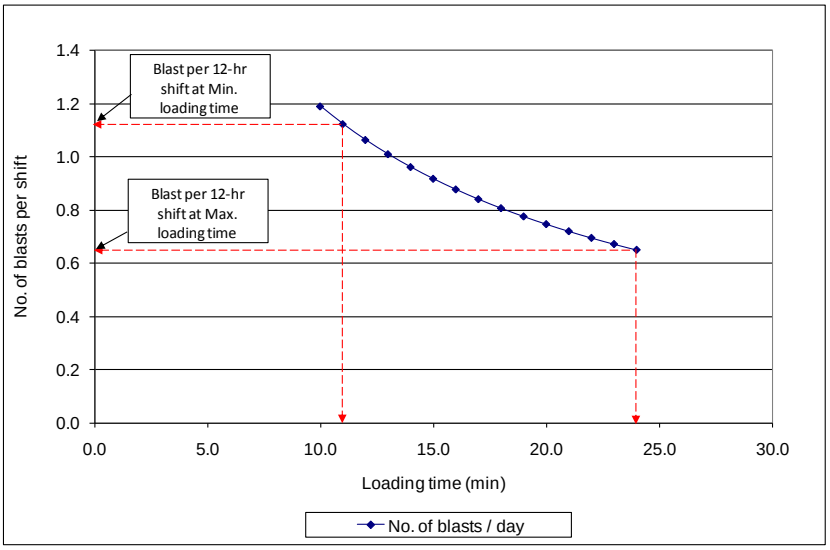

Figure 6.10: Effects of loading time on the number of blasts per shift

As shown in Figure 6.10, the loading time of the pneumatic system is inversely proportional to the number of blasts per shift. This means that the shorter the loading time, the more blasts will be achieved by the system per shift and vice versa. According to the figure, loading times of the pneumatic loading system between 11 minutes and 13 minutes will result in one blast per shift whilst loading times greater than 13 minutes will result in no blast per shift.

6.5.5 Effects of loading time on advance rates

Figure 6.11 presents the effects of loading time of the pneumatic system on decline advance rates. Results show that the loading time is inversely proportional to the advance rates. It can be seen from Figure 6.11 that the advance rates decrease with increase in loading time. According to the results, at minimum loading time (i.e. 11 minutes), the system results in one blast with an advance of 3.7m per shift (or 7.4m per 2 x 12-hour shift). At 90% advance efficiency, this results in 3.33m per shift (or 6.66m per 2 x 12-hour shift). However, at maximum loading time (i.e. 24 minutes), since there will be only one blast per day at maximum loading time, the system will result in 3.33m (per 2 x 12-hour shift) advance at 90% advance efficiency.

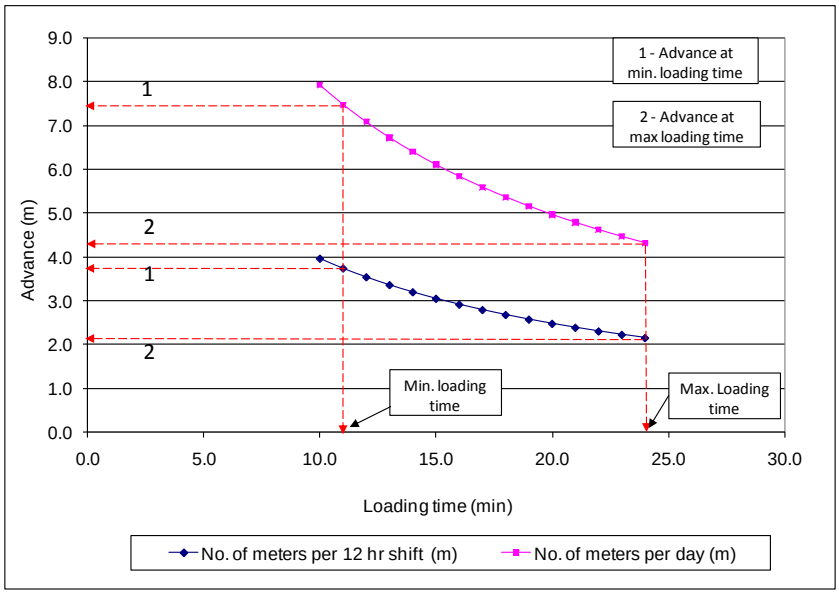

Figure 6.11: Effects of loading time on advance rates

6.6 Summary of monorail simulation results

Table 6.3 shows the summary of the simulation results for the monorail system.

Table 6.3: Monorail simulation results.

No	Description	Unit	Loading time	
			Minimum	Maximum
1	Time to clean the decline face per shift	hrs	8.95	16.75
2	Time to drilling and support decline face per shift	hrs	9.2	17.0
3	Total Drill-Blast-load-haul cycle time per shift	hrs	10.7	18.5
4	No. of blasts per shift	-	1	0
5	No. of blasts per day	-	2	1
6	Advance rate per shift (for 3.7m cut @ 90% advance recovery)	m	3.33	0
7	Advance rate per shift (for 3.7m cut @ 90% advance recovery)	m	6.66	3.33

6.7 Conventional decline development versus monorail system

To compare the monorail system with conventional method, the model was simulated with the same tonnage and decline length (Table 6.4) as used by Leppkes (2005) during studies on conventional method. Simulation results of the monorail system at minimum loading time were compared with conventional results. This section therefore, presents the results of the comparisons.

Table 6.4: Parameters used for model simulation.

Description	Unit	Value
Total tonnage	t	93.2
Decline length	m	2000
Size of face	m	3 x 3
Density of rock	Kg/m^3	2.8

The following parameters were compared for the two systems:

- Time to clean and drill the development face;
- Drill-blast-load-haul cycle times;

- Advance rates per shift; and
- Productivity of the system.

6.7.1 Time to clean and drill the development face

Figure 6.12 shows a comparison of cleaning and drilling time of the development face for conventional and monorail system. The figure shows that the total cycle time for monorail system is less than the conventional system. According to the figure, at minimum loading time, the monorail system takes 410 minutes (6.83 hours) cleaning and drilling a 3m x 3m development face whilst a total of 488 minutes (8.13 hours) will be spent in conventional method to drill the same face. The reduction in total cycle time is attributed to the following:

- Simultaneous drilling and cleaning of the face by the system;
- Automation of marking of the face using laser technology. Since the current system use manual face marking because there is no provision for automatic face marking, this increases the total drilling cycle time. However, to reduce the total drilling cycle time on the monorail system, it is suggested that the monorail system be equipped with an automatic face marking device in order to cut down on face marking time.

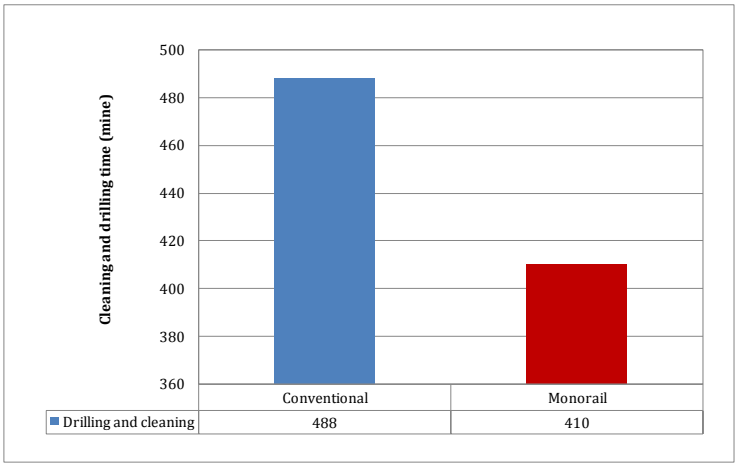

Figure 6.12: Comparison of the total cleaning and drilling time for conventional and monorail system

6.7.2 Time to charge/blast/re-entry and other activities

Figure 6.13 shows a comparison of total time to charge/blast/re-entry time of the development face for conventional and monorail system.

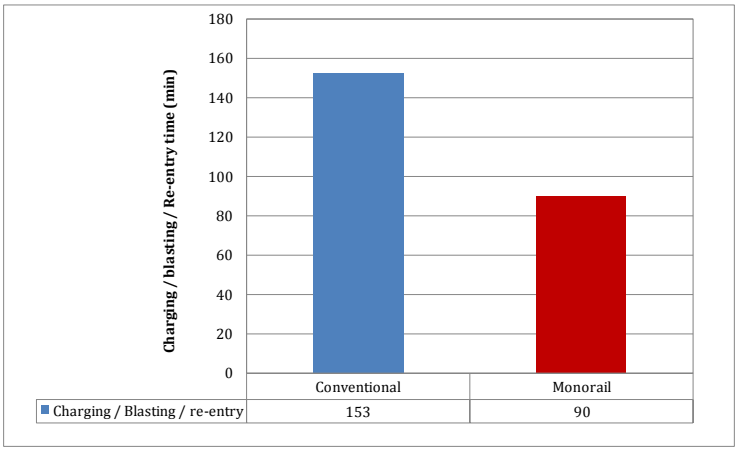

Figure 6.13: Comparison of the charging, blasting and re-entry time for conventional and monorail system

The total time to charge/blast/re-entry time is lower in monorail system than in conventional method. The reduction in time is attributed to the following:

- Since the monorail system uses electricity, there will be less diesel fumes in the decline as well as underground environment during operations. Less diesel fumes in underground mining operations resulting from the use of monorail system will improve underground environment by reducing the amount of toxic gases generated underground. This will help reduce the amount of time required to ventilate the area and make it safe after blasting hence reducing the total charge/blast/re-entry cycle time.
- Diesel engine efficiency is generally estimated at 33% (Payne and Mitra, 2008). The remaining two-thirds of the heat load are released as heat into the underground environment. Therefore, with the use of the electric monorail system in underground mining operations, significant time is saved from cooling the underground environment.

- Reduced size of development i.e. from the conventional 5.5m x 5.5m to 4m x 4m with monorail application means less heat from the development face as well as from the decline surface will be released. Thus, because of less heat on the face, less time is required to ventilate and cool the area. Also as suggested by Payne and Mitra (2008), At the design stage mines should plan on having mining excavations that are only as large as required to accommodate the equipment. The transfer of heat from the rock mass into the air will be reduced through a reduction in the area available for heat transfer.

6.7.3 Total drill-blast-load-haul cycle time

Figure 6.14 shows the comparison of the drill-blast-load and haul cycle times for the monorail and conventional systems. According to the results, the drill-blast-load-haul cycle times for conventional method is approximately 10.7 hours while simulation results indicate that the monorail system would take approximately 8.33 hours. Therefore, there is a reduction of 22.1% (or approximately 2.4 hours) in the total drill-blast-load-haul cycle time when the monorail system is applied.

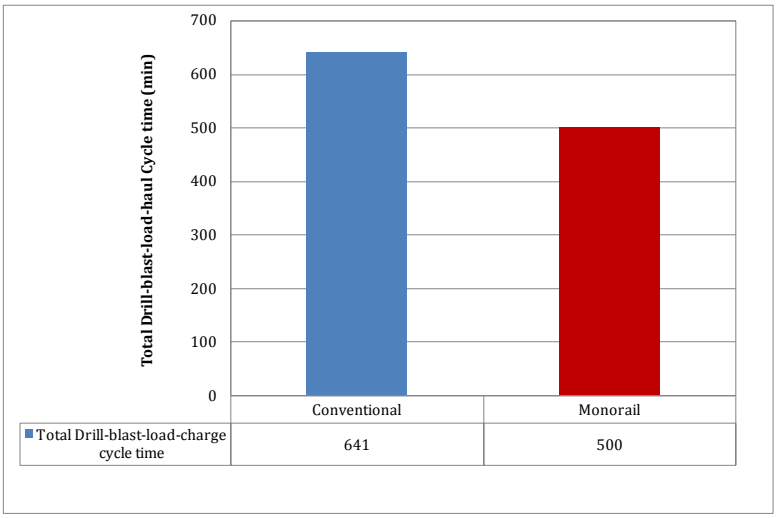

Figure 6.14: Comparison of the drill-blast-load-haul cycle time for conventional and monorail system

6.7.4 Advance rate per shift

Figure 6.15 shows a comparison of advance rates per shift for conventional and monorail systems. According to results the monorail system will have the same advance rate per shift as conventional method. The two systems will have the same advance because both systems give one blast per shift.

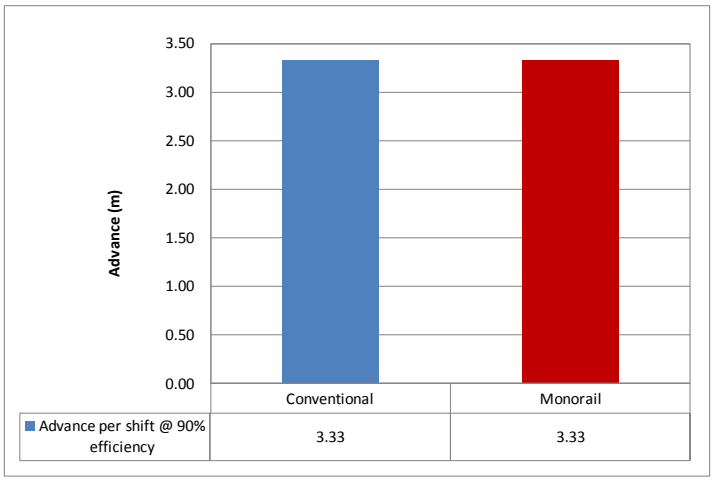

Figure 6.15: Advance rates for conventional and monorail systems

6.8 Summary

From the simulation results, the monorail system will have the same advance rate as conventional method. It has also been established that both systems will result in one blast giving the same advance. However, the total drill-blast-load-haul cycle time for the monorail system is lower than for conventional method. The decrease in total cycle time is attributed to the fact that drilling and cleaning the decline face will commence at the same time, hence there will be no waiting for the development face to be completed before drilling commences. The speed with which the material is removed from the development face at minimum loading time also contributed to reduced cycle time.

Chapter 7

7.0 Mine design for monorail system application (Jundee Case Study)

7.1 Introduction

In 2004, investigations were carried out to determine the potential of "South Deeps" narrow deposits by designing capital developments to the deposits using the conventional 1:7 decline gradient. A conceptual mine design was completed for accessing the four optimised areas in the South Deeps. Following the optimisation of the deposits, resources were found to be far from becoming potentially economic. In an effort to improve the economic viability of "South Deeps" deposits, monorail technology is used to design the decline access to these deposits. This chapter looks at mine design case study using monorail technology to "South Deeps" deposit and the results of the design compared with conventional access method. Nexus deposit is used as a case study area for designing decline access for monorail application. Mine design for the Nexus deposit was completed in Datamine. It should also be noted that the information used in this Chapter was the best available when this research project commenced.

7.2 Jundee "South Deeps" deposits

The Jundee operations are situated approximately 800 km northeast of Perth in Western Australia. The operations are owned by Newmont Mining Corporation which is one of the world's largest producers of gold. The Jundee operation began operations in 1995 and is composed of two underground mines as well as several satellite open pits about 30 km south of the operation. It produced

313,000 ounces of gold in 2006 and reported 1.48 million ounces of gold reserves at year-end. The Nim3 deposit (Figure 7.1) is the third largest underground resource of Jundee – Nimary gold field, situated beneath Nim3 open cut, immediate west of Barton Deep deposit.

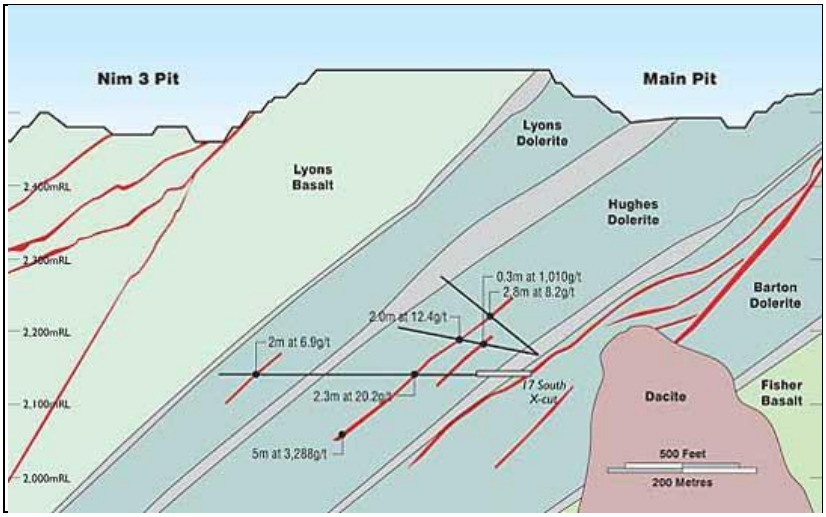

Figure 7.1: Nim3 deposit of Jundee operations (Newmont, 2004)

A number of structures; Nim3 Lyons, Nexus, Midas/Money Line, Hughes Extended and Colloform structure collectively forms the Nim3 deposit (South Deeps) and was the primary source for Nim3 open cut/underground operations. Figure 7.2 shows the ore bodies of the South Deeps mineralisation.

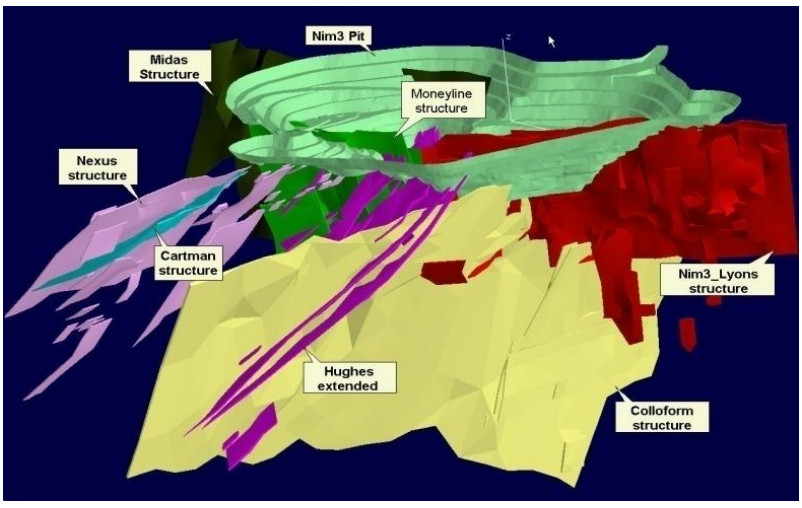

Figure 7.2: Nim3 pit and South Deep deposits at Jundee Mine (Newmont, 2004)

7.3 The Nexus Structure

The Nexus structure strikes north and dips moderately to the west at about 40°. The structure generally lies close to the basal contact with a thick overlying dacitic porphyry body (the Nexus Dacitic Porphyry), which appears to be largely concordant with the local stratigraphy. The Nexus ore body has approximate strike length of 1.1km. About 400m long of the southern portion of the structure is drilled with wide spaced drilling and geological confidence is low. The mineralisation at Nexus structure is patchy within the corridor between 96550mN and 96800mN. High grade Nexus mineralisation that occurs beneath the Nim3 pit could be modelled only for a short strike length of 125m. The structure beneath Nim3 trends north and dips steeply at 70° to the west.

7.4 Mine Design for monorail application

7.4.1 Mining method

Sublevel open stoping mining method is used for the extraction of the Nexus deposit. This is because the same mining method is applied in similar areas of the mine and has proved to be successful. The orebody characteristics also favour this mining method. Horizontal levels (crosscuts) from the decline to the deposit are developed at 10-m intervals using the monorail system.

7.4.2 Access to Nexus structures

The access to Nexus deposits is via a 4.0mH x 4.0mW size of monorail decline that is 212m long. The decline starts from the box-cut entry portal (located on the southern centre of the existing Nim3 pit). The access joins Nexus main decline at elevation 2390mL (Figure 7.3). The main decline to Nexus deposit is developed with gradient 20^0 from 2440mL and spirals down to 2140mL. According to the manufacturers of Monorail train, the minimum decline dimension for one monorail train application is 3.0m x 3.0m. However, decline

dimensions of size 4.0m x 4.0m are used in this design so as to accommodate other mine services such as ventilation tubing, air and water pipes, cable etc. Since a monorail train can negotiate curves of 4m minimum horizontal track radius (Scharf, 2007), a curve radius of 6m is used in this design. This is to avoid unnecessary stresses on the beam and on the rollers, thus causing excessive wear on the track and damage to the roller bearings. Also varying lengths of straight ramps are used to provide best access to the orebody.

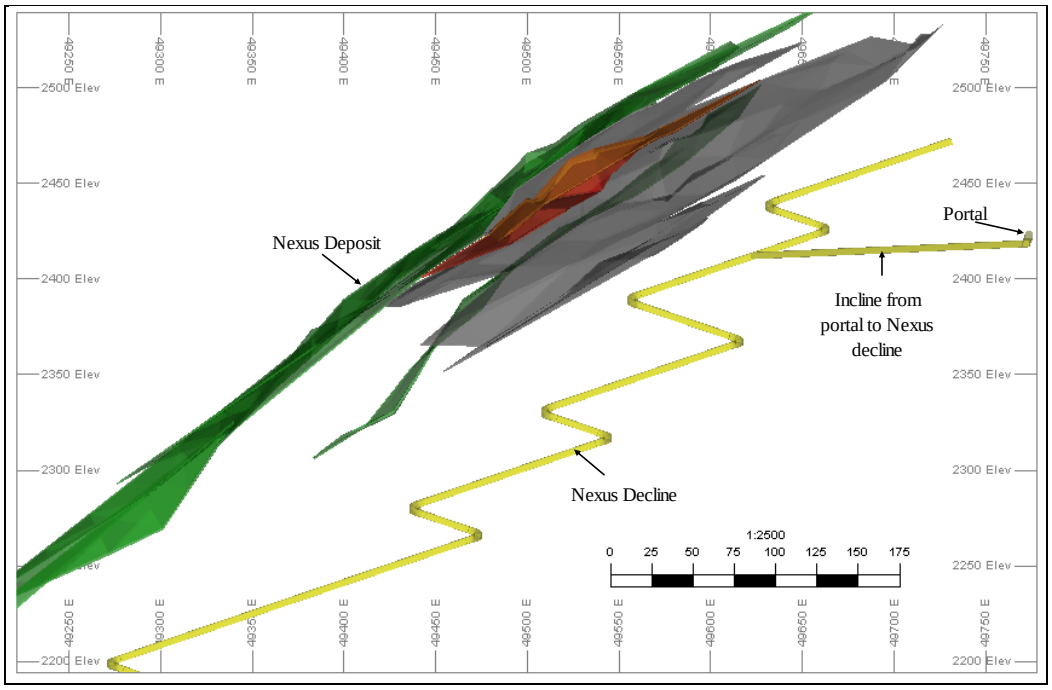

Figure 7.3: Decline design to Nexus deposits for monorail application

7.4.3 Design of cross-cuts to Nexus structures

Horizontal development headings exiting the Nexus decline provide access to stopes and draw points of the Nexus deposits. Horizontal crosscuts from the Nexus decline towards the Nexus deposits are designed with dimensions 4m x 4m as well as at 10m interval from 2440mL to 2140mL. A total of 31 crosscuts were designed with a total length of 4990m. Results of the design are shown in Figure 7.4.

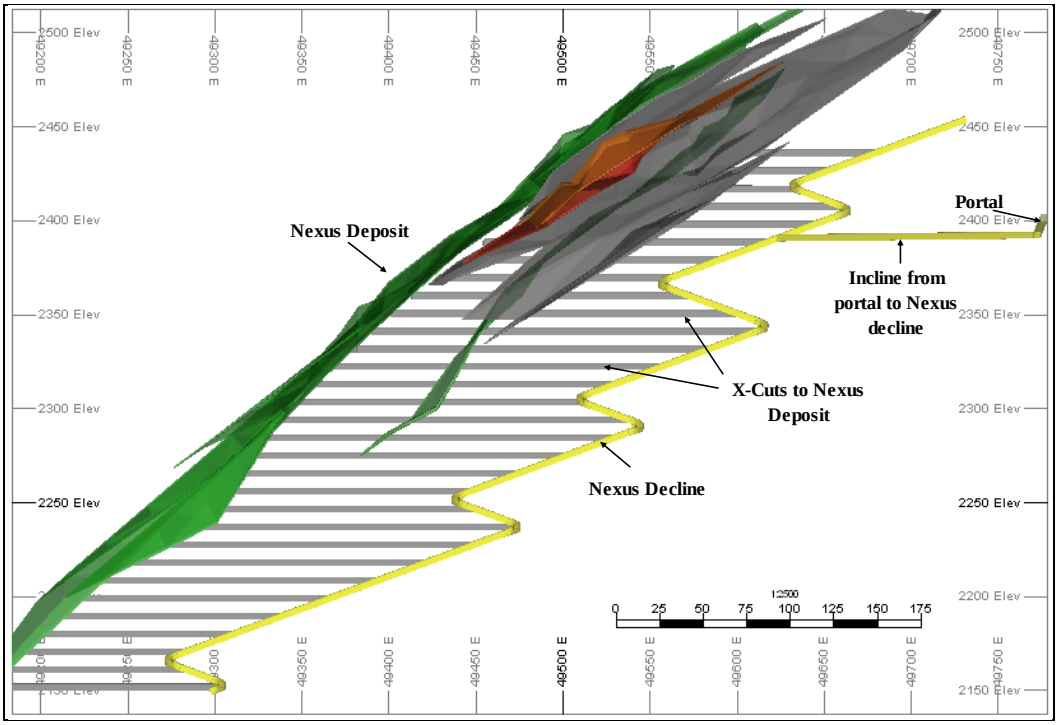

Figure 7.4: Decline design from the portal to Nexus deposits.

7.4.4 Design of fresh and exhaust ventilation drives

Figure 7.5 shows the designed fresh air intake access to Nexus deposits. Fresh air intake access (i.e. intake crosscuts and raises) is designed with dimensions 2.5m x 2.5m as compared with 3.0m x 3.0m (for intake raises) and 4.5m x 4.5m (for intake crosscuts) used in conventional design. Smaller dimensions for fresh air intake access are used because the monorail system uses electricity and it is anticipated that there will be less diesel fumes in the decline during operations. Fresh air intake access is designed on the footwall side of the deposit to take advantage of the competent ground. According to the designs, fresh air enters Nexus decline from 2390mL and is pumped down to 2140mL by means of booster fans. Several fresh air intake crosscuts supply fresh air to intermediate levels. Exhaust airways from Nexus deposits are also designed on the footwall side with dimensions of 2.5m x 2.5m. Exhaust access from Nexus deposits is also designed on the footwall side with dimensions of 2.5m x 2.5m (Figure 7.5.).

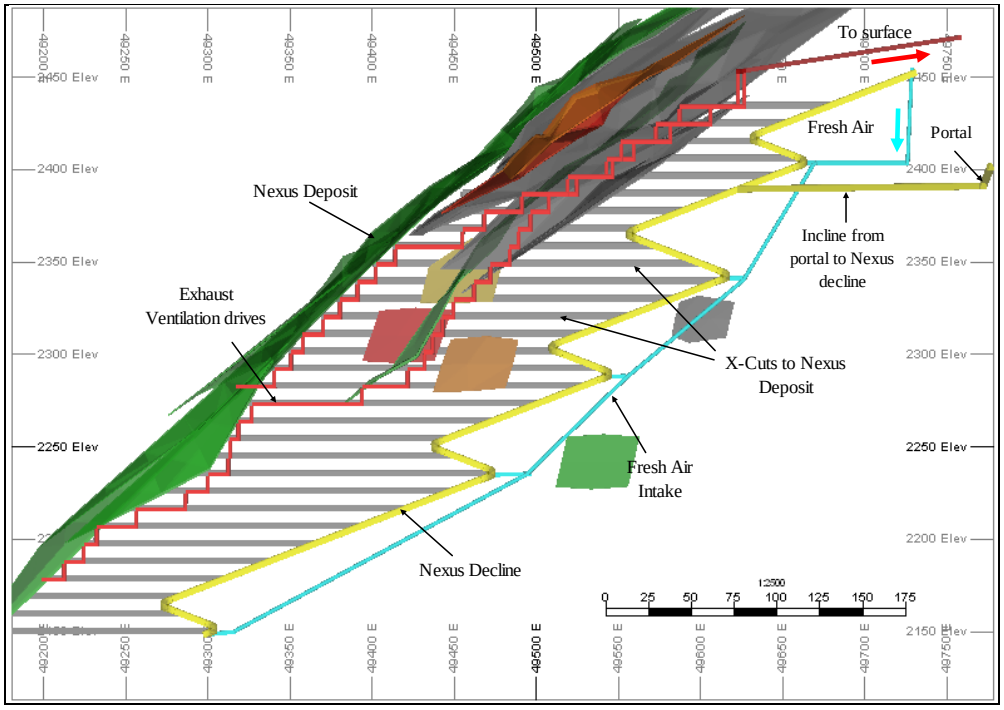

Figure 7.5: Design of fresh air intake and exhaust to Nexus structures.

7.4.5 Waste and ore handling

7.4.5.1 Waste handling

The monorail drill-load-haul system is designed specifically for development of declines. During operations of this system, waste material from decline development ends will be removed by means of a monorail pneumatic loading system. The pneumatic loader will suck rock fragments from the decline development face into the monorail hopper and once the hopper is full material is automatically discharged into the monorail containers. However, removal of waste material from access and ventilation headings will be done using conventional truck haulage system. This means that waste material from the access and ventilation heading will be removed and loaded into monorail containers using diesel Load-Haul-Dumps (LHDs). It is also anticipated that after blasting the development face, rock fragments will have oversized material that will not be sucked by the pneumatic sucker. The oversized materials will create problems during pneumatic loading operations and as such they will need to be reduced to manageable sizes by secondary breaking at the face. However, to

minimize oversized rock fragments and improve rock fragmentation, this study has determined that blasted rock fragments should have a maximum diameter of 110mm.

7.4.5.2 Ore handling

Removal of the ore from stopes may be accomplished by means of LHDs or it is being suggested that the monorail system be extended to the crosscuts to lode. If the LHDs are used to transport ore from the stopes to the monorail system via the crosscuts, special arrangements have to be made to allow the LHD load into the monorail containers in the decline. However, if the monorail system is extended into the crosscuts, LHDs will remove the ore from the stopes to the stockpile located at the end of the crosscut, and from here ore will be loaded into the monorail containers using the pneumatic system. Alternatively, LHD may be used to load ore from the stockpile into the monorail containers but this will just increase the loading time and needs to be avoided.

7.5 Results and analysis of the design

7.5.1 Development meters and tonnage to be moved

Table 7.1 shows the results in terms of development meters and tonnage to be removed for the mine design using monorail technology.

Table 7.1: Access development parameters for Nexus structures.

No	Description	Rock Tonnage (t)	Length (m)
1	Incline from portal to Nexus Decline	9400	212
	Decline from 2440mL to 2140mL	41600	895
	Total	**51000**	**1107**
2	Crosscuts (a total of 31)	227600	4991
	Total	**227600**	**4991**
3	Fresh air intake access	9800	640
	Exhaust access	27000	1674
	Total	**36800**	**2300**

According to Table 7.1, a total of 1107m is required to develop decline access to Nexus deposits from the entry portal to the end of the decline i.e. at 2140mL. Table 7.1 also shows that a total of 4990m is required to develop a total of 31 crosscuts to Nexus deposit while a total of 2300m is required for development of ventilation access to the same deposit. Table 7.1 also shows the total tonnage removed during development. Applying a tonnage factor of 2.85t/m^3, the table shows that a total of 51000 tonnes of waste material will be excavated during decline development while a total of 227600 tonnes will be excavated from the crosscuts. Ventilation access resulted in 36800 tonnes.

7.5.2 Capital development cost to Nexus deposit for monorail application

Generally, the costs of capital development to access the deposit as well as mine services are considered to be preproduction capital costs and are typically the largest component of mining capital costs. Capital developments also require the longest time period of any mine activity in preparing the mine for production. In this section an analysis of the preproduction costs associated with decline development to the Nexus deposits using monorail technology is undertaken. Development capital costs for monorail application were calculated on first principle i.e. development length multiplied by development cost per meter. This means that after determining the development meters for the decline, crosscuts and ventilation access, the development costs were calculated by multiplying the development meters by the development cost per meter as indicated in Table 7.2. The costs used for determining monorail costs are the same as those used in conventional development according to a Newmont 2004 Report.

Table 7.2: Capital development costs to Nexus deposits using monorail technology

No	Description	Length (m)	Average Development Cost (A$/m)	Development Cost** (A$'000'000)
Cost of decline access				
1	Incline from portal to Nexus Decline	212	2400	0.5
2	Decline from 2440mL to 2140mL	895	2480	2.2
	Sub-total	**1107**		**2.7**
Cost of crosscut access to Nexus deposit				
1	Crosscuts to Nexus deposits	4991	2450	12
	Sub-total	**4991**	**2450**	**12**
Cost of ventilation network				
1	Fresh air intake crosscuts	133	1650	0.2
2	Fresh air intake raise	507	2170	1.1
	Sub-total	**640**		**1.3**
1	Exhaust crosscuts	1180	1760	2.1
2	Exhaust raise	470	2070	1.0
	Sub-total	**1650**		**3.1**
	Grand Total			**19.1**

According to Table 7.2, it would cost approximately A$2.7m to develop a 212-m long incline from entry portal to the main Nexus decline as well as the development of 895m long main Nexus decline from 2440mL to 2140mL. The total cost of developing horizontal crosscuts from the decline to Nexus deposit would be approximately A$12m while a total of A$4.4m would be spent to develop ventilation access drives to the area.

7.5.3 Conventional development versus monorail system

Total development meters for the monorail system are compared with development meters obtained using conventional decline access to the Nexus deposit. Figure 7.6 shows the results of the comparison. According to Figure 7.6 the total decline development meters (i.e. from the portal to 2140mL) would reduce from 2963m using conventional development to 1107m using monorail

technology. This represents 62.6% reduction in total development meters. Also because of the reduction in the size of decline development, i.e. from the conventional 5.5mH x 5.5mW to 4mH x 4mW, the total tonnage of material to be moved per meter reduces from 91t/m to 46t/m. This means that the total tonnage of waste material to be moved would reduce from 269,000 (2963x91) tonnes in conventional development to approximately 51,000 (1107x46) tonnes using monorail technology giving a reduction of 81%.

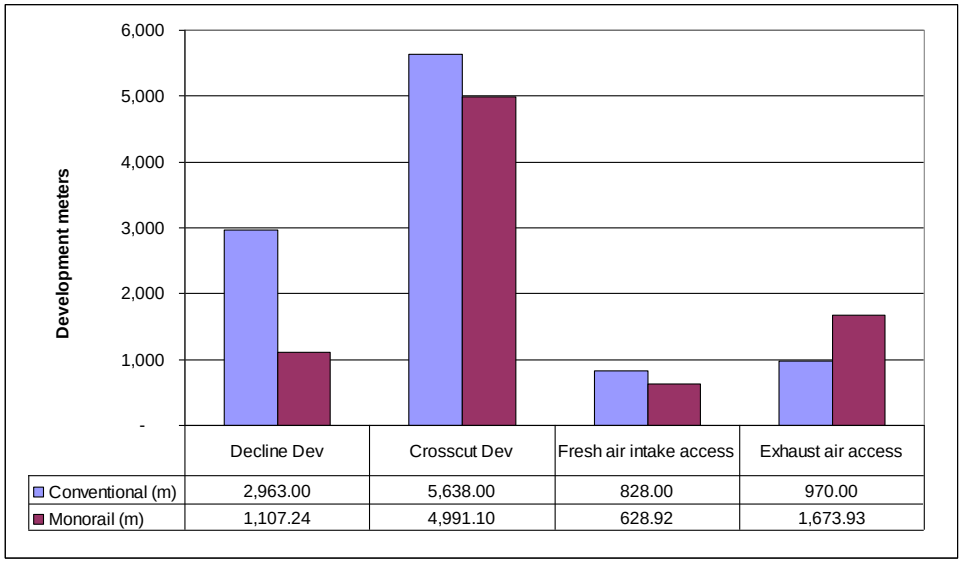

Figure 7.6: Conventional versus monorail development meters

Figure 7.6 also indicates that the total horizontal crosscut development meters would reduce by 647 meters i.e. from 5638m to 4990m (a reduction of 11.5%). Although this represents a modest reduction in the total crosscut development meters, the total tonnage reduces by 55.6% (from 513,000 to 227,600 tonnes) as shown in Figure 7.7. The reduction in total tonnage is attributed to reduced size of the crosscuts.

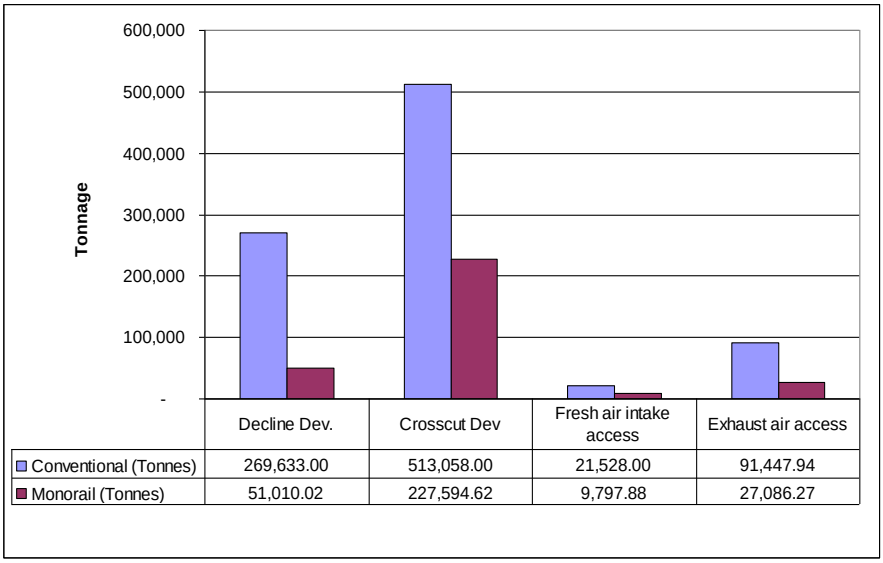

Figure 7.7: Conventional versus monorail tonnage to be removed

Fresh air intake development meters also reduce from 828m to 640m giving a reduction of 22.7%. The reduction in the size of the fresh air intake developments i.e. from 3m x 3m to 2.5m x 2.5m, resulted in the reduction in total tonnage of material to be moved from 21500 tonnes to 9300 tonnes (a reduction of 56.8%).

Further, Figure 7.6 shows that the total exhaust airway development meters increase from 970m to 1674m representing an increase of 72.6%. The increase in exhaust development meters results from the fact that LHDs will be used for ore handling in stoping areas, hence more fumes from these areas need to be exhausted. Figure 7.7 shows a corresponding reduction in tonnes to be removed for total exhaust airway development.

7.5.4 Conventional versus monorail costs

The total costs of mine design using monorail system were compared with costs of conventional method. Figure 7.8 shows the results of the comparisons. According to Figure 7.8 the total cost of decline development reduces from A$7.3m in conventional development to A$2.7m using monorail technology representing a 63% reduction.

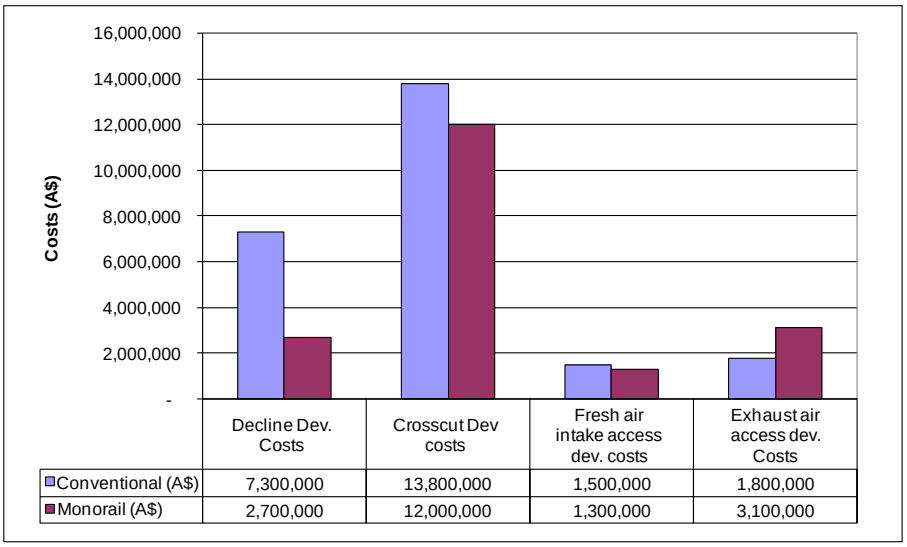

Figure 7.8: Conventional versus monorail development costs

The reduction is attributed to the reduced number of development meters due to steeper gradient as well as the reduced size of the decline. Development costs for horizontal crosscuts also reduce by A$1.8m with application of monorail technology. Compared with conventional method, this represents a reduction of 13% in total crosscut development cost. Figure 7.8 also shows that the total cost of ventilation access development would increase by 33%. This is due to increase in exhaust development meters by 72.6% based on the redesigned mine layout. However, the increase in development costs is minimal compared with the savings that will be made from the total development costs.

7.5.5 Cost analysis for purchase and installation monorail system to Nexus deposit

Capital costs for monorail operations consist of installation of a monorail and purchase of a monorail train. Table 2.7 (Chapter 2) shows capital costs, for the purchase of a monorail with two drive cabins, four drive units and six lifting beams each with a payload of 30 tonnes (Sharf, 2007). Table 2.8 (Chapter 2) shows the capital costs per meter for monorail installation. The installed power on the train is 232 kW. The total cost of monorail installation in the Nexus decline can be calculated as follows:

Total cost (monorail installation) = [Cost of monorail train] + [Installation cost per meter x Decline length]

From Table 2.7, the total cost of purchase of one monorail train (with all accessories) is A$1,316,000 while the total installation cost per meter was estimated at A$577 (Table 2.8). Also from the results of the mine design, the total decline length from the Nim3 entry portal to Nexus deposit is estimated as 1107m. Therefore, the total cost for monorail installation is estimated as indicated below:

Total cost (monorail installation) = [1,316,000] + [577 × 1107]

= **A$1,955,000**

Thus, the total cost of decline development to Nexus deposit together with purchase and installation of the monorail train is computed as follows:

= Cost of capital developments + Total monorail cost

= 19,100,000 + 1,955,000

= **A$21,055,000**

Therefore, approximately A$21m is required to develop and install the monorail system to access Nexus deposit. When compared with the total cost of using the conventional haulage system as evaluated by Newmont (2004) (Figure 7.9), there is a saving of A$5.3m for capital development to access the same deposit. This represents a 22% reduction in total capital cost for access development to Nexus deposit. Operating costs for monorail operations include maintenance of parts, power supply as well as labour costs. Table 2.9 (Chapter2) shows operating costs for the monorail train (Meyer, 2007).

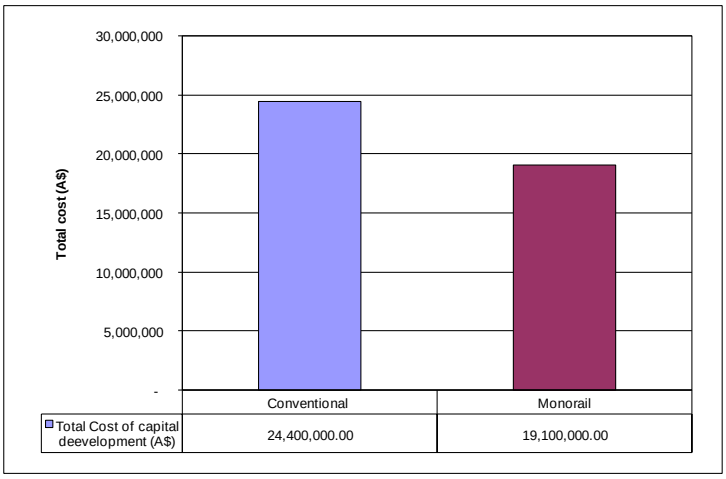

Figure 7.9: Comparison of total capital development cost to Nexus deposits

7.5.6 Duration of decline development to Nexus deposits

According to simulation results in Chapter 6, the monorail system will have the same advance rate as the conventional system (i.e. 6.66m per day). Since the total length of the decline for the Nexus deposit is known i.e. 1107m therefore, using Equation 2.5 (Chapter 2), the time taken to mine the decline is 1107÷6.66 or 166 days. Theoretically, it would take 166 days to access the Nexus orebody by means of a decline using monorail technology. In contrast, it would take 2963÷6.66 or 445 days to access the Nexus orebody using conventional decline development.

7.6 Installation of the monorail in the decline

It has been determined that the monorail technology can reduce the cost of capital development to exploit the Nexus deposit and also do it quicker. This section looks at installation of the monorail system from Nim3 box entry portal to the bottom of the decline a distance of 1107m. Sections showing monorail installation have also been indicated in this section.

The monorail system runs on an "I" beam rail suspended from the roof by chains attached to suspension bolts. Installation of a monorail is a combination of three major activities:

- Drilling support holes
- Roof bolting
- Rail placement

7.6.1 Drilling support holes

In decline development (just like in horizontal development), holes for rock bolt installation are drilled to a depth of 2m and at 3m interval perpendicular to the decline roof surface (Figure 7.10).

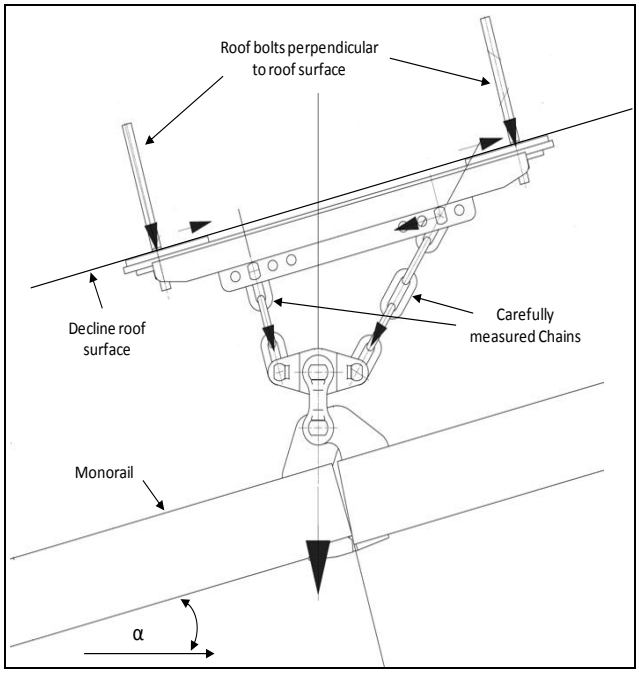

Figure 7.10: Drilling of rock bolts for monorail installation (Scharf, 2007)

Improper drilling of holes for rock bolt installation reduces the lifetime of the rock bolts (Figure 7.11). According to Oguz and Stefanko (1971) drilling time per support hole (manual drilling) for rock bolt installation (including all kinds

of work and delay) is approximately 16 minutes. Net drilling time excluding delays takes approximately 6 minutes per hole.

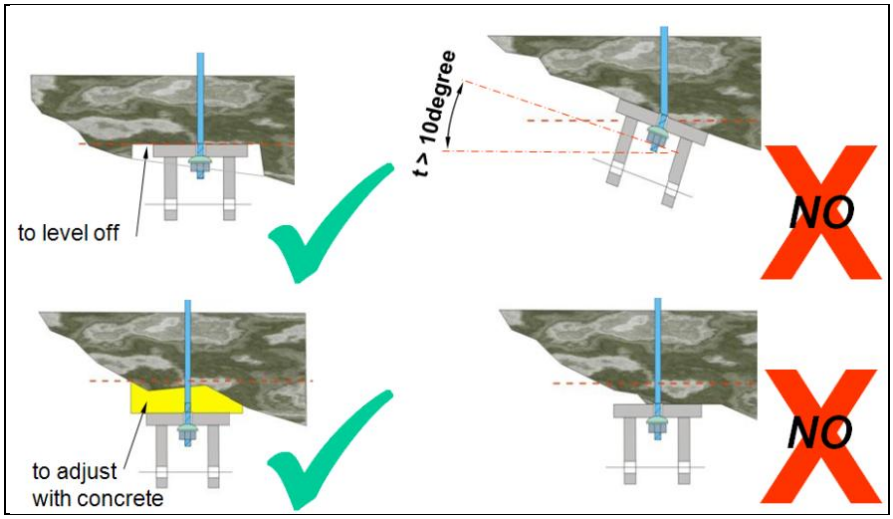

Figure 7.11: Drilling of holes for rock bolt installation (Scharf, 2007)

It should also be noted that drilling of support holes is likely to reduce when drilling with hydraulic booms. Preparatory activities for drilling such as lining and marking the hole, setting up the stoper and collaring the hole are the most important phases of the monorail installation process (Oguz and Stefanko, 1971). A badly installed monorail track will develop unnecessary tensions in the system which can lead to trouble and large power consumption.

7.6.2 Rock bolting and support

The Hilti OneStep rock bolts are used as the suspension bolts (Figure 7.12). With the monorail system, the rock bolt installation and rail extension in the decline will be done simultaneously as the face is being charged. Since supporting the roof is critical during decline development, this will be done before face drilling commences. The monorail system will drill holes that will be supported before face drilling commences. The bolts used for monorail installation has an ultimate strength of over 320kN, a diameter of 38.5mm, length of 2m and requires a 41mm diameter hole. Each bolt requires the purchase of a dispenser and an

intensifier for the installation. Resin containing rapid-curing adhesive is contained within the bolt (Scharf, 2007).

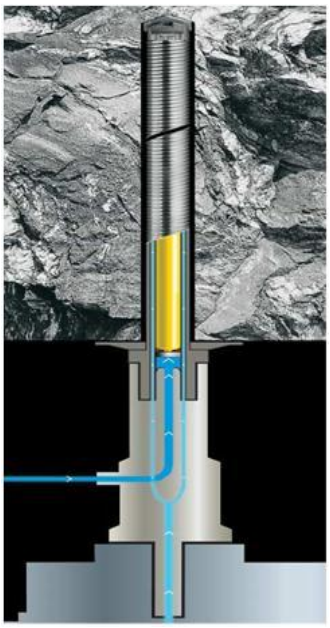

Figure 7.12: Hilti OneStep anchor bolt (Hilti Corporation, 2004)

Bolt installation requires one operator and can be installed in 40 seconds after the hole is drilled. The rock bolt for monorail application must take static and dynamic loads. Normally, dynamic load with angular transmission will cause deflection of rock bolts. This will reduce the lifetime of the rock bolts by a factor of 10 or more (Scharf, 2007). Therefore, to avoid this, a bracket with preloaded roof bolt is used.

7.6.3 Rail placement and alignment

Installation of the rock bolt is followed by attachment of a special eyebolt on the threaded end of the bolt. A shackle provides easy connection of the chain to the eyebolt (Figure 7.13). From the shackle down, the distance should be carefully measured to obtain the length of the chain for a horizontal track installation.

Measurement of the chain is done by connecting a new rail section to the one which is already installed permanently. The front end of the new rail section is lifted until it is horizontal and in line with the others. While one man holds the rail in this position, another man takes the measurement from the shackle to the hook on the top flange of the rail. Measured lengths of the chain are then cut using oxygen burner. During monorail installation at curves, the rail sections are blocked rigidly providing more stable track structure.

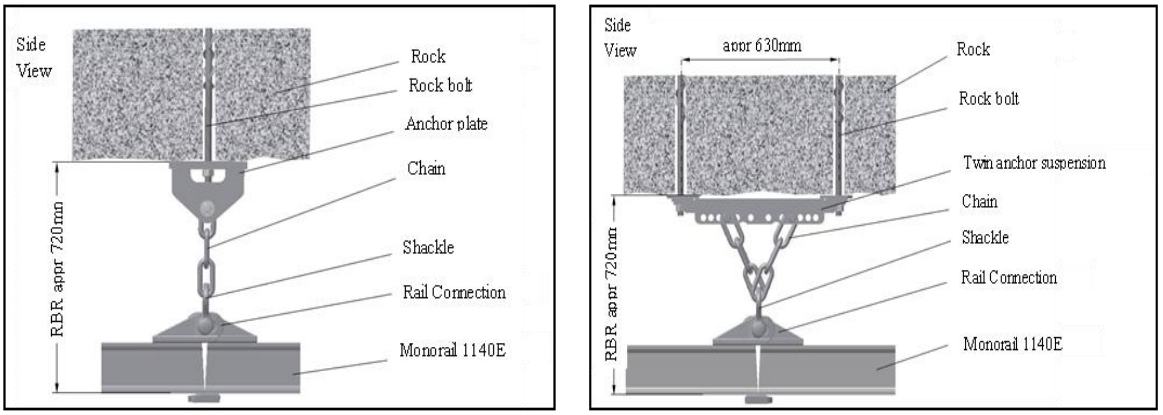

(a) (b)

Figure 7.13: Rock bolt installation and rail installation (Courtesy Scharf, 2007)

7.7 Summary

This study indicates that development of decline access to Nexus deposits using monorail technology is feasible. Compared with conventional decline development, results have shown that the monorail system has the potential of reducing the decline length to Nexus deposits by over 62.6% and decline costs by 63%. Further, the study indicates that with the monorail system, there is a potential of reducing total development costs (i.e. cost of developing the decline, crosscuts and ventilation network) by 22%. Also, due to rapid development by the monorail drill-load-haul system, the shorter decline length coupled with smaller decline openings, the duration of decline development reduces by 71.8%. This case study demonstrates that the economics of narrow vein deposits can be improved significantly by using the monorail system.

Chapter 8

8.0 Conclusion and further work

8.1 Conclusions

A distinguishing feature of modern underground hard rock mines in Australia is their seemingly invincible dependence on diesel, rubber-tyred machinery based decline development. This system has attained iconic status in the mining industry and it must be acknowledged that the model has in the past served, and in some cases continues to serve, the industry well and will be difficult to displace. However, it has to be recognized that the system suffers from a number of threats including geotechnical problems resulting from bigger cross-sections of the decline, diesel fumes from mining equipment, high ventilation requirements, and low advance rates. In contrast, the electrical monorail transport system (EMTS) uses electricity, hence providing a solution to some of the challenges faced by current system of decline development. An electro-monorail, combined with the proposed drilling and loading equipment offers a means whereby the mining industry can achieve reductions in green house gas emissions, reduce costs and improve mining rates.

The size of decline openings adopted in conventional mining (5.0mWide by 5.0mHigh) is largely driven by the need to accommodate diesel loaders and trucks. The problems associated with 'large' excavations are well known. There is elevated seismic risk, an increased likelihood of large unstable blocks forming, and falling from higher positions, having the potential to cause major damage and injury. Heat pick-up from the greater surface areas exposed can require the circulation of large volumes of ventilating air, a cost factor often obscured by the overarching ventilation demand of providing sufficient air to cool diesel engines operating underground and simultaneously maintaining adequate breathing air quality. The conventional 1:7 decline gradient and turning radius of 20m results

in unnecessarily longer decline whereas a steeper gradient and smaller turning radius results in a shorter decline; hence, an ore body can be accessed more quickly and cheaply. It has to be acknowledged that the capital cost of the monorail is significantly higher than for a similar payload truck. However, the operating cost of the monorail at a remote Western Australian mine site using diesel power generation is estimated to be the same as a similar payload underground truck (A$49 per operating hour). Rail components and installation is estimated at A$520 per metre. Interestingly, the operating cost of the monorail would be significantly less than a similar payload truck if the cost of power was significantly reduced to levels occurring in the eastern parts of Australia.

In Chapters 4 and 5 a theoretical analysis of the principles of operation of the monorail drill-and-blast system is undertaken. The stability of the monorail drilling system is critical in ensuring efficiency of the drilling process. By analyzing the balance of forces acting on the system, it was possible to determine the minimum and maximum forces required to stabilize the monorail system during drilling operations. The configuration and positioning of the monorail drilling system also has a bearing on the performance of the system. Consequently, the approximate swing and lifting angles that will enable the system to be able to cover the whole drill face during drilling operations have been determined. The use of a vacuum lift system for the transportation of fragmented rock from the face into the hopper is a new development. While it is difficult to determine how the system would perform in the actual production environment, the theory indicates that the system is capable of delivering the required productivity. As a matter of fact, the vacuum lift systems have been used in shaft sinking with excellent operating results. The productivity of the monorail system can be increased by integrating the unit operations of drilling, blasting, loading and hauling at the mining face. This is achieved by introducing a monorail mounted drill and a pneumatic face loading system. This system allows rock to be removed from the development face and loaded into the monorail containers in accelerated mining cycle.

The simulation model developed in Chapter 6 confirms the results from the analytical models. Both the monorail and conventional systems for decline development appear to have the similar advance rates (3.3 metres per shift). However, the total mining cycle is lower for the monorail system, allowing for a further drill and blast cycle.

In Chapter 7 the application of monorail technology to the development of decline access to the Nexus ore body at Jundee in Western Australia indicates that gains can be made in terms of cost saving and speed of development. Compared with conventional decline development, results show that the monorail system has the potential of reducing the decline length to the deposit by over 62.6%. Further, the study indicates that with the monorail system, there is potential to reduce decline development costs by 22%. Also, due to the reduced mining cycle using the monorail system, the shorter decline length coupled with smaller decline openings, the time it would take to develop the decline reduces by a staggering 71.8%. These results have been collaborated by the computer simulation of the system.

Clearly, the Electro-monorail drill-load-haul system is a viable alternative mining system for decline development. The system can even be used as a second level electrical reticulation component. Other benefits include elimination of diesel powered equipment in the underground environment, lower ground support and haulage costs and potential for rapid decline development.

8.2 Further Work

In going forward with this technology, it is proposed that a demonstration system be installed at a mine site in Australia. This will require the cooperation of Scharf SMT, mining companies, and government relevant agencies. The objective of setting up the demonstration system is to provide proof of concept and measure/collect operational data to be used in the subsequent design of a full scale integrated monorail system. There's need to assess the risks involved in adopting this system.

References

Alwyn, E. A. 1991, '*Mineral Deposit Evaluation, A practical Approach'. Chapman and Hall,'* ISBN 0417352907 p89.

Atlas Copco Manual, 1982, 4th Edition. pp 261.

AusIMM, 2007, '*The Mining Glossary*', The essential handbook of mining terminology, Australasian Institute of Mining and Metallurgy, ISBN 9780980425604.

Aziz, Z.B. and Klinzing, G.E. 1990,*'Dense Phase Plug Flow Transfer: The 1-inch Horizontal Flow,'* Powder Technology, 62: p. 41-49.

Bankston, J. D., and Baker F. E. 1994; '*Selecting the Proper Pump'* SRAC Publication No. 372;

Biegaj, K 2002, '*Mobile Supersucker Winzing*' – Attaining proven prior to capital commitment.'

Boyed J,T. 1993, **'***Technical Report, Independent Assessment of Coal Mining Operations at Maamba Collieries Limited*' Report 2324.2. Published by John T. Boyd and Company, Mining and Geological Engineers, Pittsburgh, Pennsylvania, United States of America – July 1993.

Bradley, M. S. A., 1989, '*An Improved Method of Predicting Pressure Drop along Pneumatic Conveying Pipelines*', Third International Conference on Bulk Materials. Storage. Handling and Transportation, Newcastle, N.S.W., June, 27-29 pp. 282-288.

Brazil, M Lee, D Rubinstein, J H Thomas, D A Weng J F and Wormald N C 2003, '*Optimisation in the Design of underground Mine Access*'; Orebody Modelling and Strategic Mine Planning Conference. Spectrum Series Volume 14

Carl, T. 2002, '*Digital Computer Simulation, Nova Publication*,' ISBN 1590333772

Chanda E.K. and Burke P.A 2007, '*Electro-Monorails; an Alternative Operating System for Deep Mining*', Australian Centre for Geomechanics Publications; ISBN: 978-0-9804185-2-1

Chanda, E.K and Corbett, C. J., 2003, '*Underground mining of shallow dipping ore bodies*' Mechanised up dip stoping versus transverse retreat stoping, Proc. 12th International Symposium on Mine Planning and Equipment Selection

(MPES), 23 -25 April, Kalgoorlie, Western Australia, CD (The Australasian Institute of Mining and Metallurgy; Melbourne).

Chanda, E.K. and Roberts, M 2005, '*Evaluation of monorail haulage system In metalliferous underground mining*' Proc. Hoist and Haul Conference, 5 – 7 September, Perth, 39 – 44 (The Australasian Institute of Mining and Metallurgy; Melbourne).

Chung C. A, 2003; Simulation Modelling Handbook, A practical approach, CRC Press, ISBN: 0849312418

Dorricott, M. G. and Jones, O. 1984, '*Vacuum Lift Systems for the Transport of Broken Rock in Shafts*' Paper presented at Regional Conference on 'Gold Mining, Metallurgy and Geology', The AusIMM Perth and Kalgoorlie Branches.

Ergun, S. 1952; Fluid flow through packed columns. Chemical Engineering Progress 48, 89–94.

Ferdinand, P.B., Russel, E.J. and DeWolf, J.T. 2002, '*Mechanics of Materials*' International Edition 3rd Edition McGraw-Hill Publishers ISBN: 0071121676.

Fisherman, G S 2001, '*Discrete Event Simulation Modelling, Programming and Analysis.*' Springer Series in Operations Research. ISBN: 0387951601.

Franklin J. and Katsabanis T., 1996; Measurement of blast fragmentation; Proceedings of the fragblast-5 workshop on measurement of blast fragmentation; Balkema / Rotterdam / Brookfield Publication. Montreal, Quebec, Canada 23-24 August. ISBN: 9054108452.

Geldart, D., 1973, 'Types of Gas Fluidization. Powder Technology', **7**: p. 285 -292.

Guse, A. and Weibezhn, K. 1997, '*Continuous transport in hard rock mining*' Colloquium – Underground Lateral Transport, 16 April, p 1-6, Randburg (South African Institute of Mining and Metallurgy; Johannesburg).

Hall, A. S, Archer F.E. and Gilbert, R. I., 1999, '*Engineering Statics*'. Second Edition. UNSW Press. ISBN 086840425X. pp 209 – 211.

Hartman, H. 2002, '*Introductory Mining Engineering*' John Willey and Sons, 2nd Edition; ISBN 0471348511.

Herbich J.B. 2000; '*Handbook of Dredging Engineering*' McGraw-Hill Professional ISBN:0071343067

Hilti Corporation 2004, FL-9494 Schaan, Principality of Liechtenstein, www.hilti.com.

Hirota, M., Y. Sogo, T. Marutani, and M. Suzuki, 2002, '*Effect of mechanical properties of powder on pneumatic conveying in inclined pipe.* Powder Technology, 122(2-3): p. 150-155.

Holland, F.A., 1995, '*Fluid flow for chemical engineers*' 2nd ed. Edward Arnold Publication London.

Howard, A 1984, '*Calculus with Analytical Geometry*' 2nd Edition. New York, Wiley Publication.

Isokangas, T. and White, B., 1993, '*Transportation and haulage practices in the Australasian mineral industry*' – underground systems, in Australasian Institute of Mining and Metallurgy, Volume 1, p91-92.

Jones I.0. 1989; '*Pneumatic Conveying in Mines*', Third International Conference on Bulk Materials, Storage, Handling and Transportation Newcastle 27-29 June

Kano T, 1985; '*Reduction of power consumption in pneumatic conveying of granular material*'. Proceedings of pneumatic conveying of bulk and powder conference. Trans Tech Publication. ISBN 0878490639 pp 185 – 192.

Kerttu S.M. 1985; '*Pipeliness - The Sealed and Quite Coal Transporters*' The National Engineering Conference, ASEA Pty. Limited, Melbourne. 2-8 March.

Klinzing, G. E. and Dhodapkar, S. V. 1993; Pressure fluctuation in pneumatic conveying systems powder technology. Vol 74, pp. 179-195.

Klinzing, G.E., Marcus, R.D., Rizk, F. and Leung, L.S., 1997; *Pneumatic Conveying of Solids -A Theoretical and Practical Approach*. Chapman & Hall.

Kraus M. N., 1980; '*Pneumatic Conveying of Bulk Materials*', 2nd Ed., McGraw-Hill, New York.

Law A.M. 2005, '*How to build valid and credible simulation models*' Proceedings of the 2005 Winter Simulation Conference, Tucson, U.S.A.

Leppkes, H 2005, '*Continuous Transport in Hard Rock Mining'*.

Liu H. 2003, '*Pipeline Engineering: Fundamentals for the Water and Wastewater Maintenance*' CRC Press ISBN:1587161400

Mason J. S, Mills D., Reed A. R. and Woodcock C. R 1980; *Introduction to pneumatic conveying*. Powder Europa 80, Industrial Awareness Seminar Lecture Notes. International Powder Institute, London, pp 1 – 57.

McCarthy, P.L. and Livingstone, R. 1993, '*Shaft of Decline? An Economic Comparison*' Open Pit to Underground: Making the transition. AIG Bulletin 14, 1993 pp 45 – 56.

McGregor, K 1967, '*The drilling of Rock' CR Books Ltd Publication*' pp 59-61,

Meriam, J. L. and Kraige L. G. 1993, 'Engineering Mechanics' Volume 1, 3rd Edition. John Wiley & Sons, Inc. p61.

Metzger, O.H. 1940, '*U.S. Bureau of Mines Information Circular*' No. 7095, Feb. 1940.

Meyer, S. 2007, Scharf, Germany – Personal communications

Meyer, S. 2008, Scharf, Germany – Personal communications

Mills D., 2004, '*Pneumatic conveying designs'*; Butterworth-Heinemann Publications 650 pp ISBN:0750654716

Mills D., Mason J. S. and Stacey R. B. 1982, '*A design study for the Pneumatic conveying of fine particulate material'*; Proceedings of Solidex 82, The Solid Handling Conference. Harrogate, England, pp C-1 to C-75.

Mills, D., 1990, '*Pneumatic Conveying Design Guide*.': Butterworth-Heinemann

Mohammed, S.A. 2005, '*Evaluation of Monorails*' BEng Thesis, WASM, Curtin University of Technology.

Morikawa, Y., Tsuji, Y., Matsui, K. and Jittani, Y., 1978, '*Pressure Drops due to Pipe Bends in Air-Solids Two Phase Flows: Circular and Elliptical Bends*', Int. J Multjphase Flow, Vol. 4, pp 575-583.

Nance, R. E., 1984, '*A tutorial view of simulation model development*' Proceedings of the Winter Simulation Conference, SIMULETTER, Vol. t5, No. 2.

Newmont, 2004: South Deeps Mining Study Report. Jundee Mine Planning Group.

Newmont, 2004; South Deeps Mining Study Report. Jundee Mine Planning Group.

Novak, T. and Kohler J. L. 1998, '*Technological innovations in deep coal mine power systems*,' IEEE Trans. Ind. Applicant., vol. 34, pp. 196–203.

Oguz, S. and Stefanko, R. 1971, '*Evaluation of a monorail mine haulage system*' Special Research Report, The PennState University, Department of Mining Engineering, 106p.

Othmer D.F. and Zenz, F.A., 1960; '*Fluidization and fluid particle systems*',: Reinhold, New York.

Ottjes, J.A., Meeuse, G.C., and Van Kuijk, G.T.L., 1976; '*Particle Velocity and Pressure Drop in Horizontal and Vertical Pipes*' Pneumotransport 3.

Pan, R. and Wypych P.W., 1997, '*Pressure Drop and Slug Velocity in Low-Velocity Pneumatic Conveying of Bulk Solids'.* Powder Technology; 94(2): pp123-132.

Pan, R. and Wypych, P.W. 1992; *Scale-up Procedures for Pneumatic ConveyingDesign.* Powder Handling and Processing; 4(2): p. 167-172.

Parfitt, N.L.C. and Griffin K.G. 1963, '*Development in transport of Men and Materials,*' The Colliery Guardian Overseas, pp 42 – 53.

Payne T. and Mitra R. 2008; A review of heat issues in underground metalliferous mines; *12th U.S./North American Mine Ventilation Symposium 2008 – Wallace (ed) The University of New South Wales, Sydney, Australia. ISBN 978-0-615-20009-5,* pp197 -201.

Pond R. 2000, '*Telephone conversation with author*' Evansville, IN: Frontier-Kemper Constructors.

Ratnayake C, 2005; '*A Comprehensive Scaling Up Technique for Pneumatic Transport Systems*' PhD Thesis Department of Technology, The Norwegian University of Sceince and Technology (NTNU), Norway.

Rhodes M., 2001; '*Pneumatic Transport of Powders*', Copyright © 2001 Martin Rhodes, Licensed to *ERPT;* Monash *University, Melbourne, Australia;*

Robertson, A.C., 1998, '*Trucking in the next Millennium*' in Underground operations Conference, Townsville, 30th June – 3rd July, 51-54 (The Australasian Institute of Mining and Metallurgy; Melbourne).

Sandvik Mining and Construction Manual, 2007, http://www.miningandconstruction.sandvik.com/

Sargent, G.R., 1991, '*Simulation Model Verification and Validation*', Proceedings of Winter Simulation Conference;

Scharf, 2007; '*EMTS Monorail*', Electric Powered Transport System Brochure.

Shannon, R. E. 1975, 'Systems Simulation: The Art and the Science', Prentice-Hall.

Sharp, J.J. 1988, '*Basic Fluid Mechanics*', Buttterworth & Company Ltd, ISBN 040801640X. pp47.

SRK-Turgis Report, 2002, '*Costs of material transport systems for incline shafts report.*'

Standridge C. R. and Tsai J. 1992; *'A method for computing discrete event simulation performance measures from traces',* Published by: SAGE Publication; ISBN: 0037 5497/91 USA

Sturgul, J. R. 2000, '*Mine Design; Examples using Simulation*.' SME Publications ISBN 0873351819

Terence, A 1997, '*Particle size measurement*' volume 1 – Powder Sampling and particle size measurement 5th Edition, Springer Published 1997, ISBN0412729504.

Toler, V.D. 1965, '*Diesel Shuttle Cars in an underground Coal Mines*,' Coal Age, p 56 – 58.

Tsuji, Y., 1982, '*Prediction of Pressure Drop and Optimal Design of Dilute Phase Pneumatic Conveying Systems'*, Pneumatech.

Udo, W P and James, A, W., 1993, '*Discrete Event Simulation; A Practical Approach*' CRC Press, ISBN 0849371740.

Wikipedia, 2007, 'Wikipedia. http://www.wikipedia.org.'

World Mining Equipment, 1996.

Wypych P.W., Kennedy O.C., Stebbins K. and Arnold P.C. 1990; '*Pneumatic Conveying of Coal*', Paper presented at the International Coal Engineering Conference, Sydney 19-21 Institution of Engineers, Australia

Wypych P.W. and Arnold P.C. 1984; '*Feasibility and Efficiency of Dense Phase Pneumatic Transportation'*, Transportation Conference, Perth, 30 October - 1 November;

Wypych, P. W. 1994; Optimising *the design and operation of pneumatic transport systems.* International Mechanical Engineering Congress. Perth Western Australia 15 – 19 May.

Wypych, P.W. and Pan, R. 1991; '*Determination of Air-only pressure Drop in Pneumatic Conveying Systems',* Powder Handling and Processing.

Yang, W., 1977, '*A Verified Theory on Dilute Phase Pneumatic Transport'*, Journal of Powder & Bulk Solids Technology, Vol. 1, No.1, Summer pp.89·95.

Zenz, F.A., 1964; '*Conveyability of Materials of Mixed Particle Size',* Industrial and Engineering Chemistry, American Chemical Society,. 3(1): p. 65-75.

Appendix 1

GPSS/H PROGRAM FOR SIMULATION OF THE MONORAIL HAULAGE SYSTEM

```
**********************************************************************************************************************
```

GPSSH Simulation program for monorail haulage system

Written by

Bunda Besa

```
**********************************************************************************************************************
        SIMULATE
MYFILE  FILEDEF         'C:\SP4\KAPEYA2.ATF'
        INTERGER        &J,&DRILL,&T,&LOADS,&NH,&FIN
        REAL            &LOAD,&DISC,&MUP,&MDOWN,&CDOWN,&OFFLOAD,&LIFT_
                        ,&DUMP,&WAIT,&TU1,&TU2,&TU3,&TU4,&TU5,&TU6,&TULIFT_
                        ,&TUS,&TD1,&TD2,&TD3,&TD4,&TD5,&TD6,&TDH,&TDS,&DR_
                        ,&TDD,&DUP,&DWAIT,&DIST1,&LWAIT,&BLAST,&FINE,&DECL
        LET     &LOAD=600               Time to load rock fragments in hopper
        LET     &DISC=20+FRN1*20        Time to connect / disconnect pipe
        LET     &MUP=1.8                Monorail upward speed (m/min)
        LET     &MDOWN=3.5              Monorail downward speed (m/min)
        LET     &CDOWN=20+FRN1*20       Time to lower monoral containers
        LET     &OFFLOAD=10+FRN1*4      Time to discharge material in cont
        LET     &LIFT=20+FRN1*20        Time to lift containers
        LET     &LWAIT=8+FRN1*4         Waiting time before lifting cont
        LET     &DUMP=80+FRN1*20        Dumping time for 6 cont. on surface
        LET     &WAIT=5                 Waiting time
        LET     &FINE=0                 Charging / Monorail start time
        LET     &J=4                    Tonnage to be loaded per round
        LET     &DR=240                 Time to drill one hole
        LET     &T=139                  Total tonnes from development end
        LET     &NH=86                  Number of holes
        LET     &DWAIT=24+FRN1*12       Drill wait time
        LET     &DIST1=30               Monorail Loading position from face
        LET     &BLAST=5400             Blasting, mark face etc
        LET     &DECL=1107              Decline length
        GENERATE    ,,,1
HOME    BPUTPIC     FILE=MYFILE,LINES=4,AC1,XID1,XID1,XID1
TIME *.****
CREATE MONO1 M*
CREATE DRILLF D*
CREATE WASTE W*
        BPUTPIC     FILE=MYFILE,LINES=2,AC1,XID1
TIME *.****
PLACE W* AT 14 17
        BPUTPIC     FILE=MYFILE,LINES=14,AC1,XID1,XID1,XID1,XID1,XID1,XID1_
        ,XID1,XID1,XID1,XID1,XID1,XID1,XID1
TIME *.****
CREATE ROD RO*
CREATE CONT1E CE1
CREATE CONT2E CE2
CREATE CONT3E CE3
CREATE CONT4E CE4
CREATE CONT5E CE5
CREATE CONT6E CE6
CREATE CONT1F CF1
CREATE CONT2F CF2
CREATE CONT3F CF3
CREATE CONT4F CF4
CREATE CONT5F CF5
CREATE CONT6F CF6
        BLET        &TDD=&DIST1/&MDOWN
        BPUTPIC     FILE=MYFILE,LINES=3,AC1,XID1,XID1,&TDD
TIME *.****
PLACE D* ON PDR
SET D* TRAVEL *.****
        ADVANCE     &TDD
        BPUTPIC     FILE=MYFILE,LINES=2,AC1,XID1
TIME *.****
```

```
PLACE D* AT 15.01 26.79
          BPUTPIC    FILE=MYFILE,LINES=8,AC1,XID1,XID1,XID1,XID1,XID1,XID1,XID1
TIME *.****
PLACE M* AT 67.74 50.36
PLACE CE1 ON C1
PLACE CE2 ON C2
PLACE CE3 ON C3
PLACE CE4 ON C4
PLACE CE5 ON C5
PLACE CE6 ON C6
          ADVANCE    &WAIT
          BPUTPIC    FILE=MYFILE,LINES=7,AC1,XID1,XID1,XID1,XID1,XID1,XID1
TIME *.****
SET CE1 TRAVEL *.****
SET CE2 TRAVEL *.****
SET CE3 TRAVEL *.****
SET CE4 TRAVEL *.****
SET CE5 TRAVEL *.****
SET CE6 TRAVEL *.****
     ADVANCE    &CDOWN
          BLET       &TDH=&DIST1/&MDOWN
          BPUTPIC    FILE=MYFILE,LINES=4,AC1,XID1,XID1,XID1,&TDH
TIME *.****
PLACE M* ON PH
SET D* CLASS DRILL
SET M* TRAVEL *.****
          ADVANCE    &TDH
          BPUTPIC    FILE=MYFILE,LINES=3,AC1,XID1,XID1
TIME *.****
CREATE ROD RD*
PLACE RD* AT 12 22.5
          BPUTPIC    FILE=MYFILE,LINES=2,AC1,AC1
TIME *.****
WRITE M8 ***.**
          BLET       &DRILL=AC1/&DR
          BPUTPIC    FILE=MYFILE,LINES=2,AC1,&DRILL
TIME *.****
WRITE M4 ***.**
          BPUTPIC    FILE=MYFILE,LINES=2,AC1,XID1
TIME *.****
DESTROY RD*
          BPUTPIC    FILE=MYFILE,LINES=3,AC1,XID1,XID1
TIME *.****
CREATE ROD RD*
PLACE RD* AT 12 22.5
          BLET       &DISC=&DISC
          BPUTPIC    FILE=MYFILE,LINES=1,AC1,&DISC
TIME *.****
          ADVANCE    &DISC
          BPUTPIC    FILE=MYFILE,LINES=4,AC1,XID1,XID1,XID1
TIME *.****
CREATE HOPPER HP*
SET M* CLASS MONO1
DESTROY HP*
          BLET       &LOAD=&LOAD
          BPUTPIC    FILE=MYFILE,LINES=5,AC1,XID1,XID1,XID1,XID1,&LOAD
TIME *.****
CREATE ROCK R*
CREATE ROCK1 RH*
PLACE RH* ON EH
SET RH* TRAVEL *.****
          ADVANCE    &LOAD
          BPUTPIC    FILE=MYFILE,LINES=2,AC1,XID1
TIME *.****
DESTROY RD*
          BPUTPIC    FILE=MYFILE,LINES=2,AC1,XID1
```

```
TIME *.****
DESTROY RH*
          BLET      &DISC=&DISC
          BPUTPIC   FILE=MYFILE,LINES=1,AC1,&DISC
TIME *.****
          ADVANCE   &DISC
          BLET      &TU1=3.5/&MUP
          BPUTPIC   FILE=MYFILE,LINES=3,AC1,XID1,XID1,&TU1
TIME *.****
PLACE M* ON P1A
SET M* TRAVEL *.****
          ADVANCE   &TU1
          BPUTPIC   FILE=MYFILE,LINES=3,AC1,XID1,XID1
TIME *.****
CREATE ROD RD*
PLACE RD* AT 12 22.5
          BLET      &OFFLOAD=&OFFLOAD
          BPUTPIC   FILE=MYFILE,LINES=3,AC1,XID1,XID1,&OFFLOAD
TIME *.****
PLACE R* ON C1
SET R* TRAVEL *.****
          ADVANCE   &OFFLOAD
          BPUTPIC   FILE=MYFILE,LINES=2,AC1,XID1
TIME *.****
DESTROY RD*
          BPUTPIC   FILE=MYFILE,LINES=5,AC1,XID1,XID1,XID1,XID1
TIME *.****
DESTROY R*
SET CE1 CLASS CONT1F
PLACE CF1 ON CC1
DESTROY CE1
          BLET      &LOADS=&LOADS+&J
          BPUTPIC   FILE=MYFILE,LINES=4,AC1,AC1,&LOADS,AC1
TIME *.****
WRITE M1 ***.**
WRITE M2 ***.**
WRITE M8 ***.**
          BPUTPIC   FILE=MYFILE,LINES=3,AC1,XID1,XID1
TIME *.****
CREATE ROD RD*
PLACE RD* AT 12 22.5
          BLET      &DRILL=AC1/&DR
          BPUTPIC   FILE=MYFILE,LINES=2,AC1,&DRILL
TIME *.****
WRITE M4 ***.**
          BLET      &TD1=3.5/&MDOWN
          BPUTPIC   FILE=MYFILE,LINES=3,AC1,XID1,XID1,&TD1
TIME *.****
PLACE M* ON P1B
SET M* TRAVEL *.****
          ADVANCE   &TD1
          BPUTPIC   FILE=MYFILE,LINES=2,AC1,XID1
TIME *.****
DESTROY RD*
     BLET      &DISC=&DISC
     BPUTPIC   FILE=MYFILE,LINES=1,AC1,&DISC
TIME *.****
          ADVANCE   &DISC
          BPUTPIC   FILE=MYFILE,LINES=4,AC1,XID1,XID1,XID1
TIME *.****
CREATE HOPPER HP*
SET M* CLASS MONO1
DESTROY HP*
          BLET      &LOAD=&LOAD
          BPUTPIC   FILE=MYFILE,LINES=5,AC1,XID1,XID1,XID1,XID1,&LOAD
TIME *.****
```

```
CREATE ROCK R*
CREATE ROCK1 RH*
PLACE RH* ON EH
SET RH* TRAVEL *.****
        ADVANCE    &LOAD
        BPUTPIC    FILE=MYFILE,LINES=3,AC1,XID1,XID1
TIME *.****
CREATE ROD RD*
PLACE RD* AT 12 22.5
        BPUTPIC    FILE=MYFILE,LINES=2,AC1,XID1
TIME *.****
DESTROY RH*
        BLET       &DISC=&DISC
        BPUTPIC    FILE=MYFILE,LINES=1,AC1,&DISC
TIME *.****
        ADVANCE    &DISC
        BLET       &TU2=7/&MUP
        BPUTPIC    FILE=MYFILE,LINES=3,AC1,XID1,XID1,&TU2
TIME *.****
PLACE M* ON P2A
SET M* TRAVEL *.****
        ADVANCE    &TU2
        BPUTPIC    FILE=MYFILE,LINES=2,AC1,XID1
TIME *.****
DESTROY RD*
        BLET       &OFFLOAD=&OFFLOAD
        BPUTPIC    FILE=MYFILE,LINES=3,AC1,XID1,XID1,&OFFLOAD
TIME *.****
PLACE R* ON C2
SET R* TRAVEL *.****
        ADVANCE    &OFFLOAD
        BPUTPIC    FILE=MYFILE,LINES=5,AC1,XID1,XID1,XID1,XID1
TIME *.****
DESTROY R*
SET CE2 CLASS CONT2F
PLACE CF2 ON CC2
DESTROY CE2
        BLET       &LOADS=&LOADS+&J
        BPUTPIC    FILE=MYFILE,LINES=4,AC1,AC1,&LOADS,AC1
TIME *.****
WRITE M1 ***.**
WRITE M2 ***.**
WRITE M8 ***.**
        BLET      &DRILL=AC1/&DR
        BPUTPIC   FILE=MYFILE,LINES=2,AC1,&DRILL
TIME *.****
WRITE M4 ***.**
        BLET       &TD2=7/&MDOWN
        BPUTPIC    FILE=MYFILE,LINES=3,AC1,XID1,XID1,&TD2
TIME *.****
PLACE M* ON P2B
SET M* TRAVEL *.****
        ADVANCE    &TD2
        BPUTPIC    FILE=MYFILE,LINES=3,AC1,XID1,XID1
TIME *.****
CREATE ROD RD*
PLACE RD* AT 12 22.5
        BLET       &DISC=&DISC
        BPUTPIC    FILE=MYFILE,LINES=1,AC1,&DISC
TIME *.****
        ADVANCE    &DISC
        BPUTPIC    FILE=MYFILE,LINES=4,AC1,XID1,XID1,XID1
TIME *.****
CREATE HOPPER HP*
SET M* CLASS MONO1
DESTROY HP*
```

```
          BLET      &LOAD=&LOAD
          BPUTPIC   FILE=MYFILE,LINES=5,AC1,XID1,XID1,XID1,XID1,&LOAD
TIME *.****
CREATE ROCK R*
CREATE ROCK1 RH*
PLACE RH* ON EH
SET RH* TRAVEL *.****
          ADVANCE   &LOAD
          BPUTPIC   FILE=MYFILE,LINES=2,AC1,XID1
TIME *.****
DESTROY RD*
          BPUTPIC   FILE=MYFILE,LINES=2,AC1,XID1
TIME *.****
DESTROY RH*
          BLET      &DISC=&DISC
          BPUTPIC   FILE=MYFILE,LINES=1,AC1,&DISC
TIME *.****
          ADVANCE   &DISC
          BLET      &TU3=10.5/&MUP
          BPUTPIC   FILE=MYFILE,LINES=3,AC1,XID1,XID1,&TU3
TIME *.****
PLACE M* ON P3A
SET M* TRAVEL *.****
          ADVANCE   &TU3
          BPUTPIC   FILE=MYFILE,LINES=3,AC1,XID1,XID1
TIME *.****
CREATE ROD RD*
PLACE RD* AT 12 22.5
          BLET      &OFFLOAD=&OFFLOAD
          BPUTPIC   FILE=MYFILE,LINES=3,AC1,XID1,XID1,&OFFLOAD
TIME *.****
PLACE R* ON C3
SET R* TRAVEL *.****
          ADVANCE   &OFFLOAD
          BPUTPIC   FILE=MYFILE,LINES=5,AC1,XID1,XID1,XID1,XID1
TIME *.****
DESTROY R*
SET CE3 CLASS CONT3F
PLACE CF3 ON CC3
DESTROY CE3
          BLET      &LOADS=&LOADS+&J
          BPUTPIC   FILE=MYFILE,LINES=4,AC1,AC1,&LOADS,AC1
TIME *.****
WRITE M1 ***.**
WRITE M2 ***.**
WRITE M8 ***.**
          BLET      &DRILL=AC1/&DR
          BPUTPIC   FILE=MYFILE,LINES=2,AC1,&DRILL
TIME *.****
WRITE M4 ***.**
          BLET      &TD3=10.5/&MDOWN
          BPUTPIC   FILE=MYFILE,LINES=3,AC1,XID1,XID1,&TD3
TIME *.****
PLACE M* ON P3B
SET M* TRAVEL *.****
          ADVANCE   &TD3
          BPUTPIC   FILE=MYFILE,LINES=2,AC1,XID1
TIME *.****
DESTROY RD*
          BLET      &DISC=&DISC
          BPUTPIC   FILE=MYFILE,LINES=1,AC1,&DISC
TIME *.****
          ADVANCE   &DISC
          BPUTPIC   FILE=MYFILE,LINES=4,AC1,XID1,XID1,XID1
TIME *.****
CREATE HOPPER HP*
```

```
SET M* CLASS MONO1
DESTROY HP*
          BLET      &LOAD=&LOAD
          BPUTPIC   FILE=MYFILE,LINES=5,AC1,XID1,XID1,XID1,XID1,&LOAD
TIME *.****
CREATE ROCK R*
CREATE ROCK1 RH*
PLACE RH* ON EH
SET RH* TRAVEL *.****
          ADVANCE   &LOAD
          BPUTPIC   FILE=MYFILE,LINES=3,AC1,XID1,XID1
TIME *.****
CREATE ROD RD*
PLACE RD* AT 12 22.5
          BPUTPIC   FILE=MYFILE,LINES=2,AC1,XID1
TIME *.****
DESTROY RH*
          BLET      &DISC=&DISC
          BPUTPIC   FILE=MYFILE,LINES=1,AC1,&DISC
TIME *.****
          ADVANCE   &DISC
          BLET      &TU4=14/&MUP
          BPUTPIC   FILE=MYFILE,LINES=3,AC1,XID1,XID1,&TU4
TIME *.****
PLACE M* ON P4A
SET M* TRAVEL *.****
          ADVANCE   &TU4
          BPUTPIC   FILE=MYFILE,LINES=2,AC1,XID1
TIME *.****
DESTROY RD*
          BLET      &OFFLOAD=&OFFLOAD
          BPUTPIC   FILE=MYFILE,LINES=3,AC1,XID1,XID1,&OFFLOAD
TIME *.****
PLACE R* ON C4
SET R* TRAVEL *.****
          ADVANCE   &OFFLOAD
          BPUTPIC   FILE=MYFILE,LINES=5,AC1,XID1,XID1,XID1,XID1
TIME *.****
DESTROY R*
SET CE4 CLASS CONT4F
PLACE CF4 ON CC4
DESTROY CE4
          BLET      &LOADS=&LOADS+&J
          BPUTPIC   FILE=MYFILE,LINES=4,AC1,AC1,&LOADS,AC1
TIME *.****
WRITE M1 ***.**
WRITE M2 ***.**
WRITE M8 ***.**
          BLET      &DRILL=AC1/&DR
          BPUTPIC   FILE=MYFILE,LINES=2,AC1,&DRILL
TIME *.****
WRITE M4 ***.**
          BLET      &TD4=14/&MDOWN
          BPUTPIC   FILE=MYFILE,LINES=3,AC1,XID1,XID1,&TD4
TIME *.****
PLACE M* ON P4B
SET M* TRAVEL *.****
          ADVANCE   &TD4
          BPUTPIC   FILE=MYFILE,LINES=3,AC1,XID1,XID1
TIME *.****
CREATE ROD RD*
PLACE RD* AT 12 22.5
          BLET      &DISC=&DISC
          BPUTPIC   FILE=MYFILE,LINES=1,AC1,&DISC
TIME *.****
          ADVANCE   &DISC
```

```
        BPUTPIC    FILE=MYFILE,LINES=4,AC1,XID1,XID1,XID1
TIME *.****
CREATE HOPPER HP*
SET M* CLASS MONO1
DESTROY HP*
        BLET       &LOAD=&LOAD
        BPUTPIC    FILE=MYFILE,LINES=5,AC1,XID1,XID1,XID1,XID1,&LOAD
TIME *.****
CREATE ROCK R*
CREATE ROCK1 RH*
PLACE RH* ON EH
SET RH* TRAVEL *.****
        ADVANCE    &LOAD
        BPUTPIC    FILE=MYFILE,LINES=2,AC1,XID1
TIME *.****
DESTROY RD*
        BPUTPIC    FILE=MYFILE,LINES=2,AC1,XID1
TIME *.****
DESTROY RH*
        BLET       &DISC=&DISC
        BPUTPIC    FILE=MYFILE,LINES=1,AC1,&DISC
TIME *.****
        ADVANCE    &DISC
        BLET       &TU5=17.5/&MUP
        BPUTPIC    FILE=MYFILE,LINES=3,AC1,XID1,XID1,&TU5
TIME *.****
PLACE M* ON P5A
SET M* TRAVEL *.****
        ADVANCE    &TU5
        BPUTPIC    FILE=MYFILE,LINES=3,AC1,XID1,XID1
TIME *.****
CREATE ROD RD*
PLACE RD* AT 12 22.5
        BLET       &OFFLOAD=&OFFLOAD
        BPUTPIC    FILE=MYFILE,LINES=3,AC1,XID1,XID1,&OFFLOAD
TIME *.****
PLACE R* ON C5
SET R* TRAVEL *.****
        ADVANCE    &OFFLOAD
        BPUTPIC    FILE=MYFILE,LINES=5,AC1,XID1,XID1,XID1,XID1
TIME *.****
DESTROY R*
SET CE5 CLASS CONT5F
PLACE CF5 ON CC5
DESTROY CE5
        BLET       &LOADS=&LOADS+&J
        BPUTPIC    FILE=MYFILE,LINES=4,AC1,AC1,&LOADS,AC1
TIME *.****
WRITE M1 ***.**
WRITE M2 ***.**
WRITE M8 ***.**
        BLET       &DRILL=AC1/&DR
        BPUTPIC    FILE=MYFILE,LINES=2,AC1,&DRILL
TIME *.****
WRITE M4 ***.**
        BLET       &TD5=17.5/&MDOWN
        BPUTPIC    FILE=MYFILE,LINES=3,AC1,XID1,XID1,&TD5
TIME *.****
PLACE M* ON P5B
SET M* TRAVEL *.****
        ADVANCE    &TD5
        BPUTPIC    FILE=MYFILE,LINES=2,AC1,XID1
TIME *.****
DESTROY RD*
        BLET       &DISC=&DISC
        BPUTPIC    FILE=MYFILE,LINES=1,AC1,&DISC
```

```
TIME *.****
          ADVANCE    &DISC
          BPUTPIC    FILE=MYFILE,LINES=4,AC1,XID1,XID1,XID1
TIME *.****
CREATE HOPPER HP*
SET M* CLASS MONO1
DESTROY HP*
          BLET       &LOAD=&LOAD
          BPUTPIC    FILE=MYFILE,LINES=5,AC1,XID1,XID1,XID1,XID1,&LOAD
TIME *.****
CREATE ROCK R*
CREATE ROCK1 RH*
PLACE RH* ON EH
SET RH* TRAVEL *.****
          ADVANCE    &LOAD
          BPUTPIC    FILE=MYFILE,LINES=2,AC1,XID1
TIME *.****
DESTROY RH*
          BLET       &DISC=&DISC
          BPUTPIC    FILE=MYFILE,LINES=1,AC1,&DISC
TIME *.****
          ADVANCE    &DISC
          BPUTPIC    FILE=MYFILE,LINES=3,AC1,XID1,XID1
TIME *.****
CREATE ROD RD*
PLACE RD* AT 12 22.5
          BLET       &TU6=21/&MUP
          BPUTPIC    FILE=MYFILE,LINES=3,AC1,XID1,XID1,&TU6
TIME *.****
PLACE M* ON P6A
SET M* TRAVEL *.****
          ADVANCE    &TU6
          BPUTPIC    FILE=MYFILE,LINES=2,AC1,XID1
TIME *.****
DESTROY RD*
          BLET       &OFFLOAD=&OFFLOAD
          BPUTPIC    FILE=MYFILE,LINES=3,AC1,XID1,XID1,&OFFLOAD
TIME *.****
PLACE R* ON C6
SET R* TRAVEL *.****
          ADVANCE    &OFFLOAD
          BPUTPIC    FILE=MYFILE,LINES=5,AC1,XID1,XID1,XID1,XID1
TIME *.****
DESTROY R*
SET CE6 CLASS CONT6F
PLACE CF6 ON CC6
DESTROY CE6
          BLET       &LOADS=&LOADS+&J
          BPUTPIC    FILE=MYFILE,LINES=4,AC1,AC1,&LOADS,AC1
TIME *.****
WRITE M1 ***.**
WRITE M2 ***.**
WRITE M8 ***.**
          TEST L     &LOADS,&T,DOWN
          BLET       &DRILL=AC1/&DR
          BPUTPIC    FILE=MYFILE,LINES=2,AC1,&DRILL
TIME *.****
WRITE M4 ***.**
          BLET       &TD6=21/&MDOWN
          BPUTPIC    FILE=MYFILE,LINES=3,AC1,XID1,XID1,&TD6
TIME *.****
PLACE M* ON P6B
SET M* TRAVEL *.****
          ADVANCE    &TD6
          BPUTPIC    FILE=MYFILE,LINES=3,AC1,XID1,XID1
TIME *.****
```

```
CREATE ROD RD*
PLACE RD* AT 12 22.5
          BLET      &DISC=&DISC
          BPUTPIC   FILE=MYFILE,LINES=1,AC1,&DISC
TIME *.****
          ADVANCE   &DISC
          BLET      &TULIFT=&DIST1/&MUP
          BPUTPIC   FILE=MYFILE,LINES=6,AC1,XID1,XID1,XID1,XID1,XID1,&TULIFT
TIME *.****
PLACE M* ON PL
CREATE HOPPER HP*
SET M* CLASS TRAIN
PLACE HP* AT 22 30
SET M* TRAVEL *.****
          ADVANCE   &TULIFT
          BPUTPIC   FILE=MYFILE,LINES=2,AC1,XID1
TIME *.****
DESTROY RD*
UPTOP   BPUTPIC   FILE=MYFILE,LINES=3,AC1,XID1,XID1
TIME *.****
PLACE M* AT 67.74 50.36
          BLET      &LWAIT=&LWAIT
          BPUTPIC   FILE=MYFILE,LINES=1,AC1,&LWAIT
TIME *.****
          ADVANCE   &LWAIT
          BLET      &LIFT=&LIFT
          BPUTPIC   FILE=MYFILE,LINES=7,AC1,XID1,XID1,XID1,XID1,XID1,XID1,&LIFT
TIME *.****
SET CF1 TRAVEL *.****
SET CF2 TRAVEL *.****
SET CF3 TRAVEL *.****
SET CF4 TRAVEL *.****
SET CF5 TRAVEL *.****
SET CF6 TRAVEL *.****
          ADVANCE   &LIFT
          BPUTPIC   FILE=MYFILE,LINES=3,AC1,XID1,XID1
TIME *.****
CREATE ROD RD*
PLACE RD* AT 12 22.5
          BPUTPIC   FILE=MYFILE,LINES=7,AC1,XID1,XID1,XID1,XID1,XID1,XID1
TIME *.****
DESTROY CF1
DESTROY CF2
DESTROY CF3
DESTROY CF4
DESTROY CF5
DESTROY CF6
          BLET      &TUS=&DECL/&MUP
          BPUTPIC   FILE=MYFILE,LINES=3,AC1,XID1,XID1,&TUS,XID1,XID1,&MUP
TIME *.****
PLACE M* ON PZ
SET M* TRAVEL *.****
          ADVANCE   &TUS
          BPUTPIC   FILE=MYFILE,LINES=2,AC1,XID1
TIME *.****
DESTROY RD*
          BPUTPIC   FILE=MYFILE,LINES=2,AC1,XID1
TIME *.****
PLACE M* AT 419.78 150.04
          BLET      &DUMP=&DUMP
          BPUTPIC   FILE=MYFILE,LINES=4,AC1,XID1,XID1,XID1,&DUMP
TIME *.****
CREATE ROCK R*
PLACE R* ON PD1
SET R* TRAVEL *.****
          ADVANCE   &DUMP
```

```
          BPUTPIC    FILE=MYFILE,LINES=2,AC1,XID1
TIME *.****
DESTROY R*
          BLET       &TDS=&DECL/&MDOWN
          BPUTPIC    FILE=MYFILE,LINES=3,AC1,XID1,XID1,&TDS
TIME *.****
PLACE M* ON PZ1
SET M* TRAVEL *.****
          ADVANCE    &TDS
          BPUTPIC    FILE=MYFILE,LINES=3,AC1,XID1,XID1
TIME *.****
CREATE ROD RD*
PLACE RD* AT 12 22.5
          BPUTPIC    FILE=MYFILE,LINES=2,AC1,XID1
TIME *.****
PLACE M* AT 67.74 50.36
          BLET       &LWAIT=&LWAIT
          BPUTPIC    FILE=MYFILE,LINES=1,AC1,&LWAIT
TIME *.****
          ADVANCE    &LWAIT
          BPUTPIC    FILE=MYFILE,LINES=13,AC1,XID1,XID1,XID1,XID1,XID1,XID1,XID1_
            ,XID1,XID1,XID1,XID1,XID1,XID1
TIME *.****
CREATE CONT1E CE1
CREATE CONT2E CE2
CREATE CONT3E CE3
CREATE CONT4E CE4
CREATE CONT5E CE5
CREATE CONT6E CE6
CREATE CONT1F CF1
CREATE CONT2F CF2
CREATE CONT3F CF3
CREATE CONT4F CF4
CREATE CONT5F CF5
CREATE CONT6F CF6
          BPUTPIC    FILE=MYFILE,LINES=7,AC1,XID1,XID1,XID1,XID1,XID1,XID1
TIME *.****
PLACE CE1 ON C1
PLACE CE2 ON C2
PLACE CE3 ON C3
PLACE CE4 ON C4
PLACE CE5 ON C5
PLACE CE6 ON C6
          BLET       &WAIT=&WAIT
          BPUTPIC    FILE=MYFILE,LINES=1,AC1,&WAIT
TIME *.****
          ADVANCE    &WAIT
          BPUTPIC    FILE=MYFILE,LINES=2,AC1,XID1
TIME *.****
DESTROY RD*
          BLET       &CDOWN=&CDOWN
          BPUTPIC    FILE=MYFILE,LINES=7,AC1,XID1,XID1,XID1,XID1,XID1,XID1_
          ,XID1,&CDOWN
TIME *.****
SET CE1 TRAVEL *.****
SET CE2 TRAVEL *.****
SET CE3 TRAVEL *.****
SET CE4 TRAVEL *.****
SET CE5 TRAVEL *.****
SET CE6 TRAVEL *.****
          ADVANCE    &CDOWN
          BLET       &TDH=&DIST1/&MDOWN
          BPUTPIC    FILE=MYFILE,LINES=3,AC1,XID1,XID1,&TDH
TIME *.****
PLACE M* ON PH
SET M* TRAVEL *.****
```

```
          ADVANCE    &TDH
          BPUTPIC    FILE=MYFILE,LINES=3,AC1,XID1,XID1
TIME *.****
CREATE ROD RD*
PLACE RD* AT 12 22.5
          BLET       &DISC=&DISC
          BPUTPIC    FILE=MYFILE,LINES=1,AC1,&DISC
TIME *.****
          ADVANCE    &DISC
          BPUTPIC    FILE=MYFILE,LINES=3,AC1,XID1,XID1
TIME *.****
SET M* CLASS MONO1
DESTROY HP*
          BLET       &LOAD=&LOAD
          BPUTPIC    FILE=MYFILE,LINES=5,AC1,XID1,XID1,XID1,XID1,&LOAD
TIME *.****
CREATE ROCK R*
CREATE ROCK1 RH*
PLACE RH* ON EH
SET RH* TRAVEL *.****
          ADVANCE    &LOAD
          BPUTPIC    FILE=MYFILE,LINES=2,AC1,XID1
TIME *.****
DESTROY RD*
          BPUTPIC    FILE=MYFILE,LINES=2,AC1,XID1
TIME *.****
DESTROY RH*
          BLET       &DISC=&DISC
          BPUTPIC    FILE=MYFILE,LINES=1,AC1,&DISC
TIME *.****
          ADVANCE    &DISC
          BLET       &TU1=3.5/&MUP
          BPUTPIC    FILE=MYFILE,LINES=3,AC1,XID1,XID1,&TU1
TIME *.****
PLACE M* ON P1A
SET M* TRAVEL *.****
          ADVANCE    &TU1
          BPUTPIC    FILE=MYFILE,LINES=3,AC1,XID1,XID1
TIME *.****
CREATE ROD RD*
PLACE RD* AT 12 22.5
          BLET       &OFFLOAD=&OFFLOAD
          BPUTPIC    FILE=MYFILE,LINES=3,AC1,XID1,XID1,&OFFLOAD
TIME *.****
PLACE R* ON C1
SET R* TRAVEL *.****
          ADVANCE    &OFFLOAD
          BPUTPIC    FILE=MYFILE,LINES=5,AC1,XID1,XID1,XID1,XID1
TIME *.****
DESTROY R*
SET CE1 CLASS CONT1F
PLACE CF1 ON CC1
DESTROY CE1
          BLET       &LOADS=&LOADS+&J
          BPUTPIC    FILE=MYFILE,LINES=4,AC1,AC1,&LOADS,AC1
TIME *.****
WRITE M1 ***.**
WRITE M2 ***.**
WRITE M8 ***.**
          BLET       &DRILL=AC1/&DR
          BPUTPIC    FILE=MYFILE,LINES=2,AC1,&DRILL
TIME *.****
WRITE M4 ***.**
          BLET       &TD1=3.5/&MDOWN
          BPUTPIC    FILE=MYFILE,LINES=3,AC1,XID1,XID1,&TD1
TIME *.****
```

```
PLACE M* ON P1B
SET M* TRAVEL *.****
          ADVANCE    &TD1
          BPUTPIC    FILE=MYFILE,LINES=2,AC1,XID1
TIME *.****
DESTROY RD*
          BLET       &DISC=&DISC
          BPUTPIC    FILE=MYFILE,LINES=1,AC1,&DISC
TIME *.****
          ADVANCE    &DISC
          BLET       &LOAD=&LOAD
          BPUTPIC    FILE=MYFILE,LINES=5,AC1,XID1,XID1,XID1,XID1,&LOAD
TIME *.****
CREATE ROCK R*
CREATE ROCK1 RH*
PLACE RH* ON EH
SET RH* TRAVEL *.****
          ADVANCE    &LOAD
          BPUTPIC    FILE=MYFILE,LINES=3,AC1,XID1,XID1
TIME *.****
CREATE ROD RD*
PLACE RD* AT 12 22.5
          BPUTPIC    FILE=MYFILE,LINES=2,AC1,XID1
TIME *.****
DESTROY RH*
          BLET       &DISC=&DISC
          BPUTPIC    FILE=MYFILE,LINES=1,AC1,&DISC
TIME *.****
          ADVANCE    &DISC
          BLET       &TU2=7/&MUP
          BPUTPIC    FILE=MYFILE,LINES=3,AC1,XID1,XID1,&TU2
TIME *.****
PLACE M* ON P2A
SET M* TRAVEL *.****
          ADVANCE    &TU2
          BPUTPIC    FILE=MYFILE,LINES=2,AC1,XID1
TIME *.****
DESTROY RD*
          BLET       &OFFLOAD=&OFFLOAD
          BPUTPIC    FILE=MYFILE,LINES=3,AC1,XID1,XID1,&OFFLOAD
TIME *.****
PLACE R* ON C2
SET R* TRAVEL *.****
          ADVANCE    &OFFLOAD
          BPUTPIC    FILE=MYFILE,LINES=5,AC1,XID1,XID1,XID1,XID1
TIME *.****
DESTROY R*
SET CE2 CLASS CONT2F
PLACE CF2 ON CC2
DESTROY CE2
          BLET       &LOADS=&LOADS+&J
          BPUTPIC    FILE=MYFILE,LINES=4,AC1,AC1,&LOADS,AC1
TIME *.****
WRITE M1 ***.**
WRITE M2 ***.**
WRITE M8 ***.**
          BLET       &DRILL=AC1/&DR
          BPUTPIC    FILE=MYFILE,LINES=2,AC1,&DRILL
TIME *.****
WRITE M4 ***.**
          BLET       &TD2=7/&MDOWN
          BPUTPIC    FILE=MYFILE,LINES=3,AC1,XID1,XID1,&TD2
TIME *.****
PLACE M* ON P2B
SET M* TRAVEL *.****
          ADVANCE    &TD2
```

```
          BPUTPIC    FILE=MYFILE,LINES=3,AC1,XID1,XID1
TIME *.****
CREATE ROD RD*
PLACE RD* AT 12 22.5
          BLET      &DISC=&DISC
          BPUTPIC    FILE=MYFILE,LINES=1,AC1,&DISC
TIME *.****
           ADVANCE    &DISC
          BPUTPIC    FILE=MYFILE,LINES=4,AC1,XID1,XID1,XID1
TIME *.****
CREATE HOPPER HP*
SET M* CLASS MONO1
DESTROY HP*
          BLET      &LOAD=&LOAD
           BPUTPIC    FILE=MYFILE,LINES=5,AC1,XID1,XID1,XID1,XID1,&LOAD
TIME *.****
CREATE ROCK R*
CREATE ROCK1 RH*
PLACE RH* ON EH
SET RH* TRAVEL *.****
          ADVANCE    &LOAD
          BPUTPIC    FILE=MYFILE,LINES=2,AC1,XID1
TIME *.****
DESTROY RD*
          BPUTPIC    FILE=MYFILE,LINES=2,AC1,XID1
TIME *.****
DESTROY RH*
          BLET      &DISC=&DISC
          BPUTPIC    FILE=MYFILE,LINES=1,AC1,&DISC
TIME *.****
          ADVANCE    &DISC
          BLET      &TU3=10.5/&MUP
          BPUTPIC    FILE=MYFILE,LINES=3,AC1,XID1,XID1,&TU3
TIME *.****
PLACE M* ON P3A
SET M* TRAVEL *.****
          ADVANCE    &TU3
          BPUTPIC    FILE=MYFILE,LINES=3,AC1,XID1,XID1
TIME *.****
CREATE ROD RD*
PLACE RD* AT 12 22.5
          BLET      &OFFLOAD=&OFFLOAD
          BPUTPIC    FILE=MYFILE,LINES=3,AC1,XID1,XID1,&OFFLOAD
TIME *.****
PLACE R* ON C3
SET R* TRAVEL *.****
          ADVANCE    &OFFLOAD
          BPUTPIC    FILE=MYFILE,LINES=5,AC1,XID1,XID1,XID1,XID1
TIME *.****
DESTROY R*
SET CE3 CLASS CONT3F
PLACE CF3 ON CC3
DESTROY CE3
          BLET      &LOADS=&LOADS+&J
          BPUTPIC    FILE=MYFILE,LINES=4,AC1,AC1,&LOADS,AC1
TIME *.****
WRITE M1 ***.**
WRITE M2 ***.**
WRITE M8 ***.**
          BLET      &DRILL=AC1/&DR
          BPUTPIC    FILE=MYFILE,LINES=2,AC1,&DRILL
TIME *.****
WRITE M4 ***.**
          BLET      &TD3=10.5/&MDOWN
          BPUTPIC    FILE=MYFILE,LINES=3,AC1,XID1,XID1,&TD3
TIME *.****
```

```
PLACE M* ON P3B
SET M* TRAVEL *.****
        ADVANCE    &TD3
        BPUTPIC    FILE=MYFILE,LINES=2,AC1,XID1
TIME *.****
DESTROY RD*
        BLET       &DISC=&DISC
        BPUTPIC    FILE=MYFILE,LINES=1,AC1,&DISC
TIME *.****
        ADVANCE    &DISC
        BPUTPIC    FILE=MYFILE,LINES=4,AC1,XID1,XID1,XID1
TIME *.****
CREATE HOPPER HP*
SET M* CLASS MONO1
DESTROY HP*
        BLET       &LOAD=&LOAD
        BPUTPIC    FILE=MYFILE,LINES=5,AC1,XID1,XID1,XID1,XID1,&LOAD
TIME *.****
CREATE ROCK R*
CREATE ROCK1 RH*
PLACE RH* ON EH
SET RH* TRAVEL *.****
        ADVANCE    &LOAD
        BPUTPIC    FILE=MYFILE,LINES=3,AC1,XID1,XID1
TIME *.****
CREATE ROD RD*
PLACE RD* AT 12 22.5
        BPUTPIC    FILE=MYFILE,LINES=2,AC1,XID1
TIME *.****
DESTROY RH*
        BLET       &DISC=&DISC
        BPUTPIC    FILE=MYFILE,LINES=1,AC1,&DISC
TIME *.****
        ADVANCE    &DISC
        BLET       &TU4=14/&MUP
        BPUTPIC    FILE=MYFILE,LINES=3,AC1,XID1,XID1,&TU4
TIME *.****
PLACE M* ON P4A
SET M* TRAVEL *.****
        ADVANCE    &TU4
        BPUTPIC    FILE=MYFILE,LINES=2,AC1,XID1
TIME *.****
DESTROY RD*
        BLET       &OFFLOAD=&OFFLOAD
        BPUTPIC    FILE=MYFILE,LINES=3,AC1,XID1,XID1,&OFFLOAD
TIME *.****
PLACE R* ON C4
SET R* TRAVEL *.****
        ADVANCE    &OFFLOAD
        BPUTPIC    FILE=MYFILE,LINES=5,AC1,XID1,XID1,XID1,XID1
TIME *.****
DESTROY R*
SET CE4 CLASS CONT4F
PLACE CF4 ON CC4
DESTROY CE4
        BLET       &LOADS=&LOADS+&J
        BPUTPIC    FILE=MYFILE,LINES=4,AC1,AC1,&LOADS,AC1
TIME *.****
WRITE M1 ***.**
WRITE M2 ***.**
WRITE M8 ***.**
        BLET       &DRILL=AC1/&DR
        BPUTPIC    FILE=MYFILE,LINES=2,AC1,&DRILL
TIME *.****
WRITE M4 ***.**
        BLET       &TD4=14/&MDOWN
```

```
          BPUTPIC    FILE=MYFILE,LINES=3,AC1,XID1,XID1,&TD4
TIME *.****
PLACE M* ON P4B
SET M* TRAVEL *.****
          ADVANCE    &TD4
          BPUTPIC    FILE=MYFILE,LINES=3,AC1,XID1,XID1
TIME *.****
CREATE ROD RD*
PLACE RD* AT 12 22.5
          BLET       &DISC=&DISC
          BPUTPIC    FILE=MYFILE,LINES=1,AC1,&DISC
TIME *.****
          ADVANCE    &DISC
          BLET       &LOAD=&LOAD
          BPUTPIC    FILE=MYFILE,LINES=5,AC1,XID1,XID1,XID1,XID1,&LOAD
TIME *.****
CREATE ROCK R*
CREATE ROCK1 RH*
PLACE RH* ON EH
SET RH* TRAVEL *.****
          ADVANCE    &LOAD
          BPUTPIC    FILE=MYFILE,LINES=2,AC1,XID1
TIME *.****
DESTROY RD*
          BPUTPIC    FILE=MYFILE,LINES=2,AC1,XID1
TIME *.****
DESTROY RH*
          BLET       &DISC=&DISC
          BPUTPIC    FILE=MYFILE,LINES=1,AC1,&DISC
TIME *.****
          ADVANCE    &DISC
          BLET       &TU5=17.5/&MUP
          BPUTPIC    FILE=MYFILE,LINES=3,AC1,XID1,XID1,&TU5
TIME *.****
PLACE M* ON P5A
SET M* TRAVEL *.****
          ADVANCE    &TU5
          BPUTPIC    FILE=MYFILE,LINES=3,AC1,XID1,XID1
TIME *.****
CREATE ROD RD*
PLACE RD* AT 12 22.5
          BLET       &OFFLOAD=&OFFLOAD
          BPUTPIC    FILE=MYFILE,LINES=3,AC1,XID1,XID1,&OFFLOAD
TIME *.****
PLACE R* ON C5
SET R* TRAVEL *.****
          ADVANCE    &OFFLOAD
          BPUTPIC    FILE=MYFILE,LINES=5,AC1,XID1,XID1,XID1,XID1
TIME *.****
DESTROY R*
SET CE5 CLASS CONT5F
PLACE CF5 ON CC5
DESTROY CE5
          BLET       &LOADS=&LOADS+&J
          BPUTPIC    FILE=MYFILE,LINES=4,AC1,AC1,&LOADS,AC1
TIME *.****
WRITE M1 ***.**
WRITE M2 ***.**
WRITE M8 ***.**
          BLET       &DRILL=AC1/&DR
          BPUTPIC    FILE=MYFILE,LINES=2,AC1,&DRILL
TIME *.****
WRITE M4 ***.**
          BLET       &TD5=17.5/&MDOWN
          BPUTPIC    FILE=MYFILE,LINES=3,AC1,XID1,XID1,&TD5
TIME *.****
```

```
PLACE M* ON P5B
SET M* TRAVEL *.****
        ADVANCE    &TD5
        BPUTPIC    FILE=MYFILE,LINES=2,AC1,XID1
TIME *.****
DESTROY RD*
        BLET       &DISC=&DISC
        BPUTPIC    FILE=MYFILE,LINES=1,AC1,&DISC
TIME *.****
        ADVANCE    &DISC
        BLET       &LOAD=&LOAD
        BPUTPIC    FILE=MYFILE,LINES=5,AC1,XID1,XID1,XID1,XID1,&LOAD
TIME *.****
CREATE ROCK R*
CREATE ROCK1 RH*
PLACE RH* ON EH
SET RH* TRAVEL *.****
        ADVANCE    &LOAD
        BPUTPIC    FILE=MYFILE,LINES=3,AC1,XID1,XID1
TIME *.****
CREATE ROD RD*
PLACE RD* AT 12 22.5
        BPUTPIC    FILE=MYFILE,LINES=2,AC1,XID1
TIME *.****
DESTROY RH*
        BLET       &DISC=&DISC
        BPUTPIC    FILE=MYFILE,LINES=1,AC1,&DISC
TIME *.****
        ADVANCE    &DISC
        BLET       &TU6=21/&MUP
        BPUTPIC    FILE=MYFILE,LINES=3,AC1,XID1,XID1,&TU6
TIME *.****
PLACE M* ON P6A
SET M* TRAVEL *.****
        ADVANCE    &TU6
        BPUTPIC    FILE=MYFILE,LINES=2,AC1,XID1
TIME *.****
DESTROY RD*
        BLET       &OFFLOAD=&OFFLOAD
        BPUTPIC    FILE=MYFILE,LINES=3,AC1,XID1,XID1,&OFFLOAD
TIME *.****
PLACE R* ON C6
SET R* TRAVEL *.****
        ADVANCE    &OFFLOAD
        BPUTPIC    FILE=MYFILE,LINES=5,AC1,XID1,XID1,XID1,XID1
TIME *.****
DESTROY R*
SET CE6 CLASS CONT6F
PLACE CF6 ON CC6
DESTROY CE6
        BLET       &LOADS=&LOADS+&J
        BPUTPIC    FILE=MYFILE,LINES=4,AC1,AC1,&LOADS,AC1
TIME *.****
WRITE M1 ***.**
WRITE M2 ***.**
WRITE M8 ***.**
        TEST L     &LOADS,&T,DOWN
        BLET       &DRILL=AC1/&DR
        BPUTPIC    FILE=MYFILE,LINES=2,AC1,&DRILL
TIME *.****
WRITE M4 ***.**
        BLET       &TD6=21/&MDOWN
        BPUTPIC    FILE=MYFILE,LINES=3,AC1,XID1,XID1,&TD6
TIME *.****
PLACE M* ON P6B
SET M* TRAVEL *.****
```

```
          ADVANCE    &TD6
          BPUTPIC    FILE=MYFILE,LINES=3,AC1,XID1,XID1
TIME *.****
CREATE ROD RD*
PLACE RD* AT 12 22.5
          BLET       &DISC=&DISC
          BPUTPIC    FILE=MYFILE,LINES=1,AC1,&DISC
TIME *.****
          ADVANCE    &DISC
          BPUTPIC    FILE=MYFILE,LINES=2,AC1,XID1
TIME *.****
DESTROY RD*
          BLET       &TULIFT=&DIST1/&MUP
          BPUTPIC    FILE=MYFILE,LINES=6,AC1,XID1,XID1,XID1,XID1,XID1,&TULIFT
TIME *.****
PLACE M* ON PL
CREATE HOPPER HP*
SET M* CLASS TRAIN
PLACE HP* AT 22 30
SET M* TRAVEL *.****
          ADVANCE    &TULIFT
          TRANSFER   ,UPTOP
DOWN    BPUTPIC    FILE=MYFILE,LINES=6,AC1,AC1,&LOADS,XID1,AC1,AC1
TIME *.****
WRITE M1 ***.**
WRITE M2 ***.**
DESTROY W*
WRITE M5 End Cleaning Completed!
WRITE M8 ***.**
          BLET       &TUS=14/&MUP
          BPUTPIC    FILE=MYFILE,LINES=3,AC1,XID1,XID1,&TUS
TIME *.****
PLACE M* ON PF
SET M* TRAVEL *.****
          ADVANCE    &TUS
          BPUTPIC    FILE=MYFILE,LINES=2,AC1,XID1
TIME *.****
PLACE M* AT 67.74 50.36
          BLET       &LWAIT=&LWAIT
          BPUTPIC    FILE=MYFILE,LINES=1,AC1,&LWAIT
TIME *.****
          ADVANCE    &LWAIT
          BLET       &LIFT=&LIFT
          BPUTPIC    FILE=MYFILE,LINES=7,AC1,XID1,XID1,XID1,XID1,XID1,XID1,&LIFT
TIME *.****
SET CF1 TRAVEL *.****
SET CF2 TRAVEL *.****
SET CF3 TRAVEL *.****
SET CF4 TRAVEL *.****
SET CF5 TRAVEL *.****
SET CF6 TRAVEL *.****
          ADVANCE    &LIFT
          BPUTPIC    FILE=MYFILE,LINES=9,AC1,XID1,XID1,XID1,XID1,XID1_
          ,XID1,XID1,XID1,&TUS
TIME *.****
PLACE M* ON PZ
SET M* TRAVEL *.****
DESTROY CF1
DESTROY CF2
DESTROY CF3
DESTROY CF4
DESTROY CF5
DESTROY CF6
          BLET       &TUS=&DECL/&MUP
          BPUTPIC    FILE=MYFILE,LINES=3,AC1,XID1,XID1,&TUS,XID1,XID1,&MUP
TIME *.****
```

```
PLACE M* ON PZ
SET M* TRAVEL *.****
          ADVANCE    &TUS
          BPUTPIC    FILE=MYFILE,LINES=2,AC1,XID1
TIME *.****
PLACE M* AT 419.78 150.04
          BLET       &DUMP=&DUMP
          BPUTPIC    FILE=MYFILE,LINES=4,AC1,XID1,XID1,XID1,&DUMP
TIME *.****
CREATE ROCK R*
PLACE R* ON PD1
SET R* TRAVEL *.****
          ADVANCE    &DUMP
          BPUTPIC    FILE=MYFILE,LINES=3,AC1,XID1,XID1
TIME *.****
DESTROY R*
DESTROY M*
FINISH   BPUTPIC    FILE=MYFILE,LINES=3,AC1,XID1,XID1
TIME *.****
CREATE ROD RD*
PLACE RD* AT 12 22.5
          BLET       &WAIT=&WAIT
          BPUTPIC    FILE=MYFILE,LINES=1,AC1,&WAIT
TIME *.****
          ADVANCE    &WAIT
          BPUTPIC    FILE=MYFILE,LINES=2,AC1,XID1
TIME *.****
DESTROY RD*
          ADVANCE    &WAIT
          BLET       &DRILL=AC1/&DR
           BPUTPIC    FILE=MYFILE,LINES=3,AC1,&DRILL,AC1
TIME *.****
WRITE M4 ***.**
WRITE M8 ***.**
          BLET       &FIN=&NH
          BPUTPIC    FILE=MYFILE,LINES=1,AC1,&FIN
TIME *.****
          TEST GE    &DRILL,&FIN,FINISH
          BPUTPIC    FILE=MYFILE,LINES=3,AC1,&NH,XID1
TIME *.****
WRITE M4 ***.**
WRITE M6 Drilling Completed!
          ADVANCE    &DWAIT
          BPUTPIC    FILE=MYFILE,LINES=2,AC1,XID1
TIME *.****
SET D* CLASS DRILLF
          BLET       &WAIT=&WAIT
          BPUTPIC    FILE=MYFILE,LINES=1,AC1,&WAIT
TIME *.****
          ADVANCE    &WAIT
          BLET       &DUP=&DIST1/&MUP
          BPUTPIC    FILE=MYFILE,LINES=3,AC1,XID1,XID1,&DUP
TIME *.****
PLACE D* ON PD
SET D* TRAVEL *.****
          ADVANCE    &DUP
          BPUTPIC    FILE=MYFILE,LINES=3,AC1,XID1,XID1
TIME *.****
DESTROY RO*
DESTROY D*
          BPUTPIC    FILE=MYFILE,LINES=2,AC1,XID1,&BLAST
TIME *.****
WRITE M11 Charging /Monorail Extension begins
LAST      BPUTPIC    FILE=MYFILE,LINES=3,AC1,XID1,XID1
TIME *.****
CREATE STAR ST*
```

```
PLACE ST* AT 7 20
          ADVANCE    &WAIT
          BPUTPIC    FILE=MYFILE,LINES=2,AC1,XID1
TIME *.****
DESTROY ST*
          ADVANCE    &WAIT
          BPUTPIC    FILE=MYFILE,LINES=2,AC1,AC1
TIME *.****
WRITE M13 ***.**
          BLET       &FINE=&FINE+10
          BPUTPIC    FILE=MYFILE,LINES=1,AC1,&FINE
TIME *.****
          TEST GE    &FINE,&BLAST,LAST
          BPUTPIC    FILE=MYFILE,LINES=3,AC1,XID1,XID1
TIME *.****
WRITE M12 Charging /Monorail Extension completed!
END
      ADVANCE              &CDOWN
      TRANSFER             ,HOME
      TERMINATE
      GENERATE             60*60*12*2
      TERMINATE            1
      START                1
      END
```

Appendix 2

SCREEN SHOTS OF COMPUTER SIMULATION PROCESS

Screen shots show (for each loading time i.e. the time to load material in the hopper), the total time to clean the development face and the number of tonnes loaded. The time it takes to drill and support the face, the number of holes drilled and the total drill-blast-load-haul cycle time for each loading time is also indicated.

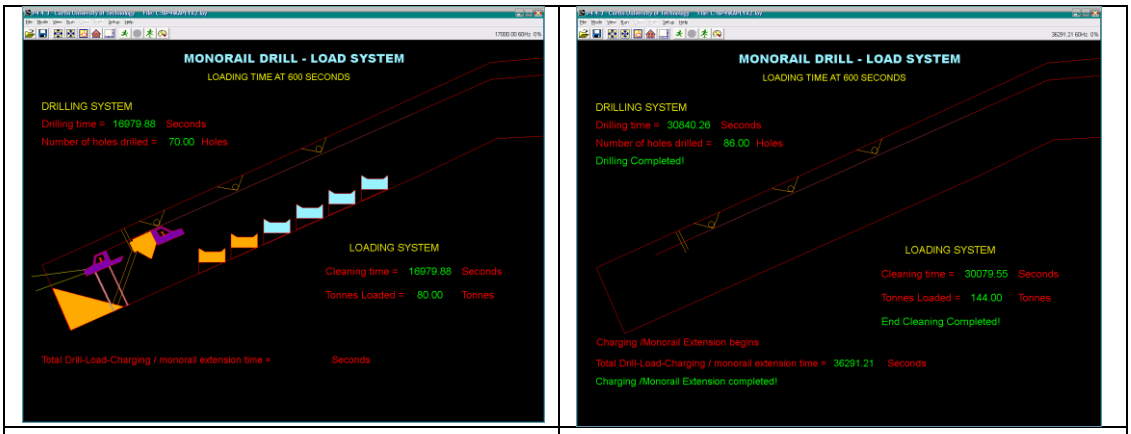

(a) (b)

Figure A1: Loading time 600 sec

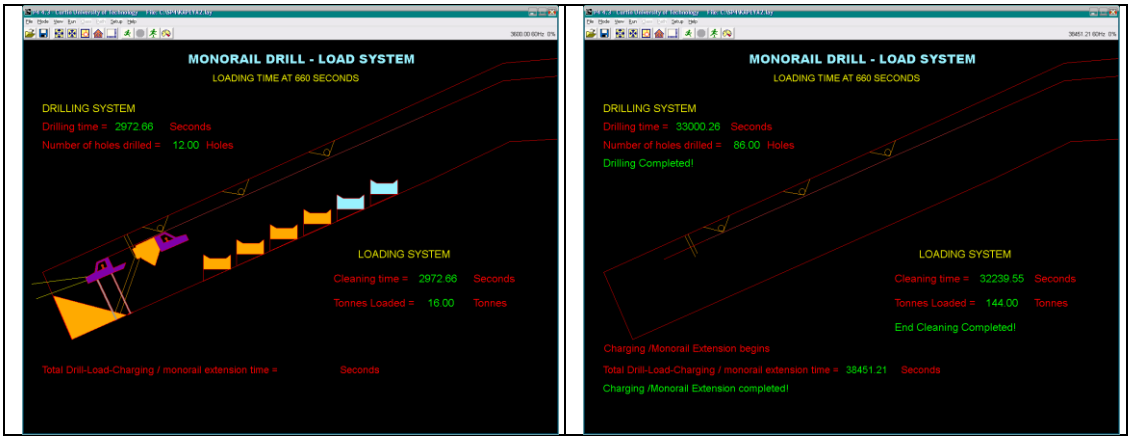

(a) (b)

Figure A2: Loading time 660 sec

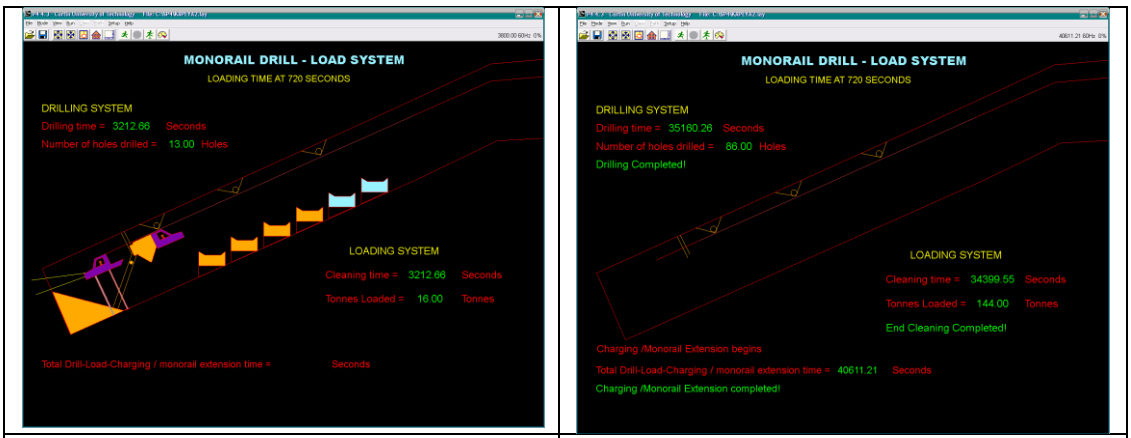

(a) (b)

Figure A3: Loading time 720 sec

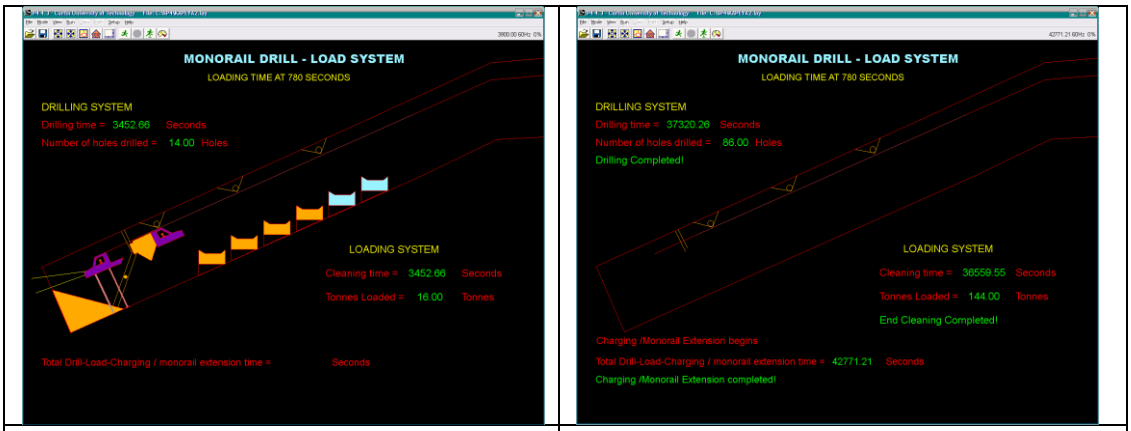

(a) (b)

Figure A4: Loading time 780 sec

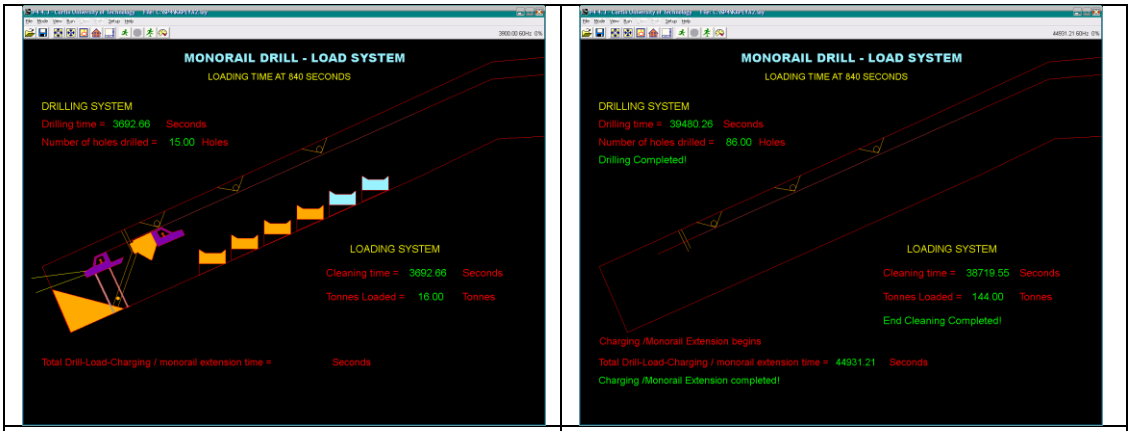

(a) (b)

Figure A5: Loading time 840 sec

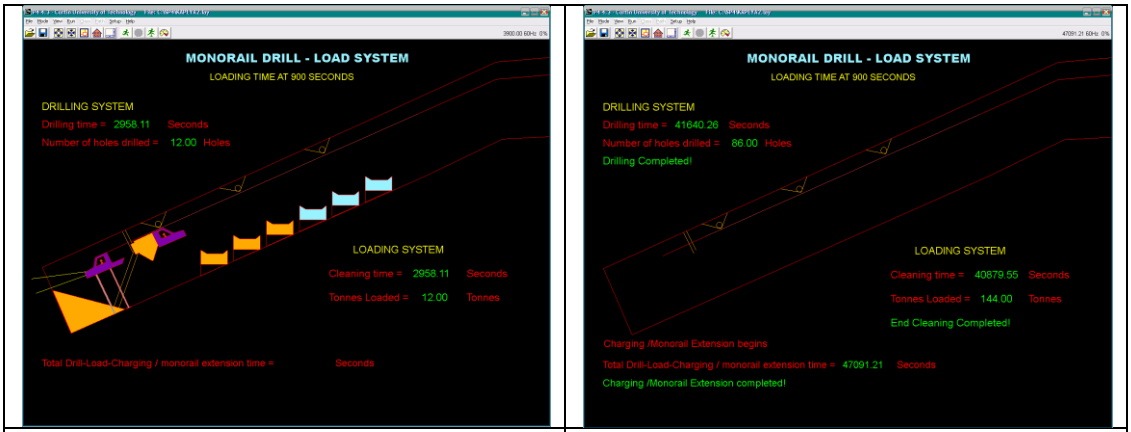

(a) (b)

Figure A6: Loading time 900 sec

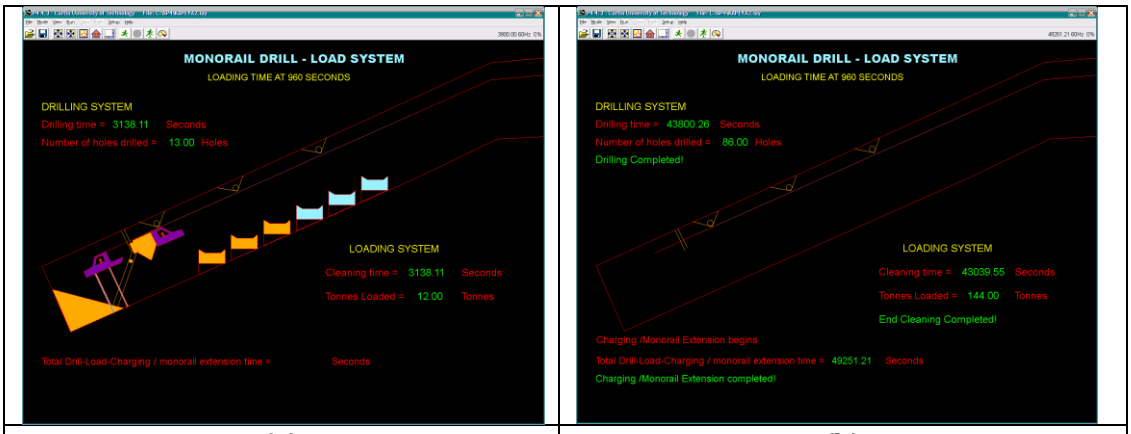

(a) (b)

Figure A7: Loading time 960 sec

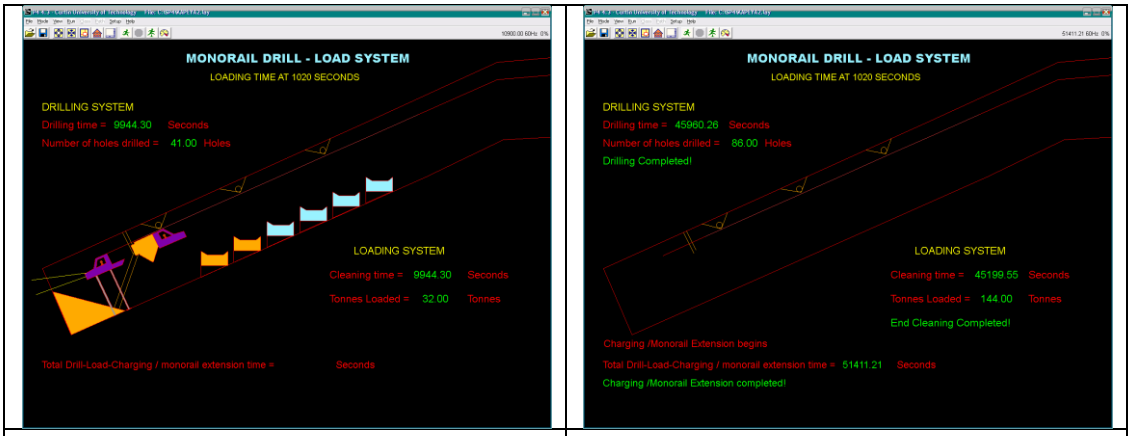

(a) (b)

Figure A8: Loading time 1020 sec

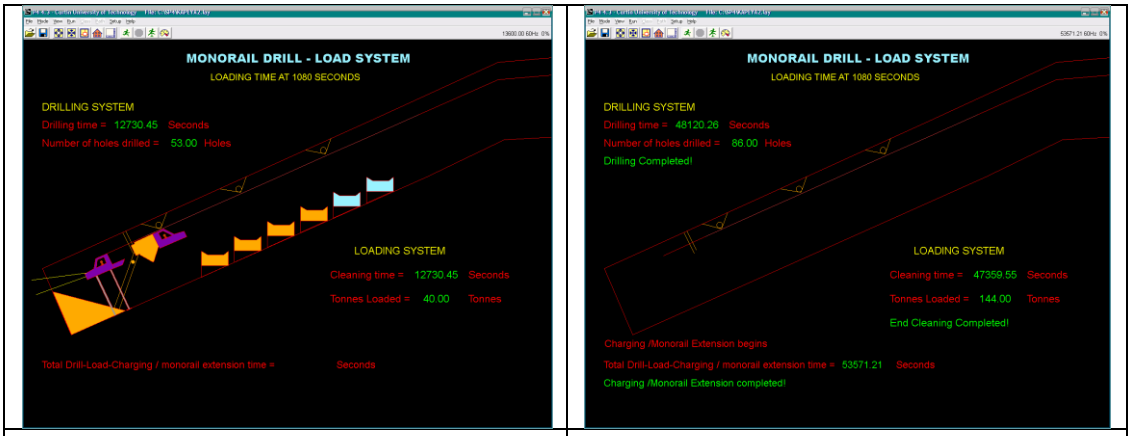

(a) (b)

Figure A9: Loading time 1080 sec

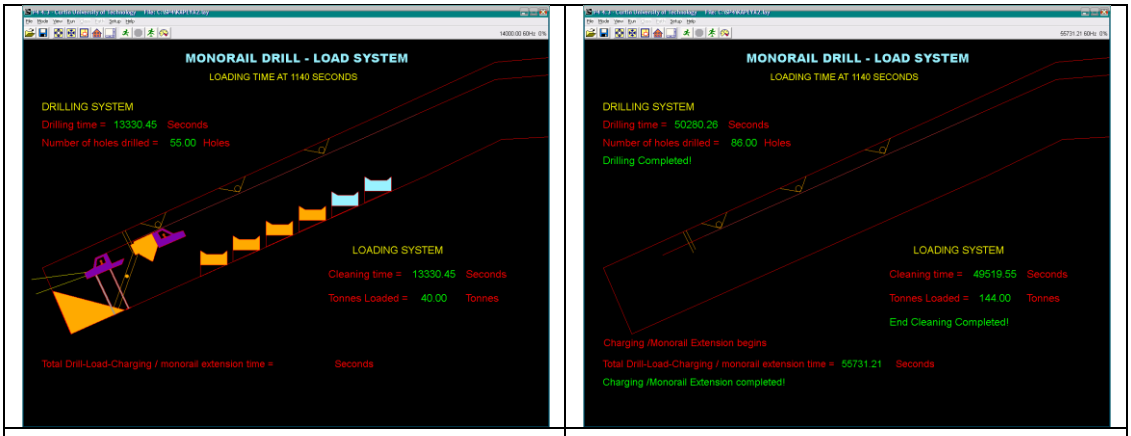

(a) (b)

Figure A10: Loading time 1140 sec

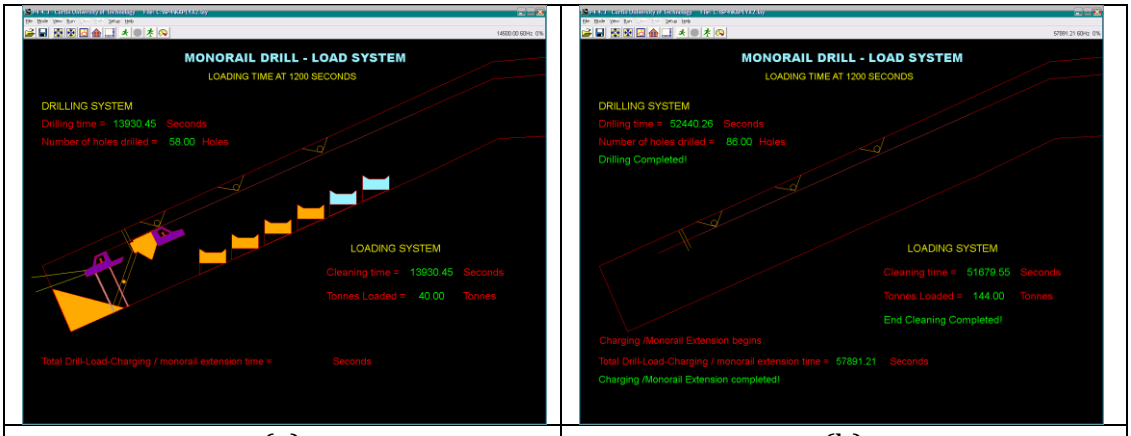

(a) (b)

Figure A11: Loading time 1200 sec

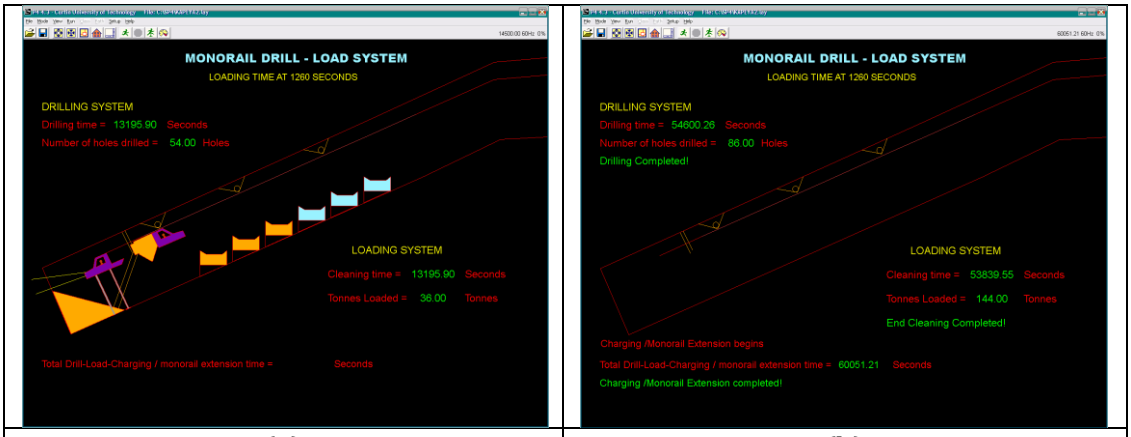

(a) (b)

Figure A12: Loading time 1260 sec

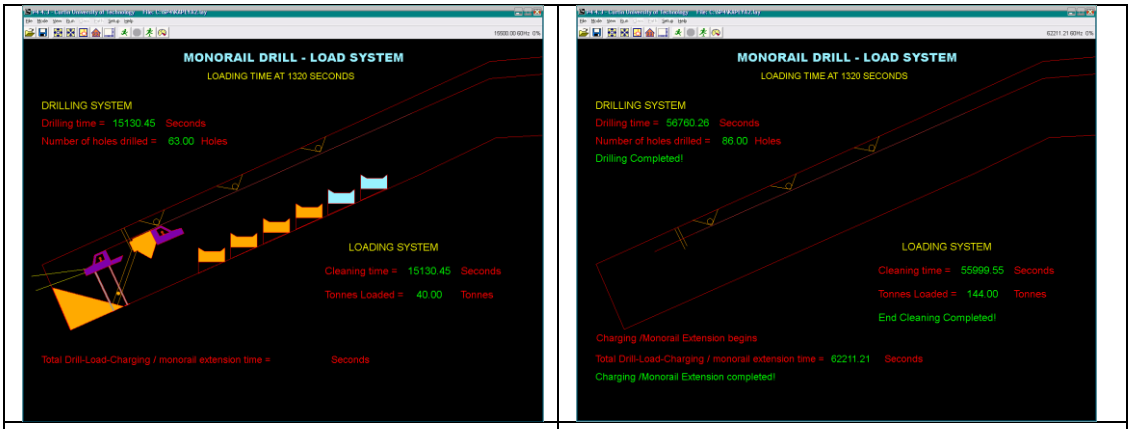

(a) (b)

Figure A13: Loading time 1320 sec

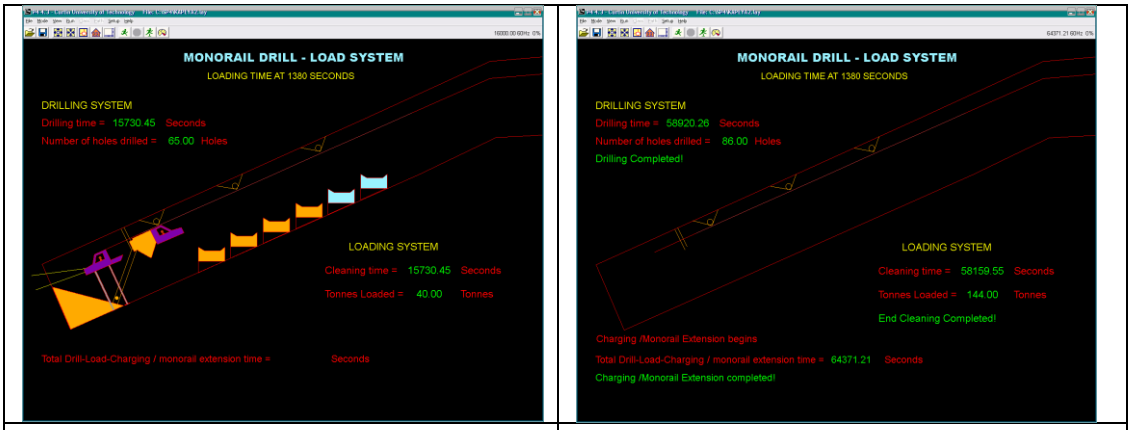

(a) (b)

Figure A14: Loading time 1380 sec

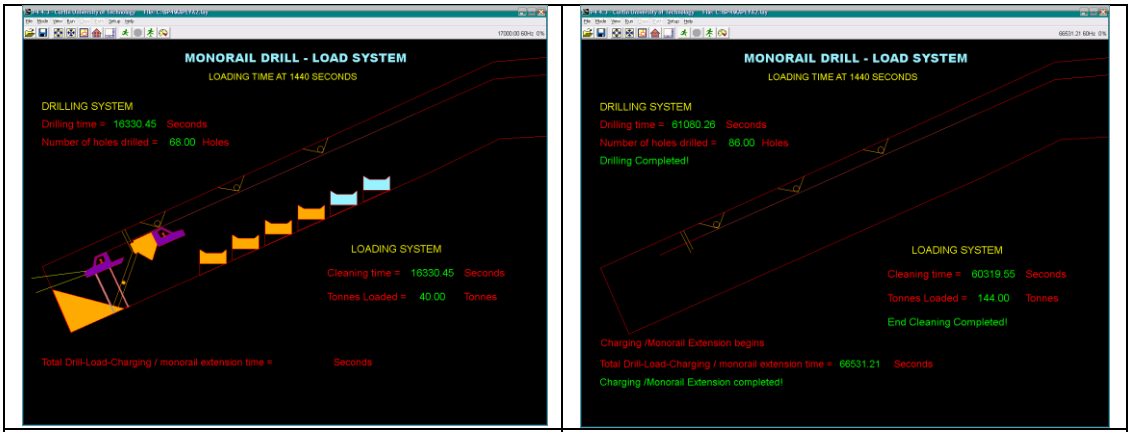

(a) (b)

Figure A15: Loading time 1440 sec